Energy, Mines and Resources Canada
Énergie, Mines et Ressources Canada

Canada

THE ENERGY OF OUR RESOURCES - THE POWER OF OUR IDEAS

L'ÉNERGIE DE NOS RESSOURCES - NOTRE FORCE CRÉATRICE

NOTICE TO LIBRARIANS AND INDEXERS

The Geological Survey's Current Research series contains many reports comparable in scope and subject matter to those appearing in scientific journals and other serials. Most contributions to Current Research include an abstract and bibliographic citation. It is hoped that these will assist you in cataloguing and indexing these reports and that this will result in a still wider dissemination of the results of the Geological Survey's research activities.

AVIS AUX BIBLIOTHÉCAIRES ET PRÉPARATEURS D'INDEX

La série Recherches en cours de la Commission géologique contient plusieurs rapports dont la portée et la nature sont comparables à ceux qui paraissent dans les revues scientifiques et autres périodiques. La plupart des articles publiés dans Recherches en cours sont accompagnés d'un résumé et d'une bibliographie, ce qui vous permettra, on l'espère, de cataloguer et d'indexer ces rapports, d'où une meilleure diffusion des résultats de recherche de la Commission géologique.

GEOLOGICAL SURVEY OF CANADA
COMMISSION GÉOLOGIQUE DU CANADA

PAPER / ÉTUDE
92-1B

CURRENT RESEARCH, PART B
INTERIOR PLAINS AND ARCTIC CANADA

RECHERCHES EN COURS, PARTIE B
PLAINES INTÉRIEURES ET RÉGION ARCTIQUE DU CANADA

1992

92-02694/

© Minister of Supply and Services Canada 1992

Available in Canada through

authorized bookstore agents and other bookstores

or by mail from

Canada Communication Group — Publishing
Ottawa, Canada K1A 0S9

and from

Geological Survey of Canada offices:

601 Booth Street
Ottawa, Canada K1A 0E8

3303-33rd Street N.W.,
Calgary, Alberta T2L 2A7

100 West Pender Street,
Vancouver, B.C. V6B 1R8

A deposit copy of this publication is also available for
reference in public libraries across Canada

Cat. No. M44-92/1B
ISBN 0-660-57063-7

Price subject to change without notice

Cover description

View to the northeast of Vendom Fiord, south-central Ellesmere Island. Recessive middle Paleozoic foredeep clastics lie along the slopes and within the fiord, and more resistant carbonates form the 600 m high peaks. Photo by T. de Freitas.

Description de la photo couverture

Perspective vers le nord-est du fjord Vendom dans la partie centre sud de l'île d'Ellesmere. Des roches clastiques d'avant-fosse en retrait (Paléozoïque moyen) longent les pentes et se remarquent dans le fjord; les roches carbonatées plus résistantes forment les pics s'élevant jusqu'à 600 m. Photo gracieuseté de T. de Freitas.

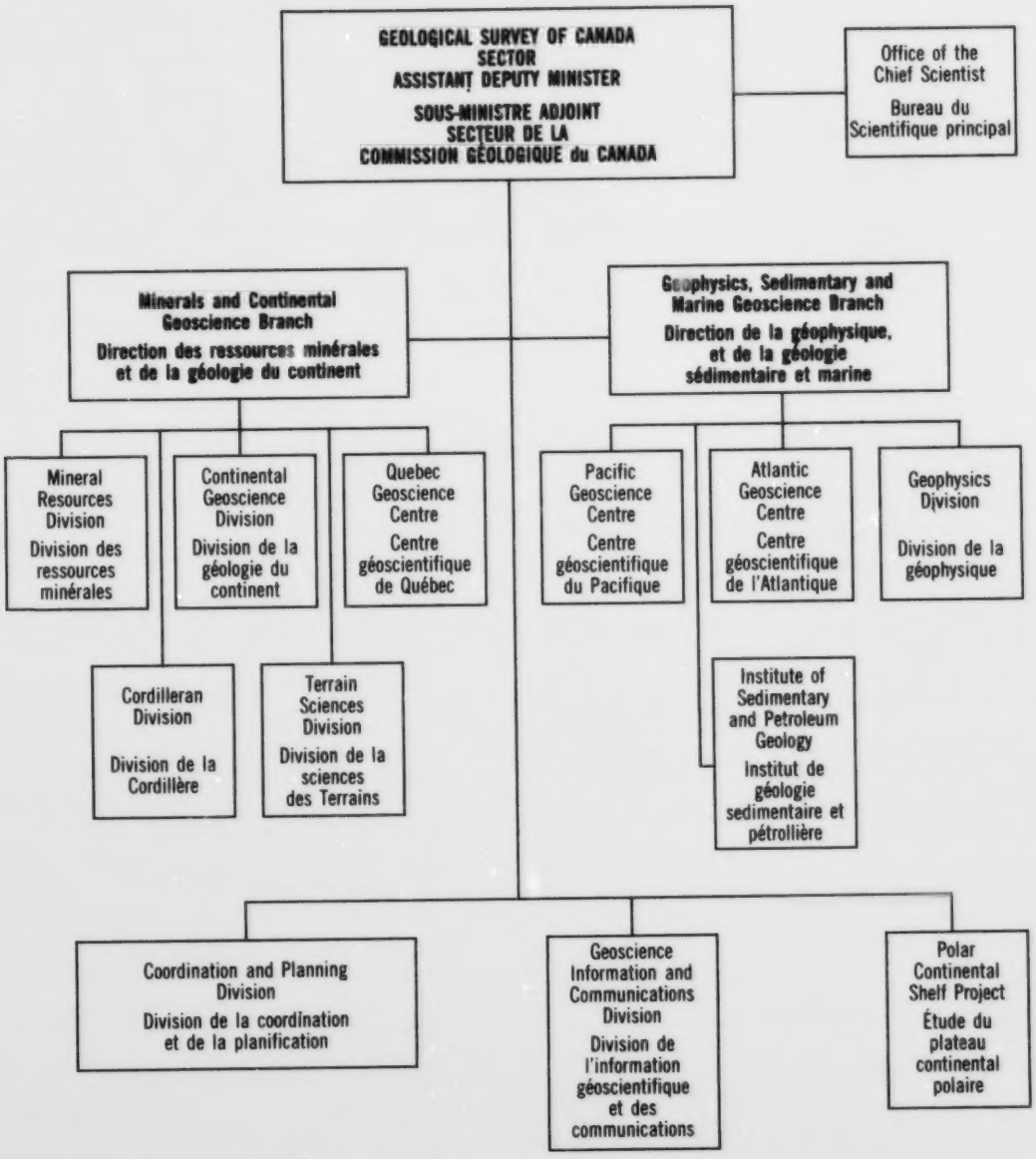
GEOLOGICAL SURVEY OF CANADA
SECTOR
ASSISTANT DEPUTY MINISTER
SOUS-MINISTRE ADJOINT
SECTEUR DE LA
COMMISSION GÉOLOGIQUE du CANADA
Office of the Chief Scientist
Bureau du Scientifique principal
Minerals and Continental Geoscience Branch
Direction des ressources minérales et de la géologie du continent
Geophysics, Sedimentary and Marine Geoscience Branch
Direction de la géophysique, et de la géologie sédimentaire et marine
Mineral Resources Division
Division des ressources minérales
Continental Geoscience Division
Division de la géologie du continent
Quebec Geoscience Centre
Centre géoscientifique de Québec
Pacific Geoscience Centre
Centre géoscientifique du Pacifique
Atlantic Geoscience Centre
Centre géoscientifique de l'Atlantique
Geophysics Division
Division de la géophysique
Cordilleran Division
Division de la Cordillère
Terrain Sciences Division
Division de la sciences des Terrains
Institute of Sedimentary and Petroleum Geology
Institut de géologie sedimentaire et pétrollière
Coordination and Planning Division
Division de la coordination et de la planification
Geoscience Information and Communications Division
Division de l'information géoscientifique et des communications
Polar Continental Shelf Project
Étude du plateau continental polaire

Separates

A limited number of separates of the papers that appear in this volume are available by direct request to the individual authors. The addresses of the Geological Survey of Canada offices follow:

601 Booth Street
OTTAWA, Ontario
K1A 0E8
(FAX: 613-996-9990)

Institute of Sedimentary and Petroleum Geology
3303-33rd Street N.W.
CALGARY, Alberta
T2L 2A7
(FAX: 403-292-5377)

Cordilleran Division
100 West Pender Street
VANCOUVER, B.C.
V6B 1R8
(FAX: 604-666-1124)

Pacific Geoscience Centre
P.O. Box 6000
9860 Saanich Road
SIDNEY, B.C.
V8L 4B2
(Fax: 604-363-6565)

Atlantic Geoscience Centre
Bedford Institute of Oceanography
P.O. Box 1006
DARTMOUTH, N.S.
B2Y 4A2
(FAX: 902-426-2256)

Québec Geoscience Centre
2700, rue Einstein
C.P. 7500
Ste-Foy (Québec)
G1V 4C7
(FAX: 418-654-2615)

When no location accompanies an author's name in the title of a paper, the Ottawa address should be used.

Tirés à part

On peut obtenir un nombre limité de «tirés à part» des articles qui paraissent dans cette publication en s'adressant directement à chaque auteur. Les adresses des différents bureaux de la Commission géologique du Canada sont les suivantes:

601, rue Booth
OTTAWA, Ontario
K1A 0E8
(facsimilé : 613-996-9990)

Institut de géologie sédimentaire et pétrolière
3303-33rd St. N.W.,
CALGARY, Alberta
T2L 2A7
(facsimilé : 403-292-5377)

Division de la Cordillère
100 West Pender Street
VANCOUVER, British Columbia
V6B 1R8
(facsimilé : 604-666-1124)

Centre géoscientifique du Pacifique
P.O. Box 6000
9860 Saanich Road
SIDNEY, British Columbia
V8L 4B2
(facsimilé : 604-363-6565)

Centre géoscientifique de l'Atlantique
Institut océanographique Bedford
B.P. 1006
DARTMOUTH, Nova Scotia
B2Y 4A2
(facsimilé : 902-426-2256)

Centre géoscientifique de Québec
2700, rue Einstein
C.P. 7500
Ste-Foy (Québec)
G1V 4C7
(facsimilé : 418-654-2615)

Lorsque l'adresse de l'auteur ne figure pas sous le titre d'un document, on doit alors utiliser l'adresse d'Ottawa.

CONTENTS

1	B.A. KJARSGAARD and T.D. PETERSON Kimberlite-derived ultramafic xenoliths from the diamond stability field: a new Cretaceous geotherm for Somerset Island, Northwest Territories
7	T.W. ANDERSON and C.F.M. LEWIS Evidence for ice margin retreat and proglacial lake (Agassiz?) drainage by about 11 ka, Clearwater River spillway area, Saskatchewan
13	C. BÉGIN, Y. MICHAUD et S. BOUCHER Données préliminaires sur la morphologie et dynamisme récent d'un système dunaire de haut de falaise dans la région de la rivière Mountain, District de Mackenzie, Territoires du Nord-Ouest
23	H.R. JACKSON, B.D. LONCAREVIC, and W. BLAKE, Jr. Shallow seismic and magnetic data from northernmost Baffin Bay: insights into geology
31	J.B. NELSON, D.A. FORSYTH, D. TESKEY, A.V. OKULITCH, D.L. MARCOTTE, C.D. HARDWICK, M.E. BOWER, and R. MACNAB The 1991 Polar Margin Aeromagnetic Survey in the Lincoln Sea, northern Ellesmere Island and northern Greenland
37	G.H. EISBACHER Structural geology of northwestern Devon Island, Arctic Canada
47	U. MAYR and T. de FREITAS Cambro-Ordovician stratigraphy of Grinnell Peninsula, northern Devon Island, Northwest Territories
53	T. de FREITAS and U. MAYR The middle Paleozoic sequence of northern Devon Island, Northwest Territories
65	P. THÉRIAULT and U. MAYR Newly discovered Carboniferous exposures at the margin of Sverdup Basin, northwestern Devon Island, Northwest Territories
73	G.S. SOULE and D.A. SPRATT Study of the Triangle Zone and Foothills structures in the Grease Creek Syncline area of Alberta
79	T. GENTZIS, F. GOODARZI, and D. GIBSON A petrographic study of coal-bearing strata in the Drumheller area, Red Deer River valley, Alberta
91	S.A. EDLUND and M-K. WOO Eolian deposition on western Fosheim Peninsula, Ellesmere Island, Northwest Territories during the winter of 1990-91
97	A.G. LEWKOWICZ and K.A. GUDJONSSON Slope hummocks on Fosheim Peninsula, Ellesmere Island, Northwest Territories
103	Author Index

Kimberlite-derived ultramafic xenoliths from the diamond stability field: a new Cretaceous geotherm for Somerset Island, Northwest Territories

B.A. Kjarsgaard[1] and T.D. Peterson
Continental Geoscience Division

Kjarsgaard, B. A. and Peterson, T. D., 1992: Kimberlite-derived ultramafic xenoliths from the diamond stability field: a new Cretaceous geotherm for Somerset Island, Northwest Territories; in Current Research, Part B; Geological Survey of Canada, Paper 92-1B, p. 1-6.

Abstract

Mantle-derived ultramafic xenoliths from the Batty Bay kimberlite complex consist predominantly of garnet and garnet + spinel lherzolites. Coarse textures are more prevalent than porphyroclastic textures in these xenoliths. The pressures and temperatures of equilibration of twenty-one lherzolite xenoliths are consistent with a 44mW/m^2 steady-state shield paleogeotherm. The geotherm is not inflected, and no correlation exists between xenolith textural type and pressure and temperature of equilibration. Three of the twenty-one xenoliths equilibrated in the diamond stability field.

Résumé

Des xénolites ultramafiques dérivés du manteau et issus du complexe kimberlitique de Batty Bay, se composent principalement de lherzolites à grenat et à grenat + spinelle. Dans ces lherzolites, les textures grossières sont prédominantes comparativement aux textures porphyroclastiques. Les pressions et températures d'équilibre de vingt et un xénolites de lherzolite concordent avec un paléogéotherme statique du bouclier, de 44 mW/m^2. Le géotherme n'est pas infléchi, et il n'existe aucune corrélation entre le type textural du xénolithe d'une part et la pression et la température d'équilibre d'autre part. Trois des vingt et un xénolites ont atteint un équilibre dans le champ de stabilité du diamant.

[1] Mineral Resources Division

INTRODUCTION

Investigation of Somerset Island kimberlites in July 1990, included sampling of all known kimberlite bodies (Fig. 1), as well as detailed mapping of the Batty Bay complex (Fig. 2). Emphasis on collecting mantle xenoliths resulted in the discovery of five new localities (Nord, and Batty Bay sites K12, K14, K16 and K24), plus the recognition that xenoliths are much more abundant at Batty Bay sites K11 and K15 than was previously inferred (Mitchell, 1987). Of the more than 200 peridotite xenoliths collected from Batty sites K11-K16, garnet lherzolites predominate over spinel lherzolites at all localities except site K13 (Nanorluk of Mitchell, 1976), where they are in approximately equal abundance. Eclogite xenoliths were not found at any locality, consistent with previous work (Mitchell, 1987). This paper presents a preliminary mantle paleogeotherm for Somerset Island based on 21 garnet and garnet + spinel lherzolite samples from the Batty Bay complex, utilizing the recently experimentally calibrated geothermobarometers of Brey et al. (1990).

GENERAL GEOLOGY

The kimberlites of Somerset Island form a belt trending approximately northeast-southwest. Localisation of kimberlite magmatism appears to have been controlled by three distinct fracture sets (north-south; northeast-southwest; southeast-northwest: Mitchell, 1975), which may be related to Paleozoic tectonism during evolution of the Boothia Uplift, and are probably, in part at least, reactivated Precambrian structures (Brown et al., 1969). In places on the western side of Somerset Island these fracture sets are continuous, extending from the basement into the Paleozoic cover (Map 3; Blackadar, 1967).

Cretaceous intrusive ages have been determined for the Ham (88 Ma: Heaman, 1989) and Elwin Bay (105 Ma: C.B. Smith, written communication to L. Heaman) kimberlites utilizing the U-Pb perovskite dating method. An age of 100 Ma (Rb-Sr, phlogopite) was determined for the Batty Bay K10 kimberlite by Smith et al. (1989). These kimberlite radiometric ages are considerably younger than the Paleozoic cover rocks (Cambro-Ordovician to Upper Silurian sedimentary rocks, predominantly dolostone) which they intrude. Emplacement of kimberlite in the Somerset Island field correlates with a worldwide Cretaceous episode of kimberlite activity.

The Somerset Island kimberlites consist principally of hypabyssal facies kimberlite. Dykes occur at Jos, Ham and Batty Bay, and enlarged fissures termed 'blows' are found at Ham, Nord, Ouest, Peuyuk and Batty Bay. Rocks containing pelletal lapilli (characteristic of diatreme facies kimberlite) were observed at Elwin Bay and Batty Bay, but are a subordinate rock type. This suggests that the current exposure level of the Somerset Island kimberlites is at the transition from the root zone (hypabyssal facies) to the lowermost diatreme (diatreme facies), indicating 1-2 km of erosion has

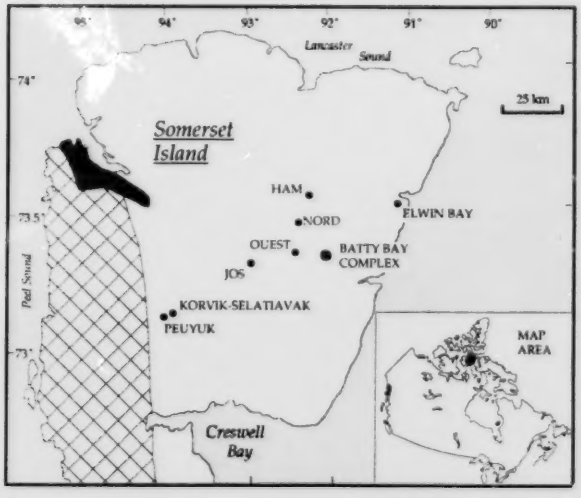

Figure 1. Location map of the Somerset Island kimberlite province. Regional geology after Stewart (1987): white = Paleozoic cover; dark stipple = Late Proterozoic cover; cross-hatch = Precambrian basement.

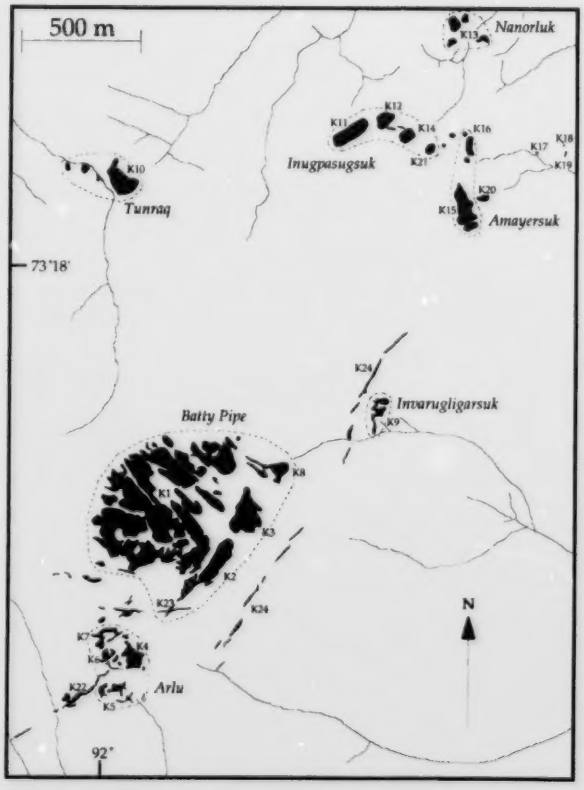

Figure 2. Detailed map of the Batty Bay kimberlites showing the surface expression of the complex (based on outcrop, frost-heaved blocks and regolith). Location names in italics are the outcrop groupings of Mitchell (1976).

Table 1. Mantle xenolith mineral assemblages and comparison of geothermometers and geobarometers. BKN = thermometer/barometer of Brey et al. (1990); BK = thermometer of Brey and Köhler (1990); MC74 and FB86 = empirical barometer and thermometer of Finnerty and Boyd (1987), see text for details. Mineralogy as follows: Gt = garnet; Sp = spinel; Ol = olivine; Opx = orthopyroxene; Cpx = clinopyroxene; Phl = phlogopite; Ru = rutile. Secondary minerals replace the primary mineral shown in brackets, i.e. (Gt). Textural types are as follows (after Harte, 1977): C-E = coarse equant; C-T = coarse tabular; P = porphyroclastic; M-P = mosaic porphyroclastic; D-P = disrupted porhyroclastic. Grain sizes of olivine neoblasts in porphyroclastic, mosaic porphyroclastic and disrupted porphyroclastic samples are: vfg = very fine grained, <0.1 mm; fg = fine grained, 0.1 - 0.5 mm; mg = medium grained, >0.5 mm.

Sample#	Primary Mineralogy	Secondary Mineralogy	Texture	P (GPa)		T (°C)		
				BKN	MC74	BKN	FB86	BK
K11A1	Gt + Ol + Opx + Cpx	rare Phl + Sp (Gt)	C-E	4.40	4.13	1146	1043	1165
K11A3	Gt + Ol + Opx + Cpx	minor Phl + Sp (Gt)	P, fg	4.12	3.99	1121	994	1175
K11A4	Gt + Ol + Opx + Cpx	minor Phl + Sp (Gt)	M-P, vfg	5.27	4.43	1234	1129	1243
K11A5	Gt + Ol + Opx + Cpx		C-E	4.20	4.08	1127	1012	1078
K11A7	Gt + Ol + Opx + Cpx	minor Sp (Cpx)	C-E	4.05	4.18	1156	1054	1192
K11A9	Gt + Ol + Opx + Cpx	minor Phl + Sp (Gt)	C-E	4.78	4.39	1192	1088	1182
K11A14	Gt + Ol + Opx + Cpx	rare Phl + Sp (Gt)	C-E	4.36	3.96	1123	997	1101
K11A15	Gt + Ol + Opx + Cpx	minor Phl + Sp (Gt)	C-E	4.21	4.19	1152	1052	1177
K11A16	Gt + Ol + Opx + Cpx		C-E	4.28	4.40	1158	1063	1172
K12A2	Gt + Ol + Opx + Cpx		C-T	4.57	4.56	1218	1142	1215
K12A3	Gt + Sp + Ol + Opx + Cpx	minor Phl + Sp (Gt)	C-E	4.35	4.44	1206	1119	1307
K12A4	Gt + Ol + Opx + Cpx	minor Phl + Sp (Gt)	C-T	3.65	3.20	995	847	1044
K12A7	Gt + Ol + Opx + Cpx	rare Sp (Gt)	C-T	4.62	4.54	1214	1132	1207
K12A8	Gt + Ol + Opx + Cpx		P, vfg	5.25	4.51	1246	1130	1277
K13B3	Gt + Sp + Ol + Opx + Cpx	Ru exsolution in Gt	D-P, mg	2.74	2.16	859	708	682
K13B5	Gt + Ol + Opx + Cpx	minor Phl + Sp (Gt)	C-T	3.80	3.66	1083	941	1147
K14A1	Gt + Sp + Ol + Opx + Cpx + Phl	rare Sp (Gt)	D-P, mg	4.96	4.39	1204	1080	1181
K15A2	Gt + Ol + Opx + Cpx		C-T	4.06	4.13	1140	1057	1167
K15A7	Gt + Ol + Opx + Cpx	rare Sp (Gt)	M-P, fg	4.79	4.47	1227	1131	1196
K16A2	Gt + Sp + Ol + Opx + Cpx	minor Phl + Sp (Gt)	C-T	3.51	3.15	999	856	1137
K16A3	Gt + Ol + Opx + Cpx	minor Sp (Gt)	C-E	3.75	3.65	1046	927	1185

occurred. Detailed petrography and geochemistry of the Somerset island kimberlites will be presented elsewhere (Kjarsgaard and Peterson, in prep.).

Davies (1975) noted that at Batty Bay the north-east kimberlites contain abundant pyrope garnet and Cr-diopside macrocrysts (derived from disaggregated mantle xenoliths) as compared to the main pipe (K1) and its satellites. This is consistent with our mapping results, as we found no mantle xenoliths at localities K1-K9 and K22, K23. The remainder of this paper presents data on a preliminary suite of 21 peridotite xenoliths collected from Batty Bay sites K11 to K16.

MANTLE XENOLITHS

The mantle xenoliths collected are all varieties of peridotite; eclogites were not found. The majority (>65%) of the xenoliths are four-phase (olivine + orthopyroxene + clinopyroxene + Al-bearing phase) garnet lherzolites, but garnet + spinel lherzolites and spinel lherzolites are also well represented in the collection. A few dunites and harzburgites were also collected. Examples of xenoliths representing metasomatised mantle include primary phlogopite- and rutile-bearing lherzolites. Serpentinization of the xenoliths is quite varied, ranging from samples in which only garnet and/or spinel is left intact along with small islands of olivine or pyroxenes, to samples which are completely unaltered. In most xenoliths, typically 5-25% of the original xenolith mineralogy is altered, but only four of fifty-nine selected samples were unsuitable for study due to the effects of serpentinization. Xenolith size ranged widely from small nodules, 0.5 cm in diameter to larger ovoids with dimensions to 15 cm X 10 cm X 8 cm. The majority of the xenoliths collected were either rounded and 4-5 cm in diameter, or irregularly shaped fragments from larger nodules with the largest dimension being 3-5 cm. Using the textural nomenclature scheme of Harte (1977), most of the xenoliths are classified as coarse equant to coarse tabular types, however, examples of porphyroclastic, mosaic porphyroclastic and disrupted porphyroclastic types occur as subordinate textural variants (see Table 1).

ANALYTICAL METHODS

Compositions of minerals were determined on a Cameca Camebax electron microprobe (Analytical Division, Geological Survey of Canada, Ottawa). All analyses were performed using WDS techniques. Accelerating potential was 15kV with a specimen current of ca. 10.0 nA for Na, K, Mg and Fe and ca. 30.0 nA for all other elements. A focussed beam with a 2-3 μm spot size was utilized for all analyses.

Counting time for all elements was 10 seconds, with the exception of Ni (200 seconds). Raw data were corrected with PAP software.

MINERAL CHEMISTRY

Olivines in all xenoliths are forsterite-rich, with Mg# of 91.3 to 92.7 (Mg# = Mg/[Mg + Fe]). NiO ranges from 0.33 to 0.45 wt%. Olivine in porphyroclastic samples has a slightly more restricted compositional range (Mg# = 91.3 to 92.3; NiO = 0.34 to 0.41 wt%). No differences in composition were found between olivines of different xenolith type, nor is there any apparent correlation between olivine Mg# or NiO content with pressure or temperature.

Garnets are similar in composition to chrome pyrope garnets found in other garnet lherzolites worldwide (Nixon, 1987), and belong to group 9 garnets in the statistical classification of Dawson and Stephens (1975). All garnets are low in TiO_2 (0.07 to 0.70 wt%) and Cr_2O_3-rich (2.92 to 7.59 wt%) with Mg# of 81.9 to 86.6. There are no compositional differences between garnets from garnet lherzolites and garnet + spinel lherzolites, or among different textural types of xenoliths.

Orthopyroxenes are enstatites (Mg# of 92.1 to 93.7) with low aluminium (1.00 to 1.39 wt% Al_2O_3), calcium (0.43 to 1.00 wt% CaO) and chromium (0.23 to 0.73 wt% Cr_2O_3) contents. There are no compositional differences between orthopyroxenes from different lherzolite textural types.

Clinopyroxenes from porphyroclastic xenoliths exhibit higher titanium (0.13 to 0.54 wt% TiO_2) and aluminium (2.34 to 3.53 wt% Al_2O_3) contents than those in coarse textured xenoliths (0.04 to 0.36 wt% TiO_2; 1.45 to 3.06 wt% Al_2O_3). The Mg# of clinopyroxenes from both textural types of xenolith are similar (90.9 to 94.0), as are the sodium (1.37 to 2.62 wt% Na_2O) and chromium (1.13 to 2.77 wt% Cr_2O_3) contents.

GEOTHERMOBAROMETRY

Temperatures and pressures of equilibration of the xenoliths have been estimated from the compositions of coexisting pyroxenes by the methods of Brey et al. (1990: T_{BKN}) and Finnerty and Boyd (1987: T_{FB86}) and from the Al-content of coexisting orthopyroxene and garnet by the methods of Brey et al. (1990: P_{BKN}) and Finnerty and Boyd (1987: P_{MC74}). Results are presented in Table 1, and shown in Fig. 3 (T_{BKN} vs P_{BKN}) and 4 (T_{FB86} vs P_{MC74}). Temperature estimates from an additional thermometer, recently calibrated by Brey and Köhler (1990: T_{BK}) utilizing the partitioning of Na between coexisting pyroxenes, are also listed in Table 1 and are similar to those obtained by the T_{BKN} thermometer.

Utilizing the preferred thermobarometers of Brey et al. (1990: Fig. 3), three of the twenty-one xenoliths plot in the diamond stability field. Figure 3 illustrates that the xenoliths define an array in P-T space which can be interpreted as a steady-state shield paleogeotherm. The majority of the lherzolites plot at temperatures on or slightly above the theoretical 44mW/m^2 continental convection-related geotherm of Gurney and Harte (1980). In contrast, use of the empirical thermobarometer of Finnerty and Boyd (Figure 4; T_{FB86} vs P_{MC74}) produces a quite different set of data points, which could be interpreted as a P-T array defining a 42mW/m^2 paleogeotherm at pressures lower than approximately 4.0 GPa, while at higher pressure the geotherm is inflected to hotter temperatures.

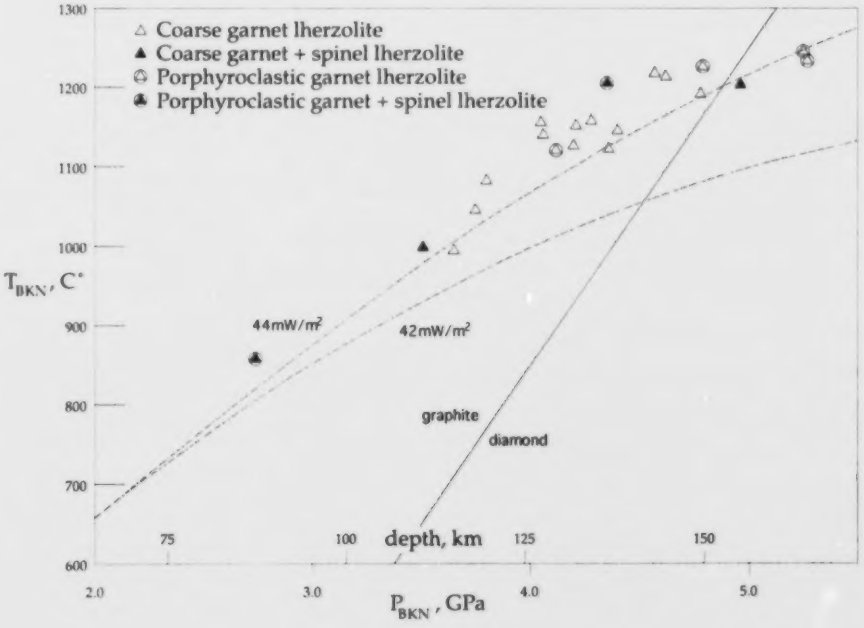

Figure 3. Pressures and temperatures of equilibration of mantle xenoliths from the Batty Bay complex, utilizing the experimentally calibrated thermobarometers of Brey et al. (1990: T_{BKN} vs P_{BKN}). The theoretical 42mW/m^2 and 44mW/m^2 geotherms are from Gurney and Harte (1980). The graphite/diamond transition is from Kennedy and Kennedy (1976).

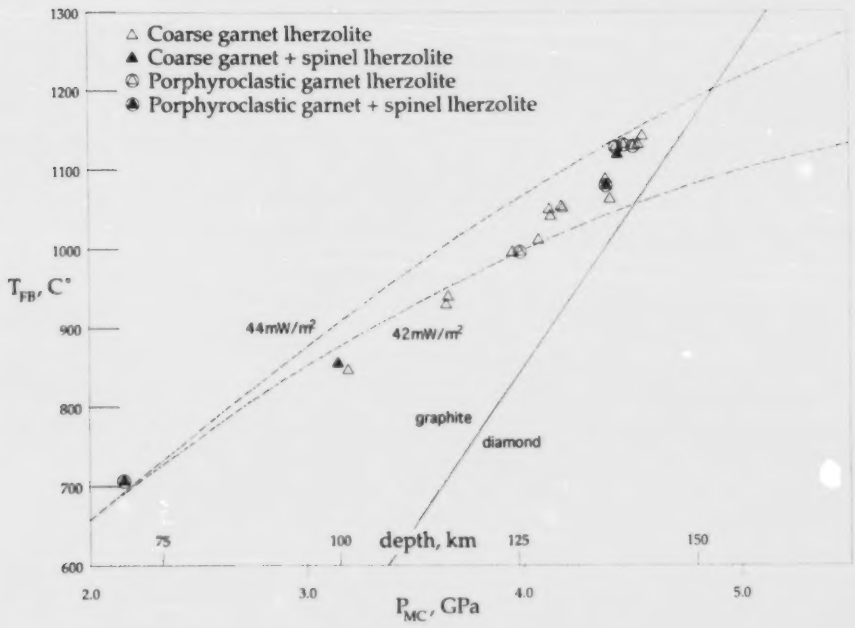

Figure 4. Pressures and temperatures of equilibration of mantle xenoliths from the Batty Bay complex, using Finnerty and Boyd's (1987) preferred empirical thermobarometers (T_{FB86} vs P_{MC74}). Theoretical geotherms and graphite/diamond transition as per Figure 3.

DISCUSSION

Although more data points are required (especially at higher pressure; thermobarometry is in progress on an additional 30 xenoliths), the results of this study provide new insights regarding the equilibration pressures and temperatures of Somerset Island mantle xenoliths. Previous work by Mitchell (1977, 1978, 1987) and Jago and Mitchell (1987) found no xenoliths which had equilibrated at pressures higher than 3.9 GPa (i.e. none in the diamond stability field). Furthermore, Jago and Mitchell (1987) and Mitchell (1987) suggested their results produced a paleogeotherm hotter than the theoretical 44mW/m^2 geotherm. Some of the apparent P-T differences between this study and previous work result from the geothermobarometers utilized (T_{Wells} vs P_{Wood}, Jago and Mitchell (1987), Mitchell (1987); T_{BKN} vs P_{BKN}, this study). According to Carswell and Gibb (1987), temperature estimates using the Wells method are considered relatively accurate (± 50°C to 3.7 GPa), but pressure estimates from the Wood method are typically low by 0.33 to 0.53 GPa. The major pressure differences (approximately >1.3 GPa uncorrected, or >0.9 GPa corrected) between the studies appears to be independent of the geobarometer used and therefore, must be sample dependent.

Jago and Mitchell (1987) state that xenoliths from the Ham blow define an inflected or perturbed paleogeotherm. In contrast, Mitchell (1987) suggested in his summary paper on all Somerset Island mantle xenoliths (including Ham) that the paleogeotherms are not inflected. Results from this study illustrate that the Batty Bay paleogeotherm is not inflected and is a good example of a steady-state geotherm. Furthermore, applying a pressure correction (see above) to previous P-T estimates for Somerset Island (Fig. 8 of Mitchell, 1987) shifts most of these data points onto the theoretical 44mW/m^2 geotherm.

The recent experimental study of Brey et al. (1990) and application by Brey (1991) of the newly calibrated thermobarometers to xenoliths from the Kaapvaal Craton (South Africa) conclusively demonstrate that the supposed inflected geotherm of Finnerty and Boyd (1987) is fictive, derived from thermobarometric measurements on high temperature disequilibrium samples. Brey (1991) suggests that equilibrium xenoliths from the Kaapvaal Craton define a 44mW/m^2 paleogeotherm. P-T determinations on equilibrium assemblages from Somerset Island (this study) lead to a similar conclusion (a 44mW/m^2 paleogeotherm). The conclusions of Brey (1991) and this study also support the hypothesis of Carswell and Gibb (1987) and Carswell (1991), who stated that interpretation of an inflected geotherm resulted from the use of Finnerty and Boyd's (1987) preferred thermobarometers (T_{FB86} vs P_{MC74}).

Although it has been suggested that correlations exist between xenolith textural type and pressure-temperature of equilibration (e.g. Kaapvaal Craton; Boyd and Nixon, 1978: Somerset Island; Mitchell, 1987), results from this study do not support such a model. At Batty Bay, porphyroclastic mantle xenoliths span the range of pressures obtained, and correlation between xenolith type and equilibration P-T does not exist. Though the three highest (and five of the ten highest) pressure xenoliths in this study are porphyroclastic, preliminary results on other coarse-texture xenoliths indicate similar or higher pressure.

SUMMARY

The pressures and temperatures of equilibration of 21 lherzolite xenoliths from the Batty Bay kimberlite complex define a 44mW/m^2 steady-state shield paleogeotherm which is not inflected. Correlation is lacking between xenolith textural type and pressure and temperature of equilibration. The results of this study are consistent with the conclusions drawn by Brey (1991) regarding the Kaapvaal Craton. Three of twenty one xenoliths equilibrated in the diamond stability field. This is consistent with bulk sampling of kimberlite in the 1970's (Davies, 1975), which yielded 2 microdiamonds.

ACKNOWLEDGMENTS

We would like to thank the Polar Continental Shelf Project for helicopter and fixed wing support and accommodation at Resolute Bay. BAK also thanks T. Frisch of the Geological Survey of Canada for use of his base camp facilities at Fiona Lake and providing helicopter flying time which allowed the Peuyuk kimberlite to be sampled. John Stirling assisted with the electron microprobe. Contribution to the Canada-NWT Geoscience Initiative 1991-1996. Comments from T. Frisch and A.N. LeCheminant plus critical review by R.F. Emslie greatly improved the manuscript.

REFERENCES

Blackadar, R.G.
1967: Precambrian geology of Boothia Peninsula, Somerset Island, and Prince of Wales Island, District of Franklin; Geological Survey of Canada, Bulletin 151, 62p.

Boyd, F.R. and Nixon, P.H.
1978: Ultramafic nodules from the Kimberley pipes, South Africa; Geochimica et Cosmochimica Acta v. 42, p. 1367-1382.

Brey, G.P.
1991: Fictive conductive geotherms beneath the Kaapvaal Craton; Extended Abstracts, Fifth International Kimberlite Conference, Araxá, Brazil. CPRM Special Publication 2/91, Brasilia, p. 23-25.

Brey, G.P. and Köhler, T.
1990: Geothermobarometry in Four-phase Lherzolites II. New thermobarometers, and Practical Assessment of Existing Thermobarometers; Journal of Petrology v. 31. p. 1353-1378.

Brey, G.P., Köhler, T. and Nickel, K.G.
1990: Geothermobarometry in Four-phase Lherzolites I. Experimental results from 10 to 60 kb; Journal of Petrology v. 31, p. 1313-1352.

Brown, R.L., Dalziel, I.W.D., and Rust, B.
1969: The structure, metamorphism and development of the Boothia Arch, Arctic Canada; Canadian Journal of Earth Sciences v. 6, p. 525-534.

Carswell, D.A.
1991: The garnet-orthopyroxene Al barometer: problematic application to natural garnet lherzolite assemblages; Mineralogical Magazine v. 55, p. 19-31.

Carswell, D.A. and Gibb, F.G.F.
1987: Evaluation of mineral thermometers and barometers applicable to garnet lherzolite assemblages; Contributions to Mineralogy and Petrology v. 95, p. 473-487.

Davies, R.
1975: Unpublished Proprietary Assessment Report, Mining Claims Batty 1-31 and Bat 1-5, Somerset Island, District of Franklin, Northwest Territories. 21 p.

Dawson, J.B. and Stephens, W.E.
1975: Statistical classification of garnets from kimberlites and associated xenoliths; Journal of Geology v. 83, p. 589-607.

Finnerty, A.A. and Boyd, F.R.
1987: Thermobarometry for garnet peridotites: basis for the determination of thermal and compositional structure of the upper mantle; in Nixon, P.H. (ed.) Mantle Xenoliths, J. Wiley and Sons, Toronto, p. 381-402.

Gurney, J.J. and Harte, B.
1980: Chemical variations in upper mantle nodules from southern African kimberlites; Philosophical Transactions of the Royal Society London, v. 297A, p. 273-293.

Harte, B.
1977: Rock nomenclature with particular relation to deformation and recrystallization textures in olivine-bearing xenoliths; Journal of Geology v. 85, p. 279-288.

Heaman, L. H.
1989: The nature of the subcontinental mantle from Sr-Nd-Pb isotopic studies on kimberlitic perovskite; Earth and Planetary Science Letters v. 92, p. 323-334.

Jago, B.C. and Mitchell, R.H.
1987: Ultrabasic xenoliths from the Ham kimberlite, Somerset Island, Northwest Territories; Canadian Mineralogist v. 25, p. 515-525.

Kennedy, C.S. and Kennedy, G.C.
1976: The equilibrium boundary between graphite and diamond; Journal of Geophysical Research v. 81, p. 2467-2470.

Mitchell, R.H.
1975: Geology, Magnetic Expression, and Structural Control of the Central Somerset Island Kimberlites; Canadian Journal of Earth Sciences v. 12, p. 757-764.
1976: Kimberlites of Somerset Island, District of Franklin; Geological Survey of Canada Paper 76-1A, p. 501-502.
1977: Ultramafic xenoliths from the Elwin Bay kimberlite: the first Canadian paleogeotherm; Canadian Journal of Earth Sciences v. 14, p. 1202-1210.
1978: Garnet lherzolites from Somerset Island, Canada and aspects of the nature of perturbed geotherms; Contributions to Mineralogy and Petrology v. 67, p. 341-347.
1987: Mantle-derived xenoliths in Canada; in Nixon, P.H. (ed.) Mantle Xenoliths, J. Wiley and Sons, Toronto, p. 33-40.

Nixon, P.H. (ed.).
1987: Mantle Xenoliths; J. Wiley and Sons, Toronto, 843 p.

Smith, C.B., Allsopp, H.L., Garvie, O.G., Kramers, J.D., Jackson, P.F.S., and Clement, C.R.
1989: Note on the U-Pb perovskite method for dating kimberlites: Examples from the Wesselton and DeBeers mines, South Africa, and Somerset Island, Canada; Chemical Geology (Isotope Geoscience Section) v. 79, p. 137-145.

Stewart, W.D.
1987: Late Proterozoic to early Tertiary stratigraphy of Somerset Island and northern Boothia Peninsula, District of Franklin, N.W.T.; Geological Survey of Canada Paper 83-26. 78 p.

Evidence for ice margin retreat and proglacial lake (Agassiz ?) drainage by about 11 ka, Clearwater River spillway area, Saskatchewan

Thane W. Anderson and C.F. Michael Lewis[1]
Terrain Sciences Division

Anderson, T.W. and Lewis, C.F.M., 1992: Evidence for ice margin retreat and proglacial lake (Agassiz ?) drainage by about 11 ka, Clearwater River spillway area, Saskatchewan; in Current Research, Part B, Geological Survey of Canada, Paper 92-1B, p. 7-11.

Abstract

Plant detritus overlying glaciolacustrine clay in two lake basins in the Clearwater River spillway area, Saskatchewan, is radiocarbon dated at 10 600 ± 120 and 11 100 ± 150 BP. The radiocarbon dates, lithological changes, and carbon measurements from across the clay-organic sediment contact imply Laurentide ice retreat, and the presence and drainage of a proglacial lake in the lowland connecting to Clearwater Valley by about 11 ka BP. Further work is needed to validate the radiocarbon dates and to determine the relationship of the proglacial lake to glacial Lake Agassiz.

Résumé

On a daté des débris végétaux qui recouvrent une argile glaciolacustre, dans deux bassins lacustres de la région du chenal de sortie de la rivière Clearwater en Saskatchewan, de 10 600 ± 120 et de 11 100 ± 150 BP. Les dates obtenues avec la méthode du radiocarbone, les variations lithologiques et les mesures radiométriques effectuées sur le carbone recueilli en deçà du contact entre l'argile et le sédiment organique, indiquent un retrait des glaces laurentidiennes, ainsi que la présence et le drainage d'un lac proglaciaire dans les basses terres aboutissant à la vallée de la rivière Clearwater, dès 11 ka BP environ. Il est nécessaire de poursuivre les recherches pour valider les datations par le radiocarbone et pour déterminer le lien entre le lac proglaciaire et le lac glaciaire Agassiz.

[1] Atlantic Geoscience Centre, Dartmouth

INTRODUCTION

The idea that glacial Lake Agassiz extended to Clearwater River valley and flowed northward to the Arctic Ocean has long been debated (Elson, 1967, 1983; Christiansen, 1979; Schreiner, 1983; Smith, 1989). Indeed, isobases on Lake Agassiz (Teller and Thorleifson, 1983) suggest that a topographic lowland 20 to 30 m below the projected Agassiz water surface (Campbell level, here 440-450 m a.s.l.) could have connected the Agassiz basin with Clearwater Valley. However, the drainage of Lake Agassiz westward is thought to have been blocked by the presence of Laurentide ice based on the absence of glacial lake sediments west of longitude 106°W (Christiansen, 1979).

Recently the senior author visited the Clearwater River spillway area to clarify the history of deglaciation and glacial lake presence by collecting cores from lake basins adjacent to the spillway and from areas to the north and south of the spillway. This report documents the lithological changes and results from carbon analyses and preliminary radiocarbon dating of the basal sediments in two lake basins that are situated in the lowland. The sedimentological and chronological data are assessed in terms of providing new evidence with respect to deglaciation of the area bordering the spillway and possible northwestward extension of glacial Lake Agassiz to the Clearwater spillway area and subsequently to the Arctic Ocean.

A large inflow of meltwater into the Arctic Ocean may have induced sea ice outflow and climatic cooling in the North Atlantic Ocean, for example, the abrupt younger Dryas cooling of northwest Europe and eastern Canada between 11-10 ka (Mott et al., 1986; Harvey, 1989). It is important, for the understanding of rapid climate change, to confirm episodes of northward drainage of large glacial lakes such as glacial Lake Agassiz.

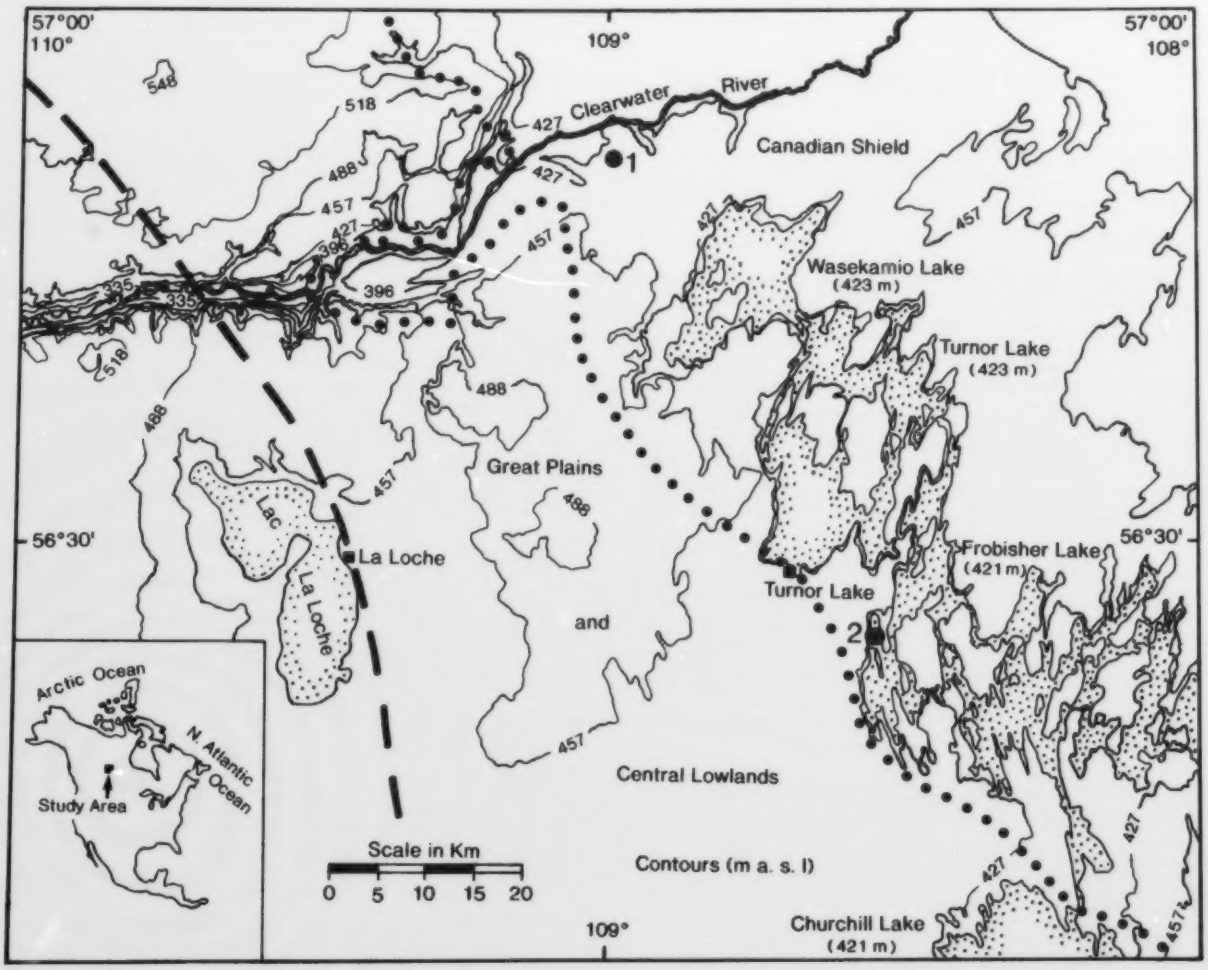

Figure 1. Location map. 1. Long Lake. 2. Nipawin Bay. The closely spaced contours (upper left) delineate the Clearwater spillway. The dotted line marks the southwest limit of Shield rocks. The position of the 11 000 BP ice margin shown by the dashed line is from Dyke and Prest (1987). Inset map shows location of study area.

GEOLOGICAL SETTING

The Saskatchewan part of the Clearwater River spillway crosses the contact between Precambrian rocks of the Canadian Shield and Paleozoic and Mesozoic rocks of the Great Plains and Central Lowlands (Fig. 1). The Shield rocks consist of granite, granodiorite, quartz monzonites, schists, and gneisses (Whitaker and Pearson, 1972). Rocks of the Great Plains and Central Lowlands comprise interbedded fine to coarse sand, silt, and clay of the Swan River-Manville Group (Whitaker and Pearson, 1972).

The study area lies well outside the maximum extent of glacial Lake Agassiz mapped by Teller et al. (1983) and slightly northeast of glacial Lake Meadow as delineated in Christiansen (1979). The study area also lies between the Late Wisconsinan ice retreat positions at 11 000 and 10 000 BP as presently understood (Dyke and Prest, 1987).

FIELD AND LABORATORY TECHNIQUES

Five sites were cored in 1988, two lake basins south of Clearwater River, two to the north of the river and an embayment off Nipawin Bay in Frobisher Lake. Results from two of the sites, Long Lake and Nipawin Bay (Fig. 1), are reported here.

Long Lake (56°51'40"N, 108°59'20"W) is situated about 50 km north northwest of La Loche, Saskatchewan, and about 4 km south of Clearwater River; it is accessible by a sideroad off Highway 955. The lake is on Shield rocks at an elevation of approximately 423 m a.s.l. (from topographic map 74C/15). Lake depth averaged about 1 m as determined by echosounding. Coring was carried out with a modified Livingstone piston sampler (using tubes of 5 and 7.5 cm diameter) from two aluminum boats bolted together in raft-like fashion. A 7.8 m core was recovered in 1.2 m water depth in a broad basin near the north end of the lake.

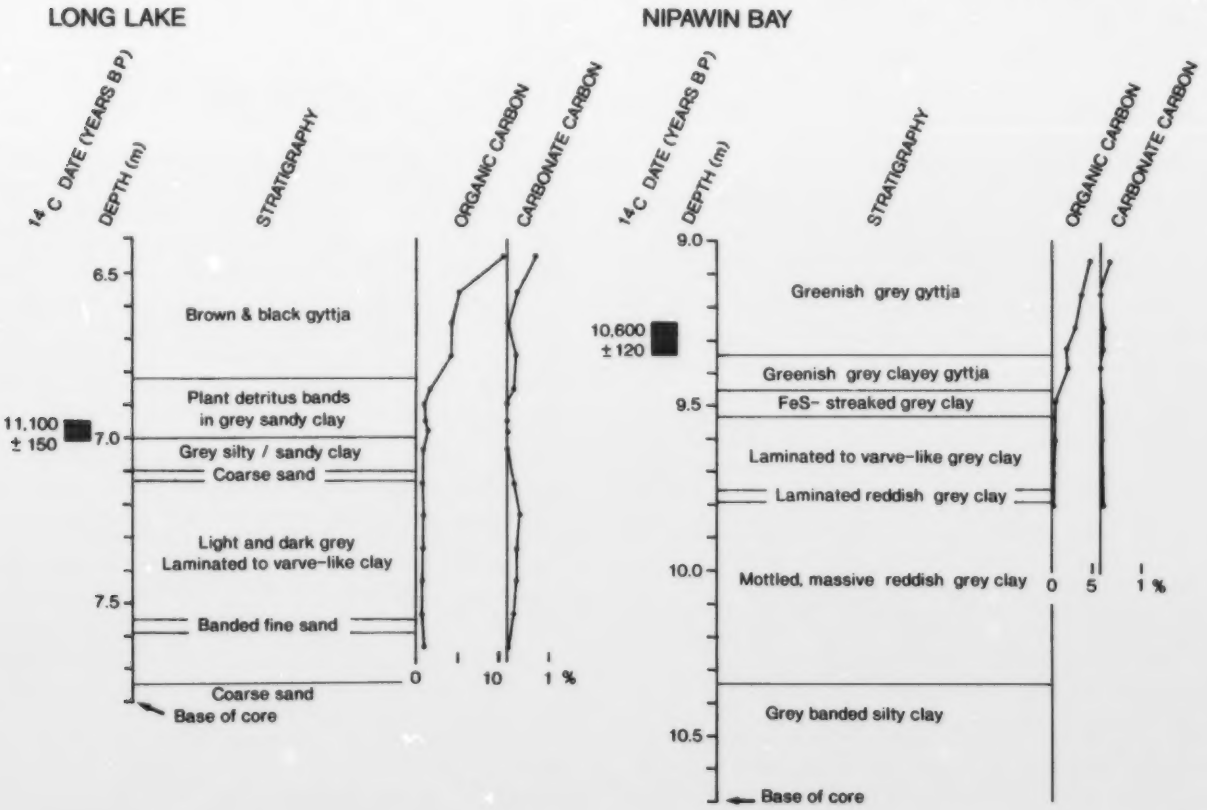

Figure 2. Stratigraphy, radiocarbon dates and carbon contents of the basal sediments at Long Lake and Nipawin Bay.

The Nipawin embayment site (56°24'28"N, 108°33'00"W) is located about 60 km southeast of Clearwater River and 12 km southeast of Turnor Lake, Saskatchewan, at the northeast terminus of Highway 909. The site lies on Shield rocks at an elevation of about 421 m a.s.l. (from topographic map 74C/7). Depth of water increased gradually southward from shore to 2.8 to 3.0 m in the centre of the embayment. A 10.7 m core of the bottom sediments was recovered here from aboard a local fisherman's boat.

The cores were extruded, described, and sampled for pollen study, carbon analysis, and radiocarbon dating. Pollen studies of the Long Lake core are part of a thesis study by C. McLeod (McMaster University) and will be reported at a later date. Total carbon contents of the basal inorganic/organic sediments were determined at approximately 10 cm intervals by the combustion of the sediment samples at 2500°C in a LECO induction furnace. The organic fraction was measured following HCl digestion; carbonate contents were calculated as differences between the foregoing. Radiocarbon dating was performed on bulk sediment at the organic/inorganic contact.

RESULTS

Sediment stratigraphy and chronology

Sediment changes in the two cores are illustrated in Figure 2. The Long Lake core bottomed in coarse sand which is overlain by firm light and dark grey varve-like, laminated clay (75 cm) interbedded in places with layers of fine to medium coarse sand. This is capped by successive layers of coarse sand (3 cm) and massive silty sandy clay (10 cm). Similar clay, highly charged with plant detritus, continues up another 18 cm to overall depth 6.82 m below the lakebed. The remainder of the core consists of organic lake sediment (gyttja). A radiocarbon date of 11 100 ± 150 BP (GSC-4807) (corrected for the sample $\delta^{13}C$ value of -23.5°/∞) was obtained on plant detritus at 6.95-7.01 m.

The basal sediments of the Nipawin embayment core consist of grey banded silty clay (35 cm) with occasional sand layers overlain by massive reddish grey clay (55 cm), in turn, succeeded by laminated reddish grey clay (5 cm) and laminated, varve-like grey clay (couplets of alternating light and dark grey) (30 cm). The overlying FeS-streaked clay and clayey gyttja units (19 cm) represent a gradational change upward to greenish grey gyttja at 9.34 m below the lakebed. The greenish grey gyttja changes at 8.9 m to brown gyttja which continues to the surface. A ^{14}C date of 10 600 ± 120 BP (GSC-4821) (corrected for the sample $\delta^{13}C$ value of -28.4°/∞) was obtained at the base (9.27-9.34 m) of the greenish grey gyttja.

Organic and carbonate carbon contents

The trends of organic carbon and carbonate carbon profiles for the two sites are illustrated in Figure 2. Organic carbon is low (less than 1%) in the basal inorganic sediments of Long Lake, increases to about 1.5% in the plant detritus-rich clay unit, and increases further across the clay-gyttja contact reaching values of about 10% maximum within the gyttja. Carbonate carbon is extremely low (less than 0.3%) or is absent in the basal inorganic clays and increases only slightly upwards (to 0.7%) in the gyttja.

The basal inorganic sediments of the Nipawin Bay core also contain less than 1% organic carbon. Values average about 2% at the transition to gyttja and increase gradually upward to about 5% within the gyttja. As in the Long Lake core, carbonate carbon is minimal (less than 0.1%) with only a slight increase (to over 0.2%) in the gyttja.

DISCUSSION

The sequences of laminated silty clay and interbedded massive clay and sand that characterize the basal sediments in Long Lake and Nipawin Bay imply deposition in a large proglacial lake in contact with the Laurentide ice. The gradational change from clay to organic lake sediment (gyttja) at Nipawin Bay suggests that, as the proglacial lake drained, the site changed gradually to the shallower and smaller basin of the present embayment with initiation of organic deposition. Sand at the top of the inorganic sequence of Long Lake, located in the constricted portion of the lowland connecting to the Clearwater valley, is probably a lag deposit that accumulated during the drawdown phase of the proglacial lake. The overlying detritus-rich clay is thought to be reworked glaciolacustrine clay that was washed into the basin prior to stabilization of the slopes by vegetation and onset of organic sedimentation in the lake.

Whether this proglacial lake was Lake Agassiz is uncertain at the present time. The presence of basal glaciolacustrine clay in both lake basins indicates inundation by possibly the same proglacial water body. The radiocarbon ages for the overlying organic sediments indicate that the Laurentide ice margin had retreated north of the lowland connecting to the Clearwater valley and the proglacial lake had drained by approximately 11 ka BP. Even though the minor traces (or absence) of carbonate carbon in the dated sediment intervals suggest hard-water error may not be a significant factor, the bulk sediment dates are viewed with caution on account of possible inherent reservoir and contamination effects (MacDonald et al., 1991).

Further studies are in progress and others are being planned to confirm the areal extent and age of the proglacial lake sediments. The reliability of the radiocarbon dates is being assessed through comparison with AMS dating of terrestrial plant macrofossil material in the cores and with the regional pollen stratigraphy. Additional lake sediment sampling between the study area and the assumed northwest limit of Lake Agassiz will help with asssessing the possible correlation of the observed glaciolacustrine sediments with those of glacial Lake Agassiz.

ACKNOWLEDGMENTS

The radiocarbon dates were made available by the Radiocarbon Dating Laboratory of the Geological Survey of Canada. The carbon analyses were determined in the

Sedimentology Laboratories also at the GSC. We thank B.R. Pelletier for his support of the pursuit of our ideas. R.J. Mott, L.H. Thorleifson, and R.N. McNeely offered helpful comments on the manuscript.

REFERENCES

Christiansen, E.A.
1979: The Wisconsinan deglaciation of southern Saskatchewan and adjacent areas; Canadian Journal of Earth Sciences, v. 16, p. 913-938.

Dyke, A.S. and Prest, V.K.
1987: Late Wisconsinan and Holocene history of the Laurentide ice sheet; Géographie physique et Quaternaire, v. 41, p. 237- 263.

Elson, J.A.
1967: Geology of Glacial Lake Agassiz; in Life, Land and Water, (ed.) W.J. Mayer-Oakes; Occasional Papers, Department of Anthropology, 1, University of Manitoba Press, p. 37-95.
1983: Lake Agassiz-discovery and a century of research; in Glacial Lake Agassiz, (ed.) J.T. Teller and L. Clayton; The Geological Association of Canada, Special Paper 26, p. 21- 41.

Harvey, L.D.D.
1989: Modelling the Younger Dryas; Quaternary Science Reviews, v. 8, p. 137-149.

MacDonald, G.M., Beukens, R.P., and Kieser, W.E.
1991: Radiocarbon dating of limnic sediments: a comparative analysis and discussion; Ecology, v. 72, p. 1150-1155.

Mott, R.J., Grant, D.R., Stea, R., and Occhietti, S.
1986: Late-glacial climatic oscillation in Atlantic Canada equivalent to the Allerød/younger Dryas event; Nature, v. 323, p. 247-250.

Schreiner, B.T.
1983: Lake Agassiz in Saskatchewan; in Glacial Lake Agassiz, (ed.) J.T. Teller and L. Clayton; The Geological Association of Canada, Special Paper 26, p. 75-96.

Smith, D.G.
1989: Catastrophic paleoflood from glacial Lake Agassiz 9,900 years ago in the Ft. McMurray region, northeast Alberta (abstract); in Program and Abstracts, Canadian Quaternary Association Biennial Meeting, August 26-27, Edmonton, Alberta, p. 47.

Teller, J.T. and Thorleifson, L.H.
1983: The Lake Agassiz-Lake Superior connection; in Glacial Lake Agassiz, (ed.) J.T. Teller and L. Clayton; The Geological Association of Canada, Special Paper 26, p. 261-290.

Teller, J.T., Thorleifson, L.H., Dredge, L.A., Hobbs, H.C., and Schreiner, B.T.
1983: Maximum extent and major features of Lake Agassiz; in Glacial Lake Agassiz, (ed.) J.T. Teller and L. Clayton; The Geological Association of Canada, Special Paper 26, p. 43-45.

Whitaker, S.H. and Pearson, D.E.
1972: Geological map of Saskatchewan; Province of Saskatchewan, Department of Mineral Resources, Geological Sciences Branch and Saskatchewan Research Council, Geology Division.

Geological Survey of Canada Project 910019

Données préliminaires sur la morphologie et dynamisme récent d'un système dunaire de haut de falaise dans la région de la rivière Mountain, District de Mackenzie, Territoires du Nord-Ouest

C. Bégin, Y. Michaud et S. Boucher[1]
Centre géoscientifique de Québec, Sainte-Foy

Bégin, C., Michaud, Y., et Boucher, S., 1992: Données préliminaires sur la morphologie et dynamisme récent d'un système dunaire de haut de falaise dans la région de la rivière Mountain, District de Mackenzie, Territoires du Nord-Ouest; dans Recherche en Cours, Partie B; Commission géologique du Canada, Étude 92-1B, p. 13-21.

Résumé

La dune de haut de falaise de la rivière Mountain représente un phénomène éolien assez répandu dans le nord-ouest canadien. Développée au sommet d'une terrasse fluvioglaciaire d'une hauteur de 85 m, la dune active est alimentée par les matériaux fins provenant de la falaise vive sous-jacente ainsi que par les sables déposés dans le lit de la rivière Mountain. La morphologie générale du système dunaire montre qu'il évolue rapidement vers une forme parabolique. Son activité actuelle affecte une surface de l'ordre de 11 300 m^2 et sa crête sommitale est d'une hauteur d'environ 20 m. La présence de plusieurs paléosols forestiers dans l'aire de déflation constitue le trait marquant de la dune et témoigne du caractère récurrent de son activité. L'analyse dendrochronologique des troncs fossiles associés au niveau organique supérieur met en évidence une avancée de la dune de près de 55 m au cours du dernier siècle. Enfin, il semble que la sédimentation nivéo-éolienne joue un rôle prépondérant dans le dynamisme actuel de la dune.

Abstract

Cliff-head dunes such as the one observed in the Mountain River area are widespread eolian features in northwestern Canada. Located atop an 85 m high glaciofluvial terrace, this sand dune is nourished in fine materials by the underlying glaciofluvial sediment and alluvium of the braided Mountain River. The general morphology of the dune shows that this feature is rapidly evolving toward a parabolic shape. It covers at present an area of about 11 300 m^2 while its crest stands about 20 m high. The presence of several paleosols in the deflation zone is the prominent feature of this dune. In fact, they indicate that eolian activity is a recurrent process at this locality. The dendrochronological analyses of fossil stumps associated with the organic horizon located in the upper portion of the deflation zone, show that the accumulation front has advanced about 55 m during the last 100 years. Finally, niveo-eolian activity seems to play an important role in the recent dynamics of this sand dune.

[1] Sciences de la Terre, UQAC, 555 boul. de l'Université, Chicoutimi, QC, G7H 2B1

INTRODUCTION

Bien que relativement importants dans certaines localités de par leur étendue et les marques qu'ils laissent dans le paysage, les systèmes dunaires de la vallée du fleuve Mackenzie demeurent, en somme, peu connus. On connaît les champs de dunes stabilisées de la région de Fort Simpson et de la rivière Trail grâce à la description générale qu'en a fournie David (1977). Dans le premier cas, la superficie des dépôts remaniés par le vent couvre 240 km^2; les formes résultantes sont des dunes de type parabolique ou transversale. Dans le second cas, la superficie du champ de dunes est d'environ 45 km^2 (David, 1977). Outre ces zones de dépôts éoliens localisées dans la partie sud de la vallée du fleuve Mackenzie, on retrouve un vaste champ de dunes stabilisées dans la partie nord-est de la péninsule de Tuktoyaktuk. Les sables, deltaïques surtout, ont été remaniés sous forme de dunes paraboliques. La surface éolisée avoisine les 500 km^2 (Michaud et Bégin, en prép.). Malgré le peu d'informations disponibles sur les conditions morphogénétiques et climatiques sous lesquelles ces grands champs de dunes se sont formés, il est généralement accepté qu'ils sont associés à des conditions périglaciaires au tardi-Wisconsinien (Niessen *et coll.*, 1984).

Ailleurs, le long de la vallée, les phénomènes éoliens apparaissent très marginaux. On les retrouve sous forme de petites dunes localisées au sommet des falaises de dépôts meubles associées à des vallées de cours d'eau ou à des milieux littoraux, lacustres ou marins. Ces dunes de haut de falaise ("cliff-top-dunes" ou "cliff-head-dunes") ont été signalées dans la région du delta du Mackenzie (Mackay, 1974; Rampton, 1988) mais également au Yukon (Nickling, 1978) et en Alaska (Kuhry-Helmens, *et coll.*, 1985). De tels phénomènes éoliens, si mineurs soient-ils sur le plan spatial, peuvent avoir un grand intérêt paléoécologique puisque, dans certains cas, il est possible d'en analyser le dynamisme grâce à la présence de paléosols forestiers dans les sables éoliens.

Dans le cadre du programme d'étude sur le changement à l'échelle planétaire initié à la Commission géologique du Canada, l'étude détaillée d'une de ces dunes de haut de falaise a été entreprise dans la région de la rivière Mountain. La présence de vestiges de forêts fossilisées dans la dune permet d'entrevoir une reconstitution fine du développement de la dune tout en la rattachant à un cadre climatique précis grâce à l'analyse dendrochronologique. Les résultats préliminaires concernant les aspects morphologiques ainsi que la dynamique récente de la dune de haut de falaise de la rivière Mountain sont présentés ici.

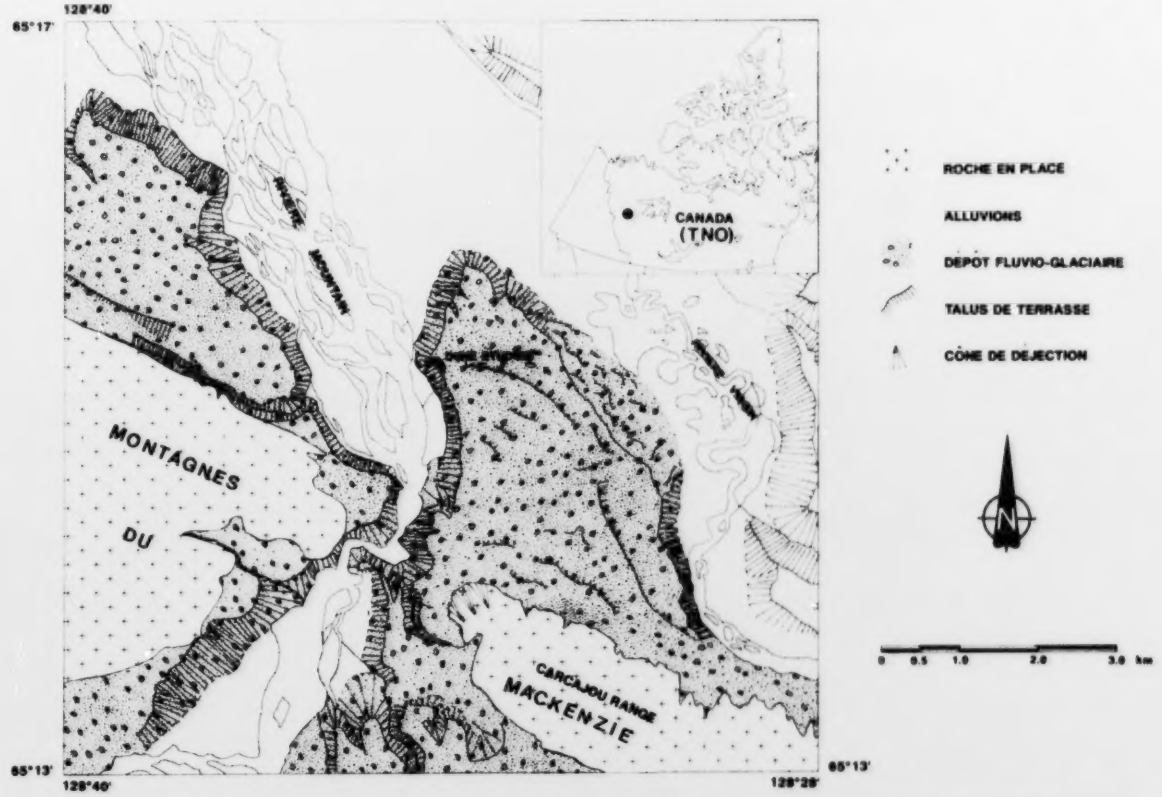

Figure 1. Localisation du site dunaire étudié. La dune s'est développée au sommet d'une terrasse fluvioglaciaire et fait face à la vallée de la rivière Mountain.

LA DUNE DE LA RIVIÈRE MOUNTAIN ET SON CONTEXTE RÉGIONAL

La dune étudiée (65° 14′ N, 128° 33′ W) est localisée à 80 km à l'ouest de Norman Wells dans les Territoires du Nord-Ouest. Elle est située directement au pied des monts Mackenzie, à la limite de la plaine du Mackenzie (fig. 1). Dans la région, les monts Mackenzie constituent l'unité physiographique dominante, en continuité avec les montagnes Rocheuses, et dont la marge est généralement orientée nord-ouest – sud-est. Cette formation de roches plissées d'âge protérozoïque et paléozoïque peut atteindre, dans le secteur immédiat, une altitude de 1300 m; mais généralement, leur altitude varie entre 800 et 900 m. La couverture sédimentaire quaternaire de la plaine du Mackenzie vient s'adosser aux monts Mackenzie. Dans la région d'étude, ces dépôt meubles surmontent une formation métasédimentaire constituée de schistes argileux peu déformés d'âge mésozoïque.

Cette situation de contact entre les montagnes et la plaine a rendu l'histoire glaciaire relativement complexe. Selon Duk-Rodkin et Hughes (1991) trois sources de glaciers sont à considérer: les grands glaciers originant des hautes chaînes des montagnes Blackbone, à la frontière du Yukon et des Territoires du Nord-Ouest, les glaciers de vallées mineurs originant des hauts sommets de la chaîne Canyon, et enfin, la calotte glaciaire Laurentidienne qui, au pléni-glaciaire, venait s'adosser au front des monts Mackenzie. Ces trois systèmes glaciaires ont laissé dans le paysage des indications géomorphologiques et stratigraphiques suffisamment claires pour en reconstituer les principaux mouvements (Duk-Rodkin et Hugues, 1991).

Figure 2. Vue aérienne de la dune et de son contexte régional. On aperçoit les deux principales sources de provenance des matériaux fins: la falaise vive directement sous la dune et la plaine alluviale.

La bordure de la chaîne Canyon aurait été une zone privilégiée pour l'évacuation vers le nord des eaux de fonte lors des périodes de retrait de la glace (Duk-Rodkin et Hugues, 1991). Les chenaux de fonte auraient alors laissé dans le secteur, sous forme de deltas au niveau des exutoires de vallées, d'épais dépôts fluvioglaciaires qui ont été entaillés par la suite en terrasses par les cours d'eau qui s'écoulent des montagnes vers la plaine du fleuve Mackenzie. La dune de sable étudiée est localisée sur le rebords supérieur d'une de ces terrasses fluvioglaciaires situées au pied des monts Mackenzie et dont l'altitude oscille autour de 360 et 460 m (fig. 2). L'aire de déflation de la dune fait face à la vallée de la rivière Mountain, à l'endroit où celle-ci dévale les monts Carcajou (voir fig. 1). La rivière s'écoule alors du sud-ouest vers le nord-est, suivant la structure des montagnes. Lorsqu'elle atteint les basses terres, elle vient se frapper contre la terrasse fluvioglaciaire où se situe la dune, puis bifurque vers le nord-ouest en chenaux anastomosés. L'abaissement du niveau de la rivière en période d'étiage met en disponibilité une quantité importante de sédiments fins susceptibles à l'emprise du vent. Au cours de l'été 1991, au moins deux tempêtes de poussière et de sables fins ont été observées.

La région étudiée est associée à la forêt boréale. Les terrasses ainsi que le fond des vallées sont colonisés par l'épinette blanche (*Picea glauca* (Moench) Voss) qui, souvent en association avec l'aulne gris (*Alnus incana* (L.) Moench), forme des pessières relativement fermées. Les zones où la sédimentation est active sont fréquemment colonisées par des populations clonales de peupliers baumier (*Populus balsamifera* L.)

La station météorologique la plus proche du site étudié est celle de Norman Wells où l'on y enregistre des données en continu depuis 1943. Ces données indiquent que le climat de la région est de type subarctique semi-humide avec une température moyenne annuelle de -6.1°C et des précipitations

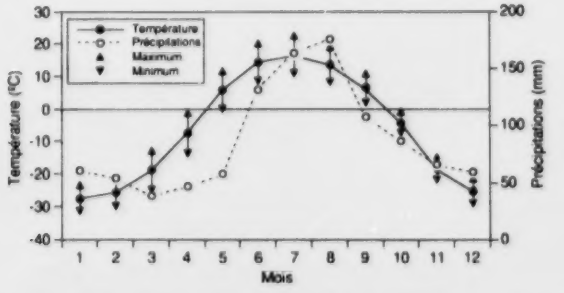

Figure 3. Données météorologiques de la station de Norman Wells pour la période de 1934 à 1989.

annuelles de l'ordre de 1010 mm (fig. 3). Les amplitudes thermiques annuelles sont très élevées. En janvier, on y observe des températures minimum de -43°C alors qu'en juillet la température peut atteindre des valeurs supérieures à 24°C.

MÉTHODES

L'étude de la dune de Mountain River a été initiée en 1990. Elle a été orientée de façon à fournir une vision la plus intégrée possible du dynamisme de la dune. Ainsi, l'échantillonnage de la dune comporte plusieurs aspects distincts.

Un quadrat de 25 200 m^2 (180 sur 140 m), divisé en 252 parcelles (10 sur 10 m) et défini par un dispositif de cordes, a été installé sur l'aire d'influence de la dune. La cartographie des principaux éléments morphologiques (falaises, micro-falaises, crêtes, etc.), écologiques (couvert végétal) et paléoécologiques (paléosols) a été effectuée. La topographie de la dune a été mesurée à l'aide d'un niveau-chaîne électronique GDD (précision de 0,01 m). Les levés ont été prises à tous les 10 m le long des lignes du quadrat orientées est-ouest et à tous les 5 m pour les lignes sud-nord. Les levées topographiques ont été ajustées par rapport au niveau zéro correspondant au sommet du dépôt fluvioglaciaire sous-jacent. La stratigraphie des dépôts éoliens dans la zone de déflation a été établie à l'intérieur de tranchées exercées au droit des coupes naturelles. On a effectué quatre forages dans la zone d'accumulation à l'aide d'une foreuse manuelle Sthil munie d'un carottier de type CRREL. Ces forages ont permis de vérifier la présence de dépôts nivéo-éoliens ainsi que la profondeur des lits de matière organique enfouis. Des câbles à senseurs thermiques reliés à un système d'enregistrement de données automatisé (R. Branker Research Ltd.) ont été installés dans deux des trous de forage.

Les arbres fossiles associés aux différents niveaux organiques dans la zone de déflation ont été cartographiés puis échantillonnés sous forme de sections transversales pour fin d'analyses dendrochronologiques. Les arbres morts et vivants de la zone d'accumulation ont été échantillonnés à l'aide d'une sonde de type Presler. Dans tous les cas, les échantillons ont été sablés puis poncés jusqu'à ce que les cellules du bois soient visibles à la loupe binoculaire (40X). La datation des tiges mortes a été effectuée selon les techniques standard d'«interdatation» ("cross dating" sensu Stokes et Smiley, 1968). La largeur des cernes annuels a été mesurée au laboratoire de dendrochronologie du Centre d'études nordiques (Université Laval) à l'aide d'un micromètre Henson (précision de 0,01 mm).

ASPECTS MORPHOLOGIQUES DE LA DUNE

Le système dunaire affecte une surface totale de 11 300 m^2. Malgré ses dimensions réduites, il comporte tous les éléments typiquement associés aux dunes paraboliques.

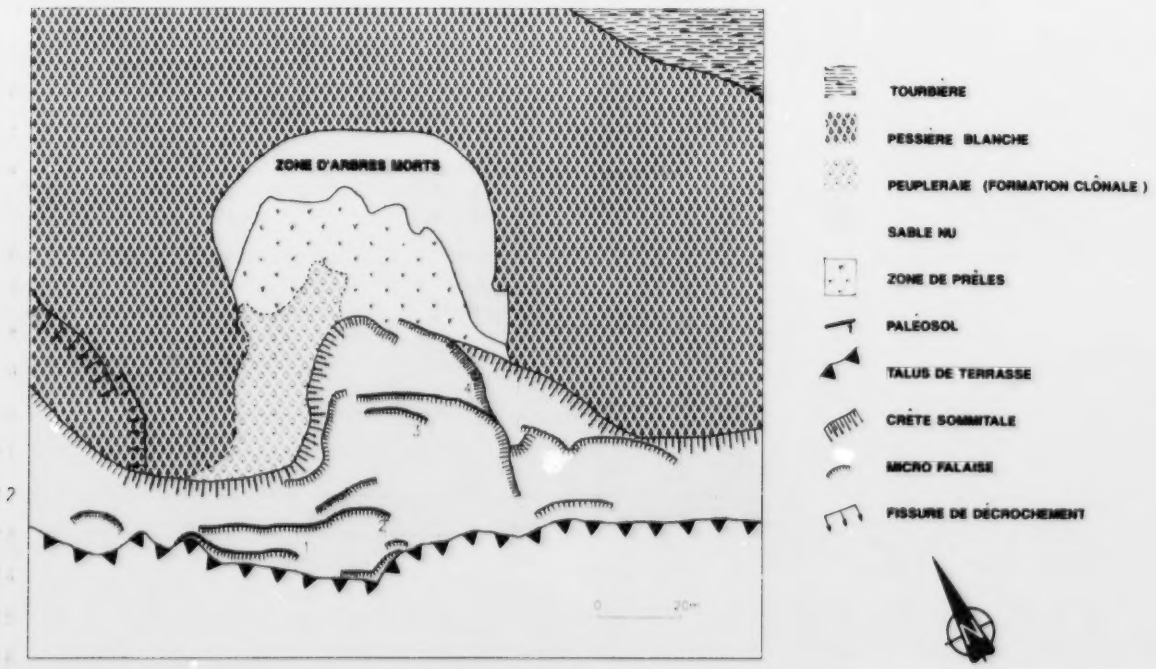

Figure 4. Cartographie des principaux éléments géomorphologiques et écologiques de la dune. L'aire de déflation s'étend du talus de la terrasse jusqu'à la crête sommitale alors que la zone d'accumulation s'étend jusque dans la pessière.

La dune est d'abord caractérisée par une aire de déflation composée d'une cuvette centrale et de deux extensions latérales qui se prolongent de part et d'autre en suivant le rebord de la terrasse (fig. 4). Au total, l'aire de déflation s'étend sur une largeur d'environ 230 m. La cuvette centrale, qui couvre une surface de 2800 m^2 (55 sur 50 m), est divisée en deux dépressions séparées par une crête médiane constituant un léger surplomb. Ces deux sous-cuvettes correspondraient à des systèmes de vent légèrement différents. Si l'on considère les prolongements latéraux de la cuvette principale, l'aire de déflation totale avoisine les 4800 m^2. Mais l'aire de déflation se caractérise surtout par la présence d'une multitude d'arbres morts qui jonchent l'ensemble de la surface d'érosion (fig. 5).

Figure 5. Vue générale de l'aire de déflation, du plancher de la cuvette vers la crête sommitale. On distingue quelques-uns des paléosols forestiers et la multitude d'arbres fossiles qui leur sont associés.

Ces arbres, qui attirent immédiatement le regard de l'observateur, sont en fait associés à des paléosols forestiers apparaissant à différents niveaux dans l'aire de déflation (fig. 6). Ces forêts enfouies, incluant litières et troncs d'arbres, constituent, sans aucun doute, le trait le plus marquant et le plus original de la dune de la rivière Mountain. Après avoir été successivement enfouies lors de périodes d'éolisation, ces forêts sont aujourd'hui remises à jour dans l'aire de déflation à la faveur de l'activité récente de la dune. Elles témoignent clairement du caractère récurrent de l'activité de la dune puisque chaque niveau organique correspond, *a priori*, à une phase de stabilisation de la dune. Au moins quatre niveaux organiques incluant des troncs d'arbres en position de vie sont facilement repérables. Ils sont situés respectivement à 4,5, 6,5, 14,5 et 15,5 m au-dessus du contact stratigraphique entre le matériel fluvioglaciaire et les sables éoliens (appellés ici, par convention, les niveaux forestiers n^{os} 1, 2, 3, et 4). Entre ce niveau de contact et le premier paléosol forestier situé à 4,5 m, on retrouve une séquence de lits organiques très compacts en alternance avec des niveaux de sables éoliens (fig. 6). Étant donné que le premier lit organique est situé à peine à 70 cm au-dessus des sédiments fluvioglaciaires, il est probable que l'on se trouve ici en présence de la séquence complète de l'activité éolienne du site depuis les premières phases d'éolisation qui ont suivi le retrait de la glace.

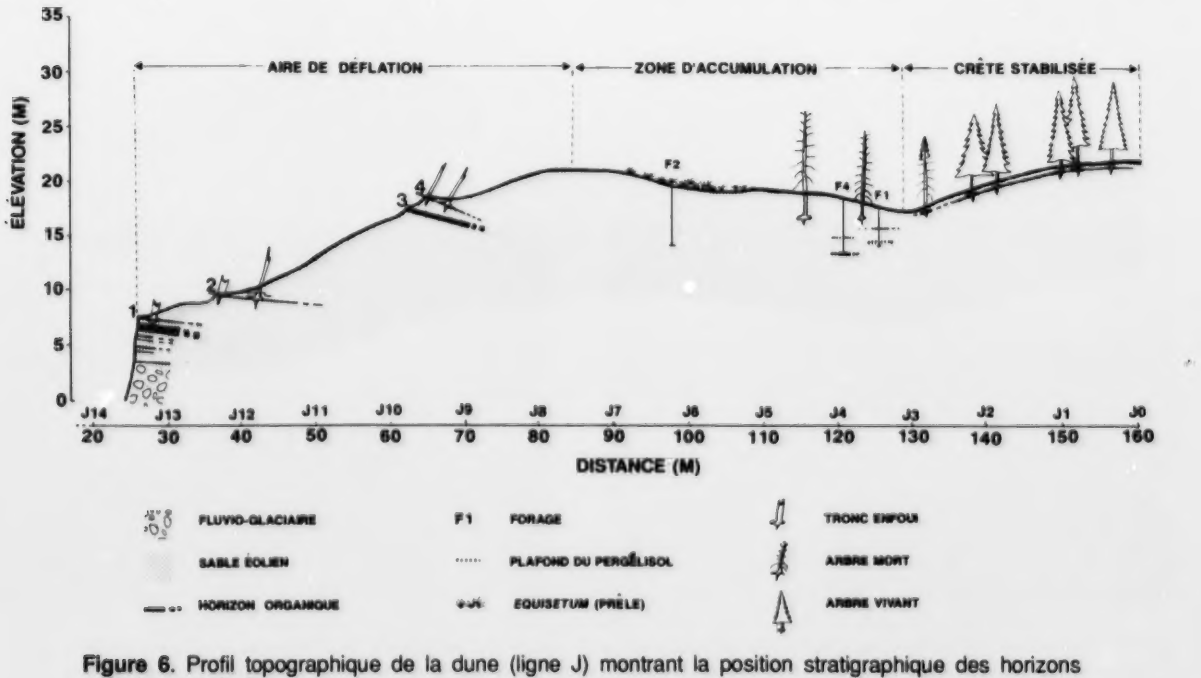

Figure 6. Profil topographique de la dune (ligne J) montrant la position stratigraphique des horizons organiques enfouis.

La présence de paléosols organiques, forestiers ou non, affecte fortement la topographie à l'intérieur de l'aire de déflation. Parce qu'ils constituent des niveaux plus résistants à l'érosion éolienne en raison de leur compaction et de leur capacité de rétention d'eau, les horizons organiques entraînent la formation de terrassettes délimitées par des micro-falaises (fig. 4). On retrouve une dizaine de ces terrassettes dans l'aire de déflation. Ces petites surfaces organiques qui affleurent contribuent également à la stabilisation du fond de la cuvette de déflation puisqu'elles constituent des milieux propices à l'installation d'une couverture muscinale et herbacée.

La limite entre l'aire de déflation et la zone d'accumulation est définie par une crête sommitale qui, à certains endroits, atteint une hauteur de 20 m par rapport au plancher de la cuvette de déflation. Dans la partie centrale de la dune, là où l'activité éolienne est maximale, la crête est défoncée et ouvre directement sur la zone d'accumulation. Les extensions latérales de la crête sont colonisées, soit par l'épinette blanche (côté sud), soit par une population clonale de peupliers baumier (côté nord). La zone d'accumulation actuelle se situe dans l'axe de la cuvette centrale de l'aire de déflation et est clairement délimitée par un front d'avancée très actif qui progresse dans la forêt selon une direction nord-nord-est (fig. 4). La surface affectée par la sédimentation actuelle est de l'ordre de 3200 m^2. La pente générale de la zone d'accumulation est de 6° dans sa partie frontale (ligne J, fig. 4) alors qu'elle peut atteindre 26° dans ses parties latérales (ligne 6, fig. 4).

Le dynamisme actuel de la sédimentation est illustré par une zonation d'entités végétales depuis la crête sommitale de la dune jusqu'au front d'accumulation (fig. 7). Le revers de la crête sommitale (côté nord) est colonisé par une population clonale de peupliers baumier qui tend à progresser vers la partie centrale de la zone d'accumulation. Cette partie centrale est caractérisée par la présence de prêles (*Equisetum pratense* Ehrh) qui, à certains endroits, forment une couverture presque continue. La zone qui suit, délimitée d'un côté par les prêles et de l'autre par la forêt actuelle, correspond à la partie la plus active de la zone d'accumulation. Le sable y est à nu et la densité d'arbres morts est comparable à celle que l'on retrouve en forêt. C'est à cet endroit que l'accumulation de sable est la plus forte (fig. 8). La pessière blanche située au-delà de la zone d'accumulation, semble s'être développée sur un ancien cordon dunaire qui, aujourd'hui, est complètement stabilisé. Plusieurs formes d'accumulation et de dénivation y sont encore visibles.

Une tranchée effectuée dans la zone d'accumulation (quadrat J-4) au mois d'août 1990 a révélé la présence d'un dépôt de neige enfoui sous 75 cm de sable. Le dépôt nival avait une épaisseur de 55 cm et était constitué d'une succession de lits de neige pure et de lits de neige interstratifiés avec du sable. Cette neige enfouie dans les sables éoliens indique l'importance de la sédimentation nivéo-éolienne dans un tel milieu. Les phénomènes de dénivation étaient d'ailleurs omniprésents dans la zone d'accumulation. On y retrouvait des placages de sable sur les branches et le tronc des arbres, des bourrelets circulaires à la base des troncs et des fissures d'effondrement le long du front d'accumulation (fig. 8). Les forages effectués à l'été 1991 ont démontré que cette neige n'est pas permanente puisqu'elle était absente des quatre carottes de sol prélevées dont la longueur variait de 3,5 à 5,5 m. Les conditions climatiques au cours de la saison estivale joueraient un rôle important dans la conservation de la neige enfouie (Koster et Dijkmans, 1988). Des été chauds et humides, par exemple, pourraient accélérer la fonte du dépôt nival. L'importance des processus nivéo-éoliens dans le développement des dunes en régions froides est de plus en plus considérée par plusieurs chercheurs. Bélanger et Filion (1991) rapportent qu'au Québec subarctique la sédimentation nivéo-éolienne peut représenter jusqu'à 75 % de l'accumulation annuelle dans les milieux à découvert. Les auteurs soulignent que les lentilles de neige peuvent persister durant plus de deux ans dans les dépôts éoliens. En Alaska, Koster et Dijkmans (1988) ont décrit en détail les formes associées à la sédimentation nivéo-éolienne. Celle-ci serait de nature annuelle dans la mesure où toutes les lentilles de neige disparaissent au cours de l'été.

Figure 7. Vue générale (vers le nord) de la zone d'accumulation avec la partie colonisée par les prêles (avant-plan) et la pessière à demi ensevelie.

Figure 8. Limite du front d'accumulation progressant dans la forêt. Les phénomènes reliés à l'accumulation et à la dénivation y sont très nombreux.

En plus de vérifier la présence de lits de neige, les forages effectués dans la zone d'accumulation ont permis de situer la profondeur du front de dégel ainsi que la position des différents horizons organiques enfouis. Ces éléments importants au niveau de la compréhension du dynamisme de la dune sont représentés à la figure 6.

Enfin, les analyses granulométriques d'une vingtaine d'échantillons, provenant de différents niveaux dans l'aire de déflation ainsi que de la zone d'accumulation de la dune, montrent qu'il s'agit de sables fins très bien triés dont la taille moyenne est de 0,2 ± 0,06 mm.

DYNAMISME RÉCENT

La présence de paléosols organiques, répartis stratigraphiquement depuis le contact avec le fluvioglaciaire jusqu'au sommet de la dune, montre que l'activité de cette dernière n'a pas été constante depuis les toutes premières phases d'éolisation. La datation des paléosols au carbone radioactif permettra de reconstituer la dynamique de la dune en situant dans le temps les périodes d'activité et de stabilisation. De plus, l'analyse des macrofossiles provenant des mêmes horizons organiques enfouis devrait permettre d'évaluer les contextes écologiques sous lesquels se seraient produites les périodes de stabilisation.

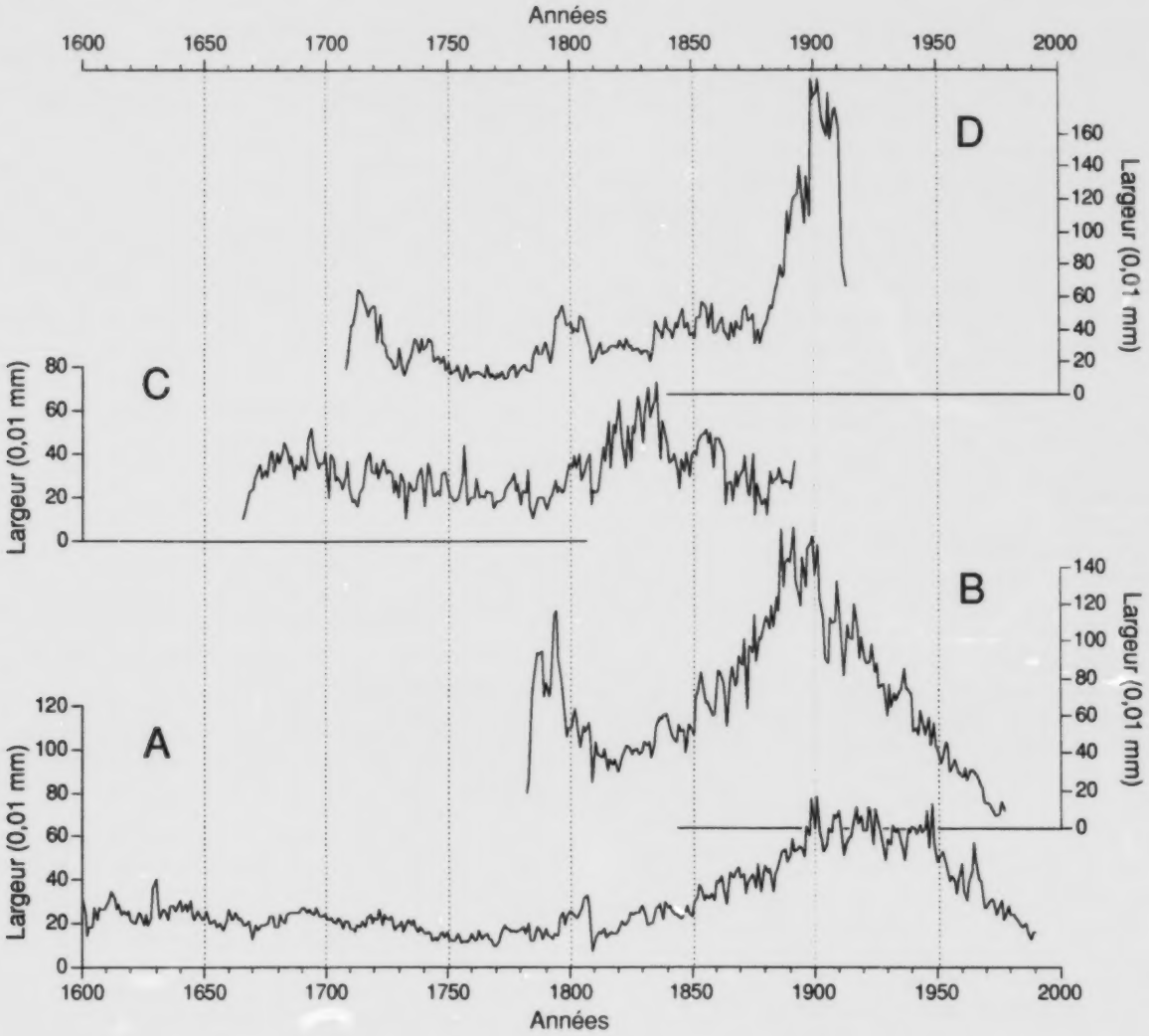

Figure 9. Recoupement dendrochronologique entre deux arbres fossiles (C et D) appartenant au niveau forestier n° 4, un arbre mort (B) situé à la limite externe du front d'accumulation et une courbe de croissance moyenne (A) établie à partir d'individus vivants situés au-delà du front de la dune.

D'autre part, les troncs d'arbres fossiles associés aux quatre horizons organiques supérieurs indiquent que la dune a été colonisée par des milieux forestiers lors des quatre plus récentes phases de stabilisation. Ils indiquent, par le fait même, que les reprises d'éolisation se sont effectuées au dépend de ces milieux forestiers. Cette situation n'est pas différente de celle que l'on connaît aujourd'hui puisque le front d'accumulation actuel progresse dans une formation conifériennne dense. L'analyse dendrochronologique du matériel ligneux fossilisé (dans l'aire de déflation) et en voie d'enfouissement (dans la zone d'accumulation), permet de cerner précisément la dynamique récente de la dune. Cette analyse comporte quatre aspects distincts: la datation des arbres fossiles associés aux paléosols forestiers dans l'aire de déflation, la datation des arbres morts dans la zone d'accumulation en fonction de leur position par rapport au front, et l'analyse des patrons de croissance radiale des arbres vivants et moribonds situés à la limite du front d'accumulation. Dans les deux premiers cas, la datation s'effectue à l'aide des techniques standard d'interdatation et de certains cernes diagnostiques (p. ex. cernes pâles); elle inclut les années d'apparition, les années de mortalité ainsi que les périodes de chute de croissance. Enfin, l'analyse dendrochronologique, par le biais des caractéristiques des cernes de croissance (largeur et densité), permet de rattacher les périodes d'activité et de stabilisation à des contextes climatiques précis.

La figure 9 présente, à titre d'exemple, le recoupement dendrochronologique effectué entre deux arbres fossiles (C et D) appartenant au niveau organique supérieur dans l'aire de déflation (niveau forestier n^{o} 4), un arbre mort (B) situé à la limite externe du front d'accumulation et une courbe de croissance moyenne (A) établie à partir d'une dizaine d'individus vivants. Ces derniers sont tous situés à l'extérieur de la zone d'accumulation; ils ne sont pas pour autant indépendants de l'activité de la dune dans la mesure où la forêt située au front de la dune est périodiquement affectée par un saupoudrage de sable. La chute de croissance qui caractérise les quarante dernières années de la courbe de croissance moyenne reflète, *a priori*, cet ensablement lent mais constant.

Le recoupement dendrochronologique montre que les arbres appartenant au niveau forestier n^{o} 4 sont morts à la charnière du XIX^{e} et du XX^{e} siècle, soit entre 1890 et 1915. Cet étalement dans les dates de mortalité est relié à la position relative des individus par rapport au front d'avancée de la dune, à la vitesse d'ensablement, mais également à l'état physiologique des arbres au moment de l'ensablement. Ainsi, certains arbres résisteront plus longtemps à l'ensablement en développant des racines adventives. Généralement, l'apparition de telles racines indiquerait un taux d'ensablement relativement lent (Filion et Marin, 1988) alors qu'un fort taux d'accumulation pourrait entraîner le dépérissement de l'arbre sans que celui-ci ait l'occasion de s'adapter en formant des racines adventives.

Les courbes de croissance individuelles C et D (fig. 9) montrent que la surface de la dune était colonisée par des arbres depuis au moins 1666 et que les conditions sont demeurées favorables au maintien d'un milieu forestier au cours des 250 années qui ont suivi. Il est difficile de dater précisément l'arrivée du front de la dune au niveau des arbres C et D puisque, de toute évidence, ces deux arbres n'ont pas réagi de la même façon à l'ensablement. Dans un cas (C), la dernière portion de la courbe est caractérisée par une diminution graduelle de la croissance qui s'échelonne sur une période d'environ 60 ans alors que dans le cas de la courbe D, la chute de croissance a été très rapide (3 années) et a été précédée par une augmentation significative de la croissance radiale. Des observations préliminaires sur la morphologie des épinettes fossiles portent les auteurs à croire qu'un tel patron de croissance (D) est typique des arbres ayant développé des racines adventives, l'augmentation de croissance étant justement reliée à l'apparition de ces racines. L'analyse des patrons de croissance des arbres situés à la limite du front d'accumulation actuel et dont la mort est récente (B) renforce cette hypothèse. Ces arbres, dont le tronc est enseveli sur une hauteur de deux à trois mètres, sont dépourvus de racines adventives et accusent une chute de croissance radiale qui peut s'étendre sur une période de 80 ans.

À partir des périodes de chute de croissance ainsi établies, on peut donc situer le début de l'ensablement des arbres C et D (niveau forestier n^{o} 4) vers 1840 alors que dans le cas de l'individu B l'ensablement aurait commencé vers 1905 et aurait finalement entraîné sa mort en 1977. Étant donné que les arbres qui affleurent au niveau forestier n^{o} 4 sont situés à 55 m du front d'accumulation actuel (arbre B), on peut estimer la vitesse d'avancée de la dune à près d'un mètre (0,85 m) par année.

Les observations effectuées au cours des étés 1990 et 1991 confirment le caractère très actif de la dune. Une sédimentation de 50 cm de sable a été mesurée entre les deux saisons et ce, à différents endroits dans la zone d'accumulation. Des valeurs du même ordre ont été mesurées au niveau de l'abaissement de la surface de l'aire de déflation. Ces mesures ont été effectuées à partir des arbres fossiles échantillonnés en 1990 au niveau du sol et qui ont été déchaussés au cours de l'année qui a suivi.

CONCLUSIONS

Malgré ses dimensions réduites, la dune de la rivière Mountain est d'un grand intérêt d'un point de vue géomorphologique, paléoécologique et paléoclimatique. Grâce à la présence de paléosols organiques et d'arbres fossiles dans l'aire de déflation, il apparait possible de reconstituer fidèlement la dynamique ancienne et récente du système dunaire en l'associant à différents contextes écologiques. Les résultats préliminaires ont montré que la dune est actuellement des plus actives. Comme cela déjà a été le cas à au moins quatre reprises dans le passé, le développement actuel de la dune se fait au dépend d'un milieu forestier accusant une vitesse de progression qui, depuis un siècle, est de l'ordre de 0,85 m par année. L'abondance des phénomènes nivéo-éoliens porte à croire que l'essentiel de la sédimentation s'effectue au cours de l'hiver.

REMERCIEMENTS

Les auteurs aimeraient remercier Ann Delwaide qui a effectué les analyses dendrochronologiques au laboratoire de dendrochronologie du Centre d'études nordiques (Université Laval) et Andrée Bolduc (Centre géoscientifique de Québec) pour ses commentaires lors de la lecture du manuscrit.

RÉFÉRENCES

Bélanger, S. et Filion, L.
1991: Niveo-aeolian sand deposition in subarctic dunes, eastern coast of Hudson Bay, Québec, Canada; Journal of Quaternary Science, v. 6, p. 27-37.

David, P.P.
1977: Sand dune occurrences in Canada. A theme and resource inventory study of aeolian landforms in Canada; Report Indian and Northern Affairs, National Parks Branch, Ottawa, 1-183.

Duk-Rodkin, A. et Hugues, O.L.
1991: Age relationships of Laurentide and montane glaciations, Mackenzie Mountains, Northwest Territories; Géographie Physique et Quaternaire, v. 45, p. 79-90.

Filion, L. et Marin, P.
1988: Modifications morphologiques de l'Épinette blanche soumise à la sédimentation éolienne en milieu dunaire, Québec subarctique; Canadian Journal of Botany, v. 66, p. 1862-1869.

Koster, E.A. et Dijkmans, J.W.A.
1988: Niveo-aeolian deposits and denivation forms, with special reference to the Great Kobuk sand dunes, Northwestern Alaska; Earth Surface Processes and Landforms, v. 13, p. 153-170.

Kuhry-Helmens, K.F., Koster, E.A., et Galloway, J.P.
1985: Photo-interpretation map of surficial deposits and landforms of the Kobuk Sand Dunes and part of the Kobuk Lowland, Alaska; U.S. Geol. Surv. Open-File Report, 85-242.

Mackay, J.R.
1974: Mackenzie Delta area, Northwest Territories; Geological Survey of Canada; Miscellaneous Report, no 23, 202 p.

Nickling, W.G.
1978: Eolian sediment transport during dust storms: Slims River Valley, Yukon Territories; Canadian Journal of Earth Sciences, v. 15, p. 1069-1084.

Niessen, A.C.H.M., Koster, E.A., et Galloway, J.P.
1984: Periglacial sand dunes and eolian sand sheets. An annotated bibliography; U.S. Geol. Surv. Open-File Report, 84-167.

Rampton, V.N.
1988: Quaternary geology of the Tuktoyaktuk coastlands, Northwest Territories; Geological Survey of Canada, Memoir 423, 98 p.

Stokes, M.A. et Smiley, T.L.
1968: An introduction to tree ring dating; University of Chicago Press, Chicago, 73 p.

Commission géologique du Canada projet 900009

Shallow seismic and magnetic data from northernmost Baffin Bay: insights into geology

H. Ruth Jackson, Bosko D. Loncarevic, and Weston Blake, Jr.[1]
Atlantic Geoscience Centre, Dartmouth

Jackson, H.R., Loncarevic, B.D. and Blake, W., Jr., 1992: Shallow seismic and magnetic data from northernmost Baffin Bay: insights into geology; in Current Research, Part B; Geological Survey of Canada, Paper 92-1B, p. 23-29.

Abstract

Four discrete seismic units are recognized on the basis of penetration, folding and stratification. Correlation of these units with the onshore geology is supported by the interpretation of the magnetic profiles. In Smith Sound, a narrow portion of Nares Strait, the Precambrian Shield and the Proterozoic Thule Group can be traced 11 km offshore. A shallow sedimentary basin south of the contact has dipping layers younger than the Proterozoic strata.

Résumé

On a identifié quatre unités sismiques discrètes en fonction de leur pénétration, plissement et stratification. La corrélation de ces unités avec la géologie du littoral est confirmée par l'interprétation des profils magnétiques. Dans le détroit de Smith, étroite portion du détroit de Nares, le Bouclier précambrien et le groupe de Thule d'âge protérozoïque peuvent être suivis au large jusqu'à 11 km de distance. Un bassin sédimentaire peu profond, au sud du contact, présente des couches inclinées plus jeunes que les strates du Protérozoïque.

[1] Terrain Sciences Division

INTRODUCTION

Five integrated geophysical and geological programs were carried out on the multidisciplinary C.S.S. Hudson cruise 91-39 to northernmost Baffin Bay: shallow seismic reflection, deep seismic refraction, magnetic and gravity measurements, and seafloor sampling. The expedition left Dartmouth, Nova Scotia on August 15, visited Thule, Greenland on September 3-5, and terminated in Goose Bay, Labrador on September 20, 1991. Only a small portion of the data gathered are discussed in this paper.

The geographical locations of the surveys in Smith Sound and northernmost Baffin Bay are shown in Figure 1. The new offshore geophysical data, available industry multichannel seismic data and the onshore geology have been considered together. These data sets shed new information on the seabed geology of the region.

METHODS

The position of the magnetic profiles collected in Smith Sound and northernmost Baffin Bay is plotted in Figure 1. A Varian V-75 magnetometer was used to acquire the magnetic data. The magnetic profiles displayed later in the paper have the IGRF 85 (International Geomagnetic Reference Field) removed.

The location of the seismic reflection profiles obtained with the 655 cm^3 Texas Instruments Sleeve Gun and the Nova Scotia Research Foundation and Seismic Engineering hydrophones is presented in Figure 2. Clear definition of the subsurface to a maximum depth of four tenths of a second was achieved. Positioning for the cruise was provided by BIONAV, the Bedford Institute integrated navigational system which received its principal input from the Global Positioning System. The fix accuracy was 50 m or better.

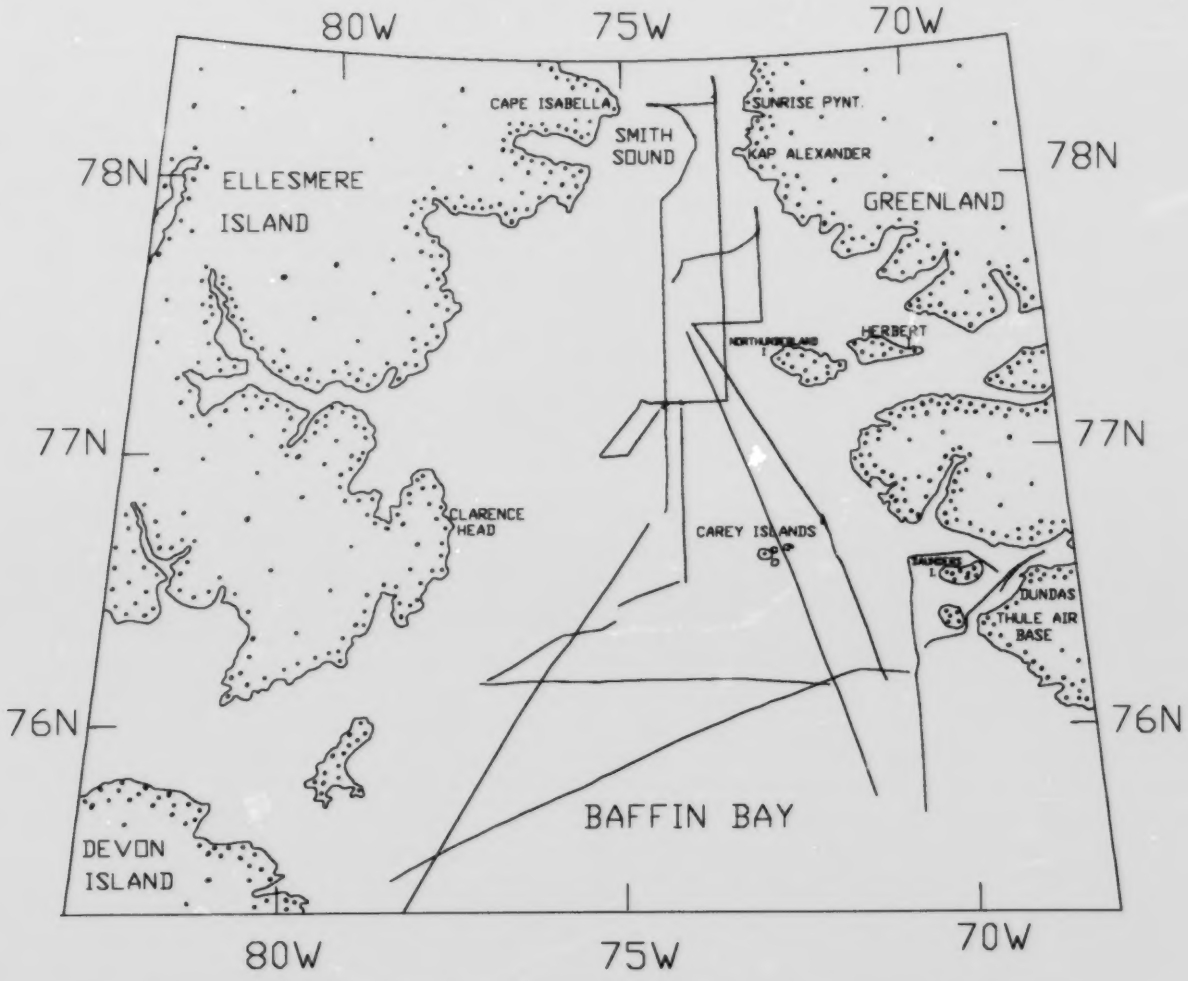

Figure 1. Location chart showing the position of the magnetic profiles discussed in the paper.

GEOLOGY

The regional onshore geology bordering northernmost Baffin Bay and Smith Sound (Fig. 2) is dominated by Archean and Proterozoic crystalline rocks of the Precambrian Shield and the unmetamorphosed strata of the Proterozoic Thule Group. The crystalline basement rocks consist primarily of gneiss, schist and granite (Escher and Watts, 1976; Frisch and Dawes, 1982). Various types of basic and ultrabasic rocks which could be the source of magnetic anomalies occur within the gneisses. The high-grade gneisses and meta-igneous rocks of the Shield are unlikely to be penetrated by energy from the seismic source.

The Proterozoic Thule Group, which consists of sedimentary and igneous rocks, provides a seismic target with the possibility of internal reflections. The Thule Group strata are in flat-lying to gently dipping homoclinal sections; in some places, broad flexures and folds due to faulting occur (Dawes et al., 1982a). On Greenland the prominent orientation of faulting in the Thule Group and of dyke swarms within it is WNW (Dawes et al., 1982b). On Ellesmere Island diabase dykes do not show any major preferred orientation and predate the deposition of Paleozoic strata (Frisch, 1988).

The north-south extent of the outcrop of the Thule Group has been carefully documented because of the controversy regarding the origin of Nares Strait (Dawes and Kerr, 1982). The contact of the Precambrian Shield rocks with the Thule Group unmetamorphosed strata is a major fault immediately to the north of Kap Alexander. Its position is at about 78°15′N (Dawes et al., 1982a). Precambrian Shield is exposed to the north and the sedimentary rocks are downfaulted to the south. On Ellesmere Island there is no Thule Group exposure known north of 78°32′N. The southern limit is between 76°48′N and 75°N (Frisch and Christie, 1982).

The Carey Islands, Northumberland Island and Saunders Island (Fig. 1) are of particular relevance to this paper because of their proximity to our geophysical data. The bedrock of the

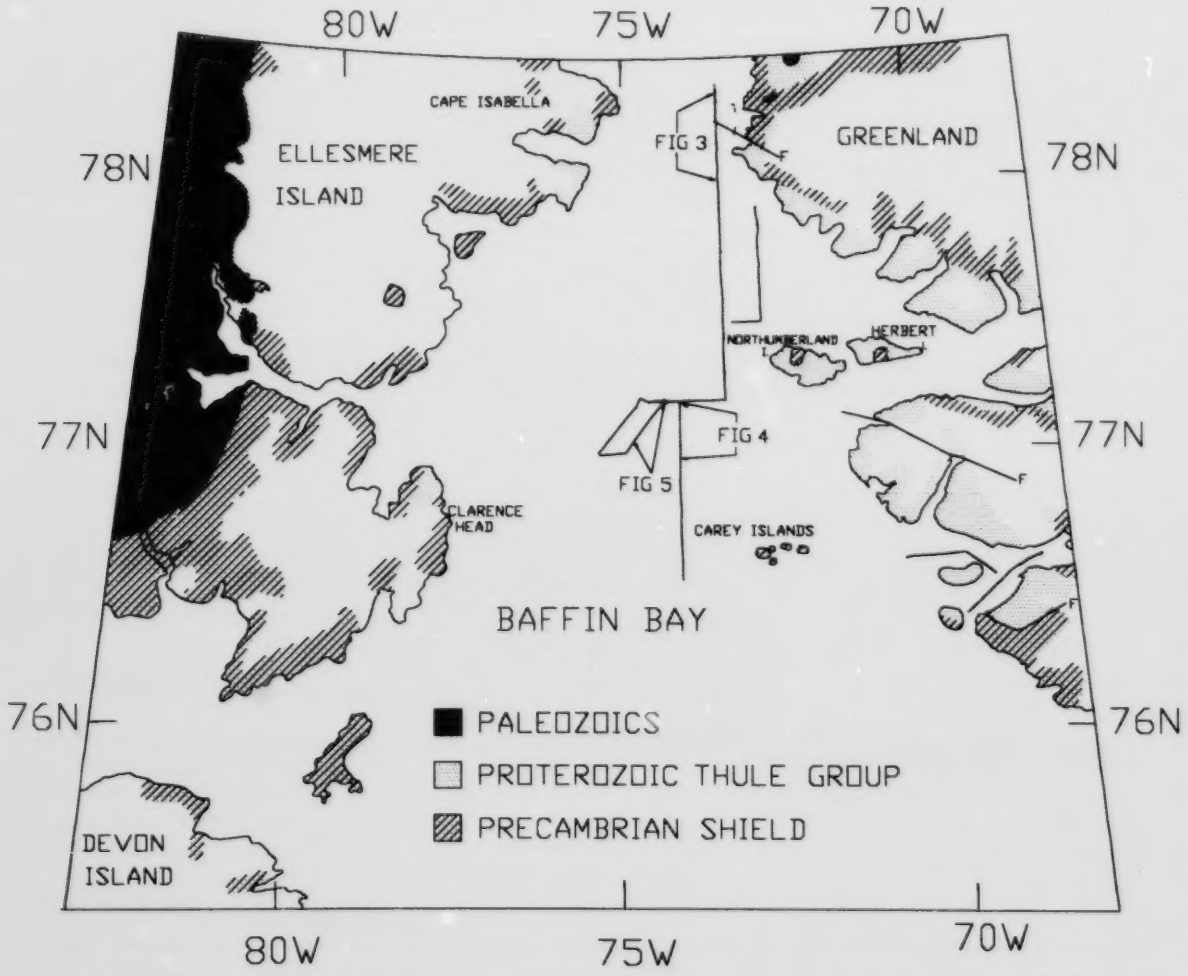

Figure 2. Map showing geology onshore and seismic tracks offshore. The "F" adjacent to solid lines indicates faults mapped onshore and their offshore extensions.

Carey Islands is composed of rocks of the Precambrian Shield intruded by dolerite dykes and sills. No sedimentary rocks have been mapped (Bendix-Almgreen et al., 1967). Northumberland and Herbert Islands contain the thickest and most complete sequences of lower Thule Group. Basic sills, lavas and tuffs are interbedded in the sedimentary sequences (Dawes et al., 1982a). On Saunders Island the upper Thule Group also contains dykes and sills (Dawes et al., 1973).

SEISMIC REFLECTION PROFILES

Four distinct types of seismic reflector were observed, each having a different seabed morphological expression. On the northernmost of the seismic lines in Smith Sound, north of Kap Alexander, there is a rough bottom with no seismic penetration. This is designated as reflection unit 1 (Fig. 3). This unit is interpreted as Precambrian Shield on the basis of its seismic properties and its position relative to the onshore geology (Fig. 2).

There is an abrupt change in the seismic profile just to the north of Kap Alexander. The seabed bathymetry south of the contact is comparatively smooth, and dipping homoclinal reflectors are observed in the subbottom (Fig. 3). About .1 sec of seismic penetration is achieved in these rocks which are labelled unit 2. Evidence of faulting with related folding is observed. Lateral variation occurs within this unit, and there are sections where the dipping reflectors are less well defined. Based on its location relative to the onshore geology and its physical traits, this unit is inferred to represent strata of the Proterozoic Thule Group.

In the third unit the maximum depth of penetration was achieved. Strong internal reflectors ranging in aspect from gently dipping with broad folds to steeply dipping and

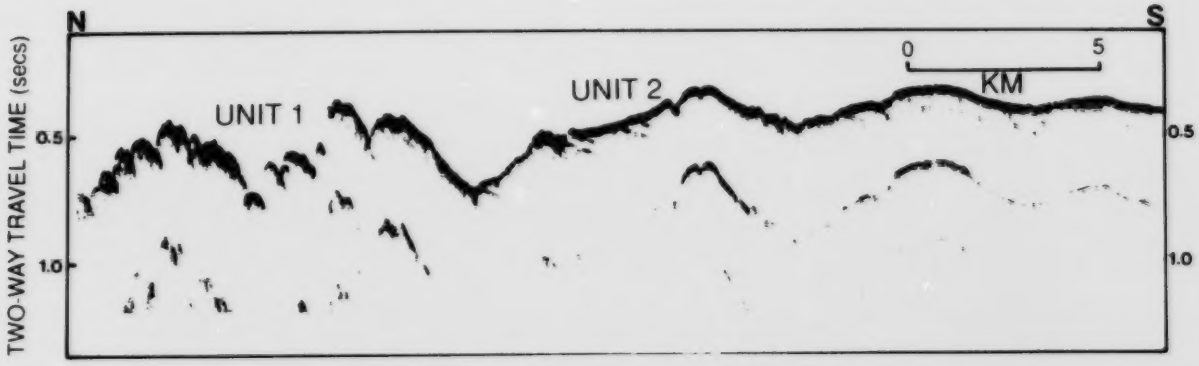

Figure 3. Seismic section showing unit one, inferred to be crystalline shield, adjacent to unit two, presumed Thule Group. The location of the seismic section is shown in Figure 2.

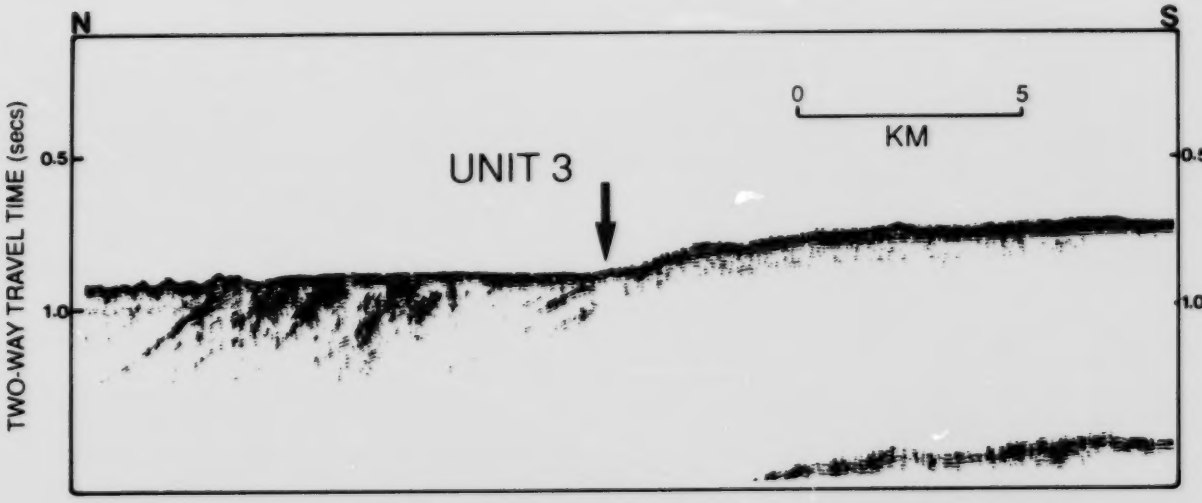

Figure 4. Seismic profile illustrating unit 3, well stratified sedimentary rocks, in abrupt possible fault contact with the basement. The location of the seismic section is shown in Figure 2.

possible prograded sequences are observed (Fig. 4). The steeper dipping section is in sharp probable fault contact with the previously described unit 2. Unit 3 forms basins within unit 2. Structural relations and acoustic characteristics suggest that unit 3 is younger than the other units.

The third and the fourth units have a flat-lying topographic expression (Fig. 5). The water depth along the seismic profile increases from about 350 m from units one and two to about 550 m. The fourth unit is given a separate status because less penetration is achieved and it consists of tight folds. However, unit 4 could also be interpreted as a disturbed zone within unit 3. The contact between unit three and four is not well defined.

MAGNETICS

On the northernmost magnetic profile closest to Greenland the character of the magnetic data is varied and correlatable with the units identified from the seismic data. To the north of the contact between seismic unit 1 and 2 larger amplitude anomalies with less short wavelength jitter are observed than to the south of the contact (Fig. 6).

Magnetic anomalies with high amplitudes of up to 500 nT and short wavelengths are observed WNW of Northumberland Island. On Northumberland Island within the Proterozoic Thule Group lavas and related sills have been documented and dated by Dawes and Rex (1986). These magnetic anomalies are inferred to be due to the presence of basic dykes that commonly intrude the Precambrian rocks. There are four episodes of Proterozoic magmatism in North-West Greenland and the dyke orientation of the oldest is WNW-ESE. This direction is consistent with the inferred extension of the dykes offshore of Northumberland Island.

Near the Carey Islands, high amplitude magnetic anomalies were measured. On the Carey Islands lavas and related sills that intrude the Precambrian basement have been described and dated by Dawes and Rex (1986). A relationship between these rocks and the observed magnetic anomalies is inferred here similar to that in the Northumberland Island area.

General negative or low amplitude, long wavelength anomalies are associated with the Carey, Glacier and North Water Basins (Fig. 6). The sedimentary basins were identified on multichannel industry reflection profiles collected in the Canadian portion of northern Baffin Bay (Jackson et al., in prep.). Within the North Water Basin the multichannel seismic survey data identified a basement high. The basement high from the multichannel survey intersects the data acquired on this cruise (Fig. 6). The magnetic anomaly becomes more positive over the multichannel basement high and is coincident with unit 4 on the shallow seismic line.

Positive amplitude, long wavelength (approximately 40 km) anomalies illustrated as smooth curves are found south of the paleoshelf boundary defined on the basis of industry multichannel data (Fig. 6). The long wavelengths are compatible with deep basement. The dip in the value of the magnetic anomaly along this southern magnetic profile may describe the southern continuation of the Carey Basin.

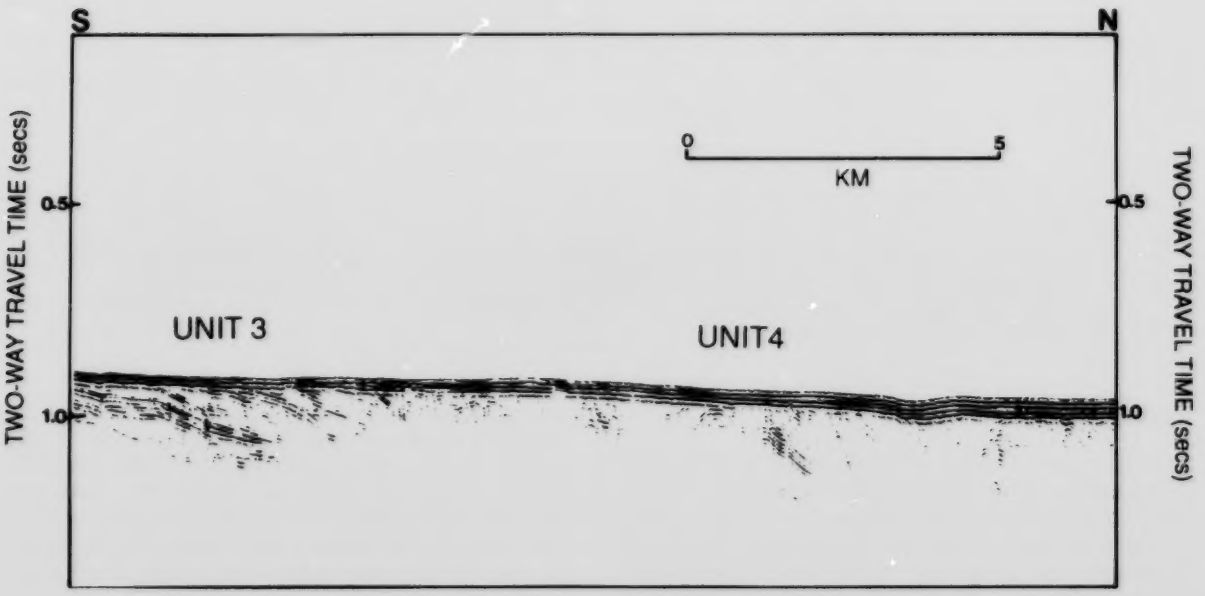

Figure 5. Seismic reflection line depicting unit 4, highly folded strata, adjacent to unit 3 with gently dipping strata. The location of the seismic section is shown in Figure 2.

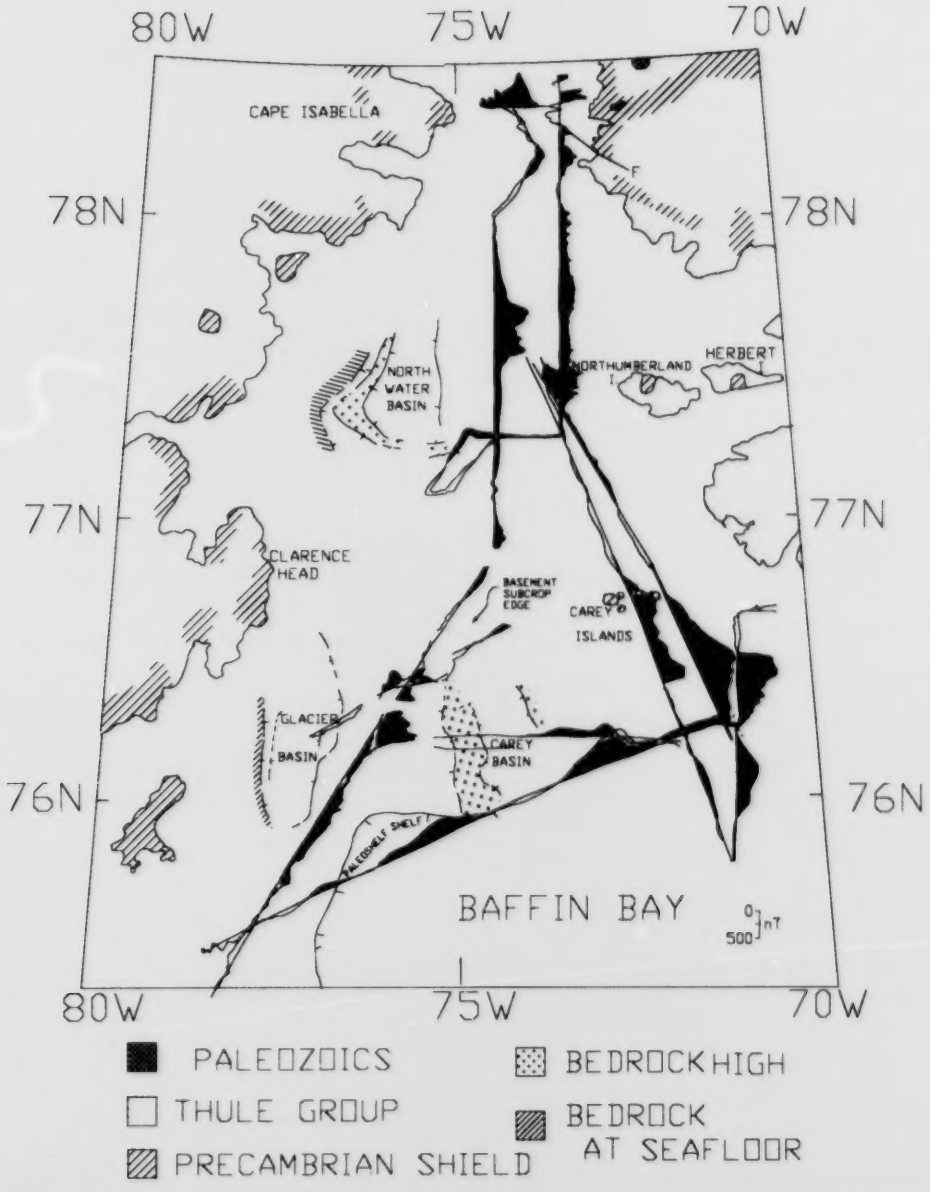

Figure 6. Magnetic anomaly along track compared with onshore geology. The line labelled "F" represents a fault. The offshore features are based on the interpretation of multichannel reflection lines and magnetic surveys. Glacier and Carey Basin are based on Jackson (et al., in prep.) and North Water Basin on Newman (1982).

CONCLUSIONS

The combination of seismic reflection, magnetic and onshore geological data allows the rock units to be extended offshore. In particular in Smith Sound, a narrow portion of Nares Strait, 11 km from Sunrise Pynt the Precambrian Shield and Proterozoic strata of Greenland can be identified confidently. The contact between the two units offshore appears to be in good alignment with the contact onshore. Furthermore, the character of the shallow seismic profiles and the magnetic anomalies indicate the probable occurrence of Thule Grou rocks WNW of Northumberland Island. The shallow seismi profiles confirm the presence of sedimentary basins tha contain strata (unit 3) inferred to be younger than Proterozoi The exact age of these strata is unknown because they hav not been sampled; however, the shallow seismic profile provide the information required for selecting sample sites t document their age.

ACKNOWLEDGMENTS

The writers are indebted to Captain L. Strum, the officers and crew of the C.S.S. Hudson for their willing support during the cruise. Technical support throughout the cruise to maintain the seismic system and potential field equipment was efficiently provided by Borden Chapman, Larry Johnston and Jess Nielsen. Art Jackson provided the navigational data and Claudia Currie the support for producing the paper. Brian MacLean and Tom Frisch reviewed the manuscript and greatly improved it.

REFERENCES

Bendix-Almgreen, S., Fristrup, B., and Nichols, R.L.
1967: Notes on the geology and geomorphology of the Carey Øer, North-West Greenland; Meddelelser om Grønland, Geoscience, nr. 8, 19 p.

Dawes, P.R. and Kerr, J.W. (ed.).
1982: Nares Strait and the drift of Greenland: a conflict in plate tectonics; Meddelelser om Grønland, Geoscience, v. 8, 393 p.

Dawes, P.R. and Rex, D.C.
1986: Proterozoic basaltic magmatic periods in North-West Greenland: evidence from K/Ar ages; Grønlands Geologiske Undersøgelse, Rapport nr. 130, p. 24-31.

Dawes, P.R., Rex, D.C., and Jepsen, H.F.
1973: K/Ar whole rock ages of dolerites from the Thule district, western North Greenland; Grønlands Geologiske Undersøgelse, Rapport nr. 95, p. 14-22.

Dawes, P.R., Frisch, T., and Christie, R.L.
1982a: The Proterozoic Thule Basin of Greenland and Ellesmere Island: importance to the Nares Strait debate: in Nares Strait and the drift of Greenland: a conflict in plate tectonics; ed. P.R.Dawes and J.W.Kerr; Meddelelser om Grønland, Geoscience, v. 8, p. 89-104.

Dawes, P.R., Peel, J.S., and Rex, D.C.
1982b: The Kap Leiper basic dyke and the age of the dolerites of Inglefield Land, North-West Greenland; Grønlands Geologiske Undersøgelse, Rapport nr. 110, p. 14-19.

Escher, A. and Watts, W.S. (ed.)
1976: Geology of Greenland; Geological Survey of Greenland, Copenhagen, 603 p.

Frisch, T.
1988: Reconnaissance geology of the Precambrian Shield of Ellesmere, Devon and Coburg islands, Canadian Arctic Archipelago; Geological Survey of Canada, Memoir 409,102 p.

Frisch, T. and Christie, R.L.
1982: Stratigraphy of the Proterozoic Thule Group, southeastern Ellesmere Island, Arctic Archipelago; Geological Survey of Canada, Paper 81-19, 12 p.

Frisch, T. and Dawes, P.R.
1982: The Precambrian Shield of northernmost Baffin Bay: correlation across Nares Strait; in Nares Strait and the drift of Greenland: a conflict in plate tectonics; ed. P.R.Dawes and J.W.Kerr; Meddelelser om Grønland, Geoscience, v. 8, p. 79-88.

Jackson, H.R., Dickie, K., and Marillier, F.
in prep: Seismic reflection interpretation bearing on the tectonic evolution of northern Baffin Bay.

Newman, P.H.
1982: Marine geophysical study of southern Nares Strait; in Nares Strait and the drift of Greenland: a conflict in plate tectonics; ed. P.R.Dawes and J.W.Kerr; Meddelelser om Grønland, Geoscience, v. 8, p. 255-260.

Geological Survey of Canada Project 890042

The 1991 Polar Margin Aeromagnetic Survey in the Lincoln Sea, northern Ellesmere Island and northern Greenland

J.B. Nelson[1], D.A. Forsyth[2], D. Teskey[3], A.V. Okulitch[4], D.L. Marcotte[5], C.D. Hardwick[5], M.E. Bower[5], and R. Macnab[6]

Nelson, J.B., Forsyth, D.A., Teskey, D., Okulitch, A.V., Marcotte, D.L., Hardwick, C.D., Bower, M.E., and Macnab, R., 1992: The 1991 Polar Margin Aeromagnetic Survey in the Lincoln Sea, northern Ellesmere Island and northern Greenland; in Current Research, Part B, Geological Survey of Canada, Paper 92-1B, p. 31-35.

Abstract

The Lincoln Sea portion of the Polar Margin High Resolution Aeromagnetic Survey Program was initiated in 1989 and completed in 1991. Approximately 4000 line km of total field and horizontal gradient data were collected in 1991. GPS and inertial systems provided positions for magnetic observations and for correcting the location of northern Greenland on a working base map.

Total field data were merged and levelled in a provisional fashion to produce a preliminary magnetic map of the Lincoln Sea survey area. Anomaly patterns are clearly related to major geological features: the Paleozoic Pearya Terrane appears to extend beneath the continental shelf, while magnetic features ascribed to Tertiary fault zones and dyke swarms cross the map area; the latter may provide constraints to estimates of relative motion between Ellesmere Island and Greenland.

Résumé

La partie du Programme de levés aéromagnétiques de haute résolution de la marge polaire concernant la mer de Lincoln a été entreprise en 1989 et complétée en 1991. Environ 4 000 km linéaires de levés du champ total et de données gradiométriques ont été recueillies en 1991. Les systèmes SPG et inertiel ont fourni des emplacements pour les observations magnétiques et pour corriger la position du Groenland septentrional sur un fond de carte conséquent.

On a provisoirement fusionné et nivelé les données sur le champ total pour produire une carte magnétique préliminaire de la région du levé de la mer de Lincoln. Les schémas des anomalies sont de toute évidence associés aux accidents majeurs de la géologie: le terrane de Pearya d'âge paléozoïque semble se prolonger au-dessous de la plate-forme continentale, tandis que les détails magnétiques attribués à des zones de failles et à des essaims de dykes d'âge tertiaire traversent la région cartographiée; ces derniers pourraient aider à définir dans certaines limites des estimations du mouvement relatif entre l'île d'Ellesmere et le Groenland.

[1] Defence Research Establishment Pacific, Victoria, British Columbia
[2] Continental Geoscience Division, Ottawa, Ontario
[3] Geophysics Division, Ottawa, Ontario
[4] Institute of Sedimentary and Petroleum Geology, Calgary, Alberta
[5] Institute for Aerospace Research, Ottawa, Ontario
[6] Atlantic Geoscience Centre, Dartmouth, Nova Scotia

INTRODUCTION

The Polar Margin High-Resolution Aeromagnetic Survey Program was initiated in 1989, with funding provided by the Department of National Defence (DND), the Geological Survey of Canada (GSC), and the Institute for Aerospace Research (IAR). The Lincoln Sea portion of this survey was completed in 1991, yielding the first high-resolution aeromagnetic survey to extend from Nares Strait, northern Ellesmere Island, and northern Greenland out to the edge of the continental margin.

Understanding the Lincoln Sea area is key to unravelling the tectonic evolution of the Arctic Ocean: the northern part of the Lincoln Sea crust may have been affected by formation of the Alpha and Lomonosov Ridges and the opening of the Fram Basin, while motion between Ellesmere Island and Greenland along Nares Strait should be reflected in the structure of the continental shelves. The objective of the survey was to collect detailed magnetic data to help clarify the relationship between these events and the crustal features observed in this part of the Arctic Ocean.

The data acquisition system was carried aboard the IAR Convair 580 aircraft. Total field magnetic data were recorded along with horizontal and vertical gradients, as well as positional information (accurate to 50 m) from GPS and inertial sensors (Nelson et al, 1991b). Four thousand line km of data were collected in 1991, bringing the total 1989-1991 Lincoln Sea survey to approximately 24000 line km. Figure 1 shows the total pattern of flight and tie lines, with 1991 lines in bold. Flown at a constant 300 m altitude offshore, and at 300 m in a draped mode onshore, the 1991 survey consisted of:

(1) nine north/south lines 4 km apart from 82°N (over northern Greenland) to 84°30'N (beyond the continental shelf break), between 44° and 50°W (Area 1);

(2) eleven east/west lines 2 km apart from 56° to 59°15'W, between 82°20' and 82°32'N (Area 2);

(3) two lines from the 1989 survey reflown;

(4) four tie lines through Area 1 and a tie line through the entire 1989-1991 survey area.

A cesium vapour magnetometer was installed in the GSC seismic vault at Alert, N.W.T. to measure and record the diurnal changes in the Earth's field. The sampling rate was 8 Hz and time synchronization with the aircraft system clock was within 1 second.

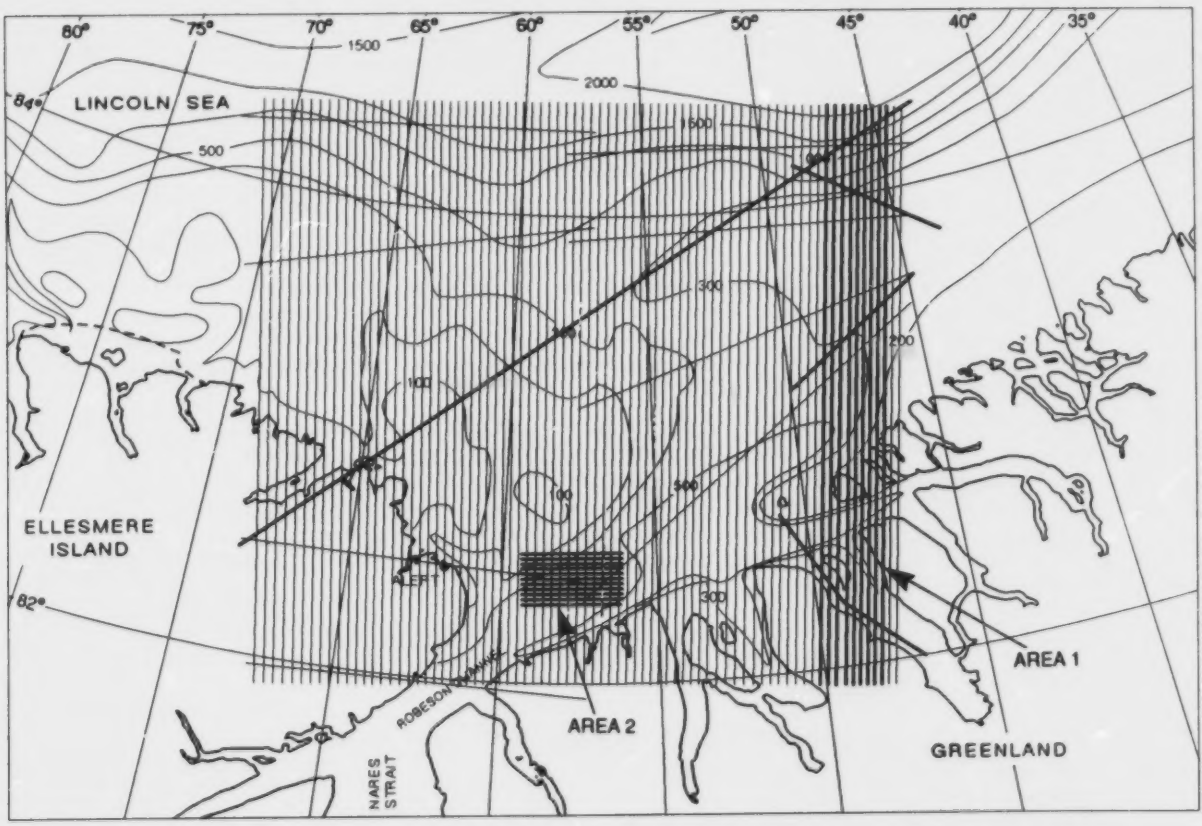

Figure 1. Flight lines for the entire 1989-1991 Lincoln Sea aeromagnetic survey (1991 portion in bold). Bathymetric contours are in metres. Profiles from Areas 1 and 2 are shown in Figures 2a and 2b, respectively.

Previous reports (Hardwick et al., 1990; Nelson et al., 1991a,b) have dealt with the 1989 and 1990 surveys. This report presents the first magnetic map of the entire Lincoln Sea survey area, produced from merged and provisionally levelled data. Correlations between significant magnetic anomaly patterns and onshore geology are discussed also.

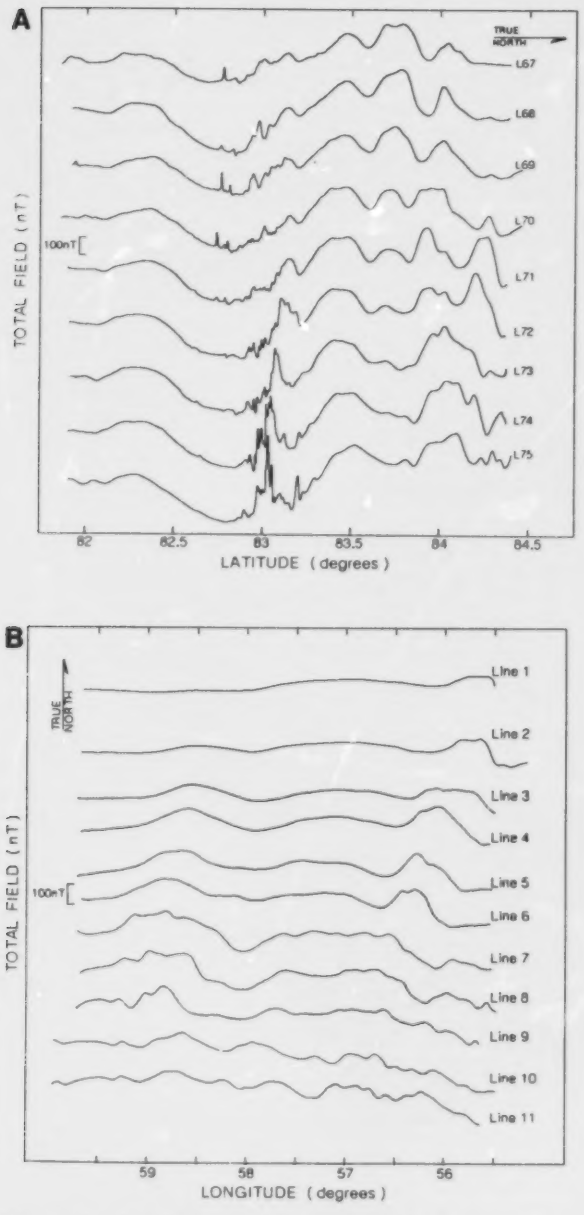

Figure 2. **A.**) Stack plot of the total field profiles measured over Area 1. **B)** Stack plot of the total field profiles measured over Area 2.

DATA

Figures 2a and 2b are stack plots of the total field profiles measured over Areas 1 and 2, respectively.

The total field data from 1989, 1990, and 1991 were merged and provisionally levelled by adjusting tie and primary survey lines to reduce cross-tie errors to zero. The resulting data were sampled on a 1 km by 1 km grid (Fig. 3); some levelling problems remain in the data, which will require treatment with de-corrugation processing. Figure 4 is a grey-scale contour plot of the total data set.

DISCUSSION

The first result of the 1991 survey relates to the inaccuracy of some published maps of Greenland. Comparison of GPS fixes with World Aeronautical Charts (WAC) indicate that the WAC maps place Greenland some 10-14 km east and slightly north of its true location. This problem is well known, as WAC map A-5 (Defence Mapping Agency, 1979) contains the following disclaimers: "Greenland is up to 5 nautical miles out of position relative to Canada", and "Arctic Institute of North America Project Nord (Control Data Corporation) indicates position discrepancies in excess of 9.2 nautical miles (Nov/68)".

Reference to Canadian Hydrographic Service (CHS) Chart 7304 confirmed our Ellesmere Island and northwestern Greenland GPS fixes, however the agreement decreased significantly east of 52° W. In this region, our GPS fixes agreed very well with a recent geological map (Geological Survey of Greenland, 1989). A copy of the CHS chart was manually revised to match the GGU map east of 52° W, and used thereafter as a base for plotting magnetic results (Hardwick and Jower, 1991).

Comparisons between the magnetic anomaly pattern and the onshore geology indicate the following relationships (Fig. 4):

(1) There are southeast trending, large amplitude, linear magnetic highs located near the shelf-slope break in the northwest map area. Such short wavelength anomalies are generally atypical of a sediment-laden shelf but may be produced by several sources including: (a) structural effects related to the development of the plateau immediately to the north and characterized by a similar magnetic anomaly pattern; (b) a continuation of an apparent linear extensional structure zone trending northwest from Greenland. The short wavelength anomalies could be caused by an extension of the Tertiary dyke system that strikes northwest along the northern Greenland coast.

(2) The east-west trending positive anomalies off the coast of Ellesmere Island are parallel to fault trends within the adjacent Pearya terrane. The anomaly trends may indicate an extension of the Pearya terrane beneath the continental shelf.

(3) Northeast trending magnetic highs extend offshore from the Clements Markham and Northern Lake Hazen Fold Belts on Ellesmere Island. Anomalies extending northeast from the Clements Markham fold belt appear to truncate east-west (Pearya terrane?) trends.

(4) A prominent northeast striking anomaly pattern parallel to a proposed major fault zone crossing the Lincoln Sea from Nares Strait is not a first-order feature. Rather, a zone of positive anomalies curves eastward from Nares Strait subparallel to the major structural trends on adjacent northwest Greenland. The Greenland coast in the eastern part of the map area is characterized by a long wavelength magnetic low of uncertain origin.

(5) Superimposed on the regional low over the southeaste part of the map area, a series of short wavelength magnet highs continues offshore from a zone of La Cretaceous-Early Tertiary basic dykes. Corroboration the offshore extent, continuity, and timing of this zo could provide an important marker and major constrai on the extent and age of the major structures in the Linco Sea.

CONCLUSION

The first high-resolution aeromagnetic survey to inclu portions of the Lincoln Sea, northern Ellesmere Island, a northern Greenland has been completed. Survey data ha been provisionally levelled and gridded to produce a to

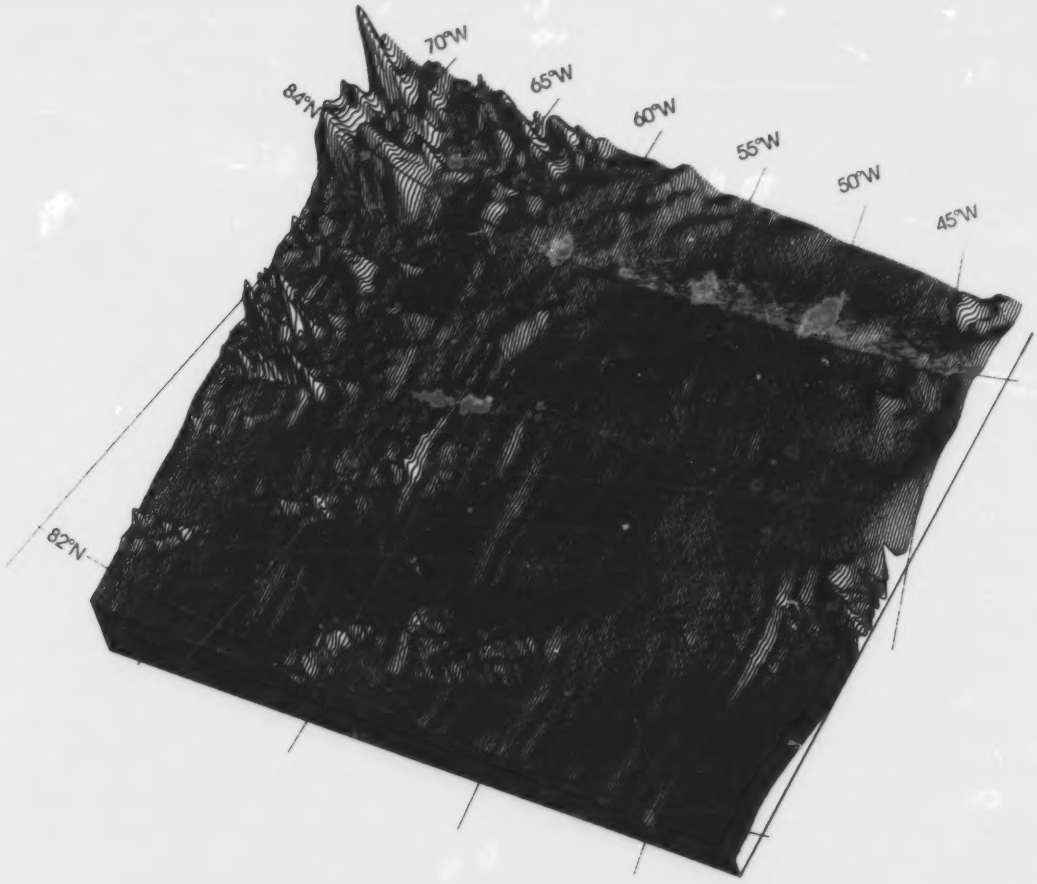

Figure 3. Surface grid plot of the entire 1989-1991 Lincoln Sea aeromagnetic survey data, provisionally levelled and sampled on a 1 km x 1 km grid. Linear perturbations remaining in the data set are due to imperfect levelling between adjacent north-south flight lines, and will be removed with a more powerful de-corrugation method.

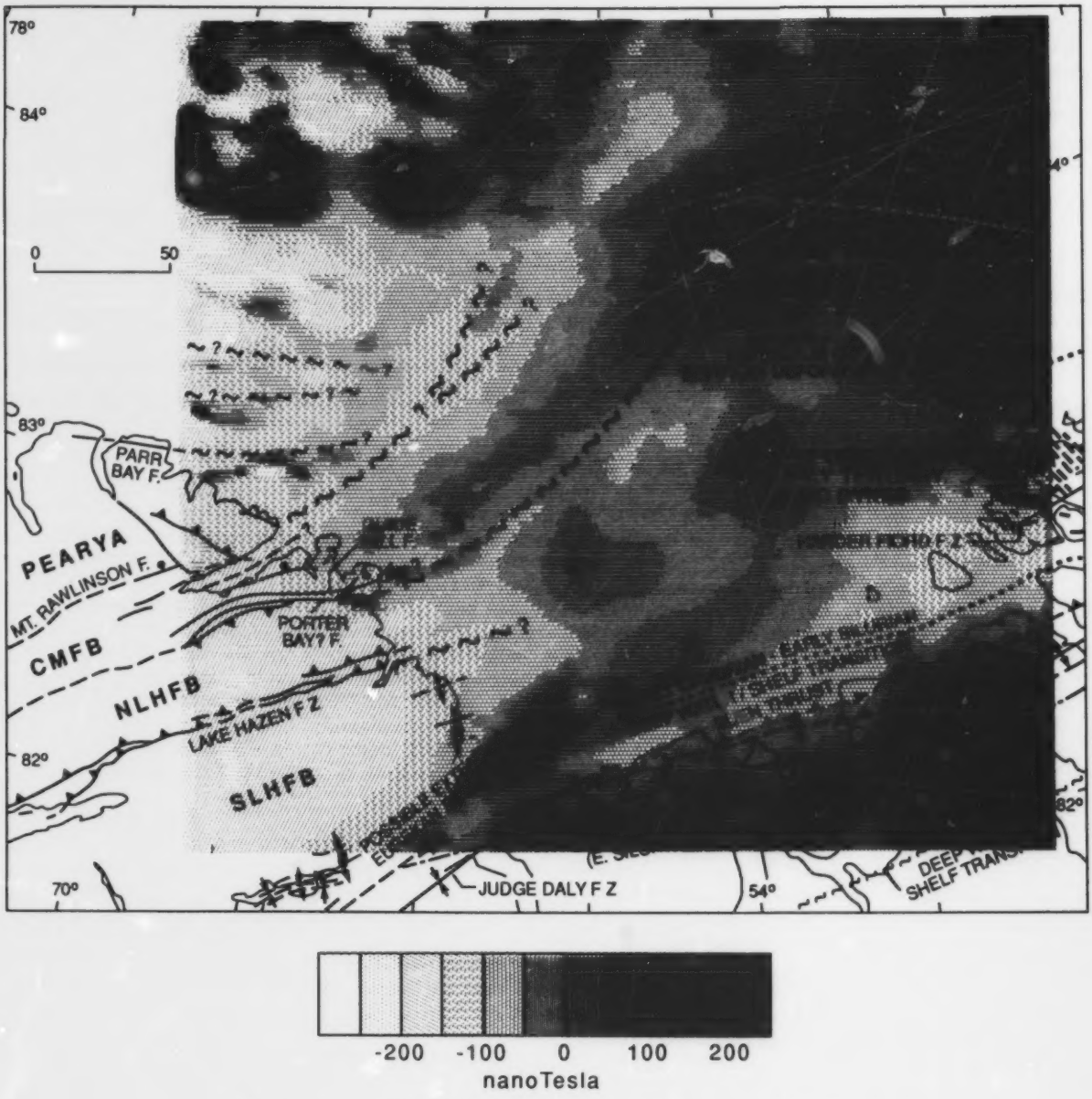

Figure 4. Contour plot of the entire 1989-1991 Lincoln Sea aeromagnetic survey data, levelled and sampled on a 1 km x 1 km grid. CMFB: Clements Markham Fold Belt; NLHFB: Northern Lake Hazen Fold Belt; SLHFB: Southern Lake Hazen Fold Belt.

field map of the area; dominant features have been correlated with known onshore geological structures. Errors in the position of northern Greenland as shown on WAC maps have been confirmed, but with appropriate modifications east of 52°W, CHS Chart 7304 has been found to be sufficiently accurate for use as a base map.

ACKNOWLEDGMENTS

The authors thank the flight crew, the ground crew, and technical support staff of the Convair 580 Project team at IAR for their invaluable assistance in collecting these data. We are also grateful for the support and encouragement received from Robin Riddihough, GSC Chief Scientist.

REFERENCES

Defence Mapping Agency
1979: World Aeronautical Chart Series ONC, sheet A-5, 2nd edition. Defence Mapping Agency Aerospace Center, St. Louis Air Force Station, Missouri 63118, Compiled April 1968, revised January 1979.

Geological Survey of Greenland (GGU)
1989: Geological Map Sheet 7, Nyeboe Land, Geological Survey of Greenland, Copenhagen, scale 1:500 000.

Hardwick, D., and Bower, M.
1991: Observed map errors – northwest coast of Greenland; IAR MSC 67, NRC #32150.

Nelson, J.B., Hardwick, D., Forsyth, D., Marcotte, D., Teskey, D., MacPherson, M., Hardwick, C.D., Nelson, J.B., Thorning, L., Bower, M., Marcotte, D.L., Forsyth, D., Macnab, R., and Teskey, D.
1990: Procedures and preliminary results of an aeromagnetic survey in the Lincoln Sea; in Current Research, Part D, Geological Survey of Canada, Paper 90-1D, p. 11-16.

Nelson, J.B., Hardwick, D., Forsyth, D., Bower, M., Marcotte, D., Macpherson, M., Macnab, R., and Teskey, D.
1991a: Preliminary analysis of data from the Lincoln Sea aeromagnetic surveys 1989-1990; in Current Research, Part B; Geological Survey of Canada, Paper 91-1B, p. 15-21.

Nelson, B., Hardwick, D., Forsyth, D.A., Marcotte, D., Teskey, D., MacPherson, M., Bower, M., and Macnab, R.
1990: Preliminary report of data acquisition and processing for the 1989-1990 lincoln sea aeromagnetic survey, Geological Survey of Canada Open File 2296.
1991b: Preliminary report of data acquisition and processing for the 1989-1990 Lincoln Sea aeromagnetic survey; Geological Survey of Canada, Open File 2296.

Geological Survey of Canada Project 890051

Structural geology of northwestern Devon Island, Arctic Canada

G.H. Eisbacher[1]
Institute of Sedimentary and Petroleum Geology, Calgary

Eisbacher, G.H., 1992: Structural geology of northwestern Devon Island, Arctic Canada; in Current Research, Part B; Geological Survey of Canada, Paper 92–1B, p. 37-45.

Abstract

The structural evolution of Paleozoic platformal to basinal successions on northwestern Devon Island can be understood in terms of three contractional and at least two extensional tectonic events. Northerly-trending latest Silurian to earliest Devonian fold structures are the expression of an intraplate shortening event along the west-directed Boothia basement thrust, whose position is probably marked by a major east-facing synsedimentary flexure on eastern Grinnell Peninsula. Late Devonian to earliest Carboniferous foreland sedimentation and subsequent deformation east of this flexure created northeasterly plunging fold–thrust structures with detachments along lower Paleozoic evaporite–shale units. Late Paleozoic and Mesozoic crustal extension of a broad region between the Sverdrup and Baffin Bay basins was followed by significant Eocene to Recent crustal contraction, expressed in the northwesterly-trending Grinnell belt; this belt is dominated by thrust faults and folds with variable vergence, segmented by high-angle cross faults. Some of these are convergent strike-slip faults which originated as thrusts or extensional faults. There are strong morphological hints that, particularly, north-northeast-trending dextral strike-slip faults with total displacement of 5 to 6 km are still active.

Résumé

On peut expliquer l'évolution structurale des successions paléozoïques de bassin passant à des successions de plate-forme du même âge, dans le nord-ouest de l'île Devon, en fonction de trois épisodes tectoniques de contraction et d'au moins deux épisodes tectoniques d'extension. Les structures plissées de direction générale nord, qui s'échelonnent du Silurien terminal au Dévonien initial, sont l'expression d'un épisode de raccourcissement intraplaque survenu le long du charriage du socle de Boothia, dirigé vers l'ouest, dont l'emplacement est marqué par une importante flexure synsédimentaire orientée vers l'est, dans l'est de la péninsule de Grinnell. La sédimentation d'avant-pays, échelonnée du Dévonien supérieur au Carbonifère initial, et la déformation ultérieure survenue à l'est de cette flexure, ont créé des structures de charriage et plissement de plongement nord-est accompagnées de décollements suivant des unités de shale et d'évaporites du Paléozoïque inférieur. La distension crustale survenue au Paléozoïque supérieur et au Mésozoïque, dans une vaste région comprise entre le bassin de Sverdrup et le bassin de la baie de Baffin, a été suivie d'une contraction crustale significative survenue de l'Éocène à l'Holocène, que traduit l'existence de la zone de Grinnell de direction générale nord-ouest; dans cette zone prédominent les failles chevauchantes et des plis de vergence variable, segmentés par des failles transversales de fort pendage. Certaines de ces failles sont des décrochements convergents qui à l'origine étaient des failles chevauchantes ou des failles d'extension. Leur morphologie indique nettement que surtout, des décrochements dextres de direction générale nord nord-est montrant un rejet total de 5 à 6 km sont encore actifs.

[1] University of Karlsruhe, Kaiserstrasse 12, 75000 KARLSRUHE, Germany

INTRODUCTION

During the 1991 field season, the author studied the regional structural geology of northwesternmost Devon Island, complementing helicopter-supported stratigraphic and sedimentological work carried out by U. Mayr, T. de Freitas, and P. Thériault (see this volume). The area investigated comprises a land mass about 180 km long and 60 km wide; it includes all of Grinnell Peninsula to the west and most of Colin Archer Peninsula to the east (Fig. 1). The region is underlain by carbonate-shale successions of a northwest facing promontory of the early Paleozoic Arctic platform. This promontory developed during Late Ordovician to Silurian differential subsidence and corresponds roughly to the present erosional coast line of Grinnell Peninsula. Progressive drowning of the carbonate shelf by eastward shale-onlap preceded latest Silurian to earliest Devonian uplift and elevation of lower Paleozoic strata, within the area encompassed by the west-directed Boothia basement thrust and the related Cornwallis Fold Belt (Kerr, 1974, 1977; Thorsteinsson and Uyeno, 1980; Miall, 1986; Okulitch et al., 1986).

Present land and offshore structures also reflect the development of a Late Devonian to earliest Carboniferous orogenic foreland fold belt, Late Carboniferous and late Mesozoic crustal extension, and, to a previously unsuspected degree, mid-Tertiary folding, thrust faulting, and convergent high-angle faulting. It was a challenge to understand the complexities created locally by superimposed and reactivated fold–thrust structures within a general regional framework dominated by gentle stratal dips.

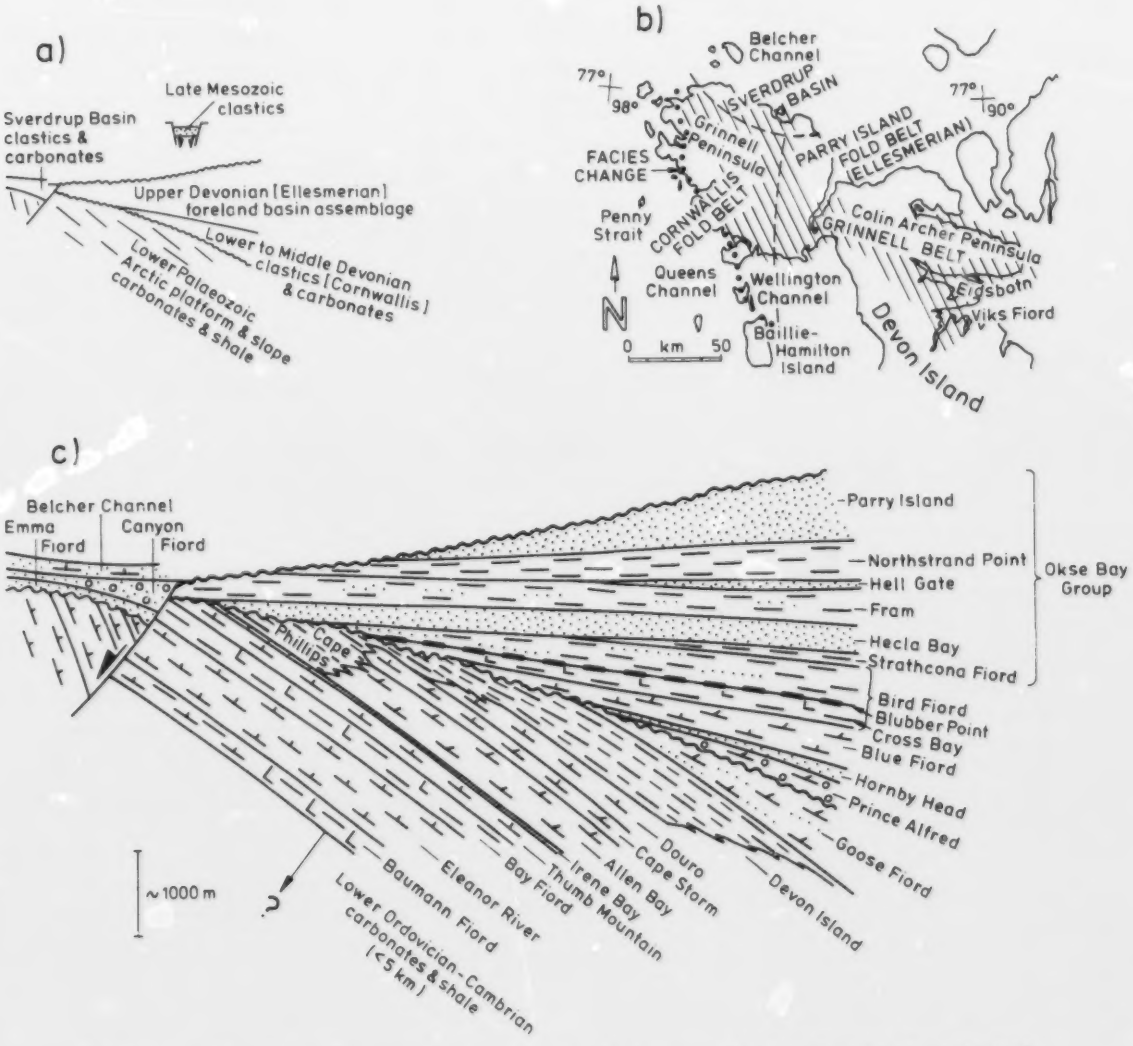

Figure 1. (a) The main tectonostratigraphic intervals **(b)**, index map, and **(c)** sedimentary formations of northwestern Devon Island.

Published and Open File reports of previous work in the area are those of Fortier et al. (1963), and Morrow and Kerr (1977, 1986). Major geophysical and crustal tectonic features have been illustrated by Sweeney et al. (1986). Preliminary airphoto interpretations and extensive fieldwork by J. Wm. Kerr have defined outstanding problems very well, in a region where accessibility, outcrop, and weather conditions hamper the formulation of a complete stratigraphic or structural hypothesis.

SEDIMENTARY TECTONICS

The major stratigraphic intervals preserved in northwestern Devon Island reflect five distinct tectonic settings or events (Fig. 1): 1) an early Paleozoic platform/slope environment along a northwest-facing, thermally subsiding passive margin that possibly graded laterally into an oceanic basin (H.P. Trettin, pers. comm., 1991); 2) a Siluro–Devonian intraplate contraction event (Cornwallis Fold Belt) with syntectonic progradation and posttectonic onlap of clastic and shallow water carbonate strata; 3) a Late Devonian foreland basin (Ellesmerian Parry Island Fold Belt); 4) Carboniferous–Permian crustal extension and stratal onlap related to the development of Sverdrup Basin; and 5) mid-Tertiary (Eurekan) to Recent intraplate shortening within the Grinnell belt, followed by erosional bevelling of a tectonically elevated land surface. Thickness and lateral facies variations and mechanical competence contrasts of rocks in the five lithotectonic intervals significantly influenced kinematics during the regional structural evolution; different deformational events also occurred under various amounts of overburden. The principal lithological heterogeneities can be summarized as follows.

The exposed 3 to 4 km of strata within the Upper Cambrian to Silurian succession probably overlie at least 7 km of older sedimentary rocks (U. Mayr, pers. comm., 1991), which rest on a west-dipping Archean and/or Proterozoic crystalline basement (Frisch, 1988). The Paleozoic Arctic platform and slope succession of northwestern Devon Island includes two structurally significant couplets of incompetent and competent strata that facilitated detachment during later flexural slip folding and thrust faulting within the Cornwallis, Parry Islands, and Grinnell belts. These couplets are: 1) the evaporitic and argillaceous Baumann Fiord Formation, which is overlain by calcareous Eleanor River Formation; and 2) the evaporitic Bay Fiord Formation, which is in turn overlain by the calcareous to dolomitic Thumb Mountain/Irene Bay/Allen Bay interval (Fig. 1c). A relatively abrupt facies change from competent Allen Bay dolostone to incompetent Cape Phillips shale (Fig. 1b) is reflected in a structural transition from long-wavelength to shorter-wavelength folds in the Cornwallis Fold Belt of southwestern Grinnell Peninsula (see below). The disappearance of Baumann Fiord evaporites in the westernmost parts of Grinnell Peninsula may contribute to the more linear, Cornwallis-aged structures there.

Northerly progradation of Silurian/Lower Devonian clastic and shallow water carbonate rocks, and a subsequent westerly onlap of Lower to Middle Devonian carbonates over erosionally truncated Silurian formations, produced a post-Cornwallis westward tapering stratal wedge (Fig. 1). This wedge includes Goose Fiord silty dolostone, Prince Alfred carbonate rudites, Hornby Head[1] siliciclastic rocks, Blue Fiord limestone and dolostone, and strata of the Cross Bay dolosiltite–evaporite member to Blubber Point limestone member of the Bird Fiord Formation (Fig. 1c). It thins dramatically along a north-trending hinge zone on eastern Grinnell Peninsula (Goodbody et al., 1988). Detachment in shales of the Late Silurian Devon Island Formation and evaporites of the Cross Bay Member, plus general westward thinning of these units, prompted the complex lateral termination of both Ellesmerian and Eurekan fold–thrust structures against the older Cornwallis Fold Belt.

The Upper Devonian foreland basin strata, which on northeastern Grinnell Peninsula belong essentially to the clastic Okse Bay Group (Embry and Klovan, 1976), also thin where they cover the Cornwallis Fold Belt. Long-wavelength folds of the Parry Islands Fold Belt are dominated by the competent Hecla Bay and Parry Islands quartzarenite formations, which alternate with the incompetent argillaceous siltstone units of the upper Bird Fiord Formation, and the Strathcona, Fram, and Northstrand formations. These incompetent formations host secondary detachments.

Profound post-Ellesmerian erosional bevelling of the folded carbonate rocks and clastic rocks is indicated by the type of deposits laid down in the low-gradient nonmarine system responsible for the pebbly sandstones of the Lower Carboniferous Emma Bay Formation. In contrast, easterly-trending synsedimentary faults and flexures controlled subsequent deposition of conglomeratic redbeds of the Upper Carboniferous Canyon Fiord Formation; these sediments were locally derived and deposited in asymmetric grabens along the southern margin of the initial Sverdrup Basin before regional onlap and overstepping of younger strata occurred along a north dipping homocline (P. Thériault, pers. comm., 1991). Probably only thin Mesozoic strata covered northwestern Devon Island; however, clastic deposits related to Late Mesozoic onlap are preserved in narrow north-northeast to northeast-trending grabens of latest Cretaceous to Paleogene age (Thorsteinsson and Mayr, 1987).

The presence of mid-Cretaceous north-northeast-trending dikes that cut Permo-Carboniferous strata on Grinnell Peninsula (Kerr, 1976) suggests that by that time a new pattern of extension, related to the opening of the Arctic Ocean, had become established within and along the margins of Sverdrup Basin. Toward the east this pattern merged with or was overlapped by the Late Cretaceous/Paleogene extensional regime within the Labrador Sea/Baffin Bay

[1] Hornby Head is an informal formation name. The unit is identical to the unnamed Devonian formation of de Freitas and Mayr (this volume).

domain (see also Kerr, 1981; Balkwill and Fox, 1982; Harrison et al., 1988; Embry and Osadetz, 1988; Okulitch et al., 1990).

Mid-Tertiary Eurekan intraplate contraction, which affected most of the northern Arctic Islands (Trettin, 1989, his Fig. 15), seems to have also reached northwestern Devon Island and possibly areas beyond to the south. However, by then most Paleozoic sedimentary rocks had been elevated, and thus their deformation occurred near the Earth's surface; pervasive cataclasis or zonal brecciation therefore dominates the deformational style near reverse and strike-slip faults of the Grinnell belt. This facilitated syn- to posttectonic erosion and bevelling of elevated land surfaces, which are sporadically covered by quartzose boulder veneers located at elevations between about 230 and 300 m.

Cornwallis Fold Belt

The Cornwallis Fold Belt of Late Silurian/earliest Devonian age consists of northerly-trending, generally open and asymmetric folds cut by related minor thrusts or cross faults; the folds are best developed on western Grinnell Peninsula and adjacent offshore islands. From east to west the fold structures decrease in wavelength, but increase in relative amplitude, structural relief, strike linearity, and the degree of westerly vergence. In the area of the observed or inferred facies change between Allen Bay dolostone and Cape Phillips shale along the southwestern platform edge, the reduced bulk competence of the succession led to tighter en echelon fold–thrust patterns and a later, complex, structural overprint similar to that documented by Kerr (1974, 1977) on nearby Bathurst Island. The following Cornwallis-aged major structures have been identified from east to west: the gently west dipping Devon Homocline, the broad Wellington downwarp, Ensorcellement Dome, Inglis Bay Syncline, Barrow Harbour Anticline, Hungry Bay Syncline, Mt. Fitzroy Anticline, and Loney Point Syncline (Fig. 2). The zone of inflection between the Wellington downwarp and Ensorcellement Dome is characterized by syndeformational erosion down to the level of the Ordovician Eleanor River Formation on the west, and by syndeformational deposition of conglomeratic Lower Devonian clastic strata on the east, with subsequent onlap and overstep of Devonian shelf carbonate rocks from east to west (T. de Freitas, pers. comm., 1991). Since Cornwallis-aged folds are tighter toward the westernmost parts of Grinnell Peninsula, blind thrusts have to be expected below. These faults probably merge with a major basement thrust similar to that proposed by Okulitch et al. (1986) for the Boothia uplift located to the south; the position of the basement thrust ramp at depth probably coincides with the Wellington–Ensorcellement inflection zone at the surface. It is interesting to note that a structural dome on the scale of Ensorcellement Dome also has been documented on central Cornwallis Island by Thorsteinsson (1988); this dome is located along strike about 200 km to the

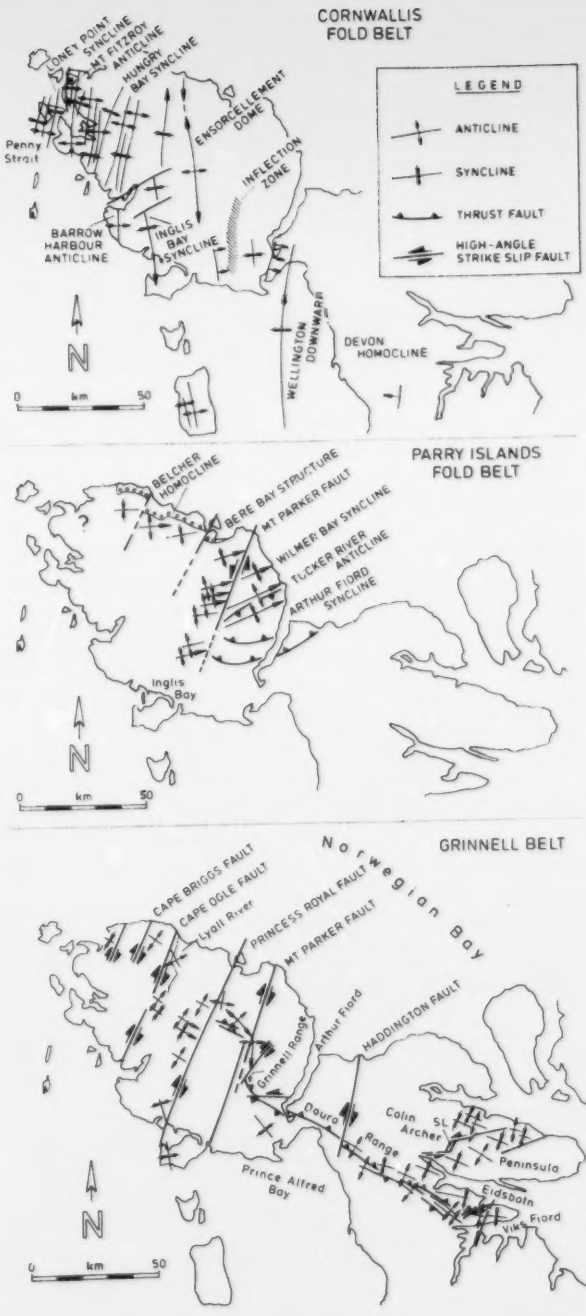

Figure 2. Major structures of the Siluro-Devonian Cornwallis Fold Belt (top), the Late Devonian/earliest Carboniferous(?) Parry Islands Fold Belt (centre), and the Tertiary Grinnell belt (bottom). Relative ages are derived from the superposition and reactivation patterns of folds, thrust faults, and high-angle cross faults.

south in alignment with the Boothia basement uplift. The total amount of east-west shortening across the Cornwallis Fold Belt on Grinnell Peninsula and in the adjacent offshore islands is difficult to evaluate, because of later structural overprinting and an increase in stratal shortening within the submerged part of the belt in Penny Strait. A rough estimate, based on stratal dips, ranges from 10 to 20 km. The continuation of the Cornwallis Fold Belt north of Grinnell Peninsula is poorly constrained. If Smith and Okulitch (1987) were correct in suggesting that the Inglefield Uplift on southeastern Ellesmere Island was an active feature during shortening of the Cornwallis Fold Belt, a major dextral transfer fault zone of earliest Devonian age might underlie southernmost Sverdrup Basin and connect the two zones of Cornwallis-aged intraplate basement shortening.

Parry Islands Fold Belt

The Late Devonian to earliest Carboniferous(?) Parry Islands Fold Belt extends from Melville Island (Fox, 1985; Harrison and Bally, 1988) through western Bathurst Island (Kerr, 1974, 1977), toward northeastern Ellesmere Island (Trettin, 1989), where more internal Ellesmerian-aged fold or thrust structures were later reactivated (Klaper, 1990). On Grinnell Peninsula, the westward thinning and onlapping wedge of Devonian carbonate rocks and the overstepping Okse Bay Group foreland clastic strata display open and gently east-northeast- to northeast-plunging folds. The folds are associated with subsidiary low-angle out-of-the-syncline thrusts; northerly-trending high-angle faults such as the Mt. Parker cross fault, probably had a dextral sense of displacement at this stage. From southeast to northwest the following major folds can be recognized in Okse Bay Group strata: the Arthur Fiord Syncline, Tucker River Anticline, Wilmer Bay Syncline, and the Bere Bay structure. The synclines are bowl shaped and open; the broad Arthur Fiord Syncline also mimics the pre-existing Cornwallis-aged Wellington downwarp. In contrast, the Tucker River Anticline is relatively narrow and slightly southeast-verging. Up the plunge and near the Mt. Parker cross fault, pre-Okse Bay Paleozoic carbonate rocks are exposed in the core of the anticline.

By analogy with the pattern described by Harrison and Bally (1988) on Melville Island, primary detachment along Bay Fiord evaporites and secondary detachment along argillaceous units higher in the succession is assumed to have facilitated the folding of stiffer layers. West of the Mt. Parker Fault, several east-plunging synclines were severely overprinted by later Eurekan events and their basinal geometry can be related only crudely to the up-plunge terminations of other folds, here termed Bere Bay structure. Toward the south, these structures grade into a disrupted second set of shallow basins and domes. Farther to the west, some east- to northeast-trending folds in pre-Okse Bay strata are probably also of Ellesmerian age, since they are overlain unconformably by Permo–Carboniferous clastic rocks (Kerr, 1976) and are overstepped by gently north dipping strata of the Sverdrup Basin (Belcher Homocline, Fig. 2). Northerly-trending Cornwallis-aged fold/fault fabrics on western Grinnell Peninsula were also reactivated and, therefore, most folds plunge steeply and their terminations are abrupt. It appears that the northernmost exposed Cornwallis structures acted as a somewhat stiffer promontory during thin-skinned Ellesmerian shortening, and that some of this shortening was transferred along north-trending sinistral faults into areas to the south (Kerr, 1977). Other northwest to west-trending structures probably originated as part of the younger Grinnell belt, although generally they have been assumed to be of late Paleozoic (Ellesmerian) age (Fortier et al., 1963). The folds and thrust faults of the Grinnell belt trend perpendicular to the main Parry Island folds, involve the Carboniferous and Permian strata of the post-Ellesmerian Belcher Homocline, and are on trend with post-Sverdrup Basin contraction structures in the offshore area north of Grinnell Peninsula (A. Okulitch, pers. comm., 1991).

Grinnell belt

The Grinnell belt of probable mid-Tertiary (Eurekan) age extends from northern Grinnell Peninsula southeast toward Colin Archer Peninsula and Viks Fiord (Fig. 2). The belt contains folds, thrust faults, and high-angle strike-slip faults which overprinted Cornwallis- and Ellesmerian-aged fold–thrust patterns or reactivated and accentuated major pre-existing structures. The axial zone of the belt is about 10 to 20 km wide and can be followed for more than 100 km along strike. Its northwestern portion coincides roughly with the present drainage divide and the topographically highest ridges of Devon Island, which are at elevations of about 500 to 600 m; there, the deformational style of the Grinnell belt is dominated by closely spaced, low-amplitude corrugations on the gently east dipping limbs of asymmetric Cornwallis-aged folds. Toward the central parts and to the southeast, the belt is more clearly defined and is possibly transitional into a zone of Eurekan-aged fold–thrust structures identified on central Ellesmere Island (Okulitch, 1982). The entire belt displays a surprisingly youthful relief and is characterized by pervasive to zonal cataclasis of competent carbonate units.

In two areas, near Lyall River to the northwest and near Eidsbotn to the southeast, it can be demonstrated that the post-Ellesmerian Carboniferous clastic strata were deformed into short and steeply plunging folds, and that the strata were also disrupted by high-angle faults. Total shortening perpendicular to the generally northwest-trending central fold–thrust structures of the Grinnell belt is in the order of 3 to 5 km. However, the belt is longitudinally segmented by high-angle transfer faults which link fold-thrust structures with varied vergence and structural style. Since shortening has generally affected previously tilted strata, the mappable fold lengths are small and plunges are steep; lateral thrust terminations are abrupt and cataclastic zones ubiquitous. Most high-angle and north-northeast trending dextral cross faults are partly of Cornwallis and/or Ellesmerian ancestry. However, regional extensional structures, some with mafic dikes (Kerr, 1976), and related to a mid-Cretaceous rifting event in Sverdrup Basin (Balkwill and Fox, 1982), have the same trend and were locally reactivated during Tertiary contraction. Late Cretaceous–Paleogene fan-shaped fault arrays, which first developed in conjunction with diffuse

extension in and around Baffin Bay (Kerr, 1980; Thorsteinsson and Mayr, 1987; Okulitch et al., 1990), were also partly inverted. On northwestern Devon Island the north-northeast-trending high-angle faults are the most remarkable structures, because they have a strong topographic expression. The main faults of this group, from southeast to northwest, are the Viks Fiord structure, Haddington Fault, Mt. Parker Fault, Princess Royal Fault, Mt. Ogle Fault, and Cape Briggs Fault (Fig. 3).

The most prominent of these faults is the Princess Royal Fault which offsets variably dipping Devonian to Carboniferous strata dextrally by about 5 km; sporadically observed shear veins along the fault zone also suggest dextral convergent movement. The fault trace is remarkable straight, it is flanked locally by steep faceted slopes, and is marked by abandoned river channels. The fault has been identified for at least 150 km into the offshore area of Norwegian Bay to the north (Okulitch, 1:1 000 000 scale compilation map, in review); on trend in the southern offshore region the extrapolated trace separates a shallow water marine area (with irregular topography) in the east from a uniformly deeper channel in the west. Where the Princess Royal Fault crosses the axial Grinnell belt, shortening by folding and thrust faulting appears to be considerably smaller to the west of the fault trace than to the east; thus, some of the dextral displacement along the northern part of the fault may have been transferred to the contraction structures of the Grinnell belt southeast of the fault. However, along the southernmost land based section of the fault, a northwest-trending syncline with a core of Okse Bay clastic rocks is also offset dextrally by about 3 km. Thus, the Princess Royal Fault, and possibly several other high-angle north-northeast-trending faults, appear to be part of a linked system of discrete faults and more broadly distributed zones of folding and thrust faulting. Two

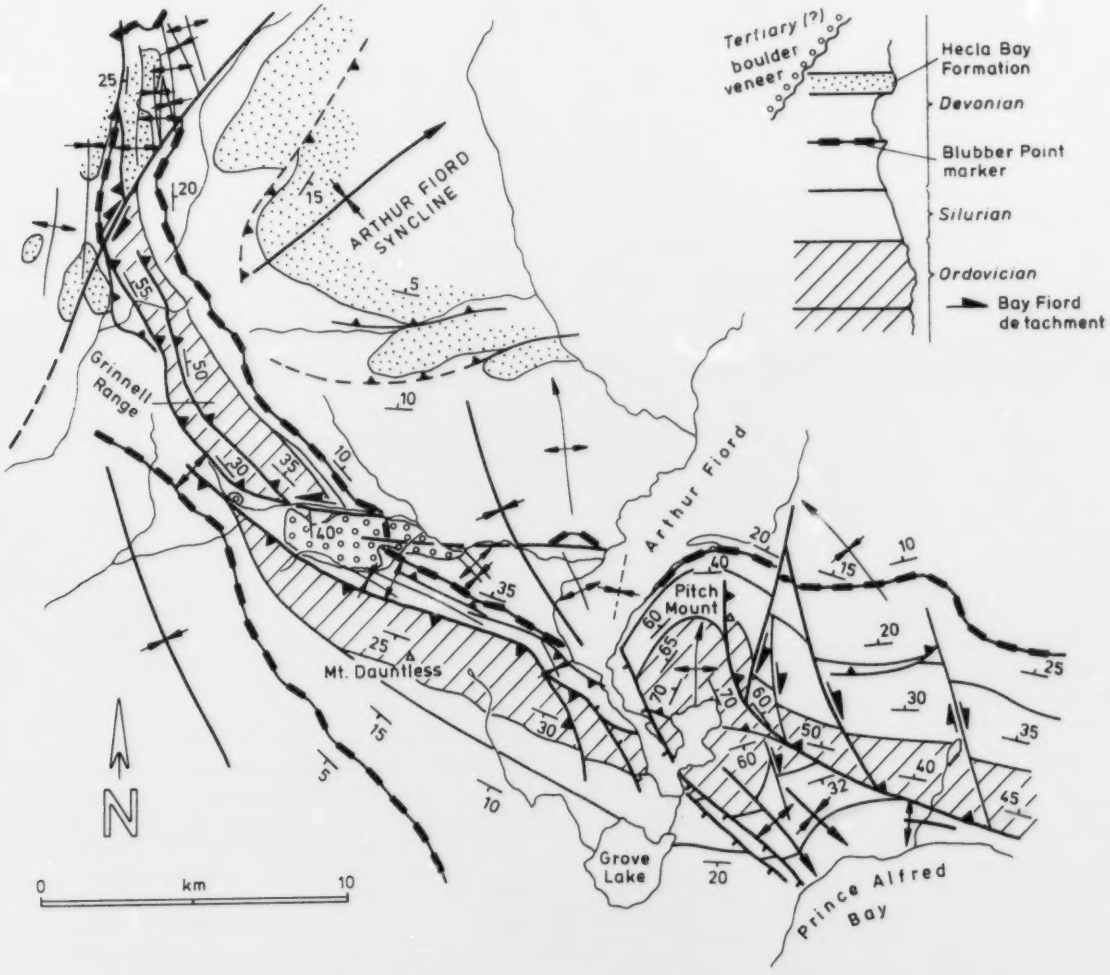

Figure 3. Sketch map of southeastern Grinnell Peninsula, where post-Cornwallis stratigraphic onlap along the Wellington Ensorcellement inflection zone created the complexities of the superposition pattern between the late, northwest-trending Grinnell belt and the earlier, northeast-trending Parry Islands Fold Belt folds and related thrust structures.

interesting examples of regional structures that provide evidence relevant to the kinematics of fault reactivation and the age of the Grinnell belt, are found in the Grinnell Range north of Prince Alfred Bay and on Colin Archer Peninsula north of Eidsbotn.

The frontal Grinnell Range consists of an internally imbricated panel made up of the competent Thumb Mountain/Irene Bay/Allen Bay interval, which was thrust southwest over folded and thrust faulted Devonian strata (Fig. 3). This panel is laterally confined by major north-northeast- and east-trending cross faults, both of which are reactivated Ellesmerian out-of-the-syncline thrust faults, originally related to the northeast-plunging Arthur Fiord Syncline. The north-northeast-trending fault seems to have transferred displacement in a dextral sense, while the east-trending fault on the south accommodated minor sinistral displacement but represents mainly a discontinuity along which thrusting changed from southwest directed to northeast directed. Thus, the structurally elevated core of the Ellesmerian Arthur Fiord Syncline was displaced southwest, akin to the keel of a boat beaching into a yielding substratum; in contrast, the structurally lower area to the south was displaced northeast above a thrust fault. In both cases detachment occurred along Bay Fiord evaporites. The zone located between the two thrust panels contains a gently northeast dipping surface of erosional bevelling covered by a fluvial boulder veneer. This veneer is at an elevation of about 230 m, at the most 10 to 15 m thick, and is made up almost entirely of Okse Bay Group quartzarenite clasts with blocks up to about 1.3 m in diameter and devoid of fine grained layers. This means that, during the tectonic uplift of the Grinnell Range, an alluvial plain, about 1 km wide and floored by bedrock, had developed parallel to the east-trending cross fault. This plain was fed laterally by torrential mountain streams, whose source areas in the Grinnell Range were made up almost entirely of Okse Bay Group quartzarenites. At present, the nearest outcrop of these quartzarenites is the Hecla Bay escarpment, located some 7 km to the north – much of the Grinnell Range immediately north the boulder veneer now consists of pre-Okse Bay carbonate rocks. A reasonable structural interpretation of these relationships requires that southwest directed thrusting of the Grinnell Range panel led to erosion and deposition of coarse Okse Bay quartzarenite material, followed by tectonic uplift of the resulting depositional boulder veneer above erosional base level. Continuing erosional downcutting of the panel reached pre-Okse Bay carbonate strata and caused the retreat of the Hecla Bay escarpment to its present position. Although the age of the boulder veneer is unknown, the relationships discussed above suggest a Tertiary age for both the thrust related uplift of the Grinnell Range panel, with respect to the area to the south, and syndeformational fluvial sedimentation along the fault controlled valley to the south. Near Arthur Fiord, the north-trending and strongly plunging anticline at Pitch Mount, which is probably of Cornwallis and/or Ellesmerian ancestry, induced another switch in structural vergence and, within a short distance to the east, displacement on the thrust fault at the base of the Douro Range increases until Bay Fiord evaporites rest on Devonian carbonate rocks. This pattern of segmentation along the Grinnell belt continues southeast toward Viks Fiord (Fig. 2).

North of Eidsbotn, the lower Paleozoic carbonate–shale strata generally dip less than 10°, and the broadly open folds with west-northwest- to northwest-trending axial surfaces are truncated or displaced by east-northeast-trending high-angle faults. In one area this pattern of faults and folds is linked directly to a short, northeast trending, asymmetrical graben structure (marked SL in Fig. 2). This structure contains an east dipping assemblage of dark green glauconitic sandstone and siltstone with grey tuffaceous bands (collectively about 100 m thick) that grade upward into light grey, silty mudstone with thin layers of resedimented coaly beds (about 30 m thick). Samples from this section have yielded Santonian(?) to Campanian palynomorphs (McIntyre, pers. comm., 1990). From its lithology and age assignment, the lower clastic unit probably correlates with the Upper Cretaceous Kanguk Formation of the adjacent Sverdrup Basin (Balkwill, 1983), and the overlying nonmarine strata correlate with the Paleogene Eureka Sound Group. Normal fault displacement, estimated from the offset of Paleozoic strata, amounts to a total of about 700 to 800 m and probably commenced in latest Cretaceous or Paleogene time, but was sustained during regional contraction as a minor extensional feature linked by

Figure 4. Possible scenario for the post-Eocene intraplate contraction responsible for the deformation along weak lithospheric zones in Arctic Canada, including northwestern Devon Island.

sinistrally convergent high-angle faults. Other high-angle fault systems on and near Devon Island (Kerr, 1980; Thorsteinsson and Mayr, 1987) show similar patterns of fault linkage.

Significance of Eurekan deformation on northwestern Devon Island

Recently published work concerning the latest Cretaceous/Paleogene history of the Arctic Islands has centred on the meaning of the widely distributed clastic deposits of the Eureka Sound Group and their regional tectonic framework (see Miall, 1985, 1988; Ricketts and McIntyre, 1986; DePaor et al., 1989; Okulitch et al., 1990; Okulitch and Trettin, in press). Most of the discrepancies in the interpretations concern the original geometry and size of the Eureka Sound Group basins, the relationships to diffuse crustal extension in and around Baffin Bay, the role of the Nares Strait strike-slip system, and the mechanisms of structural inversion in Sverdrup Basin.

It has been argued forcefully by Kerr and Ruffman (1979), Kerr (1980), Miall (1985, 1988), and Okulitch et al. (1990) that, up to about the mid-Eocene, local sedimentation patterns seem to have been controlled mainly by divergent systems of high-angle faults. However, it also emerges from ongoing discussion that, in many areas of the Arctic Islands, deposition of nonmarine Eureka Sound clastic rocks was terminated in the latest Eocene–Oligocene(?) by folding along north-northwest- to west-trending axes, by oblique dextral convergence along north-northeast- to northeast-trending reverse fault zones, and by broad regional uplift (Miall, 1988).

On northwestern Devon Island, the post-Paleozoic contractional structures suggest the existence of relatively young northeast–southwest oriented intraplate shortening that is compatible with major dextral convergence on nearby Ellesmere Island (e.g., Beauchamp, 1987) and with basin inversion by folding or reverse faulting in adjacent parts of Sverdrup Basin (Balkwill, 1983). As diffuse extension and sea-floor spreading in the Labrador Sea/Baffin Bay system ended in latest Eocene to earliest Oligocene time at about 36 Ma (Shrivastava and Tapscott, 1986), it is possible that generally northwest-trending fold–thrust structures, dextral convergence along reactivated north-northeast-trending high-angle faults, minor extension along northeast-trending grabens, and local sinistrally convergent motion on east- to east-northeast-trending high-angle faults on Devon Island were a response to post-Eocene plate-driving forces that developed simultaneously with the new spreading centres along the North Atlantic/Arctic ridge system (Fig. 4). Continuing diffuse intraplate contraction on and near Devon Island is indicated by the distribution of earthquake epicentres (Adams and Basham, 1989), by youthful land surface and submarine topography, and northeast to east-northeast orientation of the maximum horizontal stress in the area (Zoback et al., 1991). It is possible that in latest Eocene time a southwest directed mantle flow underneath the northeastern North American lithosphere initiated kinematically compatible displacements along weak and suitably oriented faults within the crust, and that this system has continued to be active, in a possibly reduced fashion, up to the present.

ACKNOWLEDGMENTS

The author wishes to acknowledge most-productive discussions with U. Mayr, T. de Freitas, and P. Thériault in the field, and much stimulating input from A. Okulitch upon his return to Calgary.

REFERENCES

Adams, J. and Basham, P.
1989: The seismicity and seismotectonics of Canada east of the Cordillera; Geoscience Canada, v. 16, p. 3-16.

Balkwill, H.R.
1983: Geology of Amund Ringnes, Cornwall, and Haig-Thomas islands, District of Franklin; Geological Survey of Canada, Memoir 390, 76 p.

Balkwill, H.R. and Fox, F.G.
1982: Incipient rift zone, western Sverdrup Basin, Arctic Canada; in Arctic Geology and Geophysics, (ed.) Embry, A.F. and Balkwill, H.R.; Canadian Society of Petroleum Geologists, Memoir 8, p. 171-187.

Beauchamp, B.
1987: Stratigraphy and facies analysis of the Upper Carboniferous to Lower Permian Canyon Fiord, Belcher Channel, and Nansen formations, southwestern Ellesmere Island; Ph.D. thesis, University of Calgary, Calgary, 370 p.

DePaor, D., Bradley, D.C., Eisenstadt, G., and Phillips, S.M.
1989: The Arctic Eurekan Orogen: a most unusual fold-and-thrust belt; Geological Society of America, Bulletin, v. 101, p. 952-967.

Embry, A.F. and Klovan, J.E.
1976: The Middle–Upper Devonian clastic wedge of the Franklinian Geosyncline; Bulletin of Canadian Petroleum Geology, v. 24, p. 485-639.

Embry, A.F. and Osadetz, K.G.
1988: Stratigraphy and tectonic significance of Cretaceous volcanism in the Queen Elizabeth Islands, Canadian Arctic Archipelago; Canadian Journal of Earth Sciences, v. 25, p. 1209-1219.

Fortier, Y.O. et al.
1963: Geology of the north-central part of the Arctic Archipelago, Northwest Territories (Operation Franklin). Geological Survey of Canada, Memoir 320, 671 p.

Fox, F.G.
1985: Structural geology of the Parry Islands Fold Belt; Bulletin of Canadian Petroleum Geology v. 33, p. 306-340.

Frisch, T.
1988: Reconnaissance geology of the Precambrian shield of Ellesmere, Devon and Coburg islands, Canadian Arctic Archipelago; Geological Survey of Canada, Memoir 409, 102 p.

Goodbody, Q.H., Uyeno, T.T., and McGregor, D.C.
1988: The Devonian sequence on Grinnell Peninsula and in the region of Arthur Fiord, Devon Island, Arctic Archipelago; in Current Research, Part D; Geological Survey of Canada, Paper 88–lD, p. 75-82.

Harrison, J.C. and Bally, A.W.
1988: Cross-sections of the Parry Islands Fold Belt on Melville Island, Canadian Arctic Islands: implications for the timing and kinematic history of some thin-skinned décollement systems; Bulletin of Canadian Petroleum Geology, v. 36, p. 311-332.

Harrison, J.C., Embry, A.F., and Poulton, T.P.
1988: Field observations on the structural and depositional history of Prince Patrick Island and adjacent areas, Canadian Arctic Islands; in Current Research, Part D; Geological Survey of Canada, Paper 88–lD, p. 41-49.

Kerr, J. Wm.
1974: Geology of Bathurst Island Group and Byam Martin Island, Arctic Canada (Operation Bathurst Island); Geological Survey of Canada, Memoir 378, 152 p.

1976: Geology of outstanding arctic aerial photographs 3, Margin of Sverdrup Basin, Lyall River, Devon Island; Bulletin of Canadian Petroleum Geology, v. 24, p. 139-153.
1977: Cornwallis Fold Belt and the mechanism of basement uplift; Canadian Journal of Earth Sciences, v. 14, p. 1374-1401.
1980: Structural framework of Lancaster aulacogen, Arctic Canada; Geological Survey of Canada, Bulletin 319, 24 p.
1981: Evolution of the Canadian Arctic Islands: a transition between the Atlantic and Arctic oceans; in The Ocean Basins and Margins, (ed.) A.E.M. Nairn, M. Churkin, and F.G. Stehli; v. 5, The Arctic Ocean, p. 105-199.

Kerr, J. Wm. and Ruffman, A.
1979: The Crozier Strait Fault Zone, Arctic Archipelago, Northwest Territories, Canada; Bulletin of Canadian Petroleum Geology, v. 27, p. 39-52.

Klaper, E.M.
1990: The mid-Paleozoic deformation in the Hazen Fold Belt, Ellesmere Island, Arctic Canada; Canadian Journal of Earth Sciences, v. 27, p. 1359-1370.

Miall, A.D.
1985: Stratigraphic and structural predictions from a plate-tectonic model of an oblique-slip orogen: the Eureka Sound Formation (Campanian–Oligocene), northeast Canadian Arctic Islands; in Strike-slip Deformation, Basin Formation, and Sedimentation, (ed.) K.T. Biddle and N. Christie-Blick; Society of Economic Paleontologists and Mineralogists, Special Publication 37, p. 361-374.
1986: Effects of Caledonian tectonism in Arctic Canada; Geology, v. 14, p. 904-907.
1988: The Eureka Sound Group: alternative interpretations of the stratigraphy and paleogeographic evolution — discussion; in Current Research, Part D; Geological Survey of Canada, Paper 88-1D, p. 143-147.

Morrow, D.W. and Kerr, J. Wm.
1977: Stratigraphy and sedimentology of lower Paleozoic formations near Prince Alfred Bay, Devon Island; Geological Survey of Canada, Bulletin 254, 122 p.
1986: Geology of Grinnell Peninsula and the Prince Alfred Bay area, Devon Island, District of Franklin, Northwest Territories; Geological Survey of Canada, Open File 1325.

Okulitch, A.V.
1982: Preliminary structure sections, southern Ellesmere Island, District of Franklin; in Current Research, Part A; Geological Survey of Canada, Paper 82-1A, p. 55-62.

Okulitch, A.V. and Trettin, H.P.
in press: Cretaceous–Early Tertiary deformation of the Arctic Islands; in Innuition Orogen and Arctic Platform, Canada and Greenland, (ed.) H.P. Trettin; Geological Survey of Canada, Geology of Canada, v. 3.

Okulitch, A.V., Dawes, P.R., Higgins, A.K., Soper, N.J., and Christie, R.L.
1990: Towards a Nares Strait solution: structural studies on southeastern Ellesmere Island and northwestern Greenland; Marine Geology, v. 93, p. 369-384.

Okulitch, A.V., Packard, J.J., and Zolnai, A.I.
1986: Evolution of the Boothia Uplift, Arctic Canada; Canadian Journal of Earth Sciences, v. 23, p. 350-358.

Ricketts, B.D. and McIntyre, D.J.
1986: The Eureka Sound Group of eastern Axel Heiberg Island: new data on the Eurekan Orogeny; in Current Research, Part B; Geological Survey of Canada, Paper 86-1B, p. 405-410.

Shrivastava, S.P. and Tapscott, C.R.
1986: Plate kinematics of the North Atlantic; in The Western North Atlantic Region, (ed.) P.R. Vogt and B.E. Tucholke; Geological Society of America, Geology of North America, v. M, p. 379-404.

Smith, G.P. and Okulitch, A.V.
1987: The Inglefield Uplift: a Devonian tectonic element, Ellesmere Island, Arctic Canada; Bulletin of Canadian Petroleum Geology, v. 35, p. 75-78.

Sweeney, J.F. et al.
1986: North American Continent–Ocean Transects Program Transect G: Canadian Arctic: Somerset Island to Canada Basin; Geological Society of America, Centennial Continent/Ocean Transect 11.

Thorsteinsson, R.
1988: Geology of Cornwallis Island and neighbouring smaller islands, Canadian Arctic Archipelago, District of Franklin, Northwest Territories; Geological Survey of Canada, Map 1626A (scale 1:250 000).

Thorsteinsson, R. and Mayr, U.
1987: The sedimentary rocks of Devon Island, Canadian Arctic Archipelago; Geological Survey of Canada, Memoir 411, 182 p.

Thorsteinsson, R. and Uyeno, T.T.
1980: Stratigraphy and conodonts of Upper Silurian and Lower Devonian rocks in the environs of the Boothia Uplift, Canadian Arctic Archipelago; Geological Survey of Canada, Bulletin 292, 75 p.

Trettin, H.P.
1989: The Arctic Islands; in The Geology of North America — An Overview, (ed.) A.W. Bally and A.R. Palmer; Geological Society of America, Geology of North America, v. A, p. 349-370.

Zoback, M.L. et al.
1991: Stress map of North America. Geological Society of America, Decade of North American Geology, Continent-scale Map-005 (scale 1:5 000 000).

Geological Survey of Canada Project 850039

Cambro-Ordovician stratigraphy of Grinnell Peninsula, northern Devon Island, Northwest Territories

Ulrich Mayr and T. de Freitas
Institute of Sedimentary and Petroleum Geology, Calgary

Mayr, U. and de Freitas, T., 1992: Cambro-Ordovician stratigraphy of Grinnell Peninsula, northern Devon Island, Northwest Territories; in Current Research, Part B; Geological Survey of Canada, Paper 92–1B, p. 47-52.

Abstract

About 3000 m of Cambrian to Upper Ordovician rocks are exposed on Grinnell Peninsula, northern Devon Island. These rocks belong to six formations, the upper five of which (in descending order the Irene Bay, Thumb Mountain, Bay Fiord, Eleanor River, and Baumann Fiord formations) are similar to their equivalents farther east on southern Ellesmere Island. The sixth, unnamed, formation, comprises the lowest part of the succession, and its upper part is eqivalent to the Baumann Fiord Formation. The unnamed formation contains large stromatolitic mounds and grainstone lenses and is interpreted as having been deposited near the margin of the Cambro–Ordovician carbonate shelf.

Résumé

Dans la péninsule de Grinnell, dans le nord de l'île Devon, affleurent environ 3 000 m de roches échelonnées du Cambrien à l'Ordovicien supérieur. Ces roches appartiennent à six formations, dont les cinq supérieures (selon un ordre descendant: formations d'Irene Bay, de Thumb Mountain, de Bay Fiord, d'Eleanor River et de Baumann Fiord) sont semblables à leurs équivalents plus à l'est situés dans le sud de l'île d'Ellesmere. La sixième formation, non dénommée, englobe la partie la plus basse de la succession, et sa partie supérieure est équivalente à la formation de Baumann Fiord. La formation non dénommée contient de vastes monticules stromatolitiques et lentilles de grainstone, et se serait constituée par sédimentation près de la marge de la plate-forme carbonatée cambro-ordovicienne.

INTRODUCTION

Most of the Cambrian and Ordovician rocks of Grinnell Peninsula are exposed in three major, north-south trending anticlines, which form the main structural elements of central and western Grinnell Peninsula. These are the Mount Fitzroy and Barrow Harbour anticlines and the Ensorcellement Dome (Fig. 1). Less extensively exposed Cambro–Ordovician strata occur in the Grinnell Range, just west of the head of Arthur Fiord. Information on some aspects of Cambro–Ordovician stratigraphy and a number of measured sections have been published previously (Morrow and Kerr, 1977, 1986) and these data have been incorporated, after field verification, into the present report. The Cambro–Ordovician sequence exposed in the Barrow Harbour Anticline is stratigraphically complex and was given particular attention during fieldwork in 1991. The oldest rocks known on Grinnell Peninsula are exposed in this anticline. These rocks are Cambrian to Early Ordovician in age and correlative with the combined Baumann Fiord, Christian Elv, Cape Clay, and Cass Fjord formations of southern Ellesmere Island to the east, but are different in lithology and evidently represent a new formation (Fig. 2), as yet unnamed. In contrast, the partly equivalent Baumann Fiord Formation, and overlying formations (the Irene Bay, Thumb Mountain, Bay Fiord, and Eleanor River formations) are comparable to strata exposed in southern and central Ellesmere Island.

IRENE BAY FORMATION

Along the Grinnell Range the Irene Bay Formation (Late Ordovician, Ashgill) is very thin and poorly exposed. No outcrops of the formation were examined there during the 1991 field season. The Irene Bay Formation is commonly represented by light grey-green weathering felsenmeer or by a muddy depression between resistant limestones of the overlying and underlying Allen Bay and Thumb Mountain formations.

Along the flanks of the Barrow Harbour Anticline the Irene Bay Formation is better exposed. In a section near Cape Sir John Franklin, the Irene Bay Formation is 25 m thick and consists of green shale and interbedded, nodular, argillaceous limestone. In contrast to occurrences elsewhere in the Arctic Islands, the Irene Bay Formation of Grinnell Peninsula is only sparsely fossiliferous.

THUMB MOUNTAIN FORMATION

The Thumb Mountain Formation (Middle to Late Ordovician, late Caradoc to early Ashgill) is about 130 m thick in the Grinnell Range and on the east side of the Barrow Harbour Anticline (Morrow and Kerr, 1977, 1986). On the west side of the Mount Fitzroy Anticline it is about 280 m thick. The formation weathers brown with a very resistant profile, in contrast to the underlying recessive and greenish weathering Bay Fiord Formation.

In the section near Barrow Harbour the Thumb Mountain Formation consists entirely of limestone. In contrast, dolostone and a lesser amount of limestone are present in the section near Cape Sir John Franklin. The rock types of the lower part of the formation include grainstone, cryptalgal laminated limestone, and minor flat-pebble conglomerate. The upper part consists of massive, burrowed and fossiliferous dolostone or limestone and probably was deposited in slightly deeper water than the lower part of the formation.

BAY FIORD FORMATION

The Bay Fiord Formation (Middle Ordovician, late Arenig to Llandeilo) is exposed in the western half of Grinnell Peninsula and at the base of the Grinnell Range on southeastern Grinnell Peninsula, where it forms the main detachment zone for northeast-verging thrust faults below the mountain range. In the Grinnell Range the formation consists of very dark grey, thin bedded dolostone with flat-pebble conglomerate and foliated and contorted gypsum with broken dolostone interbeds. Its thickness in southeastern Grinnell Peninsula is unknown.

On western Grinnell Peninsula, on the east side of the Barrow Harbour Anticline, the formation is about 180 m thick (Morrow and Kerr, 1986). Its thickness near Cape Sir John Franklin is about 420 m. The Bay Fiord Formation on western Grinnell Peninsula consists predominantly of thin bedded and laminated dolostone and limestone. These carbonate rocks weather light green and are recessive. Evaporites, characteristic of the formation farther east, were seen at only a single location on the north side of Hawker Bay. An additional significant rock type of the Bay Fiord Formation on western Grinnell Peninsula is solution breccia; it occurs in units that may exceed 70 m in thickness.

Morrow and Kerr (1986) mapped several occurrences of the Bay Fiord Formation that are overlain unconformably by Devonian carbonates of the Blue Fiord Formation, along the northeastern margin of the Ensorcellement Dome. Carbonate breccias below the unconformity are similar to those in the

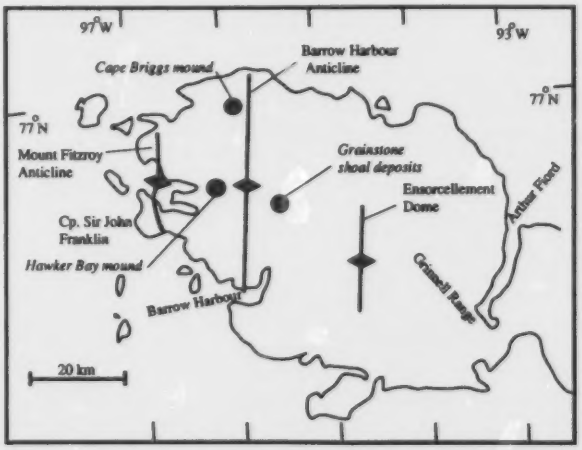

Figure 1. Index map of Grinnell Peninsula, northern Devon Island.

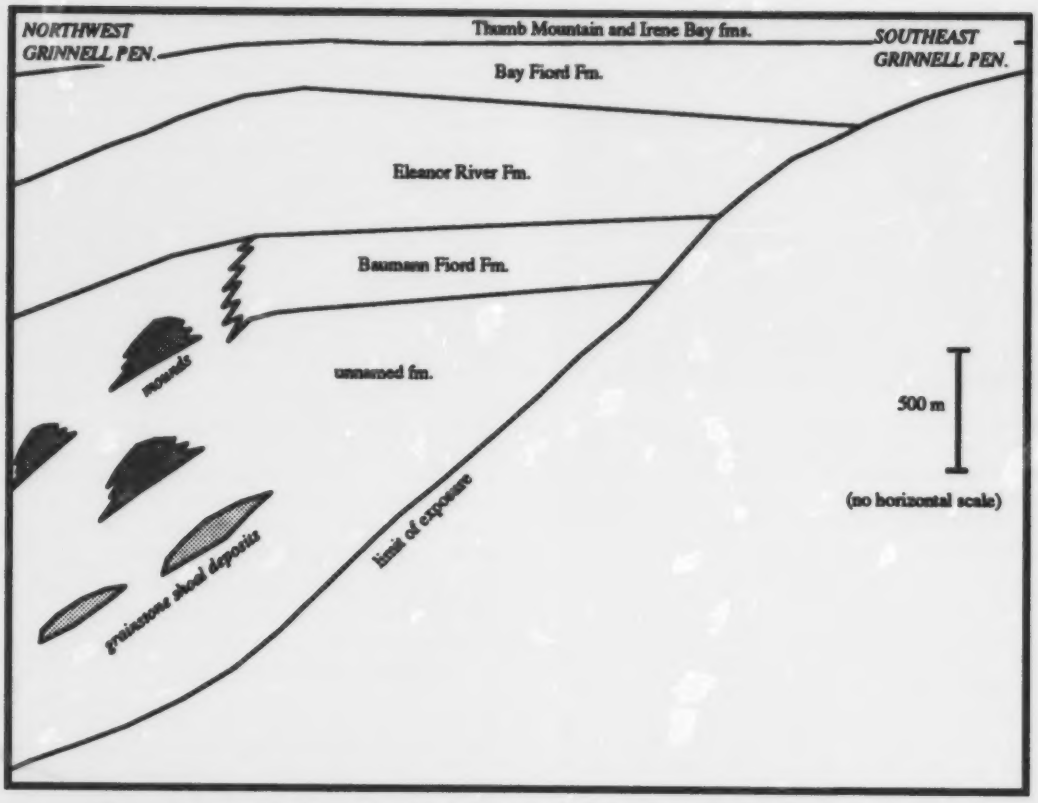

Figure 2. Stratigraphic cross-section from northwest to southeast across Grinnell Peninsula. The unnamed formation is correlative with the Christian Elv, Cape Clay, and Cass Fjord formations of southern Ellesmere Island.

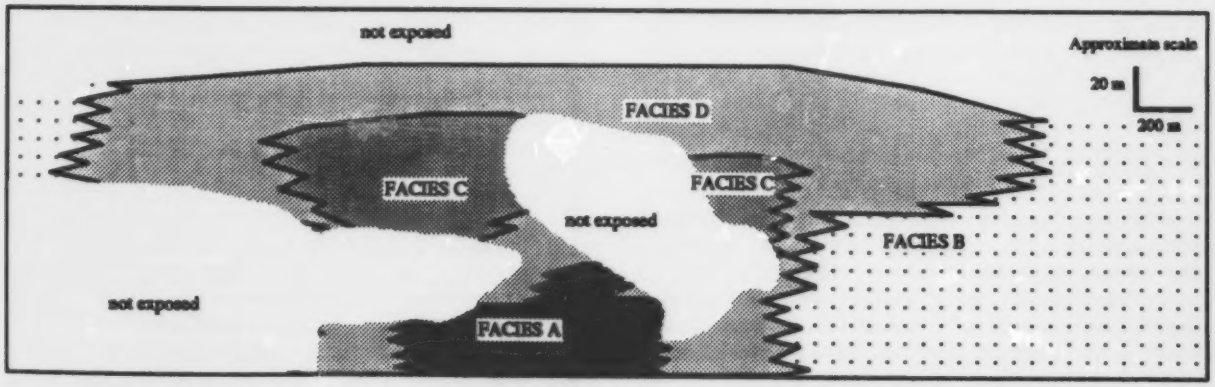

Figure 3. Facies relationships in the largest Hawker Bay carbonate mound. A – Inter-reef grainstone mound facies; B – Off-reef bedded lime mudstone and minor grainstone; C – Core facies of large microbial heads; D – Flank and cap facies of microbial heads.

Figure 4. Thrombolite/stromatolite heads in the largest Hawker Bay mound. The horizontal surface shows parts of four heads. Note the mottled thrombolitic core and the light grey cortex in each of the heads. Pencil point is resting on sediment deposited between the heads. ISPG photo. 3793–159.

Bay Fiord Formation on western Grinnell Peninsula, but in some exposures there is evidence of deposition by mass flow, which is atypical of the Bay Fiord Formation. On the other hand, evidence of mass flow is present in breccia of the Prince Alfred Formation (Lower Devonian) near Sutherland River, and for this reason some "Bay Fiord" outcrops on the northeast side of Ensorcellement Dome have been tentatively reassigned to the Prince Alfred Formation.

ELEANOR RIVER FORMATION

The Eleanor River Formation (Early Ordovician, late Tremadoc–early Arenig) is about 600 m thick on the east side of the Barrow Harbour Anticline (Morrow and Kerr, 1986), and about 650 m on the south side of Hawker Bay. Three members constitute the Eleanor River Formation. The Lower and Upper members are dark brown and resistant, whereas the Middle member is light grey-brown and is less resistant to weathering. Member thicknesses vary greatly, but generally the Middle member is the thickest.

The Upper member consists of massive limestone with minor dolostone in the Cape Sir John Franklin area. The limestone is a mottled skeletal wackestone in the lower part of the formation and a grainstone in the upper part. The Middle member of the Eleanor River Formation consists mostly of a mudcracked, very thin to thin bedded or laminated limestone with interbeds of flat-pebble conglomerate, and thicker bedded grainstone and stromatolitic beds. Most of the laminated limestone is cryptalgal laminite, although sedimentary lamination also occurs. Locally, the Middle member contains abundant, large gastropods. The Lower member consists of mottled skeletal wackestone with interbeds of grainstone.

BAUMANN FIORD FORMATION

The Baumann Fiord Formation (Early Ordovician, Tremadoc) outcrops in the central part of Ensorcellement Dome and in the vicinity of Barrow Harbour, along the eastern and southern sides of the Barrow Harbour Anticline. The formation is absent farther west or north in the Mount Fitzroy Anticline and in the northern part of the Barrow Harbour Anticline. There the Eleanor River formation is underlain directly by an unnamed Cambrian-Ordovician formation.

At Barrow Harbour the Baumann Fiord Formation is about 350 m thick and is divisible into three members. The Upper member is about 90 m thick and consists of laminated anhydrite, interbedded with stromatolitic beds and very thin bedded silty dolostone containing flat-pebble conglomerate. Thickness of the Middle member is variable, ranging from a few metres to an estimated 80 m, and it consists entirely of stromatolitic and thrombolitic rocks, which occur as large, broad mounds. The Lower member is lithologically similar to the Upper member and comprises anhydrite with interbeds consisting of large stromatolite heads and thin bedded dolostone.

UNNAMED FORMATION

In Barrow Harbour Anticline, the Eleanor River Formation and, where present, the Baumann Fiord Formation, are underlain by an unnamed formation that is at least 1900 m thick. The unnamed formation is at least as old as Late Cambrian, ranging to late Early Ordovician (Tremadoc). This age assessment is based on a preliminary conodont determination from the eastern flank of the Barrow Harbour

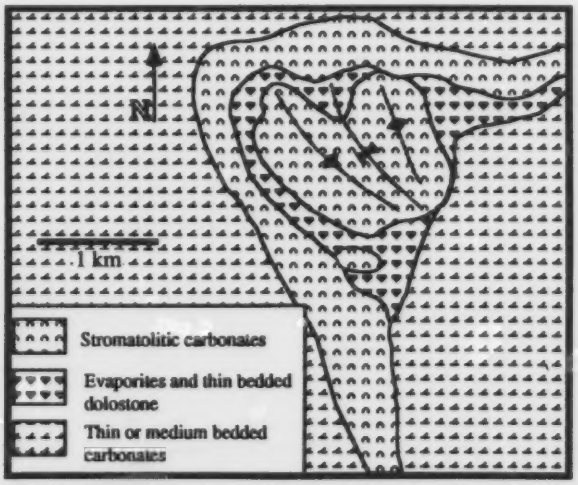

Figure 5. Map of the Cape Briggs stromatolitic mound. The mound is embedded in thin or medium bedded carbonate rocks, which have a regional dip to the northwest. The mound consists of a core of three smaller mounds and an outer, draping layer of stromatolitic beds.

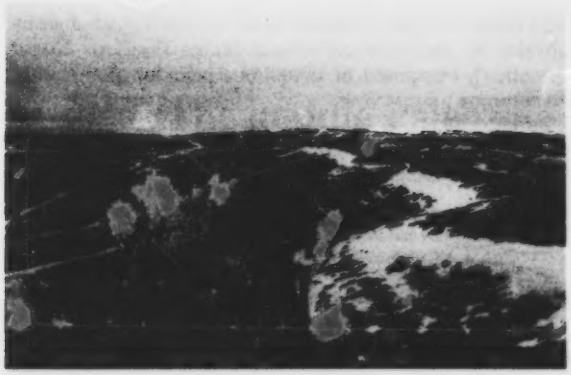

Figure 6. View north along the eastern limb of Barrow Harbour Anticline. The ridge shown on the right side of the photograph is underlain by grainstone and stromatolitic limestone. ISPG photo. 3797–49.

Anticline (GSC loc. C-155059; G.S. Nowlan, pers. comm., 1988). The unnamed formation is equivalent to the Baumann Fiord, Christian Elv, Cape Clay, and Cass Fjord formations of southern Ellesmere Island, and to the Copes Bay and Parrish Glacier formations of central Ellesmere Island.

The unnamed formation consists predominantly of recessive weathering, light grey and light brown, thin and very thin bedded lime mudstone. Dolomitic limestone and dolostone units appear to be rare. Planar and ripple crosslamination and polygonal mudcracks are common in the limestone. The thin bedded limestone is interbedded with thin beds of flat-pebble conglomerate, stromatolitic and thrombolitic beds, minor sandstone, and thin and medium bedded, burrowed limestone.

Stromatolitic mounds and isolated grainstone shoal deposits are characteristic of the unnamed formation. Two spectacular examples of microbial mounds were examined near Hawker Bay and Cape Briggs.

Near Hawker Bay, three mounds have been incised deeply by a west flowing river. The largest mound rests stratigraphically between the two smaller mounds and was examined in detail during four days of fieldwork in 1991. Main facies of the three mounds are comparable. The two smaller mounds are 0.3 to 0.8 km wide and 40 to 80 m thick; the largest mound is 2 to 2.8 km wide and more than 200 m thick. Mound strata are predominantly massive limestone in the otherwise well bedded limestone–dolostone sequence that is typical of the unnamed formation. These strata display distinctive draping over the massive mound beds. These mounds appear to be the largest Ordovician mounds known, and they contain unusual internal structures.

Four distinct facies occur in the largest mound near Hawker Bay (A to D in Fig. 3): A) an inter-reef grainstone-mound facies; B) an off-reef bedded lime mudstone and minor grainstone facies; C) a core facies containing large thrombolite/stromatolite heads of microbial origin; and D) a flank or cap facies with somewhat smaller thrombolite/stromatolite heads than in facies C. The mound is progradational in the upper part and displays facies that represent expansion and the amalgamation of other distinct mounds in the lower part.

Microbial "heads" (Fig. 4) dominate all mound facies and are unusual. Heads range in size from more than 10 m wide and 5 m high in facies D to 12 m wide and 3 to 4 m high in facies C. Larger heads of facies C form laterally elongated pillars and possess cortical stromatolitic-*Renalcis* structures; internal, vertically stacked, digitate hemispheroid stromatolites; and irregular internal thrombolites. Gastropods and cephalopods are present, particularly between heads, but are uncommon.

Microbial heads of facies C are larger than those of facies D and are built predominantly of thrombolites. Siliceous lithistid sponges (now calcitized) are also a conspicuous part of the strata between heads in this facies. The heads show much less vertical continuity and are in places upward digitate. Elongate heads show a consistent northwest orientation and are assumed to have grown perpendicular to the direction of the predominant wave energy. Thick, well sorted grainstone beds, occurring in most mound facies, are evidence of growth in shallow, agitated water.

The Cape Briggs mound is about 2.5 km wide and consists of two distinct stratigraphic sequences (Fig. 5). The inner, lower sequence is formed by three separate, ellipsoidal mounds that are up to 1.5 km in length. Gypsum and very thin bedded dolostone surround and overlie these internal mounds. The three internal mounds and the evaporites and dolostone form the core facies over which beds of the larger, outer part of the mound are draped. The bedding of the entire mound is laterally and vertically uniform and each bed consists of a single layer of large stromatolite heads up to 5 m in diameter. Individual heads in the inner mounds contain thin (1 to 2 cm in diameter) columnar, branching stromatolites; in addition, the outer mound beds contain thrombolitic heads.

The topographic expression of the unnamed formation in the Barrow Harbour Anticline is characterized by long (10 km or more) topographic ridges and domal hills (Fig. 6). These features are capped by beds of resistant weathering stromatolites and by large, bedded grainstone lenses. One of these grainstone lenses, situated in the core of the Barrow Harbour Anticline, was examined in detail. It has a length of at least 6 km, and a minimum width of 2 km. It is formed by a number of smaller lenses, each with an exposure width of about 300 to 500 m. The smaller individual lenses are about 10 to 15 m thick and consist of thin bedded to massive grainstone. Ripple crosslamination is present in some beds. Thrombolitic units, flat-pebble conglomerate and burrowed limestone, locally with flaser bedding, form minor constituents of the grainstone lenses.

CONCLUSIONS

The Ordovician and Cambrian rocks of Grinnell Peninsula were part of an extensive and thick lower Paleozoic carbonate shelf extending from Greenland to Arctic Canada (Trettin, 1989). The carbonate rocks and associated evaporites in the

interior of this shelf were deposited in subtidal and peritidal settings. The unnamed formation of Grinnell Peninsula forms a unique Cambro–Ordovician sequence in the Arctic Islands. Its facies are representative of deposition on a platform margin and are in marked contrast to the platform interior facies, which occur farther east on Devon Island and throughout much of the Arctic Islands. Giant stromatolite mounds and high-energy carbonate grainstone deposits characterized the platform margin environments on western Grinnell Peninsula, and periodically formed an extensive barrier that contributed to the deposition of peritidal sediments (Cass Fjord and Christian Elv formations) or evaporites (Baumann Fiord Formation) in the platform interior. A comparable relationship has been observed in somewhat younger strata at the platform margin on southwestern Judge Daly Promontory in north-central Ellesmere Island (Trettin, 1989). There, facies of a subtidal intrashelf basin of Early to Middle Ordovician age (equivalent to the Baumann Fiord, Eleanor River, and Bay Fiord formations) are bordered on the northwest by a shallow subtidal to peritidal carbonate facies (Bulleys Lump Formation), composed of ubiquitous peloidal microbalites and common grainstones.

REFERENCES

Morrow, D.W. and Kerr, J.Wm.

1977: Stratigraphy and sedimentology of lower Paleozoic formations near Prince Alfred Bay, Devon Island; Geological Survey of Canada, Bulletin 254.

1986: Geology of Grinnell Peninsula and Prince Alfred area, Devon Island, District of Franklin, Northwest Territories; Geological Survey of Canada, Open File Report 1325.

Trettin, H.P.

1989: The Arctic Islands; in The Geology of North America – An overview, (ed.) A.W. Bally, and A.R. Palmer; Geological Society of America, The Geology of North America, v. A.

Geological Survey of Canada Project 850039

The middle Paleozoic sequence of northern Devon Island, Northwest Territories

T. de Freitas and U. Mayr
Institute of Sedimentary and Petroleum Geology, Calgary

de Freitas, T. and Mayr, U., 1992: The middle Paleozoic sequence of northern Devon Island; in Current Research, Part B; Geological Survey of Canada, Paper 92–1B, p. 53-63.

Abstract

The middle Paleozoic sequence of northern Devon Island is extremely variable lithologically. Formations widely distributed in the eastern part of the study area and in many areas of the Arctic Archipelago were deposited on the shelf interior and are isochronous with the shelf-margin oolitic grainstone and reef lithofacies that outcrop on western Grinnell Peninsula. Uplift of western Grinnell Peninsula, which constitutes a northern segment of Boothia Uplift, and low amplitude flexure of the Paleozoic sequence occurred near, and east of, the Douro Range in the Lower Devonian. Breccias formed in the foundered platform sequence east of the Douro Range and in paleo-lows associated with the unconformity on central Grinnell Peninsula, and sandstone and conglomerates were deposited proximally to the uplift and in depressions associated with platform flexure. During Emsian and Eifelian time, the uplift remained a positive feature, as suggested by the facies changes within, and onlapping relationship of, the Blue Fiord Formation and parts of the Bird Fiord Formation; however, little detritus was shed from the structure during this time.

Résumé

La séquence du Paléozoïque moyen dans le nord de l'île Devon présente une très grande variabilité lithologique. Les formations, largement distribuées dans la partie orientale de la région étudiée et dans de nombreuses régions de l'archipel Arctique, sont le résultat de la sédimentation dans la portion interne de la plate-forme et sont contemporaines du grainstone oolitique de la marge de la plate-forme et du lithofaciès récifal, qui affleurent dans l'ouest de la péninsule de Grinnell. Le soulèvement de l'ouest de la péninsule de Grinnell, qui constitue un fragment septentrional du soulèvement de Boothia, et la flexure de faible amplitude de la séquence paléozoïque, sont apparus à proximité et à l'est du chaînon Douro dans les strates du Dévonien inférieur. Des brèches formées dans la séquence de plate-forme effondrée à l'ouest du chaînon Douro et dans les paléodépressions associées à la discordance présente dans le centre de la péninsule de Grinnell, ainsi qu'un grès et des conglomérats, se sont déposés en position proximale par rapport au soulèvement et dans des dépressions associées à la flexure de la plate-forme. Au cours de l'Emsien et de l'Eifélien, le soulèvement est demeuré une structure positive, comme le suggèrent les variations de faciès à l'intérieur de la formation de Fiord et de parties de la formation de Blue Fiord, et les recouvrements partiels de ces formations; cependant, peu de matériaux détritiques provenaient de cette structure à cette époque.

INTRODUCTION

The northern part of Devon Island is stratigraphically and structurally complex. The following represents a preliminary account of the Upper Ordovician to Upper Devonian stratigraphy of Grinnell and Colin Archer peninsulas (Fig. 1). This report highlights data collected during the 1991 field season in addition to information published by Goodbody et al. (1988) and by Prosh et al. (1988).

ALLEN BAY FORMATION

On Colin Archer Peninsula, three distinct members are recognized, herein referred to as the Lower, Middle, and Upper members of the Allen Bay Formation (Table 1).

The *Lower member* generally comprises a sparsely fossiliferous, thickly stylobedded or massive, pale olive to pale yellowish brown, finely crystalline, mottled dolomitic limestone. At locality 33 (Fig. 1) near Sandhook Bay, where the only complete section was measured, the Lower member is 170 m thick, and contains, in the lower part, an approximately 3 m thick, rubbly, greyish green weathering lime mudstone unit that is lithologically similar to the underlying Irene Bay Formation.

The lower contact with the Irene Bay Formation and the upper contact with the Middle member are sharp and conformable; it has been suggested that the latter contact is unconformable and is related to a glacioeustatic sea-level fall spanning the Ordovician–Silurian boundary (Thorsteinsson and Mayr, 1987), but fossil identifications from the Sandhook Bay locality are lacking or in progress, and lithological evidence does not support this contention. The upper contact is placed at the base of the lowest sequence containing light brown and grey, laminated, bioclastic-rich calcisiltite and calcarenite, and the lower contact is placed above the light greyish green, rubbly weathering limestone beds of the Irene Bay Formation.

The tripartite division of the Allen Bay Formation recognized in the eastern part of the study area generally does not occur in western and central Grinnell Peninsula. Although the lower, mottled, dolomitic limestone member occurs in parts of Grinnell Peninsula, it is less than 2 to 5 m thick and is overlain by a thin argillaceous limestone and calcareous mudrock unit, approximately 40 cm thick, that has yielded abundant *Orthograptus fastigatus*, a common middle Ashgill graptolite in the Arctic Islands. This unit represents a thin tongue of the Cape Phillips Formation in onlapping relationship with the platform carbonates. Also, onlapping appears to have coincided with widespread platform backstepping in the Arctic Islands, and with the development of a deep-water basin west of Grinnell Peninsula.

The *Middle member* comprises very resistant, petroliferous, thickly stylobedded and massive, finely to medium crystalline, pale yellowish brown to light brown dolostone. No complete sections of the Middle member were measured, although it is at least 410 m thick (loc. 34). The member is thoroughly bioturbated (ichnofabric index of about 4 or 5, on the scale of Droser and Bottjer, 1986) and

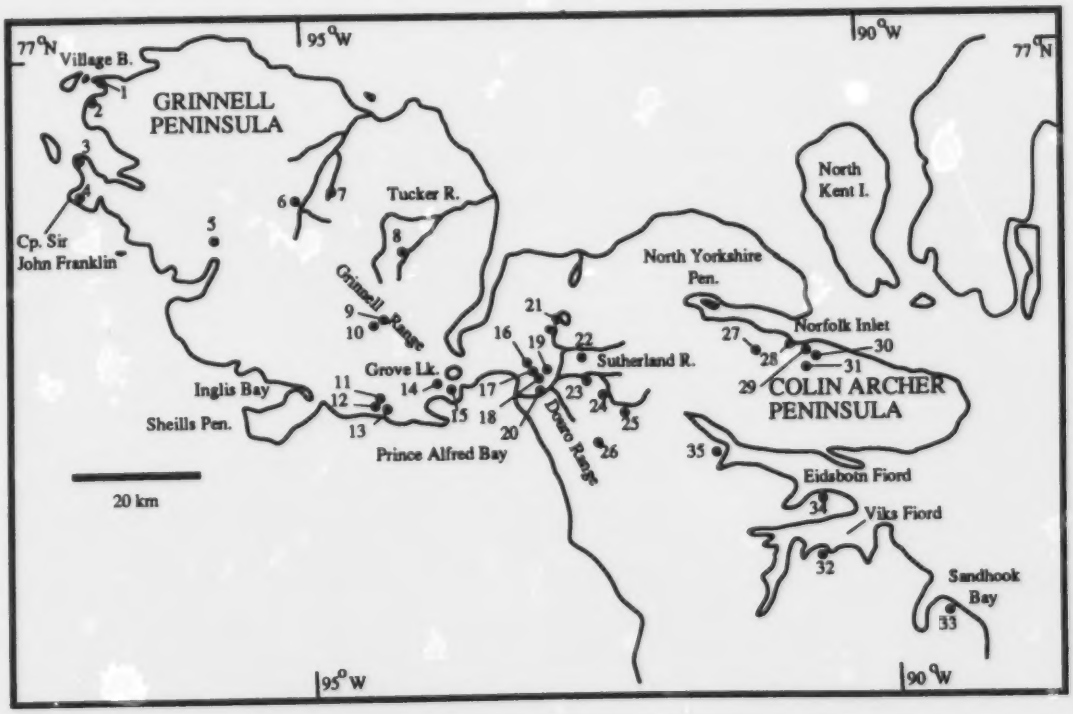

Figure 1. Study localities on northern Devon Island.

very fossiliferous. Common disarticulated pentamerid bivalve beds, up to 3 m thick, are interbedded with sparsely fossiliferous dololutite and stromatoporoid floatstone. Several small dololutite-rich stromatoporoid mounds occur at localities 33 and 35. Near the top of the member, in the eastern part of the study area (particularly at locality 35), stromatoporoid boundstone and floatstone biostromes are common in the basal parts of 2 to 5 m thick rhythms (Fig. 2).

The contact with the overlying Upper member is gradational over several metres and is placed below the lowest interval in section where light grey and yellowish grey dolostone predominates over brown dolostone. In the Douro and Grinnell ranges, this contact is not so well defined. Calcareous grainstone units, several metres to tens of metres thick, are common and represent eastern tongues of the platform margin facies. These units are uncharacteristic of the Upper member. Similarly, as discussed below, the Cape Storm Formation, although lithologically distinct in the eastern part of the study area, also shows a westward interfingering with the shelf margin facies, such that the formation is not recognizable in the southern part, and west of, the Grinnell Range.

The *Upper member* is 320 to 370 m thick and is characterized by thin to medium bedded, yellowish grey, light grey, and light yellowish brown, finely crystalline dolostone and, locally, limestone. The basal part contains abundant and distinct shallowing-upward rhythms, as discussed above (Fig. 2), which are particularly well developed at the base of the Upper member and at the top of the Middle member. Subtidal parts of the rhythms are progressively replaced by microbialites and other tidal deposits in the upper part of the member, so that individual rhythms are not identifiable in that interval.

In the eastern part of the study area, on Colin Archer Peninsula and along the southern shore of Eidsbotn Fiord, the upper contact with the Cape Storm Formation is sharp and is placed below the first yellowish grey, thin to medium bedded, silty dolostone. The contact corresponds to a break in slope and to an increase in the abundance of interbeds of light and

Table 1. Upper Ordovician to Upper Devonian Stratigraphy of Grinnell and Clin Archer peninsulas

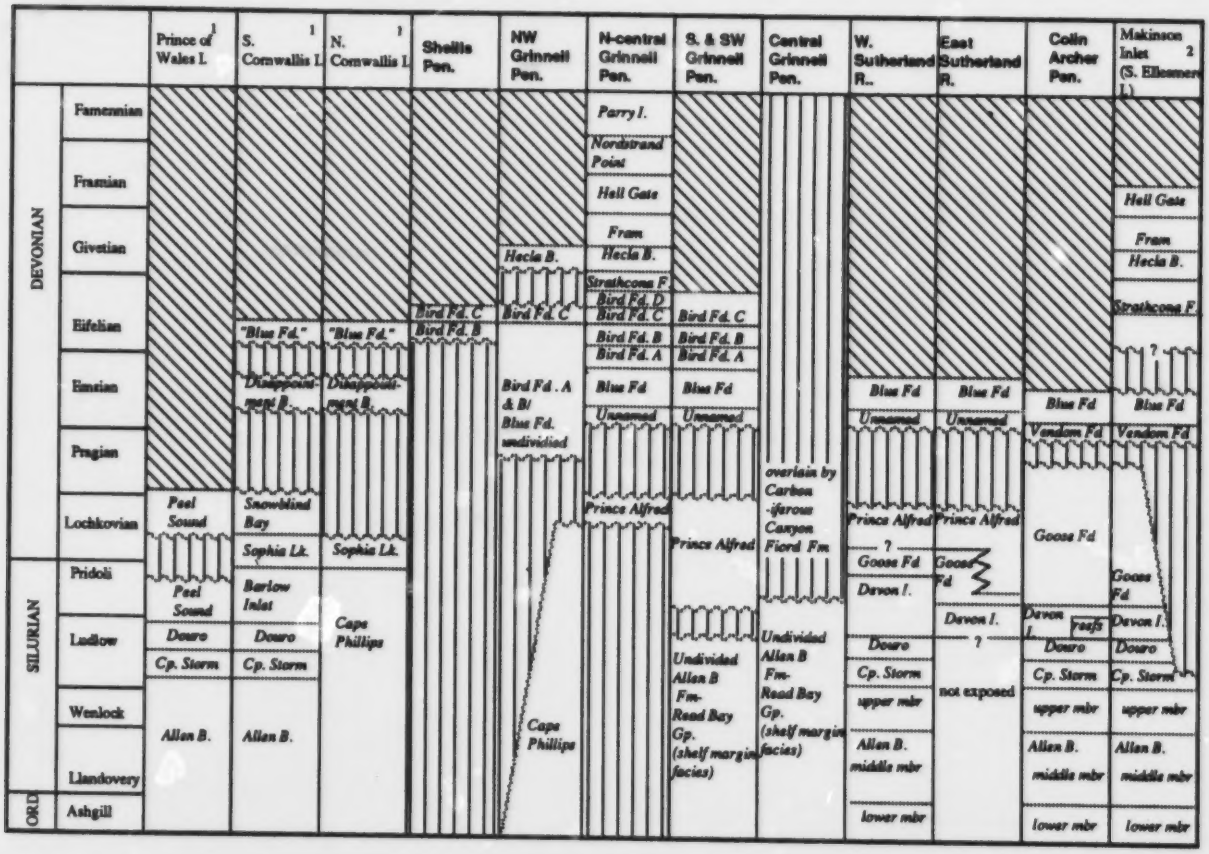

dark brown and yellowish grey dolostone that gives the Cape Storm Formation a distinctly striped appearance in outcrop. In the Douro Range, this contact is not as well defined, and, although the contact is identified on approximately the same criteria, the Cape Storm Formation beds are not as arenaceous, and the break in slope is not as prominent as in the east.

ALLEN BAY FORMATION – READ BAY GROUP UNDIVIDED (shelf margin carbonate facies of western and central Grinnell Peninsula)

A stratigraphically important facies change occurs in the study area. On central and western Grinnell Peninsula, up to 900 m of oolitic grainstone and reefal deposits occur (loc. 5). These lithotypes are isochronous with the Cape Storm and the Allen Bay formations, and part or all of the Douro Formation. Reefs are up to 230 m thick (loc. 5) and generally contain a variety of lithotypes, including stromatoporoid boundstone (most abundant), *stromatactis*-rich lime mudstone, peloidal-skeletal wackestone, and microbial boundstone. Reefs are overlain by, and interfinger with, the predominant grainstone lithology of the shelf margin facies, and megalodont bivalve floatstone is a conspicuous rock type in the upper, probable Ludlow, part of this sequence.

The Silurian platform margin facies of Grinnell Peninsula are an unusual occurrence within the Franklinian succession; they are the thickest Silurian oolitic grainstone deposits known in the world and are preserved predominantly as limestone, which is in marked contrast to coeval, intensely dolomitized shelf-margin rocks outcropping elsewhere in the Arctic Islands. The Silurian platform margin facies change coincides with the western flank of the Grinnell segment of Boothia Uplift, suggesting that this area was a zone of crustal weakness for more than 40 Ma The main features of this uplift are discussed further below.

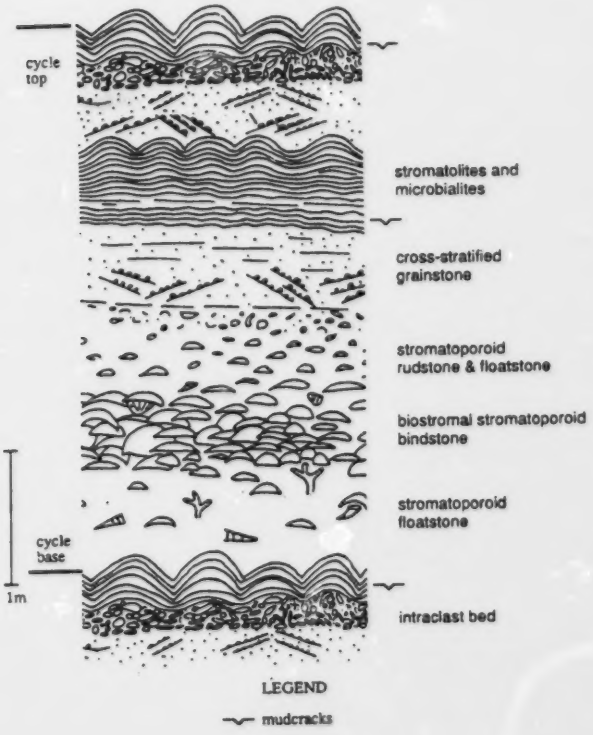

Figure 2. Schematic representation of the main rock features occurring in the upper part of the Middle member, and the lower part of the Upper member, in the Allen Bay Formation at locality 35. These thin, shallowing-upward sequences occur over most the study area east of the Douro Range.

CAPE STORM FORMATION

Based primarily on a reconnaissance examination of outcrops on Colin Archer Peninsula and a measured section in the eastern part of the study area (loc. 32), the Cape Storm Formation shows little lateral facies variability, and is characterized chiefly by yellowish grey, finely crystalline, thinly laminated, thinly to medium bedded, silty and sandy, generally unfossiliferous dolostone. The formation shows an east-to-west decrease in silt content, an increase in limestone content, and an interfingering relationship with the Silurian shelf margin facies, as discussed above.

Measured thicknesses of the Cape Storm Formation vary: near Viks Fiord (loc. 32), the formation is 587 m thick, and 289 to 430 m thick in the Douro Range (locs. 17 and 18). However, the great thickness variation in the Douro Range is likely related to tectonic repetition, as suggested by the drastic change in bedding attitude among adjacent, isolated exposures in each of these poorly exposed sections. A conspicuous development of favositid-microbial boundstone occurs in the upper part of the formation on Colin Archer Peninsula (loc. 30). This rock type comprises small mounds, 3 to 5 m wide by 2 to 3 m high, and laterally extensive biostromes.

The upper contact with the Douro Formation is arbitrarily placed at the base of a unit in which medium grey, bioturbated, fossiliferous to unfossiliferous, dolomitic limestone predominates over yellowish grey, laminated dolostone.

DOURO FORMATION

Two sections of the Douro formation were measured (location 30, where the Douro Formation is 214 m thick; and location 18, where it is 263 m thick). In both areas, the formation is characterized by interbedded, rubbly weathering, fossiliferous, argillaceous limestone, sparsely fossiliferous mottled dolomitic limestone, and thick bedded to massive limestone. Atrypids are locally abundant.

A subtle facies change occurs across the study area. The upper part of the formation on Colin Archer Peninsula is considerably thicker bedded, more resistant to weathering,

and less argillaceous than at the type section in the Douro Range (loc. 18). A notable occurrence in the uppermost 10 m of the Douro Formation are several phosphatic, bored, and cement-encrusted hardgrounds. The most conspicuous of these hardgrounds, in the highest bed of the formation, contains abundant, aligned cephalopods, which are phosphate cemented and contain fossil epibionts.

The contact with the overlying Devon Island Formation is abrupt but conformable, and is placed below a thick succession of graptolitic, thin bedded, calcareous mudrock and argillaceous limestone, assignable to the Devon Island Formation.

DEVON ISLAND FORMATION

Two sections of the Devon Island Formation were measured (location 16, the type section, where the formation is 278 m thick; and location 29, where it is 180 m thick). The formation contains two members: a lower member (approximately 50 m thick), consisting predominantly of interbedded, very thin bedded, calcareous mudrock and thin bedded, argillaceous limestone; and an upper member (130 to 220 m thick), consisting predominantly of thin bedded argillaceous limestone that is progressively more dolomitic toward the top of the formation. The Lower member weathers to a pale yellowish orange to light grey, and the Upper member weathers to a very pale orange to yellowish grey. The formation is sparsely fossiliferous, but graptolites tend to be abundant in the lower part and fish fragments and brachiopods occur rarely throughout.

A preliminary identification of graptolites indicates that the lower part of the formation is condensed and Late Silurian in age. Abundant *Bohemograptus bohemicus* ssp. (Ludlow) occur in the lowest one metre of strata at both localities (locs. 16, 29), but abundant monoserial graptolites of probable Lochkovian age (*Monograptus hercynicus*? or *Monograptus uniformis*?) occur 20 m, or less, above the base of the formation. The occurrence of several phosphatic beds, some reworked into current-stratified beds, is additional evidence of slow rates of sedimentation that followed apparently synchronous termination of carbonate deposition over most, if not all, of the study area.

The upper contact with the Goose Fiord Formation is gradational over several tens of metres and is placed at the base of the lowest occurrence of very light grey weathering dolostone that is typical of the Goose Fiord Formation.

Reefs of the Devon Island Formation

Two small reefs occur in the northern part of Colin Archer Peninsula (loc. 27, 31). Both reefs are poorly exposed, isolated carbonate bodies in an otherwise mudrock- and limestone-dominated sequence. The eastern reef (loc. 31) is about 20 m thick by 120 m wide, and is mainly composed of *stromatactis*-rich calcilutite. *Stromatactis* constitutes up to 80 per cent of the rock volume and is locally laminar and continuous, forming zebroid *stromatactis*. Layered, isopachous cement is abundant in *stromatactis* cavities and is locally interlaminated with calcilutite. *Stromatactis* calcilutite appears to grade upward into silicified coral and minor bryozoan bafflestone and rudstone, a facies succession that appears to represent shallowing. The corals are extremely well preserved. This facies is in turn overlain by crinoid-rich grainstone and packstone, representing reef-flank facies onlapping, perhaps during increased water depth over the reef.

The western reef exposure (loc. 27) appears to comprise primarily reef-slope facies. Large, variably dolomitized, allochthonous blocks are richly fossiliferous, contain abundant stromatoporoids (some up to 2 m in width), and consist predominantly of rudstone and boundstone. Early marine cement is locally very abundant, and porosity may be as high as 20 per cent in the dolomitized parts of the allochthonous blocks.

CAPE PHILLIPS FORMATION

A complete, although very poorly exposed, section of the Cape Phillips Formation was measured on western Grinnell Peninsula, near Cape Sir John Franklin (loc. 4). The formation is 1420 m thick at this locality and is divisible into two members. The lower, lithologically heterogenous member, about 170 m thick, consists predominantly of interbedded, thin bedded and fissile, argillaceous, silty, calcareous mudrock and argillaceous limestone. In contrast, the upper member, about 1250 m thick, is very homogeneous lithologically, and consists predominantly a yellowish grey weathering, calcareous mudrock and argillaceous limestone, rock types that are very similar to, and largely isochronous with, the Devon Island Formation in the study area.

A preliminary identification of graptolites indicates that the Llandovery part of the Cape Phillips Formation at Cape Sir John Franklin is about 130 m thick, the Wenlock less than 13 m, and the Ludlow about 200 to 400 m, although strata of Ludlow and Pridoli ages are very poorly exposed.

Two features of this section are noteworthy: 1) a bioturbated stylobedded limestone occurs very close to, or straddles, the Ordovician–Silurian boundary and may be a correlative of a similar, isochronous unit occurring in parts of Ellesmere and Cornwallis islands; and 2) a yellowish orange and light olive-brown weathering, well indurated, calcareous mudrock unit occurs in beds dated as Ludlow, based on the occurrence of abundant *Bohemograptus bohemicus* ssp. The lower contact of the latter unit corresponds to that of the upper member and, based on preliminary graptolite identification, may also be time-equivalent to the lower contact of the Devon Island Formation.

The Cape Phillips Formation is unconformably overlain by dolostone of the undivided Blue Fiord/Bird Fiord formations. The lower contact is gradational, over several metres, with the Allen Bay Formation — here represented by a thin, 5 m thick limestone tongue. The lowest Cape Phillips beds contain abundant *fastigatus* Zone (middle Ashgill) graptolites and *Pseudogygites* trilobites.

GOOSE FIORD FORMATION (formerly the Sutherland River Formation)

The Goose Fiord Formation is 227 m thick on Colin Archer Peninsula (loc. 28), and 370 m thick in the Douro Range (loc. 19). The formation comprises a rather monotonous succession of very light grey, slightly to very sandy, finely laminated, finely crystalline, stylobedded dolostone. The upper part, however, contains abundant beds of dolomitic, fine sandstone that likely represent the distal facies equivalents of the Prince Alfred Formation exposed to the west (Fig. 3). On Colin Archer Peninsula, this sandstone is fine to medium, yellowish orange, bioturbated, cross-stratified, and interbedded with brecciated dolostone, together comprising a succession about 65 m thick. Noteworthy in terms of regional tectonics are low amplitude (10-20 m wavelengths) slump folds in the upper part of the formation on southern North Kent Island. On the eastern flank of the Douro Range, the lower part of the Goose Fiord Formation is abundantly cross-stratified. The upper contact is probably conformable in the Sutherland River depression but unconformable on Colin Archer Peninsula (Fig. 3).

PRINCE ALFRED FORMATION

Uplift of Grinnell Peninsula occurred during the Early Devonian, and four main structural elements formed at about the same time. The Grinnell segment of Boothia Uplift represents the main area of uplift in the western part of the study area, and two small depressions (the Grove Lake and Sutherland River depressions), separated by an arch, the Douro Arch, occur to the east of the main uplift (Fig. 3). The depressions formed main depocentres for the Prince Alfred Formation sediments, and stratigraphic pinchouts occur adjacent to the arch and uplift (Fig. 3).

The Prince Alfred Formation is lithologically heterogeneous throughout the study area. Its facies are complex and, prior to the 1991 field season, despite studies by several workers since the early 1970s, its depositional history was very poorly understood. Numerous sections were studied (loc. 8, 10–14, 20, 22–25), including the type section along Sutherland River (loc. 20). There, the formation is 105 m thick and consists of interbedded, medium bedded, well sorted, light grey to light brownish grey, fine grained sandstone; monomict, sandy dolostone breccia; and thin and medium bedded, light grey, finely crystalline, light grey dolostone. The contact with the underlying Goose Fiord Formation is gradational (and conformable) and is placed at the base of the lowest unit in which sandstone predominates over dolostone.

In the Grove Lake depression (loc. 14), the formation is lithologically heterogeneous: in the upper part, cross-stratified, moderate-red siltstone and fine grained sandstone predominate, and, in the lower part, interbedded red siltstone, yellowish grey sandstone, and finely laminated, light grey, silty dolostone occur. This facies coarsens northward (from locality 14 to locality 10) and is eventually replaced by a fluviatile boulder conglomerate (Fig. 3). Clastic content shows a westward increase over dolostone in the Grove Lake depression, such that, near locality 11, strata of the formation consist entirely of pale olive weathering, thin bedded, fine grained sandstone and siltstone, interbedded

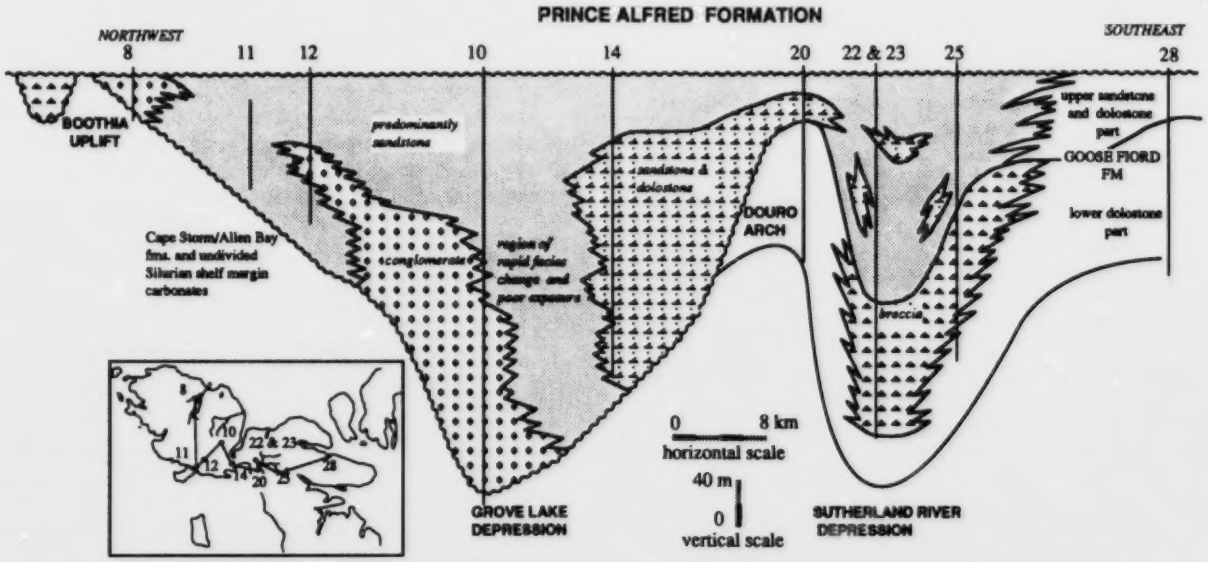

Figure 3. Generalized schematic reconstruction of the main lithofacies of the Prince Alfred Formation. The Goose Fiord Formation at locality 28 is characterized by interbedded sandstone, breccia, and dolostone in the upper part, and by dolostone in the lower part. The upper part is interpreted as representing a distal facies equivalent of the Prince Alfred Formation, although still mapped as part of the Goose Fiord Formation on Colin Archer Peninsula.

with fluviatile, carbonate-pebble conglomerate and cross-stratified dolarenite. The contact between the conglomerate and dolarenite and the fine clastic deposits (probably deposited in a tidal flat environment) is erosional. Boulder conglomerates at locality 10 and cobble and pebble conglomerates at locality 12 are likely correlatives and show a southward transport direction (Fig. 3, 4a).

Two main facies of the Prince Alfred Formation occur in the Sutherland River depression (Fig. 3, loc. 22, 23): 1) interbedded greyish yellow-orange, cross-stratified, bioturbated, fine grained sandstone, sandy dolostone breccia, and laminated, silty, light grey dolostone; and 2) interbedded dolostone and limestone breccia. Although varying amounts of carbonate breccia are present in most sections of the Prince Alfred Formation, nowhere are they as thick and as widespread as in the Sutherland River depression (Fig. 3). A maximum thickness of 140 m of limestone and dolostone breccia was observed along the northern bank of the Sutherland River (loc. 23). These breccias are stratified, mostly monomictic, but polymictic in the upper part, and generally very poorly sorted. In places, large slump folds are present, and a facies change from well bedded Goose Fiord Formation dolostones to chaotic breccia deposits can be observed at three separate localities near Sutherland River. These facies changes are abrupt and occur over less than 20 m laterally.

Breccia units up to 50 m thick and overlying Ordovician Bay Fiord Formation dolostone are common in an area of about 5 km^2 south of locality 7. These breccias were included previously in the Bay Fiord Formation (Morrow and Kerr, 1986); however, in contrast to the Bay Fiord breccias, these deposits are stratified, polymictic, and show some evidence of reworking in the form of clast rounding and sorting. About three kilometres east of locality 6, breccia beds occur within an apparently conformable Bay Fiord Formation succession. In exposures of the Prince Alfred Formation in the same area, thin bedded, greyish green mudrock and light brown sandstone occur on a very irregular erosion surface that exhibits a paleorelief greater than 20 m. The facts that the breccia deposits are confined to the area south of locality 7 (not considering breccia of the Sutherland River depression), a region of great relative uplift, and they appear to be thickest where overlying evaporite-rich Bay Fiord Formation carbonate rocks, suggest deposition over an irregular, possibly karstic, unconformity surface. Breccias, as such, were transported to paleo-lows by mass flow, or represent collapse of an extensively karstified terrain. East of this area

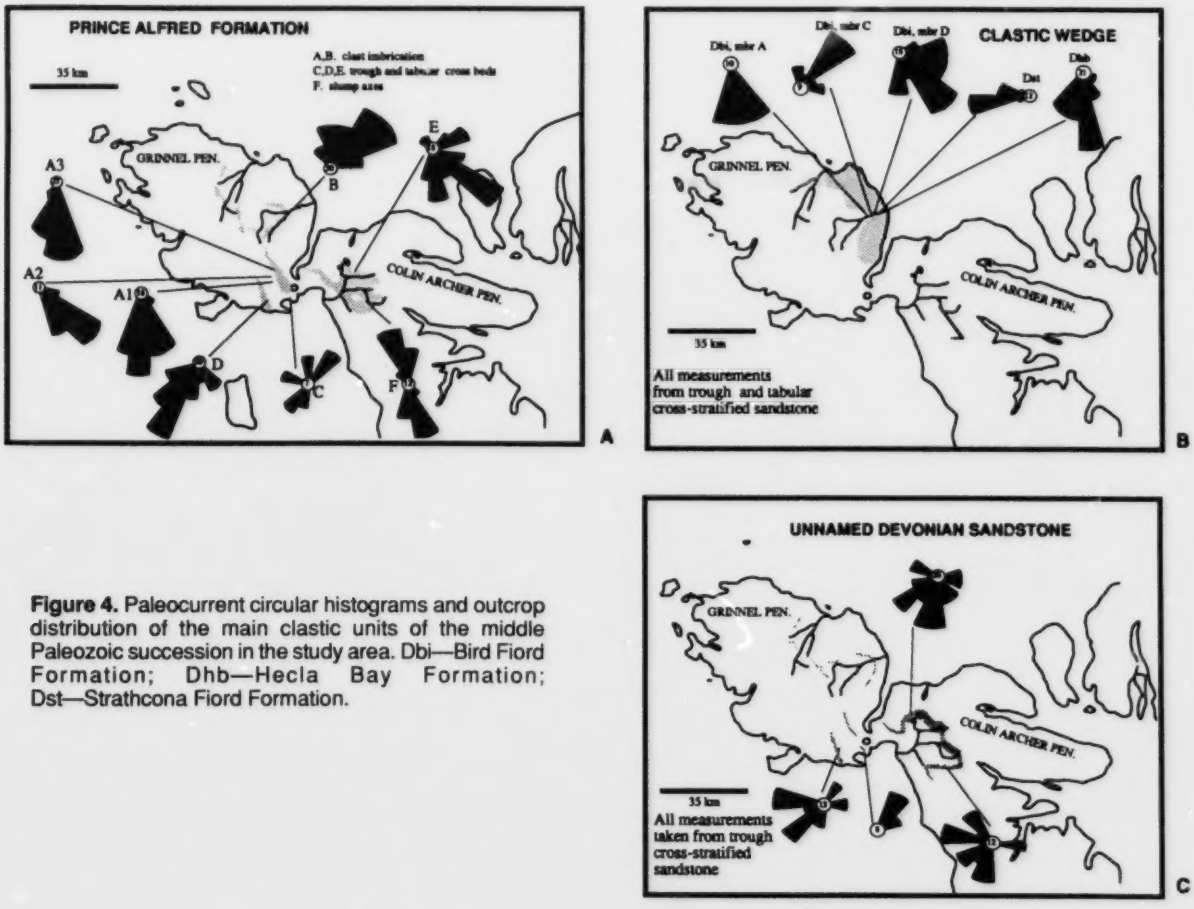

Figure 4. Paleocurrent circular histograms and outcrop distribution of the main clastic units of the middle Paleozoic succession in the study area. Dbi—Bird Fiord Formation; Dhb—Hecla Bay Formation; Dst—Strathcona Fiord Formation.

of breccia, at locality 7, an approximately 50 m thick, fluvial carbonate conglomerate unit occurs. Clast imbrication indicates a northeastward transport direction for this succession (Fig. 4a).

The age of the Prince Alfred Formation is not certain, but regional stratigraphic relationships suggest a Lochkovian age. The contact between the Prince Alfred and Goose Fiord formations is gradational and conformable in the eastern part of the study area, and, on Colin Archer Peninsula, Prince Alfred-like sandstone beds occur in the upper part of the Goose Fiord Formation. Based on this lithological correlation, the Prince Alfred Formation is partly age-equivalent to the upper part of the Goose Fiord Formation. On Ellesmere Island, the upper part of the Goose Fiord Formation is Early Devonian in age (Thorsteinsson and Uyeno, 1980) and, thus, the Prince Alfred Formation is probably Early Devonian in age and a correlative of the Snowblind Bay Formation. The base of the Prince Alfred Formation is unconformable and progressively overlies older units in the western part of the study area, suggestin onlapping and perhaps also slight diachroneity of the bas contact.

UNNAMED DEVONIAN SANDSTONE

This lithologically distinctive and mappable unit is preser throughout much of the study area. It is dominantly a troug cross-stratified, dusky yellow, well indurated c unconsolidated, well sorted, fine grained sandstone. It thickest in the Grove Lake and Sutherland River depressior (85 m at locality 21, and 65 m at locality 15, respectively) an thins generally in all directions from these areas. Its lowe contact, although poorly exposed in most areas, is considere unconformable, based on the truncation of light gre sandstone in the Prince Alfred Formation, visible o airphotos of the head of Sutherland River. The upper conta of the unnamed sandstone is gradational and is placed at th base of massive dolostone beds that form the lower part c the overlying Blue Fiord Formation.

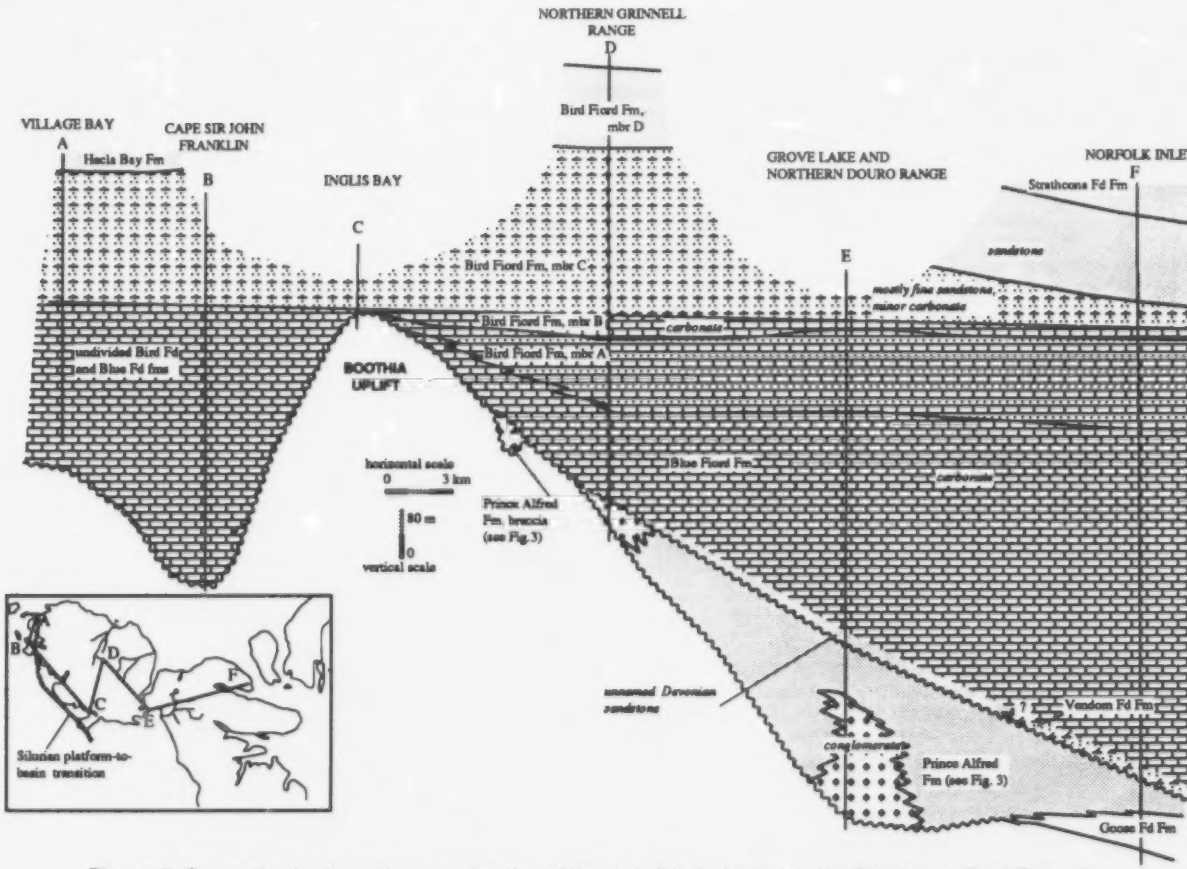

Figure 5. Generalized schematic reconstruction of the main lithofacies below the Strathcona Fiord Formation. Line along the western edge of Grinnell Peninsula on the inset shows the approximate western edge of Boothia Uplift, which also coincides with the Silurian platform-to-basin facies change. Carbonate rocks were deposited east, and deep-water clastic rocks and carbonate rocks west, of the line.

Its stratigraphic position below the Blue Fiord Formation and its dominantly clastic composition suggest that this sandstone succession may be assigned to the Vendom Fiord Formation; however, the latter formation is a fluviatile, moderately red sandstone and conglomerate that shows marked lithological heterogeneity throughout southern and central Ellesmere Island. Also, it represents sediments derived predominantly from the Bache Peninsula Uplift. In contrast, the unnamed formation is lithologically homogeneous and likely represents Prince Alfred Formation sandstone deposits reworked during a marine transgression. The similarity in distribution of the Prince Alfred Formation and the unnamed sandstone tends to support this interpretation (see Fig. 5).

BLUE FIORD FORMATION

The Blue Fiord Formation was examined briefly by the senior author; detailed accounts of this formation can be found in Goodbody et al. (1989) and Prosh et al. (1988). Only additional information is given below.

At locality 9, the Blue Fiord Formation is 588 m thick and divisible generally into two distinct units: a lower, bioturbated, richly to sparsely fossiliferous dolostone and minor limestone unit, and an upper, fenestral and partly silty dolostone unit. This general facies succession can be recognized on North Yorkshire Peninsula, and exposures there are much better. The entire formation could be interpreted as representing a general upward restriction in water circulation, such that fossiliferous lime muds (representing open marine deposition) in the lower part were replaced by fenestral lime muds in the upper part. The facies in the western part of the study area are slightly more complex.

The Blue Fiord Formation pinches out westward against, and distinctive facies occur near, Boothia Uplift on western Grinnell Peninsula. Near the head of Tucker River, at two separate localities, several features of the formation are noteworthy. At locality 7, the lower, fossiliferous, carbonate unit of the Blue Fiord Formation, common to most exposures throughout the study area, is absent, and a fenestral dolostone predominates throughout. At locality 6, three units can be recognized: a basal, 5 m thick, well sorted, well rounded pebble and granule carbonate-conglomerate; a middle, 80 m thick, cross-stratified oolite that is interbedded with the conglomerate in the lower part; and an upper fenestral lime mudstone of unknown thickness. The oolites, representing an unusual rock type in the Blue Fiord Formation, were likely deposited in an agitated nearshore setting associated with the eastern flank of Boothia Uplift on western Grinnell Peninsula. The lack of a lower, bioturbated and fossiliferous carbonate unit proximal to the uplift may be related to onlapping and to slight diachroneity of the basal part of the Blue Fiord Formation.

BIRD FIORD FORMATION

The Bird Fiord Formation is described in Goodbody et al. (1988) and in Goodbody (1989), and only additional information is given here.

Four members occur in the study area; these were referred to as the Cross Bay, Blubber Point, Baad Fiord, and Cardigan Straight members by Goodbody (1989); however, because this nomenclature does not clarify stratigraphic relationships within the formation, the members are referred to herein as members A, B, C, and D.

Member A is a generally poorly exposed, yellowish grey, thin bedded, silty dolostone and dolomitic siltstone that shows relatively uniform thickness east of, and is not present west of, Boothia Uplift (Fig. 5). It is 120 m thick near Arthur Fiord (photogrammetrically measured), 160 m near Norfolk Inlet, and 170 m at locality 7. Characteristic sedimentary structures include mudcracks, cross-stratification, and thin parallel lamination, structures that collectively suggest deposition in restricted or peritidal settings. In the vicinity of Tucker River, Member A is considerably more calcareous and less gypsiferous than near Arthur Fiord, Prince Alfred Bay, and Norfolk Inlet. Although paleocurrent information is difficult to obtain, a southward transport direction appears to have prevailed. Cross-stratification probably resulted from tidal currents, perhaps in this case indicating dominantly ebb-current sediment transport, assuming the presence of a land mass north or northeast of the study area.

Member B is a distinctive and laterally extensive cliff-forming unit throughout much of the study area. It mainly comprises interbedded, fossiliferous, bioturbated limestone, fenestral limestone, and siltstone. It shows slight westward thinning, from about 40 m on North Yorkshire Peninsula to about 28 m in the vicinity of Arthur Fiord (Fig. 5). Near Inglis Bay, Member A is missing, and Member B is approximately 25 m thick and unconformably overlies Ordovician and Silurian carbonate rocks. It is, in part, a correlative of the thick succession of carbonates exposed along the western flank of the Grinnell segment of Boothia Uplift (loc. 1–3), but these carbonates may also include correlatives of the Blue Fiord Formation and Member A of the Bird Fiord Formation (as discussed below).

Member C is generally a recessive, dusky yellow weathering, thin bedded, locally very fossiliferous, calcareous, fine to medium sandstone, containing minor interbedded fossiliferous calcirudite. The member is 182 m thick near Village Bay, 250 m near Tucker River, and 50 m on North Yorkshire Peninsula. Upper and lower contacts of the member are gradational and conformable. Unusually well preserved trace fossils are characteristic and "brachiopod gravel" can be found around some weathered sandstone or siltstone exposures. Paleocurrent information is not easily obtainable, but tabular and trough crosslamination indicate a predominantly northeastward transport direction. The sequence is interpreted as a storm-influenced shelf deposit, and cross-stratification likely formed through combined flow during storm activity.

Member D is a light to medium grey, cross-stratified, poorly indurated, plant-fragment-rich, micaceous, quartzose sandstone. It is generally poorly exposed, and is known to occur only in the vicinities of Tucker River and North Yorkshire Peninsula (Fig. 5). It shows a general southward transport direction, and its basal contact is gradational and

placed below the lowest occurrence in section of light grey weathering, noncalcareous sandstone (Fig. 5). The upper contact, with the Strathcona Fiord Formation, is sharp but conformable and is placed below the lowest occurrence of moderate-red siltstone. The member is 120 to 130 m thick in the two areas and is interpreted as representing fluvial and delta front environments.

UNDIVIDED LOWER DEVONIAN CARBONATE ROCKS: BIRD FIORD – BLUE FIORD FORMATION EQUIVALENTS WEST OF THE GRINNELL SEGMENT OF BOOTHIA UPLIFT

A thick carbonate succession of Devonian age occurs along the western flank of Boothia uplift (loc. 1, 3; Fig. 5). The succession is more than 400 m thick and consists predominantly of a fenestral lime mudstone and fossiliferous, bioturbated limestone. Light grey, thinly laminated, thin bedded dolostone and thick bedded, commonly trough cross-stratified encrinite grainstone are minor rock types. These carbonate rocks are gradationally overlain by Member C of the Bird Fiord Formation near Village Bay, and unconformably overlie numerous middle and lower Paleozoic formations. The contact is represented by an angular unconformity near Village Bay, and overturned Allen Bay, Thumb Mountain, and Irene Bay carbonates occur beneath these gently dipping Devonian carbonates.

DEVONIAN CLASTIC WEDGE

Little additional information was collected to supplement that reported by Goodbody et al. (1988), and the reader is referred to this work for a synopsis of the main facies of these formations. However, this report provides data on paleocurrent determinations, not obtained from this area previously (Fig. 4b).

Paleocurrent measurements were made only for the Hecla Bay, Strathcona Fiord formations and for part of the Bird Fiord Formation. Paleocurrent determinations presented herein are comparable to determinations published elsewhere (Embry and Klovan, 1976; Trettin, 1978) and indicate a general westward and southward transport direction for the lower two formations of the Okse Bay Group and for Member D of the Bird Fiord Formation.

THE GRINNELL SEGMENT OF BOOTHIA UPLIFT

Although epeirogenesis did not occur until the Early Devonian, there is some evidence to indicate that Grinnell Peninsula was subjected to significantly older but very minor tectonic activity. During the latest Ordovician, throughout most of the Arctic Islands, platform drowning occurred, and mudrocks were deposited over an extensive area. However, the western part of Grinnell Peninsula was perhaps an area of relatively low subsidence and, as such, marked the platform-to-basin facies change during most of the Silurian (Fig. 5, inset). The facies boundary also coincides with the western flank of the uplift, suggesting that western Grinnell Peninsula was an area of crustal weakness for more than 40 Ma.

Epeirogenesis of western Grinnell Peninsula occurred in Devonian time, and clastic material was shed from uplifted Paleozoic carbonates (Prince Alfred Formation; Fig. 3, 5). However, coarse clastic rocks outcrop east, but not west, of the uplift; this facies asymmetry, assuming that it is not an artifact of preservation, is in marked contrast to facies associated with uplift in the vicinity of Somerset Island (Miall, 1970). There, westward-transported gravel occurs as conglomerates west but generally not east of gently sloping, west-verging thrusts that formed the uplift. Moreover, in both the Prince Alfred and Snowblind Bay formations (Table 1) (Muir and Rust, 1982), paleocurrent directions derived from conglomeratic units are generally southward oriented, and clastic deposition was chiefly east of Boothia Uplift, suggesting that uplift style and associated sedimentation patterns varied from Somerset Island to Cornwallis Island and Grinnell Peninsula. Also, epeirogenesis was generally younger in the north.

Toward the eastern part of the map area, uplift was less, and manifested as gentle flexure in the sedimentary cover. Flexure caused two depocentres to form, the Grove Lake and Sutherland River depressions (Fig. 3), and also resulted in the development of an unstable situation for the carbonate sequence laid down prior to uplift, producing extensive slumping and brecciation of the Goose Fiord Formation. In areas of maximum uplift, such as in western and central Grinnell Peninsula, paleorelief developed on the unconformity surface, and associated breccias were formed through collapse or by minor transport of material into paleo-lows.

The uplift remained a positive feature through much of "Blue Fiord time", as this formation shows an onlapping relationship and a facies change associated with the uplift. The unnamed Devonian sandstone shows a similar onlapping relationship; however, its distribution and ultimate source are closely tied to the underlying Prince Alfred Formation (as suggested in Fig. 5). During the Emsian and part of the Eifelian, the uplift did not shed appreciable detritus, but remained a positive feature that caused onlapping of, and facies variation within, the Blue Fiord Formation and parts of the Bird Fiord Formation (Fig. 5). In the early Eifelian, the uplift was submerged and had little influence on sedimentation.

REFERENCES

Droser, M.L. and Bottjer, D.J.
1986: A semiquantitative classification of ichnofabric; Journal of Sedimentary Petrology, v. 56, p. 558–569.

Embry, A.F. and Klovan, J.E.
1976: The Middle–Upper Devonian clastic wedge of the Franklinian Geosyncline; Bulletin of Canadian Petroleum Geology, v. 24, p. 485–639.

Goodbody, Q.H., Uyeno, T.T., and McGregor, D.C.
1988: The Devonian sequence on Grinnell Peninsula and in the region of Arthur Fiord, Devon Island, Arctic Archipelago; in Current Research, Part D; Geological Survey of Canada, Paper 88-1D, p. 75–82.

Miall, A.D.
1970: Continental marine transition in the Devonian of Prince of Wales Island, Northwest Territories; Canadian Journal of Earth Sciences, v. 7, p. 125–144.

Morrow, D.W. and Kerr, J.Wm.
1986: Geology of Grinnell Peninsula, Devon Island, District of Franklin, Northwest Territories; Geological Survey of Canada, Open File 1325, 45 p. and 1 map.

Muir, I. and Rust, B.R.
1982: Sedimentology of a Lower Devonian coastal alluvial fan complex: the Snowblind Bay Formation of Cornwallis Island, Northwest Territories, Canada; Bulletin of Canadian Petroleum Geology, v. 30, p. 245–263.

Prosh, E.C., Lesack, K.A., and Mayr, U.
1988: Devonian stratigraphy of northwestern Devon Island, District of Franklin; in Current Research, Part D; Geological Survey of Canada, Paper 88–1D, p. 1–10

Thorsteinsson, R. and Mayr, U.
1987: The sedimentary rocks of Devon Island, Canadian Arctic Archipelago; Geological Survey of Canada, Memoir 411.

Trettin, H.P.
1978: Devonian stratigraphy, west-central Ellesmere Island, Arctic Archipelago; Geological Survey of Canada, Bulletin 302.

Geological Survey of Canada Project 850039

Newly discovered Carboniferous exposures at the margin of Sverdrup Basin, northwestern Devon Island, Northwest Territories

Pierre Thériault[1] and Ulrich Mayr
Institute of Sedimentary and Petroleum Geology, Calgary

Thériault, P. and Mayr, U., 1992: Newly discovered Carboniferous exposures at the margin of Sverdrup Basin, northwestern Devon Island, Northwest Territories; in Current Research, Part B; Geological Survey of Canada, Paper 92-1B, p. 65-72.

Abstract

The Lower Carboniferous Emma Fiord Formation and the Upper Carboniferous Canyon Fiord Formation are exposed in a small area of northwestern Devon Island, that lies approximately 100 km south and cratonward of the margin of the Sverdrup Basin. Strata from this newly recognized occurrence were deposited in a small extensional basin, here called the "Nesodden depression", and are now preserved in a Tertiary graben.

The Emma Fiord Formation is characterized by two distinct assemblages: a basal conglomerate sandstone assemblage of high-energy fluvial origin, and an overlying, largely covered, mudstone assemblage interpreted as having a fluvio-lacustrine origin. The Canyon Fiord Formation consists of a lower sandstone assemblage of low-energy fluvial origin.

Résumé

Les formations d'Emma Fiord et de Canyon Fiord, respectivement du Carbonifère inférieur et supérieur, s'observent en affleurement dans une zone restreinte de la partie nord-ouest de l'île Devon, qui se trouve approximativement à 100 km au sud de la marge du bassin de Sverdrup, dans sa section faisant face au craton. Les strates de ces lithologies récemment découvertes se sont accumulées dans un petit bassin d'extension, dans le cas présent appelé la «dépression de Nesodden»; elles se trouvent actuellement dans un graben tertiaire.

La formation d'Emma Fiord comprend deux assemblages distincts qui sont les suivants : à la base, des grès et des conglomérats dérivant d'un milieu fluviatile de haute énergie, et au-dessus, des mudstones (affleurant peu) d'origine vraisemblablement fluvio-lacustre. Quant à la formation de Canyon Fiord, elle consiste en un assemblage inférieur de grès de milieu fluviatile de basse énergie.

[1] Geological Institute, avd. A, University of Bergen, 5007 Bergen, Norway

INTRODUCTION

A newly recognized occurrence of Carboniferous strata in the Sverdrup Basin was investigated at the end of the 1991 field season. Located on northwestern Devon Island and first observed by U. Mayr, during regional mapping in 1986, the occurrence is somewhat exceptional in that the strata are contained within a small, isolated tectonic depression, lying approximately 100 km cratonward of the margin of the main Sverdrup Basin depocentre. This small depression will be informally referred to as the "Nesodden depression", after the peninsula between Eidsbotn and Viks fiords[1].

The Carboniferous rocks of the Nesodden depression cover an area approximately 9 km in length by 3 km in width, and have been preserved within a Tertiary graben that is also 3 km wide, but which extends in a west-northwest direction for 25 km. The graben's east-southeast extension coincides approximately with that of the Nesodden depression, about 4 km east of the small lake shown in Figure 1. The Tertiar graben is bounded on each side by a linear arrangement c normal and thrust fault segments (Fig. 2) that randoml alternate in nature and vergence (G. Eisbacher, pers. comm. These faults are most likely reactivated structures that als bounded the Nesodden depression and controlle sedimentation during the Carboniferous. Othe Carboniferous depressions are also present farther northwes within the Tertiary graben. Unfortunately, strata do nc outcrop at these localities, and the Carboniferous record ther is limited to scree material.

This paper provides: 1) a summary of sedimentologica field observations recorded in the study area during three day in early August 1991; 2) preliminary interpretation regarding the paleogeography and structural framework c the Nesodden depression; and 3) speculations about th regional tectonic evolution of Sverdrup Basin during th Carboniferous.

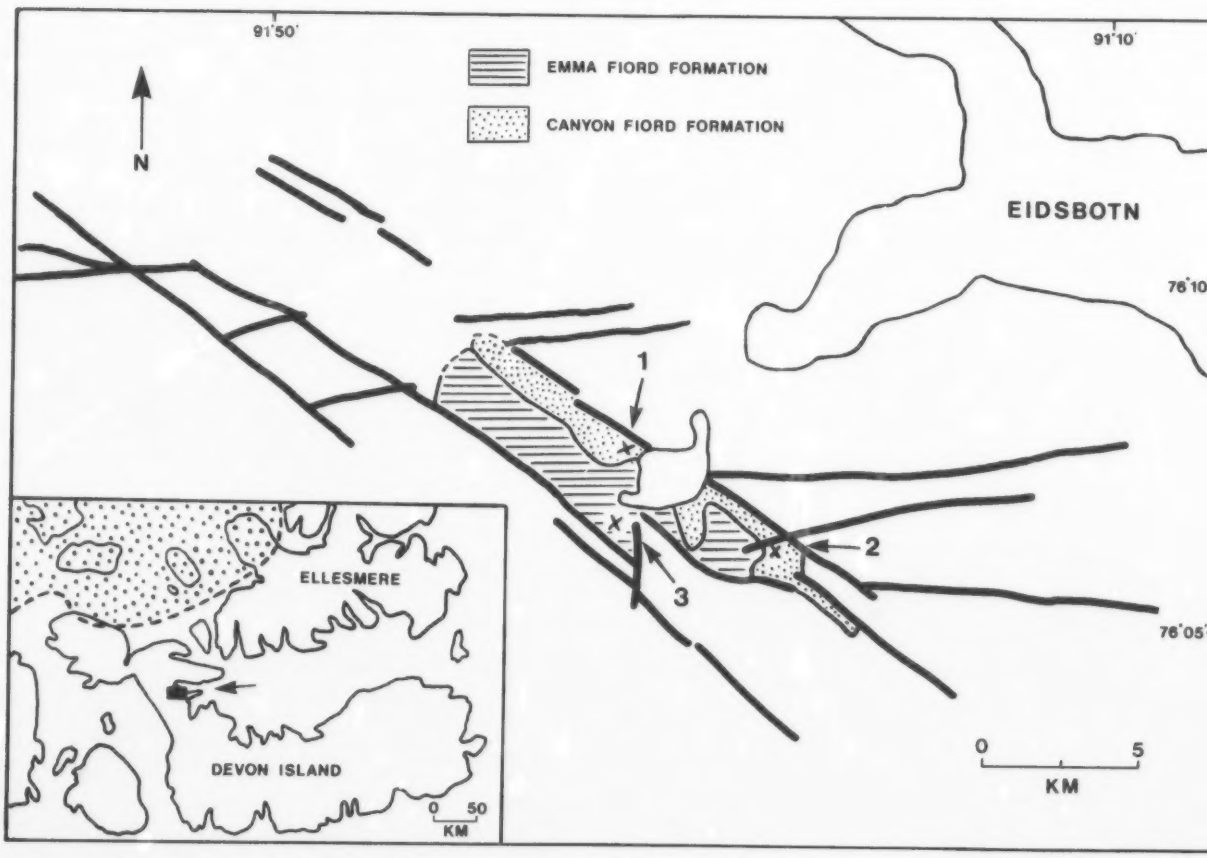

Figure 1. Map of the Nesodden area, showing main Tertiary faults (heavy lines) and distribution of the Carboniferous Emma Fiord and Canyon Fiord formations. The area surrounding the Carboniferous formations is underlain by Ordovician and Silurian rocks.

[1]Informal name, submitted for approval

GEOLOGICAL SETTING

Sedimentation within the Nesodden depression is believed to have been controlled more or less by the same tectonosedimentary events that affected the main depocentre of the Sverdrup Basin, a continental rift basin underlying much of the Canadian Arctic Archipelago. Initiation of fault-controlled subsidence in the Sverdrup Basin occurred during the Viséan with the lithospheric extension and local collapse of the Franklinian Mobile Belt. In consequence, the fluvial to lacustrine Emma Fiord Formation (Davies and Nassichuk, 1988) was deposited locally within small isolated depressions on northern Axel Heiberg Island, northern Ellesmere Island, and northwestern Devon Island. It is argued below that these tectonic depressions are of strike-slip origin, and form part of a regional wrench faulting system across the western Arctic and North Atlantic (Ziegler, 1988). Lithospheric extensional stresses appear to have been reoriented in Serpukhovian time, leading to the basin-wide failure and collapse of the Franklinian basement by dip-slip extension, and resulting in fluvial clastic sedimentation within longitudinal subbasins at the basin centre (Borup Fiord sandstone/conglomerate – Thorsteinsson, 1974); and also possibly within less prominent incipient subbasins at the basin margin (lower sandstone assemblage of the basal Canyon Fiord Formation – Thériault, 1991). A second dip-slip extensional event during the Bashkirian resulted in the marine submergence of the subbasins in central areas of Sverdrup Basin (Otto Fiord evaporites – Nassichuk and Davies, 1980; Nansen limestones – Thorsteinsson, 1974), and in fluvial sedimentation within the now fully developed subbasins of marginal areas (conglomerate assemblage of the basal Canyon Fiord Formation – Thériault, 1991).

The depositional sequences associated with these three tectonosedimentary events are the oldest of eight similar low-order sequences that characterize the upper Paleozoic succession of Sverdrup Basin (Beauchamp et al., 1986b).

Figure 2. Northeastern fault escarpment of the Nesodden graben. View is to the southeast. The fault is outlined by the linear snowfield. The lighter coloured rocks on the left of the fault belong to the Ordovician Silurian Allen Bay and Cape Storm formations. The darker rocks on the right side of the fault are the Emma Fiord and Canyon Fiord formations. ISPG photo. 3797-41

The Nesodden depression of northwestern Devon Island is situated approximately 100 km to the southeast of the margin of the main Sverdrup Basin depocentre. Despite this isolation, its sedimentary record is comparable to that of certain marginal areas of the Sverdrup Basin, such as on Grinnell Peninsula, northwestern Devon Island (Davies and Nassichuk, 1988). In both areas of Devon Island, the Carboniferous succession includes the Emma Fiord Formation and the basal sandstone and conglomerate assemblages of the Canyon Fiord Formation.

The Emma Fiord Formation is a clastic-dominated unit occurring in small isolated depressions throughout the Sverdrup Basin. It has been assigned a Viséan age (middle Early Carboniferous) from many studies of microfloral assemblages (see the review in Davies and Nassichuk, 1988), and is, therefore, the oldest unit in the Sverdrup Basin. Isolated occurrences throughout the Sverdrup Basin have shown the Emma Fiord Formation to be predominantly nonmarine, comprising variable proportions of lacustrine to fluvial, carbonaceous and calcareous shale, siltstone, sandstone, pebble conglomerate, and algal-tufa limestone (Davies and Nassichuk, 1988). Marine shale, siltstone, sandstone, and limestone have also been reported by Mayr (in press) from one locality in the Parker Bay area on northeastern Ellesmere Island. Including the present study, exposures have now been reported from seven different areas of Sverdrup Basin; namely, Svartevaeg Cliffs on northern Axel Heiberg Island, Kleybolte Peninsula on northwestern Ellesmere Island (type locality), M'Clintock Glacier, Clements Markham River and Parker Bay on northeastern Ellesmere Island, northern Grinnell Peninsula on northwesternmost Devon Island, and Nesodden peninsula on northwestern Devon Island (Fig. 1). The formation is thickest at the Parker Bay locality in northeastern Ellesmere Island, where it attains 700 m or more (Mayr, in press). Maximum stratigraphic thickness is less than 100 m at the other two northeastern Ellesmere Island localities (Mayr, in press), but is 345 m on Kleybolte Peninsula (Thorsteinsson, 1974), approximately 120 m at Svartevaeg Cliffs (Davies and Nassichuk, 1988), 430 m on Grinnell Peninsula, and at least 375 m on Nesodden Peninsula. Most Emma Fiord exposures are of limited areal extent, reaching probably no more that 5 or 10 km along strike.

The Canyon Fiord Formation is a redbed-dominated unit exposed as a relatively continuous band along the margin of Sverdrup Basin (Thériault, 1991; Thériault and Beauchamp, 1991; Fig. 1). It unconformably overlies either the Emma Fiord Formation, or deformed strata of the Franklinian Mobile Belt. Beauchamp (1987) subdivided the Canyon Fiord Formation, which spans the Bashkirian (early Late Carboniferous) to Sakmarian (early Early Permian) time interval, into three informal members: i) a lower clastic member, consisting mainly of fluvial conglomerate and sandstone; ii) a middle limestone member, consisting mainly of shallow marine limestone; and iii) an upper clastic member, consisting mainly of shallow marine sandstone with subordinate limestone. In a subsequent study on southeastern Ellesmere Island, Thériault (1991) further subdivided the lower clastic member into four distinct facies assemblages: i) a lower sandstone assemblage, deposited in the floodplain

environment of high sinuosity streams, and locally in a paludal environment; ii) a conglomerate assemblage, deposited in an alluvial fan to proximal braided stream environment; iii) an upper sandstone assemblage, deposited in braided stream and coastal plain environments; and iv) an evaporite assemblage, deposited in a local coastal playa that evolved into a hypersaline lagoon. These assemblages are early Bashkirian to middle Moscovian (earliest to middle Late Carboniferous) in age, based on the ammonoid, conodont, and foraminifer content of interlayered and overlying limestones (Thorsteinsson, 1974; Nassichuk, 1975; Beauchamp et al., 1989b; Thériault, 1991).

Only the lower sandstone and conglomerate assemblages are present in the Nesodden depression, and it is at present impossible to determine whether younger Canyon Fiord sediments, or any other upper Paleozoic unit, were ever deposited and subsequently eroded, or if the present record is relatively complete.

The lower sandstone assemblage of the Canyon Fiord Formation is only exposed near the head of Trold Fiord on southwestern Ellesmere Island (Thériault, 1991), and on Nesodden Peninsula (Section 3, this study). It reaches 130 m in thickness near the head of Trold Fiord (Thériault, 1991), and is 105 m thick on Nesodden Peninsula.

The conglomerate assemblage is widespread throughout the margin of Sverdrup Basin, occurring at several localities on northern Melville Island, northwestern Devon Island, and across Ellesmere Island (Thériault, 1991; Fig. 1). The assemblage attains a maximum thickness of 240 m between Trold Fiord and Blind Fiord on southwestern Ellesmere Island. It is at least 70 m thick on Nesodden Peninsula.

STRATIGRAPHY

Three stratigraphic sections were measured within the Nesodden depression (Fig. 3). Section 1 is located near the northwestern margin, and includes 105 m of the lower sandstone assemblage and 100 m of the conglomerate assemblage of the Canyon Fiord Formation, as well as a covered interval, of unknown thickness, of the Emma Fiord Formation. Section 2 is close to the northeastern margin of the depression, and comprises 100 m of the conglomerate assemblage of the Canyon Fiord Formation, overlain by 270 m or more of Emma Fiord strata. Section 3 was measured at the southern edge of the depression and consists of a 45 m thick interval at the base of the Emma Fiord Formation. Due to the overall poor exposure and structural complexity of the area, stratigraphic correlations were made only between Sections 1 and 2.

The fact that the Lower Carboniferous Emma Fiord Formation appears to overlie the Upper Carboniferous Canyon Fiord Formation at Sections 1 and 2, implies that the two units are fault bounded. This fault is either normal and north-dipping, or reverse and south-dipping. The latter possibility is preferred because: 1) Tertiary deformation in the area, in relation to the Eurekan Orogeny, was mainly transpressive to compressive (Eisbacher, 1992); and 2) Emma Fiord strata are intensely folded in the area immediately west, as well as to the south of the stream gully where Section 1 was measured (Fig. 1). An intersecting fault of east-west orientation, underlying this gully and extending beyond the Nesodden depression, may have contributed significantly to the present stratigraphic and structural configuration. Field relationships show that this fault underwent sinistral strike-slip motion during the Tertiary, a scenario under which the Emma FiordCanyon Fiord contact could represent a northwest-southeast subsidiary thrust fault situated in the restraining bend of the strike-slip system.

SEDIMENTOLOGY

Emma Fiord Formation (Viséan)

The Emma Fiord Formation exposed within the Nesodden depression is nonmarine, and consists of two distinct assemblages: a basal conglomerate/sandstone assemblage (~130 m thick), present at Sections 2 and 3, and an overlying mudstone assemblage (140 m or more), restricted to Section 2. A basal conglomeratic assemblage comparable to the one reported herein has also been described by Mayr (in press) for the M'Clintock Glacier locality of northeastern Ellesmere Island. Similarly, the upper part of the formation at this locality is also represented by a fine grained, clastic assemblage.

Conglomerate/sandstone assemblage

This assemblage forms the base of the Emma Fiord Formation at two of the three measured sections (Fig. 3), and comprises interlayered, light brownish grey, pebble to cobble conglomerate, and light grey, fine sandstone to siltstone. Medium to pebbly sandstone and bituminous shale are minor constituents. The conglomerate intervals are medium bedded, sheetlike to lenticular, and display parallel and tabular cross-stratification. Normal grading is common, with the basal part locally displaying an openwork fabric, and the upper part commonly consisting of pebbly sandstone. The conglomerates are also clast-supported and pebbly to cobbly with maximum particle sizes (MPS) ranging from 2 to 25 cm. Individual clasts are angular to subrounded, and are composed of roughly equal proportions of limestone and sandstone, with up to 5% chert. The matrix is sand-rich, moderately well sorted, and generally amounts to less than 15%.

The interlayers of very fine to pebbly sandstone and siltstone are very thin to medium bedded, and parallel to tabular cross-stratified or massive. Normal grading is relatively common. The subordinate bituminous shale intervals are no more than 10 cm thick, and invariably parallel laminated. The sandstone/siltstone/shale units are most abundant in the upper part of the assemblage, where they host local concentrations of secondary gypsum, occurring mainly as thin sheets infilling subvertical and bedding-parallel fractures. These sheets are up to 5 cm in thickness, make up less than 5 per cent of total rock volume, and interconnect to form a random meshlike pattern. The gypsum is either massive or fibrous, with individual fibres showing a preferred orientation that is perpendicular to the sheet's long axis. A

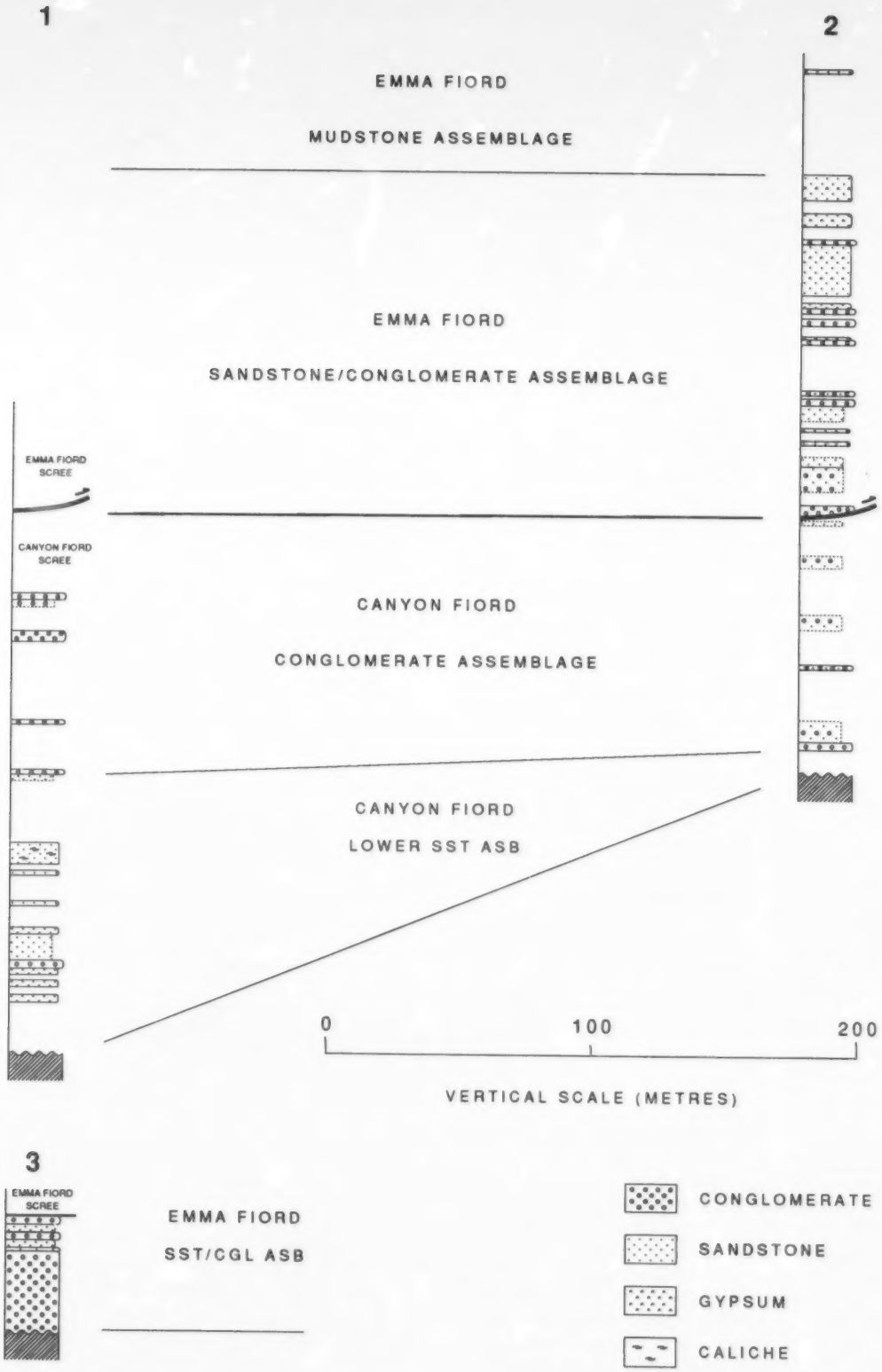

Figure 3. Columnar stratigraphic cross-section of the Emma Fiord and Canyon Fiord formations.

subordinate fabric, consisting of euhedral gypsum crystals or their associated moulds, also occurs locally within the sandstones. These crystals or moulds are less than 1 cm across. In general, the gypsum sheets or isolated crystals vary greatly in colour, with bright orange, light yellowish orange, dark greyish brown, and whitish varieties.

The conglomerate/sandstone assemblage is interpreted as streamflow deposits of probable distal alluvial fan to proximal braided stream origin, based on sedimentary structures, grain size, lack of overbank mudstones, and the structural configuration of the Nesodden depression. Many conglomerate beds have maximum particle size values above 10 cm, which is unique for the Emma Fiord Formation: at other localities, clasts seldom exceed 5 cm in size. This suggests that a relatively strong topographic gradient, most likely fault-controlled, existed at the margin of the Nesodden depression in Early Carboniferous time. Moreover, the limestone and sandstone composition of most clasts is evidence of limited transport, suggesting derivation from a local source where Franklinian formations had been exhumed along fault scarps. At all other Emma Fiord localities, the conglomerates are composed mostly of chert, a feature interpreted as representing both significant transport along regional topographic slopes, and the presence of a silicified pre-Carboniferous surface (Davies and Nassichuk, 1988). This silicified surface, which would have been formed during and following the Ellesmerian Orogeny in Late Devonian time, possibly contributed to supply the Nesodden depression with the minor chert clasts observed, while the bulk of the sediments was being shed from underlying limestone and sandstone units exposed by block faulting.

The predominant fracture-filling mode of occurrence for the gypsum indicates a secondary origin. It is believed that its emplacement was directly related to compressional folding and faulting during the middle Tertiary Eurekan Orogeny, a tectonic event that could have induced the upward migration of saline brines into newly fractured Emma Fiord strata. It is significant that the gypsum tends to be much more concentrated in strata showing intense deformation, as in the area north of the master strike-slip fault, and adjacent to Section 2 (Fig. 1). Furthermore, a fault-bounded salt diapir immediately south of Section 3, along the southwestern margin of the Nesodden depression, was probably derived from the Ordovician Bay Fiord Formation. This unit may also have been the source of saline fluids for the Emma Fiord secondary gypsum.

Mudstone assemblage

The mudstone assemblage of the Emma Fiord Formation occupies the axial part of the Nesodden depression, where it occurs as a covered recessive interval of shale/siltstone material with only minor outcropping sandstone ledges. These exposed sandstone intervals reach 2 m in thickness, and the sandstones are parallel laminated and tabular crossbedded, grey, and very fine to fine grained. The recessive intervals are believed to represent mudstone units, on the basis of the fine grain and dark grey colour of the scree material, and on the widespread occurrence of a comparable assemblage at the other Emma Fiord localities in the Sverdrup Basin (Thorsteinsson, 1974; Davies and Nassichuk, 1988). By analogy with the lacustrine interpretation invoked for much of the assemblage at these other localities, where exposures are significantly better, the covered mudstone assemblage in the Nesodden depression is considered to be at least partly lacustrine. The subordinate sandstone ledges possibly represent low-energy fluvial deposits.

The ubiquitous greyish colouration of the continental deposits and the presence of bituminous shale, not only in the Nesodden depression but in all Sverdrup Basin occurrences, indicate that deposition of the Emma Fiord Formation during Viséan time occurred under the influence of a tropical humid or subhumid climate. Generic and specific identifications of microflora and macroscopic plant fragments also point to such a setting (Davies and Nassichuk, 1988), as do the paleogeographic plate reconstructions for that time interval, in which the northern tip of North America is positioned at a latitude of approximately 20 to 25°N (Scotese et al., 1979; Smith et al., 1981).

Canyon Fiord Formation

The Canyon Fiord Formation of the Nesodden depression consists of two distinct assemblages: a lower sandstone assemblage, exposed at Section 2, and an overlying conglomerate assemblage, exposed at Sections 1 and 2. These two assemblages are similar to those described by Thériault (1991) from the Trold Fiord area of southwestern Ellesmere Island.

Lower sandstone assemblage

This assemblage is exposed in a river gully on the west side of the lake, where Section 3 was measured (Fig. 1). It is composed of three distinct lithofacies: a sandstone lithofacies, a conglomerate lithofacies, and a heterogeneous sandstone/limestone lithofacies. The sandstone lithofacies accounts for approximately 80 per cent of the assemblage, and consists of very fine to fine sandstone that is mottled (light grey to medium reddish brown colour), fine to medium bedded, and parallel laminated to tabular cross-stratified. Desiccation cracks have been observed on a few scree blocks. Individual grains are composed predominantly of quartz, with a small amount of generally muddy yet locally calcareous matrix. The conglomerate lithofacies is represented solely by a resistant 3 m thick interval in the lower part of the assemblage at Section 1. This interval appears to consist of 5 to 6 different crude beds that are internally massive, clast-supported, and composed of 80% limestone and 20% sandstone clasts. The clasts show no preferred orientation, are mainly subrounded in outline, and have maximum particle size values varying between 8 cm and 15 cm from bed to bed. Matrix forms approximately 10%, is medium brownish red, and consists of coarse to fine sand with subordinate mud. The heterogeneous sandstone/limestone lithofacies forms the uppermost part of the lower sandstone assemblage, and occurs as a continuous 8 m thick interval comprising layers of reddish sandstone hosting

minor calcareous aggregates, alternating with layers of nodular, massive, or laminated limestone with interstitial reddish sandstone. The sandstone-rich layers compare well with reported examples of nodular caliche, a type of paleosol commonly found in recent surficial sediments from semiarid settings. Similarly, the limestone-rich layers are interpreted as nodular, massive, and laminar caliche, which represent progressively more mature stages of development.

The lower sandstone assemblage is interpreted as low-energy fluvial deposits, based on the presence of streamflow-related sedimentary structures, the relatively fine grained nature and reddish colouration of the sediment, and the presence of secondary limestone of caliche origin. The orientation of the corresponding river system remains equivocal, as paleocurrent orientations could not be recovered. The poorly defined nature of foreset laminae and the spherical shape of most of the larger particles or clasts is such that cross-stratification measurements would not have been reliable, and clast imbrication was simply not observed.

Conglomerate assemblage

The conglomerate assemblage is overall red weathering, and consists of clast-supported pebble conglomerate, occurring in relatively sheetlike units, and subordinate fine sandstone interlayers. Individual conglomerate beds are 10 to 30 cm thick on average, and are generally crudely stratified, and internally normal-graded or ungraded. They are composed of 80 to 90% limestone, 10% sandstone, and less than 10% chert clasts, with grain outlines ranging from subrounded to subangular. Maximum particle size values vary from 8 to 15 cm, and display no apparent vertical trend. Matrix is sandy and constitutes less than 15%.

The reddish colouration of the conglomerate assemblage sugggests a continental environment of deposition. In addition, the clast-supported framework and relatively organized nature of the conglomerates suggest deposition mainly from traction currents of streamflow origin, probably in the distal alluvial fan or proximal braided stream environment. The more massive beds were probably deposited by mass-flow processes. Although no paleocurrent indicators were observed, it is believed that the coarse clastic material was shed in a southwesterly direction, away from an adjacent fault scarp. The fact that the conglomerate assemblage is absent from the southern part of the Nesodden depression reflects either preferential erosion along the southern fault scarp in post-Canyon Fiord time, or asymmetric distribution of the assemblage due to half-graben sedimentation, essentially along a master fault located in the northern part of the depression.

The consistent reddish colouration of the lower sandstone and conglomerate assemblages of the Canyon Fiord Formation, together with the occurrence of well developed caliche paleosols, are indicative of a warm arid or semiarid climate at the time of deposition (most likely Bashkirian). Additional features displayed elsewhere but not in the Nesodden succession include the presence of local evaporites and widespread beresellid-rich limestones interbedded with Canyon Fiord redbeds, as found on southwestern Ellesmere Island (Thériault, 1991).

DISCUSSION

Carboniferous strata of the Emma Fiord and basal Canyon Fiord formations have been discovered in a Tertiary graben on northwestern Devon Island. Because this succession is restricted to the confines of the graben, and because the Emma Fiord conglomerates display unusually proximal characteristics for this unit, it is thought that an extensional tectonic depression existed in Carboniferous time and controlled local sedimentation. Bounded more or less by the same northeast-southwest fault system as that of the Tertiary graben, this depression is herein named the "Nesodden despression."

Indirect evidence of a transtensive origin is provided in a basinwide context. Most Emma Fiord occurrences throughout Sverdrup Basin have been shown to be separated from the overlying unit (either the Canyon Fiord Formation at the basin margin, or the Borup Fiord Formation at the basin centre) by an angular unconformity or disconformity (Thorsteinsson, 1974; Davies and Nassichuk, 1988). Unfortunately, this contact in the Nesodden depression is fault-bounded, and a depositional hiatus in the area can only be suggested on the basis of the marked sedimentological differences between the Emma Fiord and Canyon Fiord formations. It is unlikely that Tertiary faulting stripped away a transitional interval between the two units, since the contact is erosional and sharply distinct at all other occurrences. In any case, the unconformity at the top of the Emma Fiord is taken to reflect a change from a regime of tectonic subsidence and sediment accumulation, to a regime of tectonic uplift and associated erosion within the many fault-bounded depressions. This phase of tectonic uplift, or basin inversion, is possibly transpressive in nature, and followed a phase of transtension during which Emma Fiord sedimentation occurred. It appears to be the norm rather than the exception for successor rift basins to be initiated with a short episode of wrench faulting, followed by a longer lasting episode of relatively pure extensional faulting. Well known examples include the Devonian basins of the North Atlantic region, and some Late CarboniferousEarly Permian basins of northwestern Europe (Ziegler, 1982). Likewise, in the Canadian Arctic, the last compressional stages of the Franklinian Mobile Belt in latest Devonian could very well have been succeeded by a wrench faulting event, leading to deposition and partial erosion of the Emma Fiord Formation in the Early Carboniferous, followed by ongoing extensional rifting in the Late Carboniferous and Early Permian. The hypothetical shift from transtension to pure extension appears to be related to a major plate reorganization in the circum Arctic regions, as sedimentological and biogenic evidence demonstrates a sharp climatic change from tropical humid in Emma Fiord time (Viséan), to tropical semiarid in Canyon Fiord and Borup Fiord time (Serpukhovian-Bashkirian). A comparable climatic change has also been reported from the Carboniferous succession of Svalbard (Steel and Worsley, 1984).

Also relevant is the fact that the distribution of Emma Fiord strata is unrelated to major depocentres developed later in the Carboniferous or Early Permian. Localities at which the thickest successions of post-Emma Fiord strata are found do not generally contain Emma Fiord sediments. This peculiarity suggests that the formation accumulated in small depressions that did not evolve into major depocentres. Instead, new faults were activated, probably in association with a reorientation of lithospheric stresses at the scale of the basin. At the same time, the depressions hosting Emma Fiord sediments probably evolved from being controlled by strike-slip fault systems in the Viséan, to dip-slip fault systems in the Serpukhovian (Borup Fiord time) and Bashkirian (Canyon Fiord time). These depressions may not have undergone any significant tectonic inversion until the late Early Permian Melvillian Disturbance (Beauchamp et al., 1989a), an event which accompanied the abortion of Sverdrup Basin rifting.

ACKNOWLEDGMENTS

We wish to thank Benoit Beauchamp for reviewing the manuscript, and providing helpful comments.

REFERENCES

Beauchamp, B.
1987: Stratigraphy and facies analysis of the Upper Carboniferous to Lower Permian Canyon Fiord, Belcher Channel and Nansen formations, southwestern Ellesmere Island; Ph.D. Thesis, University of Calgary, June 1987, 370 p.

Beauchamp, B., Harrison J.C., and Henderson, C.M.
1989a: Upper Paleozic stratigraphy and basin analysis of the Sverdrup Basin, Canadian Arctic Archipelago: Part 1, time frame and tectonic evolution; in Current Research, Part G; Geological Survey of Canada, Paper 89-1G, p. 105-113.

Beauchamp, B., Harrison, J.C., and Henderson, C.M.
1989b: Upper Paleozoic stratigraphy and basin analysis of the Sverdrup Basin, Canadian Arctic Archipelago: Part 2, transgressive-regressive sequences; in Current Research, Part G; Geological Survey of Canada, Paper 89-1G, p. 115-124.

Davies, G.R. and Nassichuk, W.W.
1988: An Early Carboniferous (Viséan) lacustrine oil shale in Canadian Arctic Archipelago; American Association of Petroleum Geologists, Bulletin, v. 92, p. 8-20.

Eisbacher, G.H.
1992: Structural geology of northwestern Devon Island, Arctic Canada; in Current Research, Part B; Geological Survey of Canada, Paper 92-1B.

Embry, A.F.
1988: Triassic sea-level changes: evidence from the Canadian Arctic Archipelago; in Sea-Level Changes – An Integrated Approach; Society of Economic Paleontologists and Mineralogists, Special Publication No. 42.

Mayr, U.
in press: Reconnaissance and preliminary interpretation of Upper Devonian to Permian stratigraphy of northeastern Ellesmere Island, Canadian Arctic Archipelago; Geological Survey of Canada, Paper 91-8.

Miall, A.D.
1983: The Nares Strait problem: a re-evaluation of the geological evidence in terms of a diffuse oblique-slip plate boundary between Greenland and the Canadian Arctic Islands; Tectonophysics, v. 100, p. 227-239.

Nassichuk, W.W.
1975: Carboniferous ammonoids and stratigraphy in the Canadian Arctic Archipelago; Geological Survey of Canada; Bulletin 237, 240 p.

Nassichuk, W.W. and Davies, G.R.
1980: Stratigraphy and sedimentation of the Otto Fiord Formation; Geological Survey of Canada, Bulletin 286.

Scotese, C.R., Bambach, R.K., Barton, C., Van der Voo, R., and Ziegler, A.M.
1979: Paleozoic base maps; Journal of Geology, v. 87, p. 217-277.

Smith, A.G., Hurley, A.M., and Briden, J.C.
1981: Phanerozoic Continental World Maps; Cambridge University Press, Cambridge.

Steel, R.J. and Worsley, D.
1984: Svalbard's post-Caledonian strata — an atlas of sedimentation patterns and palaeogeographic evolution; in Petroleum Geology of the North European Margin, (ed.) Graham and Trotman; Norwegian Petroleum Society, p. 109-135.

Thériault, P.
1991: Synrift sedimentation in the Upper Carboniferous Canyon Fiord Formation, SW Ellesmere Island, Canadian Arctic; M.Sc. Thesis, University of Ottawa, March 1991, 210 p.

Thériault, P. and Beauchamp, B.
1991: Preliminary interpretation of the depositional history and tectonic significance of the Carboniferous to Permian Canyon Fiord Formation, west-central Ellesmere Island, Arctic Archipelago; in Current Research, Part B; Geological Survey of Canada, Paper 91-1B, p. 93-103.

Thorsteinsson, R.
1974: Carboniferous and Permian stratigraphy of Axel Heiberg Island and western Ellesmere Island, Canadian Arctic Archipelago; Geological Survey of Canada, Bulletin 224.

Trettin, H.P.
1989: The Arctic Islands; in The Geology of North America An Overview, Boulder, Colorado, Geological Society of America, (ed.) A.W. Bally and A.R. Palmer; The Geology of North America, v. A, p. 349-370.

Ziegler, P.A.
1982: Geological Atlas of Western and Central Europe; Shell Internationale Petroleum, (ed.) B.V. Maatschappij; Elsevier Scientific Publishing Company, Amsterdam, 130 p.
1988: Evolution of the ArcticNorth Atlantic and the Western Tethys; American Association of Petroleum Geologists, v. 43, 198 p.

Geological Survey of Canada Project 850039

Study of the Triangle Zone and Foothills structures in the Grease Creek Syncline area of Alberta

Gregory S. Soule[1] and Deborah A. Spratt[1]
Institute of Sedimentary and Petroleum Geology, Calgary

Soule, G.S. and Spratt, D.A., 1992: Study of the Triangle Zone and Foothills structures in the Grease Creek Syncline area of Alberta; in Current Research, Part B; Geological Survey of Canada, Paper 92–1B, p. 73-78.

Abstract

Foothills structures and stratigraphy in southwestern Alberta between Little Red Deer River and Red Deer River were mapped at a scale of 1:20 000 during the summer of 1991. The Triangle Zone structure at the leading edge of the Foothills is shown to have an en echelon geometry. Four east-dipping backthrusts or 'upper detachment' horizons were recognized east of the surface expression of the Triangle Zone on Silver Creek. Stratigraphic thicknesses estimated from palynology will help to demonstrate whether or not these east-dipping faults structurally thicken the section and aid in the determination of fault displacement magnitudes. There are few stratigraphic markers within the Brazeau Group. A chert-pebble conglomerate divides the "Lower" and "Upper" parts of the Brazeau on Fallentimber Creek, although it is not yet clear whether the conglomerate is present at the same stratigraphic level throughout the study area.

Résumé

Les structures et la stratigraphie des Foothills dans le sud-ouest de l'Alberta, entre les rivières Little Red Deer et Red Deer, ont été cartographiées à l'échelle de 1/20 000 au cours de l'été 1991. Deux parties de la zone Triangle à la limite frontale des Foothills sont en échelon. Quatre chevauchements à pendage vers l'est, qui sont des décollements supérieurs, affleurent à l'est de la zone Triangle, dans la région de Silver Creek. La palynologie aidera à déterminer l'épaisseur stratigraphique ainsi qu'à déterminer si les chevauchements à pendage vers l'est causent l'épaississement de la structure, et contribuera à établir la magnitude du déplacement le long de ces failles. Il n'y a que quelques marqueurs stratigraphiques dans le groupe de Brazeau; un conglomérat à galets de chert se trouve entre les parties inférieure et supérieure du groupe, mais il n'est pas certain que ce conglomérat se présente au même niveau stratigraphique dans tout la région à l'étude.

[1] Department of Geology and Geophysics, University of Calgary, Calgary, Alberta T2N 1N4

INTRODUCTION

A Triangle Zone, or zone of underthrusting, occurs along the eastern edge of the Foothills Belt. The Grease Creek Syncline area is the only place in the southern Alberta Foothills where Tertiary rocks are preserved in the hanging wall of the Triangle Zone's upper detachment west of the surface anticline.

The study area is located approximately 60 km northwest of Calgary, Alberta. The area extends from the Little Red Deer River in the south to the Red Deer River, 25 km farther north (Fig. 1). Field investigations focused on the structure of the Foothills Belt along Little Red Deer River and Fallentimber Creek in the north. During the summer of 1991, 1:20 000 scale mapping was conducted from the eastern edge of the deformation belt, continuing westward for approximately 30 km. The Triangle Zone was also mapped along strike on the Red Deer River and Dogpound Creek (Fig. 1).

The term 'Triangle Zone' was introduced by Gordy et al. (1977) to describe the antiformal surface geometry underlain by horizontal strata at the eastern edge of the deformation belt. The Triangle Zone was formed by the delamination of the foreland basin strata and the eastward wedging of a duplex along the delaminated horizon (Fig. 2). The foreland basin

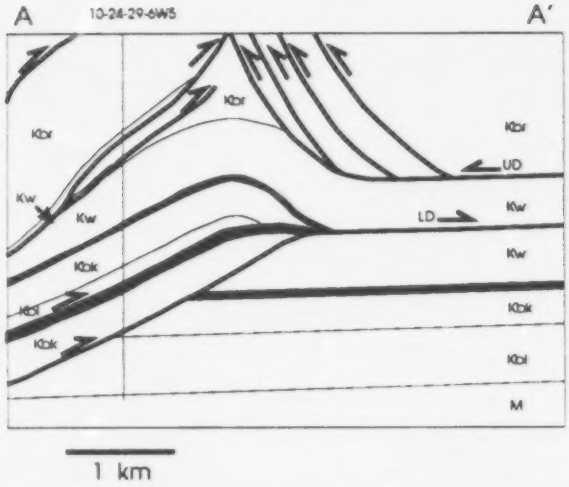

Figure 2. Schematic cross-section of the Triangle Zone showing emplacement of a wedge of strata along a detachment horizon at the top of the Wapiabi Formation (Kw). Note that the upper (UD) and lower (LD) detachments do not converge in this part of the Triangle Zone. Line of section A–A is shown in Figure 4. M = Mississippian, Fernie Formation, and Kootenay Group (undivided); Kbl = Blairmore Group; Kbk = Blackstone Formation; Kc = Cardium Formation; Kbr = Brazeau Group.

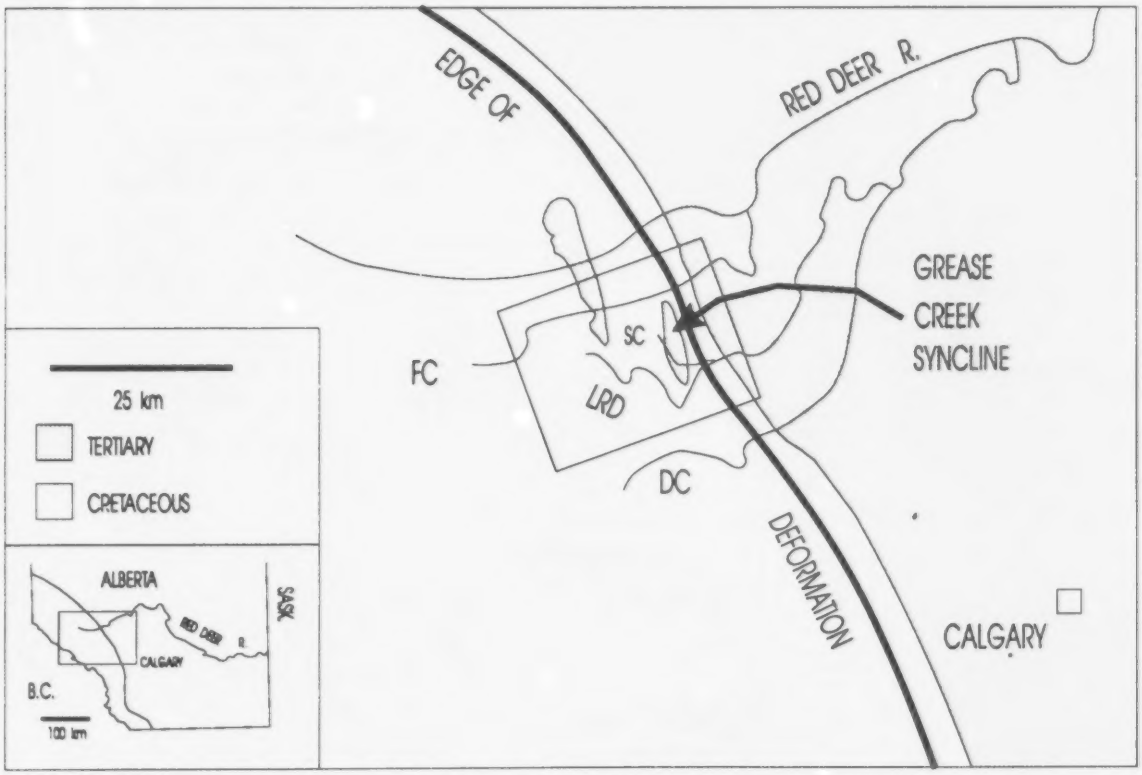

Figure 1. Location map, showing the Grease Creek area (in box) extending southwestward from the edge of deformation. Field mapping was also conducted near the edge of deformation along Dogpound Creek (DC) and the Red Deer River; FC = Fallentimber Creek; LRD = Little Red Deer River; SC = Silver Creek. The boundaries of Figure 1 are delineated on the regional map (inset).

strata above the delaminated horizon were tilted to the east by this progressive wedging, and an east-dipping 'backthrust' or upper detachment surface was formed (Fig. 2).

The upper detachment has been recognized as a part of the Triangle Zone structure (Jones, 1982; Charlesworth and Gagnon, 1985; Price, 1986), but the east-dipping faults are not shown on published maps of the Grease Creek area, and the nature of these faults (do they ramp upsection in the direction of transport?) is also in question. The Grease Creek area was chosen as a favourable locality in which to investigate the behaviour of faulting, and upper detachment surfaces in particular, at the eastern edge of deformation, because Tertiary strata are preserved within the Foothills Belt in this area. The presence of these Tertiary rocks west of the surface expression of the Triangle Zone indicates that, structurally, the level of exposure in the study area is higher than in the Wildcat Hills and Jumpingpound areas to the south (Ollerenshaw, 1978).

STRATIGRAPHY

Figure 3 shows a generalized stratigraphic column. The carbonate rocks and calcareous shales (Oswald, 1964) of the Mississippian Rundle Group outcrop to the west of the study area in the Panther River Culmination, and to the north (Ollerenshaw, 1978). The top of the Mississippian, although not exposed in the study area, is a good marker on seismic sections and well logs, as is the Jurassic Fernie Formation. The Fernie Formation comprises 40 m of black, platy shale with thin limestone interbeds, and is separated from the underlying Mississippian by a major unconformity (Hall, 1987).

The Kootenay Group is the oldest stratigraphic unit exposed in the field area. The Kootenay is approximately 60 m thick and consists of interbedded sandstone, shale, and coal seams (Hamblin and Walker, 1979). The Blairmore Group is 455 to 515 m thick (Workum, 1978), and includes the Cadomin, Gladstone, and Beaver Mines formations in the study area. The Cadomin is a chert-pebble conglomerate that unconformably overlies the Kootenay Group. The Gladstone Formation comprises sandstone, shale and limestone, with limestone and calcareous shale at the top, and overlies the Cadomin Formation. The Beaver Mines Formation consists of nonmarine, greenish grey or grey mudstone and sandstone overlying the Calcareous member of the Gladstone Formation (Ollerenshaw and Hayes, 1982). The overlying Blackstone Formation is 300 m thick and consists of dark grey to black, marine shale with siltstone interbeds (Stott, 1963). The Cardium Formation is a very good marker on seismic sections and well logs, and the fine, grey sandstone with crystalline cement is easily recognized in the field. It is about 60 m thick (Stott, 1963).

Because the focus was on structures exposed in the eastern Foothills, the stratigraphy studied was primarily that of the overlying Wapiabi Formation, Brazeau Group, and Coalspur Formation. The Wapiabi Formation is 540 m thick and consists of dark grey to black marine shale with varying amounts of siltstone interbeds (Stott, 1963). Ammonites and pelecypods are commonly found near the base, and there are varying quantities of rust weathering concretions throughout. The Brazeau Group comprises approximately 1000 m of strata (Stott, 1963) of continental origin (Jerzykiewicz and Sweet, 1986), and consists of channelled, greenish or light grey sandstone, and green-grey or light brown shale and mudstone. It is correlative with the Belly River, Bearpaw, and St. Mary River formations to the south; however, the marine shale of the Bearpaw is not present in the study area, so that differentiation of the formations is not possible (Jerzykiewicz and Sweet, 1988). Marker horizons in the Brazeau Group are rare; the sandstones are of a channelled nature and are compositionally very similar throughout. It is therefore very difficult to determine the offset on faults that occur solely within the Brazeau. There are few coal seams in the Brazeau Group of the study area to serve as markers. Within the Brazeau, the only marker horizon recognizable in the field is present primarily in the northern part of the area; there is a chert-pebble conglomerate that occurs in the middle of the group, allowing it to be divided into the Lower and Upper Brazeau [this division also appears on geological maps by Ollerenshaw (1967, 1978)]. The chert-pebble conglomerate is well exposed in the nearly complete Brazeau section on Red

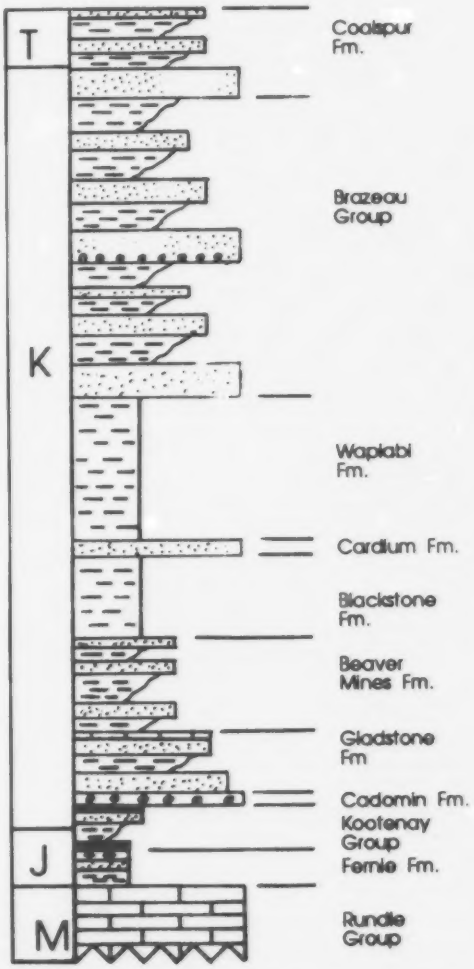

Figure 3. Generalized stratigraphy of the field area. M = Mississippian, J = Jurassic, K = Cretaceous, T = Tertiary.

Deer River (UTM 462284), and it can be correlated with the conglomerate on Fallentimber Creek. Chert-pebble conglomerates are also present in the Brazeau Formation on Little Red Deer River; however, their stratigraphic relationship to those farther north is unclear.

Defining the "base of the Tertiary" presents another problem for field mapping. Recognition of the Tertiary has been based on the presence of fossilized leaves – this is how previous workers in the Foothills have mapped the base (Jerzykiewicz, pers. comm., 1991). The inherent problems of preservation of these fossils makes it difficult to map the boundary precisely [it should be noted the Cretaceous–Tertiary boundary actually occurs in the middle of the Coalspur Formation (Fig. 3) (Jerzykiewicz and Sweet, 1986)]. The base of the Coalspur Formation was mapped at the base of a thick (5-10 m) sandstone above which fossilized leaves are found. This practice coincides with the stratigraphic definitions of Jerzykiewicz and Sweet (1986).

STRUCTURE

The most significant result of the study to date has been the recognition of four successive upper detachment surfaces on Silver Creek (Fig. 4). The surface expression of the Triangle

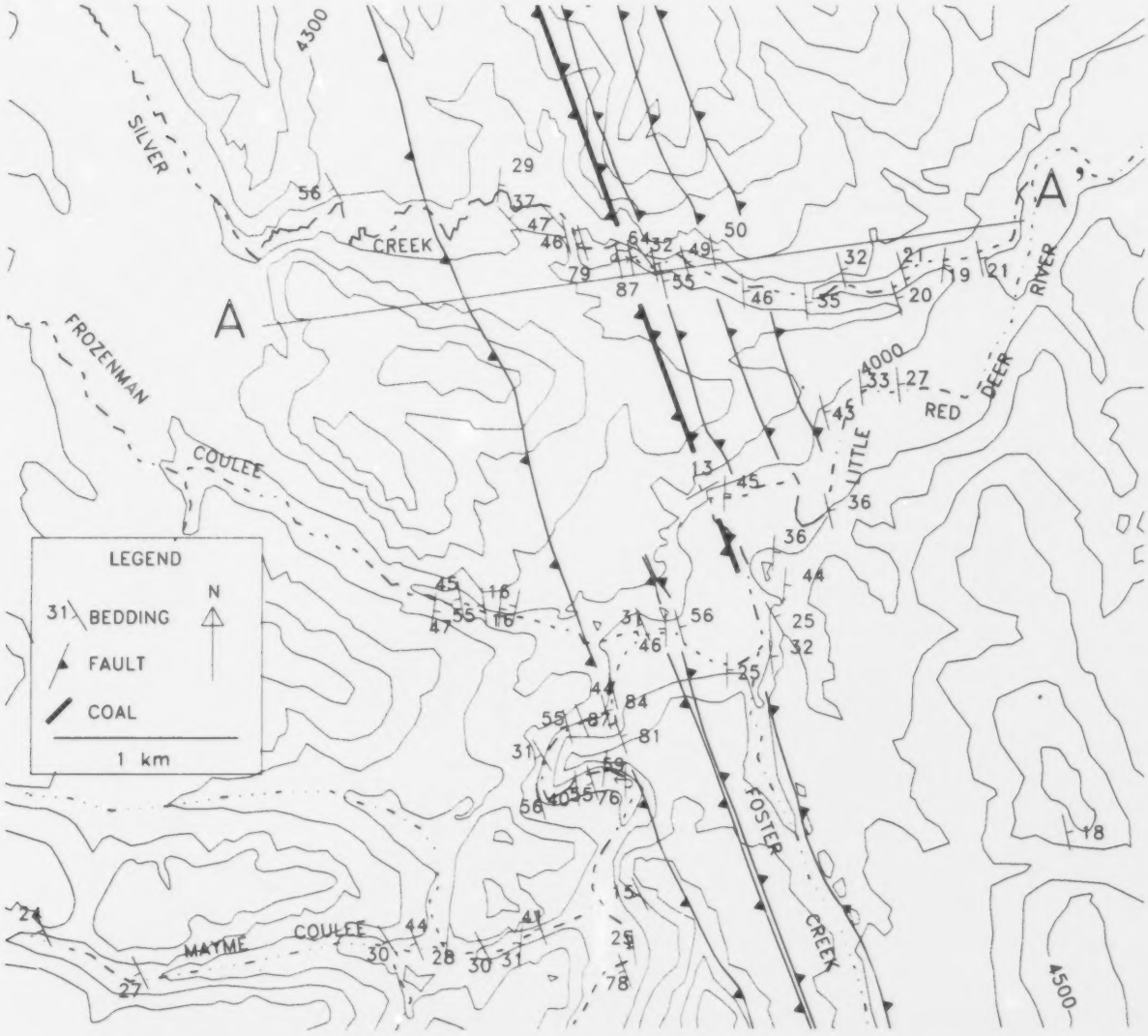

Figure 4. Map showing two, en echelon segments of the Triangle Zone core exposed near the confluence of Silver Creek and Little Red Deer River (see Fig. 1 for location). The narrow core of the Triangle Zone is bounded by east- and west-dipping faults; coal exists in the core in the northern part of the area shown on the map. All rocks mapped are Cretaceous Brazeau Group; part of the east limb of Grease Creek Syncline is exposed in Mayme Coulee (in the southwest corner of the map). Tertiary rocks in the core of Grease Creek Syncline lie just west of the area covered by this map.

Zone on Silver Creek is a tight anticline, with both west- and east-verging faults cutting through the core (Fig. 2). Vergence directions in the study area are determined from the shear sense indicated by offset on minor faults (e.g., Fig. 5) and by asymmetric minor folds. The west-dipping, east-verging thrust appears to be the most important fault on Silver Creek, since the minor structures in the core of the anticline are predominantly east-verging minor folds. Bedding inclination decreases from approximately 60° east at the Triangle Zone to approximately 20° east 2 km farther east (Fig. 4). The east-dipping strata are for the most part parallel strata that are tilted but not internally deformed. However, three fault zones are identified from their somewhat fractured footwalls, and particularly from slickensides on parallel and subparallel bedding surfaces. Furthermore, local steepening of upper detachment hanging wall strata, presumably caused by footwall ramps, interrupts the progressive eastward shallowing of bedding dips. The slickensides indicate hanging wall (east side) motion that is up-to-the-west. Further investigation of Silver Creek is needed to determine whether the west-verging upper detachment surfaces ramp upsection in the direction of transport, as the east-verging thrusts do. A minor fault in the footwall of an upper detachment clearly ramps upsection (Fig. 5), suggesting that the upper detachment surfaces do as well.

Figure 5. A minor, east-dipping thrust fault in the footwall of an upper detachment surface on Silver Creek. Looking south; notebook is 20 cm long.

The horizontal spacing of upper detachment surfaces on Silver Creek seems to be fairly regular at about 200 to 250 m (Fig. 4). The number of upper detachments initiated may be related to the progressive wedging occurring in the Triangle Zone below. The magnitude of displacement on the upper detachment surfaces is currently unknown, since none of the faults offsets any formational contacts or other marker horizons. In future studies we will attempt to determine the magnitude of the offset, based on seismic and well data, and palynological analysis of selected samples. Palynology of the coal that outcrops in the Triangle Zone on Silver Creek will be used to estimate the stratigraphic position of the coal and the thickness of the Brazeau Group above the detachment faults. The actual thickness of the Brazeau above that coal (determined from surface and well data) will then be compared with the estimated total thickness, to see if any structural thickening has occurred. It is expected that some structural thickening has occurred, given that these upper detachment surfaces probably ramp upsection (as shown in Fig. 5), repeating older strata on top of younger strata. An estimate of the minimum displacement on the four upper detachment surfaces will be made and incorporated in balanced geological cross-sections.

Detailed 1:20 000 scale mapping in the study area shows the en echelon nature of faults within the Triangle Zone (Fig. 4). Previously published maps of the area (Mackay, 1937; Hage and Hume, 1941; Ollerenshaw, 1978) were not detailed enough to show this en echelon geometry. The core of the Triangle Zone is very narrow and is well exposed on Silver Creek and Little Red Deer River (Fig. 4), yet appears to die out along strike to the south, since all rocks exposed near the mouth of Foster Creek are east dipping. The core of the Triangle Zone, shown in Figure 4 (southern part), outcrops approximately 400 m farther west. An implication of the en echelon nature of the Triangle Zones is that hanging wall splays from the west-verging upper detachment surfaces, which occur on the eastern flanks of triangle zones, must also be en echelon. Detailed mapping of these west-verging faults may aid in the delineation of en echelon triangle zone cores in areas where the core itself is not well exposed.

Jones (1982, Figure 18) depicted Grease Creek Syncline as a klippe in the west-verging hanging wall of the folded upper detachment. His duplex model for triangle zone development assumes that the upper detachment is bedding parallel, whereas the Charlesworth et al. (1985, 1987) model involves an upper detachment that ramps upsection to the west. The trajectory of the upper detachment is critical in the construction of balanced cross-sections and in establishing whether the Jones model (1978, 1982) or the Charlesworth et al. model (1985, 1987) is applicable. To date, the few vergence indicators that we have found on the east and west limbs of Grease Creek Syncline indicate east vergence, and ramping of the upper detachment is not demonstrable in the field; suggesting that the Grease Creek area does not fit either of the proposed triangle zone models exactly.

FUTURE WORK

Determination of the structural relationships between Grease Creek Syncline and the rocks beneath, east, and west of it, will require the compilation of well, seismic, palynological, and field data during 1991-1992. Balanced cross-sections will be produced, extending westward from the Triangle Zone to the Burnt Timber or McConnell thrusts. These cross-sections will be constrained by data from surface exposures, seismic sections, and boreholes, and will be used to construct sequentially restored sections to demonstrate the development of the Triangle Zone. The ramp and flat horizons, and the detachment levels identified in the cross-sections will be compared with those in the Wildcat Hills and Jumpingpound areas (Spratt and Lawton, 1990) to the south, in an attempt to demonstrate a controlling factor (e.g., lithology) for the stratigraphic position of detachments. Finally, the overall Triangle Zone geometry will be compared with that in the Wildcat Hills, Jumpingpound (Spratt and Lawton, 1990), and Turner Valley (MacKay, 1991) areas.

ACKNOWLEDGMENTS

Fieldwork for this study was funded by the Department of Energy, Mines and Resources (Contract No. 23294-1-0525/01-XSG). Ted Bergman assisted Greg Soule in the field and digitized map data.

REFERENCES

Charlesworth, H.A.K. and Gagnon, L.G.
1985: Intercutaneous wedges, the Triangle Zone and structural thickening of the Mynheer coal seam at Coal Valley in the Rocky Mountain Foothills of central Alberta; Bulletin of Canadian Petroleum Geology, v. 33, p. 22-30.

Charlesworth, H.A.K., Johnston, S.T., and Gagnon, L.G.
1987: Evolution of the Triangle Zone in the Rocky Mountain Foothills near Coalspur, central Alberta; Canadian Journal of Earth Sciences, v. 24, p. 1668–1678.

Gordy, P.L., Frey, F.R., and Norris, D.K.
1977: Geological guide for the Canadian Society of Petroleum Geologists and 1977 Waterton – Glacier Park Field Conference; Calgary, Canadian Society of Petroleum Geologists, 93 p.

Hage, C.O. and Hume, G.S.
1941: Wildcat Hills (East Half) Alberta; Geological Survey of Canada, Map 652A (scale 1:63 360).

Hall, R.L.
1987: New Lower Jurassic ammonite faunas from the Fernie Formation, southern Canadian Rocky Mountains; Canadian Journal of Earth Sciences, v. 24, p. 1688-1704.

Hamblin, A.P. and Walker, R.G.
1979: Storm dominated shallow marine deposits: the Fernie–Kootenay (Jurassic) transition, southern Rocky Mountains; Canadian Journal of Earth Sciences, v. 16, p. 1673-1690.

Jerzykiewicz, T. and Sweet, A.R.
1986: The Cretaceous–Tertiary boundary in the central Alberta Foothills. I: Stratigraphy; Canadian Journal of Earth Sciences, v. 23, p. 1356-1374.
1988: Sedimentological and palynological evidence of regional climatic changes in the Campanian to Paleocene sediments of the Rocky Mountain Foothills, Canada; Sedimentary Geology, v. 59, p. 77-92.

Jones, P.B.
1978: Notes on the geologic structures of the Foothills and eastern Rocky Mountains between Rocky Mountain House and Saskatchewan Crossing, Alberta; in Geological Guide to the Central Foothills and Rocky Mountains of Alberta, (ed.) P.B. Jones and R.H. Workum; Canadian Society of Petroleum Geologists, p. 16–23.
1982: Oil and gas beneath east-dipping underthrust faults in the Alberta Foothills; in Geologic Studies of the Cordilleran Thrust Belt, (ed.) R.B. Powers; Rocky Mountain Association of Geologists, v. 1, p. 61-74.

MacKay, B.R.
1937: Fallentimber (West Half) Alberta; Geological Survey of Canada, Map 549A (scale 1:63 360).
1939: Fallentimber (East Half) Alberta; Geological Survey of Canada, Map 548A (scale 1:63 360).

MacKay, P.A.
1991: A geometric, kinematic and dynamic analysis of the structural geology at Turner Valley, Alberta; Ph.D. thesis, University of Calgary, Calgary, 138 p.

Ollerenshaw, N.C.
1967: Geology, Wildcat Hills (West Half), Alberta; Geological Survey of Canada, Map 1351A (scale 1:50 000).
1978: Geology, Calgary, Alberta–British Columbia; Geological Survey of Canada, Map 1457A (scale 1:250 000; five cross-sections at 1:125 000 scale).

Ollerenshaw, N.C. and Hayes, B.
1982: Burnt Timber Creek Guidebook; Canadian Society of Petroleum Geologists, Calgary.

Oswald, D.H.
1964: Mississippian stratigraphy of south-eastern British Columbia; Bulletin of Canadian Petroleum Geology, v. 12, p. 452-459.

Price, R.A.
1986: The southeastern Canadian Cordillera: thrust faulting, tectonic wedging, and delamination of the lithosphere; Journal of Structural Geology, v. 8, p. 239-254.

Spratt, D.A. and Lawton, D.C.
1990: Displacement transfer in the Triangle Zone of S.W. Alberta; Geological Society of America, Abstracts with Programs, Rocky Mountain Section, v. 22, no. 6, p. 45.

Stott, D.F.
1963: The Cretaceous Alberta Group and equivalent rocks, Rocky Mountain Foothills, Alberta; Geological Survey of Canada, Memoir 317, 306 p.

Workum, R.H.
1978: Stratigraphy, central Foothills and eastern Rockies of Alberta; in Geological Guide to the Central Foothills and Rocky Mountains of Alberta, (ed.) P.B. Jones and R.H. Workum; Canadian Society of Petroleum Geologists, Calgary, p. 3-16.

Geological Survey of Canada Project 870007

A petrographic study of coal-bearing strata in the Drumheller area, Red Deer River valley, Alberta

Thomas Gentzis[1], Fariborz Goodarzi, and David Gibson
Institute of Sedimentary and Petroleum Geology, Calgary

Gentzis, T., Goodarzi, F., and Gibson, D., 1992: A petrographic study of coal-bearing strata in the Drumheller area, Red Deer River valley, Alberta; in Current Research, Part B; Geological Survey of Canada, Paper 92-1B, p. 79-89.

Abstract

The petrography of eight, major, subbituminous coal seams of the Edmonton Group in the Drumheller area of the Red Deer River valley in the Alberta Plains was investigated in 1991. The coals are dominated by huminite group macerals (humotelinite and humocollinite predominate), with a minor to moderate content of liptinite and inertinite.

The predominance of cellular and massive macerals over detrital macerals is indicative of the autochthonous nature of the peat. Reflectance values range from 0.38 to 0.51%, highest in the coal seams and lowest in the carbonaceous shales, in agreement with previous results for subbituminous and bituminous coals. The depositional environment of the peat/coal, indicated by the Tissue Preservation and Gelification indices, ranges from wet-forest/swamp to limnic and fen. The boron content averages 120 to 130 ppm, suggesting deposition in slightly brackish to brackish water. This agrees with the depositional environment previously postulated by other workers, based on sedimentological and paleontological evidence.

Résumé

On a examiné en 1991 la pétrographie de huit grands filons houillers sub-bitumineux du groupe d'Edmonton dans la région de Drumheller, dans la vallée de la rivière Red Deer, dans les plaines de l'Alberta. Les charbons contiennent en prédominance des macéraux du groupe de l'huminite (humotélinite et humocollinite en majorité), avec une teneur mineure à modérée en liptinite et en inertinite.

La prédominance des macéraux cellulaires et massifs par rapport aux macéraux détritiques indique le caractère autochtone de la tourbe. Les valeurs de la réflectance se situent entre 0,38 et 0,51 %, atteignent leur maximum dans les filons houillers et leur minimum dans les shales carbonés, en conformité avec les résultats précédents obtenus pour les charbons sub-bitumineux et bitumineux. Le milieu de sédimentation de la tourbe et du charbon, indiqués par les indices de conservation et de gélification des tissus, se situe entre un milieu de forêt humide et marécageuse et un milieu limnique et de tourbière minérotrophe. La teneur en bore est en moyenne de 120 à 130 ppm, ce qui suggère une sédimentation en eau légèrement saumâtre à saumâtre. Ceci concorde avec le milieu sédimentaire autrefois postulé par d'autres chercheurs, d'après les indices sédimentologiques et paléontologiques.

[1] Alberta Research Council, Coal Research Centre Devon, One Oil Patch Drive, Devon, Alberta T0C 1E0

INTRODUCTION

Deposition of sediments in the Drumheller area of the western Canadian Plains, during the late Mesozoic/early Cenozoic, was mainly characterized by a combination of marine transgressions and nonmarine regressions, resulting in the accumulation of thick alternations of marine and continental deposits (Williams and Burk, 1964; Shepheard and Hills, 1970).

The coal seams in the Red Deer River valley of the Drumheller region (Fig. 1) occur in the Edmonton Group, which consists of a sequence of interbedded sandstone, siltstone, mudstone, shale, and coal. The Edmonton Group is divided into four distinct formations which, in ascending order, are: the Horseshoe Canyon, the Whitemud, the Battle, and the Scollard. Previous work includes papers by Elliott (1960), Ower (1960), Campbell (1962, 1967), Campbell and Almadi (1964), Clemens and Russell (1965), Srivastava (1966, 1967, 1968a,b), Russell and Chamney (1967), Irish (1967, 1970), Irish and Havard (1968), Binda and Srivastava (1968), Binda (1969), Snead (1969), Shepheard and Hills (1970), Carrigy (1970, 1971), Binda and Lerbekmo (1973), Holter et al. (1975), Gibson (1977) and Rahmani (1983). These studies, like some of the earlier investigations, are concerned mainly with regional mapping and correlation, lithostratigraphy, biostratigraphy, sedimentary petrology, vertebrate paleontology, and palynology.

According to Irish (1970), the Horseshoe Canyon Formation comprises a predominantly nonmarine sequence of fluviodeltaic siliciclastic rocks, coal, and coaly shale. Marine and brackish water strata are found near, and at, the base of the formation; at the contact with the underlying marine Bearpaw Formation; and in the "Drumheller Marine Tongue", near the middle of the formation. In the Drumheller region the Horseshoe Canyon Formation has a total thickness of approximately 267 m (Gibson, 1977). The overlying Whitemud Formation is relatively thin (3.4-7.9 m) and consists of argillaceous sandstone, siltstone and shale. The overlying Battle Formation is a dark weathering, bentonitic claystone/mudstone with volcanic tuff (Kneehills Tuff), with a maximum thickness of 11 m (Gibson, 1977). Finally, the Scollard Formation, which is not exposed in the Drumheller area, consists of interfingering sequences of argillaceous sandstone, siltstone, mudstone, and shale, with thick coal seams near the top of the formation. The Scollard Formation ranges in thickness from 50 to 85 m (Gibson, 1977).

Shepheard and Hills (1970) recognized several deltaic lithofacies in the Horseshoe Canyon Formation, which they attributed to major distributary, marginal swamp, levee, backswamp, interdistributary bay, open and partly restricted bay, and point bar deltaic subenvironments. The thick sandstone units are believed to be major distributary channel deposits; the shale and mudstone units may represent backswamp and mud flat deposits; whereas the carbonaceous shale and coals are interpreted as marsh or swamp deposits. Gibson (1977) generally agreed with the deltaic model proposed by Shepheard and Hills (1970), but suggested the possibility that part of the Horseshoe Canyon succession was deposited in a braided, fluvial distributary system . Almost all of the coal seams are very thin (<1.0 m) and lenticular, a feature common in floodplain areas. Gibson (1977) suggested that, in a delta plain environment, such as the one envisaged during the deposition of the Horseshoe Canyon Formation, thin layers of vegetation accumulate between numerous small braided streams, thus leading to the formation of thin coal seams or carbonaceous shales. The few thick coal seams present in the succession (up to 3 m) are laterally more extensive, and represent vegetal accumulation over longer periods of time, when the clastic sediment influx was low.

The most recent account of the facies relationships and paleoenvironments represented by the Horseshoe Canyon Formation was by Rahmani (1983). Generally, he agreed with the interpretation given by Shepheard and Hills (1970, 1979), and drew an analogy with modern estuaries and deltas, such as the Rhine delta of southwestern Netherlands, and areas off the coasts of Georgia and Washington State in the United States (Rahmani, 1983).

Fifteen, regionally prominent coal seams or major coal-bearing intervals have been identified in the Edmonton Group of the Red Deer River Valley area, and these have been studied by numerous workers, such as Allan (1943), Stansfield and Lang (1944), Campbell (1962, 1967), and Steiner el al. (1972). All the above studies dealt with the chemical properties and lateral continuity of the coal seams. In addition, the paper by Gibson (1977) presents a detailed study of the thickness, distribution, and sedimentology of the major and minor coal seams, based on 56 measured field sections, exposed along the Red Deer River valley between Drumheller and Ardley (Fig. 1).

The paper describes the coal petrography of eight major seams and/or coal-bearing intervals of the Horseshoe Canyon and Scollard formations.

EXPERIMENTAL

All coals were collected as channel samples and were crushed and mixed with epoxy resin. The resulting particulate blocks (pellets) were ground and polished according to the method recommended by Mackowsky (1982). Random reflectance was measured using a Zeiss MPM II reflected light microscope fitted with both white (halogen) and fluorescent (HBO) light sources, and with the aid of an oil immersion objective lens (N.A. = 0.90 x 40; n_o = 1.615 at 23°C). Point counting was performed on 300 points under both white and fluorescent light using a Swift, Model F automatic point counter.

RESULTS

Petrographic composition

Section 73-15

The No. 4 and No. 6 coal seams of the Horseshoe Canyon Formation are exposed in this section. The Horseshoe Canyon Formation has a total thickness of 18.2 m at this locality (Fig. 2). Seam no. 4 is divided into a lower part (50 cm thick) and an upper part (25 cm thick), whereas seam

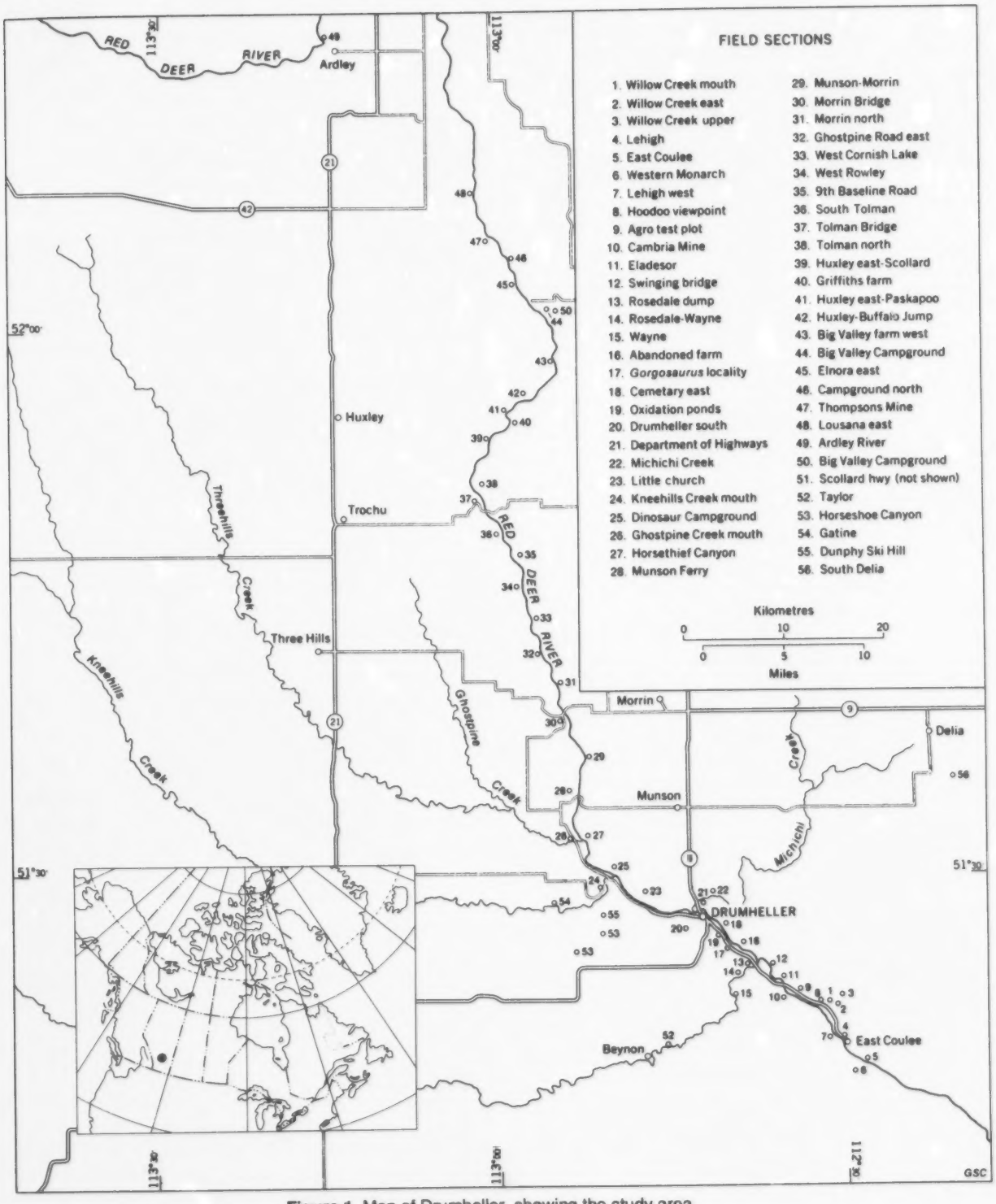

Figure 1. Map of Drumheller, showing the study area.

no. 6 has a thickness of 25 cm. Both seams are separated by carbonaceous shale and sandy units of varying thickness (Fig. 2).

The total huminite contents of the lower and upper parts of seam no. 4 are very similar (83% and 81.3%, respectively). Liptinite and inertinite contents are also similar. However, the lower part of seam no. 4 has higher humotelinite and humodetrinite contents and a much lower humocollinite content than the upper part (Fig. 2; Table 1).

The composition of seam no. 6 is such that humocollinite and humodetrinite are present in almost equal amounts (22.7% and 21.3%, respectively). There is a slight predominance of humotelinite (32.7%), meaning a higher woody tissue contribution, and liptinite and inertinite contents are similar to those in seam no. 4 (Fig. 2; Table 1).

It is worth noting the presence of two coaly units (each 1 m thick) between seams no. 4 and no. 6, an interval presumably occupied by seam no. 5 in other areas. One of the two units has the highest liptinite content of all the samples in this section (8%), and low inertinite and high humocollinite (44%) contents (Fig. 2). This unit contains 35 per cent mineral matter, and is, therefore, near the borderline of being classified as coal. It may represent seam no. 5, or the no. 5 coal-bearing interval.

Reflectance of eu-ulminite B in the section ranges from 0.47 to 0.50 per cent. The highest Ro values were obtained from the clean coaly units and the lower values from the carbonaceous shale or carbominerite intervals (Fig. 2). The

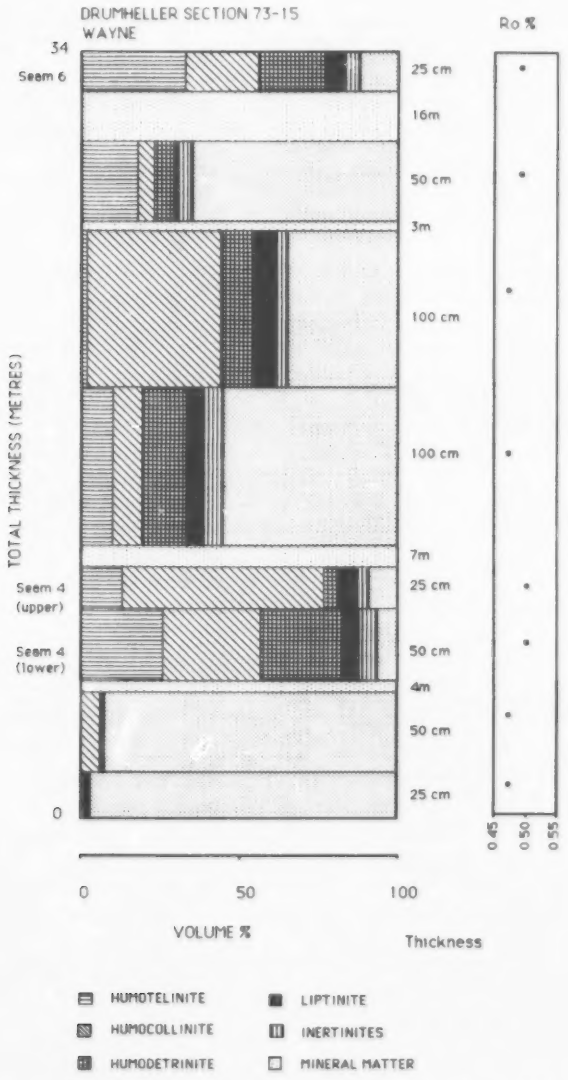

Figure 2. Maceral and reflectance profile of Section 73-15.

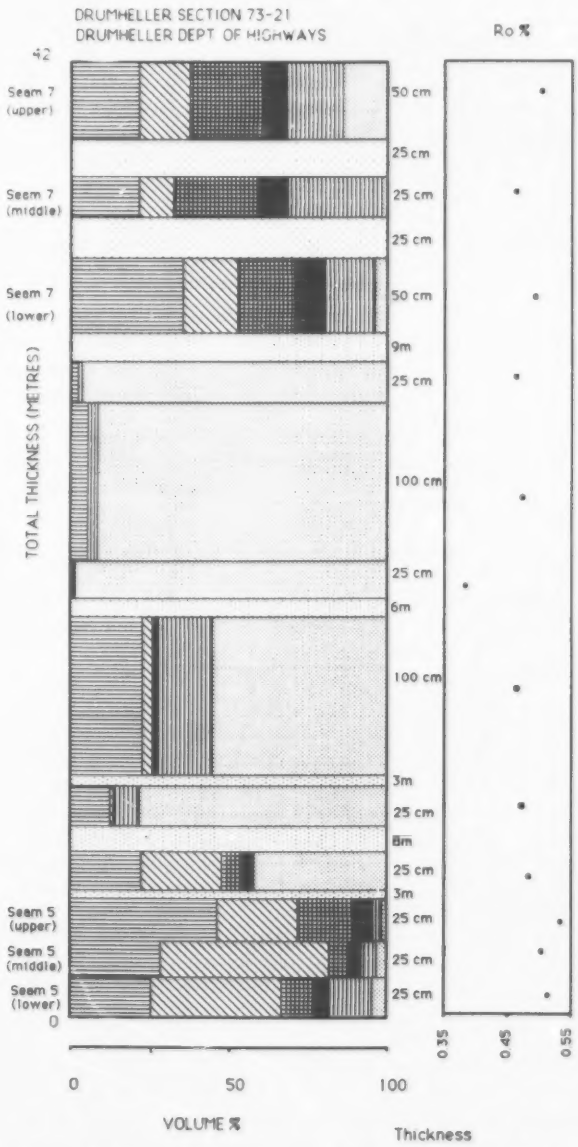

Figure 3. Maceral and reflectance profile of Section 73-21.

low Ro of the coaly unit (with the highest liptinite content) representing seam no. 5 may be related to the unit's maceral composition.

Section 73-21

This section of the Horseshoe Canyon Formation has a total thickness of 34.5 m, and includes coal seams no. 5 and no. 7 (Fig. 3). Seam no. 5 is divided into three parts: a lower (25 cm thick), a middle (25 cm thick), and an upper (25 cm thick). Huminite is the dominant maceral group in the coals (77.9 to 89.6%), followed by inertinite (2 to 13.3%) and liptinite (4.3 to 7.3%) (Table 1). Humotelinite, mainly in the form of eu-ulminite B and texto-ulminite, is present in large quantities, and the amount of humotelinite increases toward the upper part of seam no. 5, at the expense of inertinite (Fig. 3). Humocollinite comprises mainly phlobaphinite and gelinite, and humocollinite content ranges from 26 to 31.3 per cent (Table 1). Humodetrinite is made up of densinite, cementing fragments of angular inertodetrinite and liptinite (mainly sporinite). Humodetrinite content ranges from 6 to 17.3 per cent, with the minimum value found in the middle

Table 1. Maceral analysis and reflectance of the Drumheller coals

Sample	HT	HC	HD	L	I	MM	% Ro, random
Section 73-15 Wayne							
8 Seam No.6	32.7	22.7	21.3	6.3	5.3	11.7	0.49
7	18.0	5.3	5.7	0.6	4.7	65.7	0.49
6	2.0	44.0	8.0	8.0	3.0	35.0	0.47
5	10.3	9.3	14.7	5.3	6.3	54.0	0.47
4 Seam No. 4 (upper)	12.7	64.3	4.3	5.7	4.0	9.0	0.50
3	26.3	30.7	26.0	4.7	6.7	5.7	0.50
2	-	6.3	-	0.3	1.3	92.0	0.47
1	0.7	1.6	-	-	-	97.7	0.47
Section 73-21 Drumheller Department of Highways							
12 Seam No. 7 (upper)	22.3	16.0	22.7	6.7	17.7	14.6	0.50
11 Seam No. 7 (middle)	22.3	11.3	26.7	8.7	29.7	1.3	0.46
10 Seam No. 7 (upper)	36.0	16.7	17.7	10.3	16.7	2.7	0.49
9	3.0	-	-	-	1.3	95.7	0.46
8	5.7	-	-	0.3	3.3	90.6	0.47
7	1.3	-	-	-	2.3	96.3	0.38
6	23.3	2.7	0.6	2.0	16.7	54.6	0.46
5	13.3	1.0	-	-	7.7	78.0	0.47
4	23.3	25.0	6.3	5.3	0.7	39.3	0.48
3 Seam No. 5 (upper)	46.3	26.0	17.3	7.3	2.0	1.0	0.53
2 Seam No. 5 (middle)	39.3	42.7	6.0	4.3	5.3	2.3	0.50
1 Seam No. 5 (lower)	36.3	31.3	10.3	5.3	13.3	3.3	0.51
Section 73-27 Horsethief Canyon							
Sample	**HT**	**HC**	**HD**	**L**	**I**	**MM**	**% Ro, random**
9	2.3	0.7	-	-	0.3	96.7	0.41
8 Seam No.10	43.0	17.0	19.3	10.0	3.3	7.3	0.43
7	12.3	0.7	-	-	2.7	84.3	0.46
6	11.7	1.0	2.7	-	2.3	82.3	0.48
5 Seam No.9	37.3	5.3	28.7	6.0	1.3	21.3	0.51
4 Seam No.8	65.7	4.0	13.7	3.7	7.3	5.7	0.51
3	12.7	2.7	0.7	8.3	1.7	74.0	0.50
2	25.7	5.3	14.0	1.0	1.7	52.3	0.49
1	9.3	-	-	1.7	0.3	88.7	0.47
Section 73-41 Huxley East - Paskapoo Locality							
5	-	1.7	-	0.3	8.0	90.0	0.40
4	-	39.7	2.7	3.0	14.7	40.0	0.42
3	6.0	30.3	2.7	0.7	22.0	38.3	0.46
2	0.3	77.3	1.7	2.0	2.7	16.0	0.47
1C Seam No. 14 (upper)	-	54.3	9.6	5.3	24.7	6.0	0.48
1B Seam No. 14 (middle)	-	64.0	6.3	1.7	26.0	2.0	0.48
1A Seam No. 14 (lower)	3.7	69.7	6.7	7.0	8.3	4.7	0.40

part of seam no. 5. Liptinite is composed of microspores, cutinite, resinite, suberinite, and liptodetrinite. The liptinite content remains almost constant throughout the seam.

Seam no. 7 is also divided into three parts: a lower (50 cm thick), a middle (25 cm thick) and an upper (50 cm thick) (Fig. 3). The maceral groups consist of huminite (60.3 to 70.4%), liptinite (6.7 to 10.3%), and inertinite (16.7 to 29.7%). Humotelinite and humodetrinite predominate and are present in approximately similar amounts in the middle and upper parts of the seam (22.7% and 24.7%, respectively), followed by humocollinite (13.6%) (Table 1). The humotelinite content decreases toward the upper part of the seam and inertinite content is highest in the middle part of the seam (Fig. 3).

Reflectance values for eu-ulminite B range from 0.38 to 0.51 per cent, and appear to be higher in the coaly intervals (<20% mineral matter content) and lower in the sandy intervals (>40% mineral matter content) (Fig. 3; Table 1).

Section 73-27

At this locality, coal seams no. 8, no. 9, and no. 10 are exposed in a 59.8 m thick section of the Horseshoe Canyon Formation (Fig. 4). Seams no. 8 and no. 9 are 50 cm thick, whereas seam no. 10 is thinner (~25 cm). All coal seams are separated by sandstone, siltstone, and shale beds of varying thickness.

Seam no. 8 consists of 83.4% huminite, 7.3% inertinite, and 3.7% liptinite (Table 1). Humotelinite consists of eu-ulminite, showing faint cell-wall structure, and forms the bulk of the huminite (65.7%). Humodetrinite is the next most abundant (13.7%), whereas humocollinite is present in small amounts (4%) only (Fig. 4).

Seam no. 9 has a higher mineral matter content (21.3%), a lower huminite content (71.3%), a similar liptinite content (6%), but much less inertinite (1.3%) than seam no. 8 (Fig. 4). Seam no. 9 has approximately half the amount of humotelinite found in seam no. 8; however, the amount of humodetrinite in seam no. 9 is twice that of seam no. 8, with a similar concentration of humocollinite.

Seam no. 10 has a high liptinite content (10%), three times that found in seam no. 8. The liptinite is dominated by resinite, sporinite, cutinite, and liptodetrinite. The inertinite content is very low (3.3%) and huminite (79.3%) dominates the maceral composition. Humodetrinite and humocollinite are present in almost equal amounts (19.3% and 17%, respectively). Humotelinite is the most abundant (43%) (Fig. 4; Table 1).

Reflectance values in the section range from 0.41 to 0.51 per cent, and are generally higher in the coal seams, with the exception of seam no. 10 (0.43%). It should be noted that seam no. 10 also has the highest liptinite content, and reflectance suppression may be responsible for the reflectance observed.

Section 73-41

This section, east of Huxley, is 19.2 m thick and forms the uppermost 19 m of the Scollard Formation. It contains one major coal seam and several thin seams and carbonaceous units. The most obvious and thickest coal occurs in seam no. 14, which is divided into lower (30 cm thick), middle (75 cm thick) and upper (100 cm thick) parts. A 30 cm thick unit of sandstone separates the lower and middle parts (Fig. 5). Petrologically, seam no. 14 is dominated by huminite macerals (63.9 to 80.1 %), followed by inertinite (8.3 to 26%) and liptinite (1.7 to 7%) (Fig. 5; Table 1). The inertinite content increases from the base of the seam upward. Liptinite content is lowest in the middle part. Humodetrinite increases slightly in the upper part, whereas humocollinite, which is the dominant maceral (54.3 to 69.7%) shows a definite decrease from the lower to the upper part of seam no. 14 (Fig. 5). The humotelinite content is very low in seam no. 14, and humotelinite only occurs in small amounts in the lower part of the seam. Humocollinite is dominated by phlobaphinite, gelinite, and microcoprolites.

Humocollinite is the dominant maceral occurring in three units which range in thickness from 20 cm to 30 cm, in the upper part of the section (Fig. 5). However, the liptinite and inertinite content in these three units is lower than that in seam no. 14. This is attributable to the high mineral matter content.

Reflectance of eu-ulminite B shows a pronounced increase from the top to the bottom of the field section. The reflectance ranges from 0.40 to 0.49%. As expected, the higher Ro values are associated with seam no. 14, and the lower values with the more carbonaceous and shaly intervals in the upper part of the Scollard Formation.

DISCUSSION

Humotelinite and humocollinite generally form from the lignin and cellulose of plant cell-wall material of peat that accumulated in a swamp environment, when conditions for the preservation of woody tissue were most favourable. The cell walls of huminite are commonly impregnated by phlobaphinite. Such impregnation may actually increase resistance to bacterial attack (Teichmüller, 1982).

The coals of the Horseshoe Canyon Formation are humic coals dominated by huminite, as shown on the ternary compositional diagram (Fig. 6). The high huminite concentrations likely reflect acidic (<4.5 pH) water conditions in the peat/coal-forming environment, a suppression of bacterial degradation, and a water table that was high enough to prevent continuous exposure of the peat surface to the atmosphere and prevent extensive oxidation (Renton and Bird, 1988). The above conditions are unfavourable for plant decay, whereas the formation of inertinite requires high bacterial activity, aerobic conditions, and a constantly oxidizing environment (Hagelskamp and Snyman, 1988).

Although conditions in the original peat swamp environment allowed the preservation of considerable amounts of cellular macerals of the huminite group, during certain periods a fraction of the plant-derived matter was 'fusinitized' to form inertinite. The inertinite is dominated by semifusinite, fusinite, angular inertodetrinite, and sclerotinite. The layers containing inertinite in the middle and upper parts of seam no. 7 in Section 73-21, and in the middle and upper parts of seam no. 4 in Section 73-41, represent periods of increased oxidation and erosion of the peat. Inertinite is present in the above intervals as fusinite, showing white colour, high relief, and broken and collapsed cell-wall structure ('bogen structure'), whereas semifusinite has a lower reflectance and a greyish colour.

The cellular (humotelinite) and massive (humocollinite) macerals predominate over the detrital (humodetrinite) macerals, indicating the autochthonous nature of the peat. However, certain intervals, such as the middle and upper parts of seam no. 7 in Section 73-21 and seam no. 9 in Section 73-27, are indicative of hypautochthonous peat. Peat transportation presumably took place during the formation of the small crevasse splays and overbank deposits recognized as one of several deltaic lithofacies within the Horseshoe Canyon Formation by Shepheard and Hills (1970).

One of the most obvious trends observed in the four field sections is the decrease of huminite toward the upper parts of the seams - clearly seen in seam no. 14 of Section 73-41 and to a lesser extent in seam no. 7 of Section 73-21. This is consistent with a model of peat swamp development with a forest/swamp plant assemblage at the base and an accumulation of less lignin-rich material at the top (Teichmüller and Teichmüller, 1982). In Section 73-21, seam no. 7 contains higher liptinite and inertinite concentrations than seam no. 5, an indication that deposition of seam no. 7 may have been terminated by a slow rise in the water table. The same also may be true for seam no. 14 in Section 73-41. Here, although the swamp persisted, the plant materials were continuously subjected to increased alteration, which is reflected in the decrease in the concentration of the total huminite and the increase in the inertinite and, to a lesser extent, the liptinite. The contacts between the coal seams and the overlying sandstones is sharp, and this is to be expected because the sandstones are distributary or fluvial channel deposits which terminated the peat growth in the interdistributary bay or fluvial overbank areas of the deltaic complex.

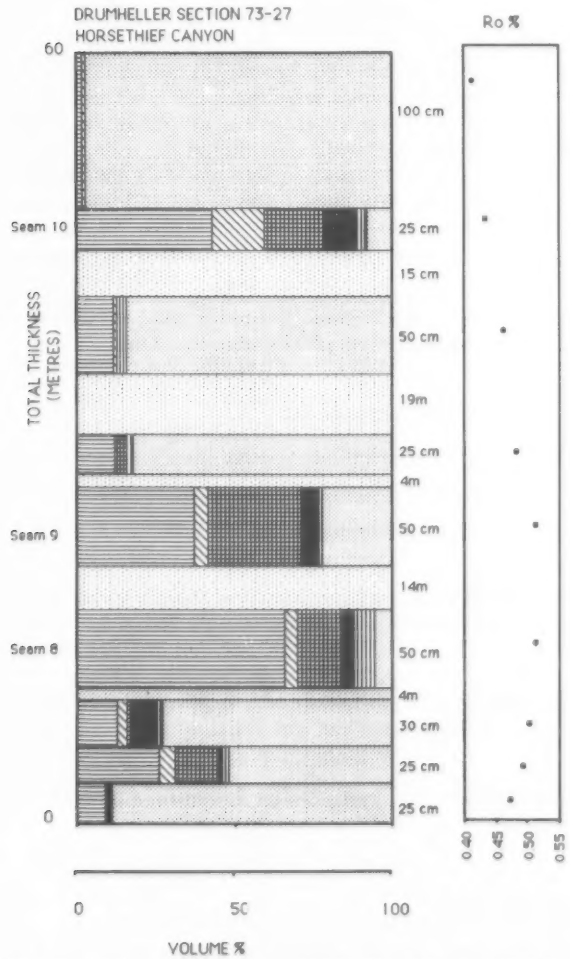

Figure 4. Maceral and reflectance profile of Section 73-27.

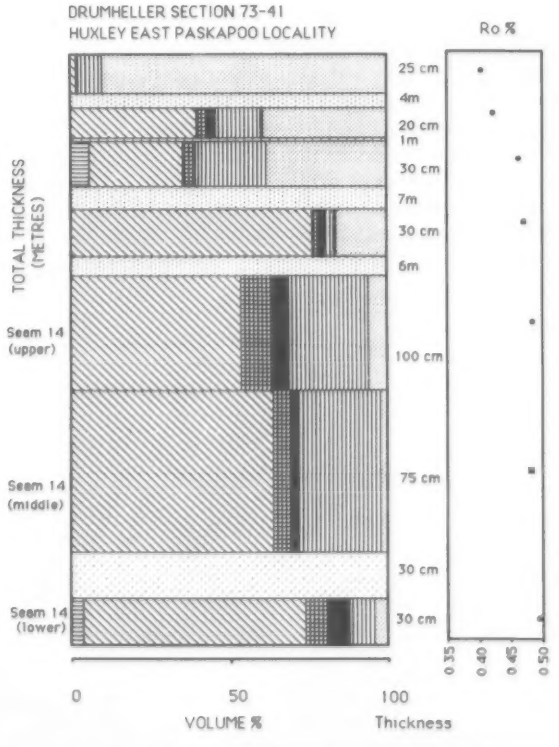

Figure 5. Maceral and reflectance profile of Section 73-41.

An interesting observation made from some of the samples is the presence of coprolites, which appear as oval to rounded bodies, a few showing a hollow in the central part and high reflectance. They range in diameter from 5 to 30m and many appear to be oxidized.

Reflectance variations

Random reflectance values measured on eu-ulminite B are as low as 0.38% in carbonaceous shales and as high as 0.51% in the coals. Reflectance measurements show consistent differences depending on whether the measurements were obtained from eu-ulminite in a coaly or a shaly matrix. Clearly, eu-ulminite B reflectance in coal has a higher value (up to 0.1%) than the same maceral variety found in shales (Goodarzi et al. 1988; Goodarzi et al., in press).

Variations in the reflectance values of huminite/vitrinite in association with different matrix lithologies have been reported previously by Teichmüller and Teichmüller (1968), Jones et al. (1971), Bostick and Foster (1975), Timofeev and Bogolyubova (1975), Goodarzi et al. (1988), and others. Several mechanisms have been proposed to explain these variations. Teichmüller and Teichmüller (1968) and Jones et al. (1971) suggested that differences in measured reflectance values may be the result of thermal conductivity differences in the section studied. Other mechanisms to explain the reflectance value variations include differences in relative retention and efficiency in the removal of reaction products, and clay catalysis, where clay minerals play an catalytic important role in the process of organic maturation (Gawley, 1970; Johns and Shimoyama, 1972; Goldstein, 1983).

No matter which mechanism is responsible, there are certain consistent variations in reflectance values, depending on the matrix lithology, as shown by Goodarzi et al. (1988) in a study of the subbituminous Hat Creek coals and the bituminous Kootenay Group coals from British Columbia (Goodarzi et al., in press). In the latter case, differences in vitrinite reflectance values were observed to depend on the matrix lithology and also on the organic matter (measured) present in thick coal seams (>1 m), thin seams (<1 m) or coal lenses (<30 cm). These reflectance value variations are not as obvious in the coals from the Red Deer River valley and near Drumheller, due to the coal seams being thinner and generally equal in thickness.

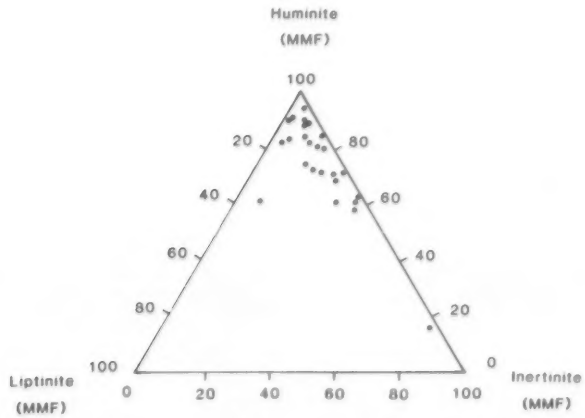

Figure 6. Ternary composition diagram of the coals studied.

Depositional environment based on Diessel's model

To help interpret the depositional conditions prevailing at the time of peat accumulation, Diessel (1982, 1986) and others derived the following ratios to relate the petrographic variations in coal to differences in the types of swamps in which the peats were deposited:

(1) $\frac{\text{humotelinite + semifusinite + fusinite}}{\text{humocollinite + macrinite + inertodetrinite}}$ Tissue Preservation Index (TPI)

(2) $\frac{\text{huminite + macrinite}}{\text{semifusinite + fusinite + inertodetrinite}}$ Gelification Index (GI)

As indicated in Figure 7, the petrographic composition of Drumheller coals plots mainly in areas indicative of subenvironments that range from a wet-forest swamp to limnic and fen. The coals possess relatively high GI values and low to intermediate TPI values. The coals from Sections 73-15 and 73-41 have the lowest TPI values. The values indicate that these peats were deposited in a deeper water environment, possibly in open, or partly restricted, interdistributary or interfluvial areas of the delta complex. The TPI values of the coals in Sections 73-21 and 73-27 are higher, pointing to a more forested, but still wet, swamp subenvironment in which the preservation of structured huminite (mainly humotelinite) and structured inertinite prevailed.

In addition, the following two ratios, taken from the work of Mastalerz and Smyth (1988), were calculated:

(3) $\frac{\text{humotelinite + humocollinite}}{\text{semifusinite + fusinite}}$

(4) $\frac{\text{humotelinite + humocollinite + semifusinite + fusinite}}{\text{sporinite + inertodetrinite}}$

The third ratio indicates the degree of dryness and wetness in the peat swamp, and the fourth ratio shows the input of plant tissue material into the peat-forming environment (Mastalerz and Smyth, 1988). As indicated in Figure 8, the samples plot in areas indicative of relatively wet conditions and a reasonable supply of woody tissue.

Environment of deposition as determined by boron content

The concentration of boron (B) in coal and interbedded sediments has been used to determine the paleosalinity of the depositional environment (Swaine, 1962; Bohor and Gluskoter, 1973; Chou, 1984; Lindhal and Finkelman, 1986; Goodarzi, 1988). Coals with B values ranging from 50 to

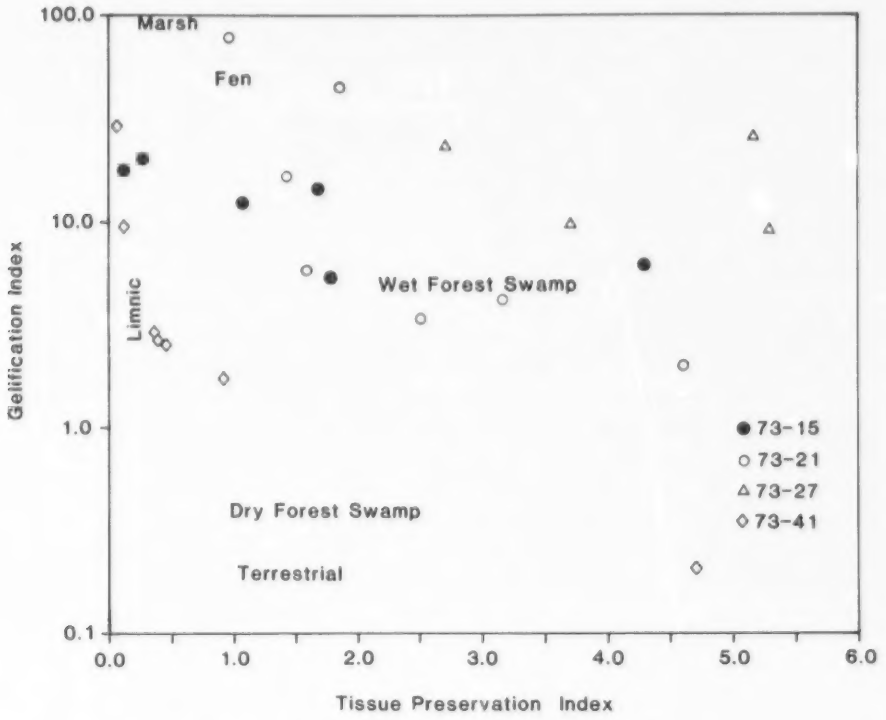

Figure 7. A plot of the Tissue Preservation (TPI) versus Gelification (Gi) indices.

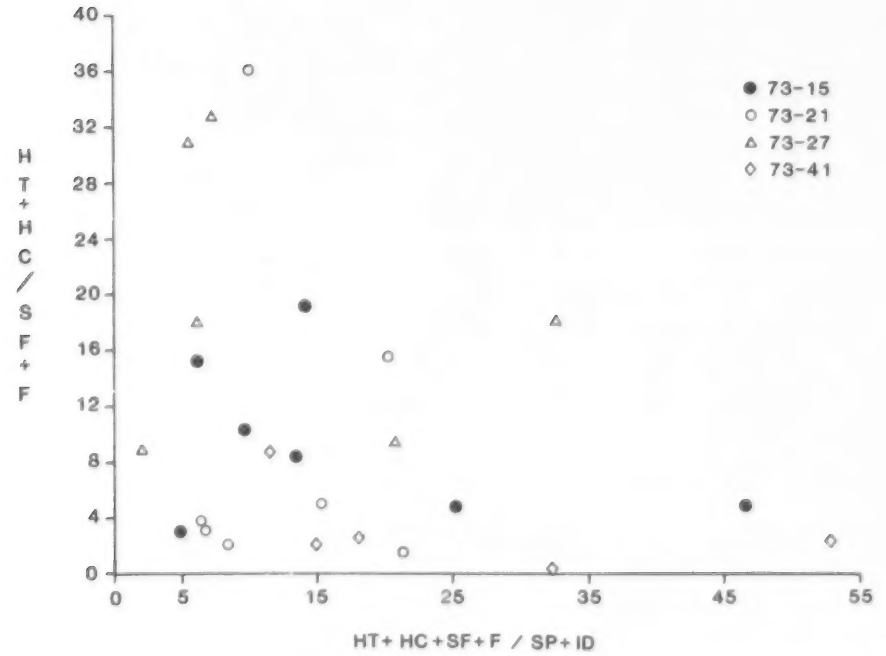

Figure 8. A plot of the degree of wetness versus the degree of input of plant tissue material into the peat-forming environment.

110 ppm indicate deposition in mildly brackish water, whereas those with a B content exceeding 110 ppm indicate brackish water deposition. The B content of the coals studied varies from 30 ppm for the Scollard Formation coals to 170 ppm for the Horseshoe Canyon Formation coals, with the majority of samples having values of 120 to 130 ppm (Goodarzi, unpublished data). This indicates that the coals formed in an environment dominated by fresh (Scollard) to brackish (Horseshoe Canyon) water. The occurrence of the oyster *Ostrea* in a "marine tongue" within the Horseshoe Canyon Formation, and the B content, to the brackish-water depositional environment - in agreement with the sedimentological interpretations given by Allan and Sanderson (1945) and Irish (1970).

CONCLUSIONS

The study shows that the subbituminous coals in the Red Deer River valley area near Drumheller are dominated by the huminite group of macerals, followed by inertinite and liptinite. The coal petrography indicates an autochthonous origin for most of the peat. It also indicates a coal/peat-forming environment ranging from wet-forest/swamp to limnic and fen. The boron content points to peat accumulation in slightly brackish to brackish waters.

Reflectance of eu-ulminite in coal is systematically higher than reflectance of eu-ulminite in carbonaceous shale, a pattern observed previously in both subbituminous and bituminous coals.

ACKNOWLEDGMENTS

The technical assistance of Kanwal Lali and Joyce Hollenbeck of the Coal and Hydrocarbon Processing Department, Alberta Research Council, is greatly appreciated. Andrew Beaton, Department of Geology, University of Western Ontario, is thanked for reviewing the manuscript.

REFERENCES

Allan, J.A.
1943: Coal areas of Alberta; Research Council of Alberta, Report No. 34.

Allan, J.A. and Sanderson, J.O.G.
1945: Geology of the Red Deer and Rosebud sheets, Alberta; Research Council of Alberta, Report No. 13.

Binda, P.L.
1969: Provenance of the Upper Cretaceous Kneehills Tuff, southern Alberta; Canadian Journal of Earth Sciences, v. 6, no. 3, p. 510-513.

Binda, P.L. and Lerbekmo, J.F.
1973: Grain-size distribution and depositional environment of Whitemud sandstones, Edmonton Formation (Upper Cretaceous), Alberta; Bulletin of Canadian Petroleum Geology, v. 21, no. 1, p. 52-80.

Binda, P.L. and Srivastava, S.K.
1968: Silicified megaspores from Upper Cretaceous beds of southern Alberta, Canada; Micropaleontology, v. 14, no. 1, p. 105-113.

Bohor, B.F. and Gluskoter, H.J.
1973: Boron in illite as a paleosalinity indicator of Illinois coals; Journal of Sedimentary Petrology, v. 43, no. 4, p. 945-956.

Bostick, N.H. and Foster, N.
1975: Comparison of vitrinite reflectance in coal seams and in kerogen of sandstone, shale and limestones in the same part of the sedimentary section; in Pétrographie de la matière organique des sédiments, relations avec la paléotempérature et le potentiel pétrolier, (ed.) B. Alpern; Paris, 1973, p. 13-25.

Campbell, J.D.
1962: Boundaries of the Edmonton Formation in the central Alberta Plains; Journal of the Alberta Society of Petroleum Geologists, v. 10, no. 6, p. 308-319.
1967: Ardley coal zone in the Alberta Plains: central Red Deer River area; Research Council of Alberta, Report No. 67-1.

Campbell, J.D. and Almadi, I.S.
1964: Coal occurrences of the VulcanGleichen area; Research Council of Alberta, Preliminary Report No. 64-2.

Carrigy, M.A.
1970: Proposed revision of the boundaries of the Paskapoo Formation in the Alberta Plains; Bulletin of Canadian Petroleum Geology, v. 18, no. 2, p. 156-165.
1971: Lithostratigraphy of the uppermost Cretaceous (Lance) and Paleocene strata of the Alberta Plains; Research Council of Alberta, Bulletin No. 27.

Chou, C.
1984: Relationship between geochemistry of coal and nature of strata overlying the Herrin Coal in the Illinois Basin, U.S.A.; Geological Society of China, Memoir, v. 5, p. 269-280.

Clemens, W.A. and Russell, L.S.
1965: Mammalian fossils from the Upper Edmonton Formation; in Vertebrate Paleontology in Alberta, Confidential Report, University of Alberta (1963), p. 32-40.

Diessel, C.F.K.
1982: An appraisal of coal facies based on maceral characteristics; Australian Coal Geology, v. 4, no. 2, p. 478-483.
1986: On the correlation between coal facies and depositional environment. Advances in the study of the Sydney Basin; Proceedings of the 12th Symposium, Department of Geology, University of Newcastle, Australia, p. 19-22.

Elliott, R.H.J.
1960: Subsurface correlation of the Edmonton Formation; Journal of the Alberta Society of Petroleum Geologists, v. 8, no. 11, p. 324-337.

Gawley, A.K.
1970: Reactions of alcohols and of hydrocarbons on montmorillonite surface; Journal of Catalysis, v. 19, p. 330-342.

Gibson, D.W.
1977: Upper Cretaceous and Tertiary coal-bearing strata in the DrumhellerArdley region, Red Deer River valley, Alberta; Geological Survey of Canada, Paper 76-35, 41 p.

Goldstein, T.P.
1983: Geocatalytic reactions in the formation and maturation of petroleum; American Association of Petroleum Geologists, Bulletin, v. 67, p. 152-159.

Goodarzi, F., Gentzis, T., Feinstein, S., and Snowdon, L.R.
1988: Effect of maceral sub-types and mineral matrix on measured reflectance of subbituminous coals and dispersed organic matter; International Journal of Coal Geology, v. 10, p. 383-398.

Goodarzi, F., Gentzis, T., Snowdon, L.R., Bustin, R.M., Feinstein, S., and Labonté, M.
in press: The effect of mineral matrix and seam thickness on reflectance of vitrinite in high to low-volatile bituminous coals: an enigma; Marine and Petroleum Geology.

Hagelskamp, H.H.B. and Snyman, C.P.
1988: On the origin of low-reflecting inertinites in coals from the Highveld Coalfield, South Africa; Fuel, v. 67, p. 307-313.

Holter, M.E., Yurko, J.R., and Chu, M.
1975: Geology and coal reserves of the Ardley coal zone of central Alberta; Alberta Research Council, Report 75-7.

Irish, E.J.W.
1967: Drumheller map area, Alberta; Geological Survey of Canada, Map 5-1907.
1970: The Edmonton Group of south-central Alberta; Bulletin of Canadian Petroleum Geology, v. 18, no. 2, p. 125-155.

Irish, E.J.W. and Havard, C.J.
1968: The Whitemud and Battle formations ("Kneehills Tuff Zone"), a stratigraphic marker; Geological Survey of Canada, Paper 67-73.

Holter, M.E., Yurko, J.R., and Chu, M.
1975: Geology and coal reserves of the Ardley coal zone of central Alberta; Alberta Research Council, Report 75-7.
Johns, W.D. and Shimoyama, A.
1972: Clay minerals and petroleum-forming reactions during burial and diagenesis; American Association of Petroleum Geologists, Bulletin, v. 56, p. 2160-2167.
Jones, J.M., Murchison, D.G., and Saleh, S.A.
1971: Variation of vitrinite reflectivity in relation to lithology; in Advances in Organic Geochemistry, (ed.) H.W. Gaertner and H. Wehner; Pergamon Press, p. 601-612.
Lindhal, P.C. and Finkelman, R.B.
1986: Factors influencing major, minor and trace element variation in U.S. coals; in Mineral Matter and Ash in Coal, (ed.) K.S. Vorres; American Chemical Society, Washington, D.C., p. 61-69.
Mackowsky, M-Th.
1982: Preparation of polished surfaces from particulate samples; in Coal Petrology, (ed.) E. Stach, M-Th. Mackowsky, M. Teichmüller, G.H. Taylor, D. Chandra, and R. Teichmüller; Gebruder Borntraeger, Berlin-Stuttgart, p. 296-299.
Mastalerz, M. and Smyth, M.
1988: Petrography and depositional conditions of the 64/65 coal seam in the Intrasudetic Basin, SW Poland; International Journal of Coal Geology, v. 10, p. 309-336.
Ower, J.R.
1960: The Edmonton Formation; Journal of the Alberta Society of Petroleum Geologists, v. 8, no. 11, p. 309-338.
Rahmani, R.A.
1983: Facies relationships and paleoenvironments of a Late Cretaceous tide-dominated delta, Drumheller, Alberta: The Mesozoic of Middle North America; Canadian Society of Petroleum Geologists, Fieldtrip Guidebook, no. 2, 36 p.
Renton, J.J. and Bird, D.S.
1988: Petrographic zonation within the Pittsburgh coal; International Journal of Coal Geology, v. 10, p. 109-139.
Shepheard, W.W. and Hills, L.V.
1970: Depositional environments of the Bearpaw-Horseshoe Canyon (Upper Cretaceous) transition zone, Drumheller "Badlands", Alberta; Bulletin of Canadian Petroleum Geology, v. 18, no. 2, p. 166-215.
1979: Upper Cretaceous: Drumheller "Badlands", Alberta; Canadian Society of Petroleum Geologists, Fieldtrip Guidebook, 4 p., 6 figs.
Snead, R.G.
1969: Microfloral diagnosis of the CretaceousTertiary boundary, central Alberta; Research Council of Alberta, Bulletin 25.
Srivastava, S.K.
1966: Upper Cretaceous microflora (Maestrichtian) from Scollard, Alberta (Canada); Pollen et Spores, v. 8, no. 3, p. 497-552.
1967: Palynology of Late Cretaceous mammal-beds, Scollard, Alberta (Canada); Palaeogeography, Palaeoclimatology, Palaeoecology, v. 3, no. 1, p. 133-150.
1968a: Ephedralean pollen from the Upper Cretaceous Edmonton Formation of Alberta (Canada) and their paleoecological significance; Canadian Journal of Earth Sciences, v. 5, no. 2, p. 211-221.
1968b: Angiosperm microflora of the Edmonton Formation, Alberta, Canada; Ph.D. thesis, University of Alberta, Edmonton, Alberta.
Stansfield, E. and Lang, W.A.
1944: Coals of Alberta, their occurrence, analysis and utilization; Research Council of Alberta, Report No. 35.
Steiner, J., Williams, G.D., and Dickie, G.J.
1972: Coal deposits of the Alberta Plains; Research Council of Alberta, Information Series No. 60, p. 85-108.
Swaine, D.J.
1962: Boron in New South Wales Permian coals; Australian Journal of Earth Sciences, v. 26, no. 6, p. 265, 266.
Teichmüller, M.
1982: Origin of the petrographic constituents of coal; in Stach's Textbook Stach's of Coal Petrology, (ed.) E. Stach, M-Th. Mackowsky, M. Teichmüller, G.H. Taylor, D. Chandra, and R. Teichmüller; Gebruder Borntreger, Berlin-Stuttgart, p. 219-275.
Teichmüller, M. and Teichmüller, R.
1968: Geological aspects of coal metamorphism; in Coal and Coal Bearing Strata, (ed.) D. Murchison and T.S. Westoll; Oliver and Boyd, Edinburgh, p. 233-267.
1982: The geological basis of coal formation; in Stach's Textbook Stach's of Coal Petrology, (ed.) E. Stach, M.-Th. Mackowsky, M. Teichmüller, G.H. Taylor, D. Chandra, and R. Teichmüller; Gebruder Borntraeger, Berlin-Stuttgart, p. 5-85.
Timofeev, P.P. and Bogolyubova, L.I.
1975: Relation of changes of organic and clay substances in deposits of the recent peat accumulation areas; in Pétrographie de la matière organique des sédiments, relations avec la paléotempérature et le potentiel pétrolier, (ed.) B. Alpern; Paris, 1973, p. 153-172.
Williams, G.D. and Burk, C.F.
1964: Upper Cretaceous; in Geological History of Western Canada, (ed.) R.G. McCrossan and R.P. Glaister; Alberta Society of Petroleum Geologists, Special Publication, p. 169-190.

Geological Survey of Canada Project 780006

Eolian deposition on western Fosheim Peninsula, Ellesmere Island, Northwest Territories during the winter of 1990-91

Sylvia A. Edlund and Ming-Ko Woo[1]
Terrain Sciences Division

Edlund, S.A. and Woo, M-K., 1992: Eolian deposition on western Fosheim Peninsula, Ellesmere Island, Northwest Territories during the winter of 1990-91; in Current Research, Part B; Geological Survey of Canada, Paper 92-1B, p. 91-96.

Abstract

Significant eolian deposition occurred during winter 1990-91 on western Fosheim Peninsula. Snow-cored barchan dunes coated with sand and gravel developed on the sea ice of Slidre Fiord adjacent to an airstrip. Dust was distributed throughout snow layers at many sites and thick blankets of silty clay draped some slopes near Hot Weather Creek base camp. Low regional winter snowfall and the redistribution of snow by strong winds created substantial bare areas which became sources for such deposition. An experiment confirmed that snowmelt could be accelerated by a week by manual dusting of a snow surface. This suggests that dust layers help create the observed zones of early melt. After snowmelt, eolian activity impacts on vegetation by delaying stabilization, by smothering vegetation, or by causing a shift in species dominance.

Résumé

Pendant l'hiver 1990-1991, a eu lieu une sédimentation éolienne significative dans la péninsule de Fosheim. Des dunes en croissant à noyau de neige recouvertes par des sables et graviers se sont formées sur les glaces de mer du fjord Slidre à proximité d'une piste d'atterrissage. La poussière était distribuée dans l'ensemble des couches de neige en de nombreux sites, et d'épaisses couvertures d'argile silteuse drapaient certains versants près du camp de base de Hot River Creek. De faibles précipitations nivales en hiver, à l'échelle régionale et la redistribution de la neige par des vents violents, ont généré des zones dénudées de superficie importante qui ont alimenté ce type de sédimentation. Une expérience a confirmé que la fonte des neiges pouvait être accélérée d'une semaine, si la surface de neige était manuellement poudrée. Ceci suggère que les couches de poussière aident à créer les zones observées de fonte précoce. Après la fonte des neiges, l'activité éolienne agit sur la végétation, en retardant la stabilisation, en étouffant la végétation, ou en déplaçant la dominance de certaines espèces.

[1] Department of Geography, McMaster University, Hamilton, Ontario L8S 4K1

INTRODUCTION

Eolian activity during winter, a common process in the Arctic Islands and on Fosheim Peninsula (Woo et al., 1990, 1991; Lewkowicz and Young, in press), was prominent during the winter of 1990-91. Although snow cover generally masks most surfaces in winter, affording some protection from eolian erosion, redistribution of snow by wind can create bare area on ridges and knolls even in winter. These become source areas for eolian activity. This paper discusses critical winter climate factors which affect eolian transported materials, describes several types of fresh eolian deposits encountered in spring 1991, explores possible reasons for enhanced eolian activity in winter 1991, and discusses some consequences of such deposition.

METHODS

Snow surveys (5-16 May 1991) were conducted from Eureka, east to the Hot Weather Creek Basin and adjacent areas (Fig. 1). Six plateau sites were surveyed to determine snow depth, density, and water equivalency on comparable topography. At each site 35 to 50 snow depth measurements were taken by plunging a steel rod into the snow. Six density measurements were also obtained using MSC snow sampler for deep (>25 cm) snow and by marking out a 15 X 15 cm^2 sampling plot for shallower snow. Snow samples were weighed, melted, and filtered for sediment content and volume.

Snowmelt experiments were conducted at Hot Weather Creek in mid May, to compare the rate of melt on artificially dusted snow cover with nondusted snow. Two experimental plots measuring 2.5 x 4 m were filled with snow to a depth of 0.47 m. The snow was compacted to a density of 380 kg/m^3 to simulate wind-packed conditions. On 13 May 1991, one of the plots was dusted with local materials (greyish brown silt with a dry color 2.5Y5/2) at an average concentration of 1230 g/m^2. Daily ablation was followed until all snow disappeared from the plots. Active layer development was monitored through the third week of August, using a frost table probe.

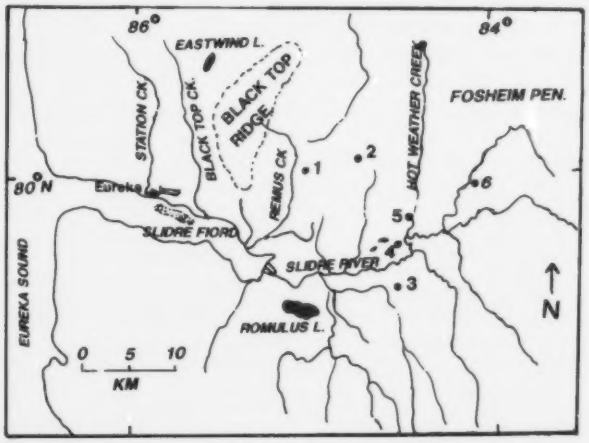

Figure 1. West-central Fosheim Peninsula, Ellesmere Island, showing location of Hot Weather Creek Base Camp and plateau sites where snow survey was conducted. Eolian deposition in Slidre Fiord is indicated by stippling. Sites are: 1. Remus central, 2. Remus east 3. east of Romulus Lake, 4. Coal Lake, 5. Hot Weather Creek, and 6. Gemini well head.

Depths and lateral extent of eolian deposits near Hot Weather Creek base camp were measured in mid June 1991. The most substantial deposits and their probable source area were sampled for grain-size analysis. The current vegetation cover was compared with previous records. On 20 August thickness and extent of deposits were again measured, and plant survival was assessed.

Data on winter 1990-91 temperature, radiation, snow accumulation, and wind speed were obtained from the weather logs at Eureka weather station and from the automatic weather station at Hot Weather Creek (see Edlund et al., 1989 for site details and specifications).

CLIMATIC FACTORS INFLUENCING WINTER EOLIAN ACTIVITY

Winter snow accumulation

Fosheim Peninsula had very low snow accumulation in winter 1990-91. Snowfall for the period of late August 1990 to early May 1991 at Eureka was only 32 mm water eqivalent. Our snow surveys showed only 43 mm snow water equivalents at Hot Weather Creek weather station, and between 17 and 44 mm snow water equivalent from other sites (Table 1).

Winter wind

Both Eureka and Hot Weather Creek weather stations recorded numerous strong wind events during winter 1990-91. Such events are relatively rare in the Arctic in winter. Days with peak wind speeds exceeding 40 km/h occurred 20 October, 6-7, 14-15, 30-31 December, 2, 17-18 February, and 25-28 March. Winds exceeded 60 km/h on 20 October, 30-31 December, 16-18 February, 27, 28 March. Peak winds reached more than 80 km/h at Eureka on 31 December, 17 February, and 27 March. Wind direction during these high wind events was northerly (290-030°) except for the late March event, which had southerly direction (170°).

WINTER EOLIAN ACTIVITY

Snow-free areas

The May 1991 snow survey detected large, snow-free areas on the north side of Slidre Fiord, the upper slopes and crest of Black Top Ridge, and the mouth of Slidre River. In other years these sites were snow covered in early May. These bare areas resulted from wind removal of snow rather than from melt, because they were present when temperatures were well below freezing.

Table 1. Snow conditions at selected plateau sites 5-14 May 1991 (see Fig. 1 for locations of samples)

	SAMPLE SITES					
	REMUS CENTRAL	REMUS EAST	EAST OF ROMULUS	COAL LAKE	HOT WR CR	GEMINI WELL
DEPTH						
mean (mm)	110.5	107.9	50.9	146.1	161.0	73.6
s.d.1	89	69	42	79	84	57
DENSITY						
(kg/m^3)	380	280	330	300	270	296
WATER EQUIV.						
(mm)	42.5	30.0	16.6	43.8	43.0	21.7
DUST CONTENT						
(g/L)*	-	T	12.2	1.5	3.0	3.7
mean						
s.d.[1]	-	-	4.2	1.1	3.9	5.6
(g/m^2)*						
mean	-	T	1029	116	73	112
s.d.[1]	-	-	727	105	74	97

[1] s.d. = Standard Deviation
* Dust content refers to total column of snow, except for Remus where only surface samples were taken
T Trace dust content

Barchan dunes on sea ice

A 2 km long field of barchan dunes 15-20 cm high composed of sand and gravel was encountered on the sea ice near the north shore of Slidre Fiord, between Eureka and Black Top Creek (Fig. 1, 2). The volume of sediments tapered off southwards. The orientations of barchan horns and plumes of sediment which bracketed large icebergs trapped in the sea ice within the dune field show that they were deposited by northerly winds.

Snow pits dug in these dunes showed that they resulted from several episodes of eolian activity (Fig. 2). A continuous, 70 mm layer of compacted, dusty snow lay directly on top of the sea ice. This was covered by a 20 to 110-130 mm layer of white snow with minimal dust which was shaped into dunes. A layer of sand and gravel, 20 to 150 mm thick (including platey fragments with long axis up to 60 mm), was deposited on top of the snow dunes, and formed snow cored barchans. The dune crests and some slopes were armoured with gravel lag, indicating that fines had been subsequently winnowed. Fine grained materials occurred in the swales of these dune fields. At no other sites did we encounter eolian deposits with such volume or coarseness, although A.G. Lewkowicz (pers. comm., September, 1991) observed such clastic deposits on land near Black Top Creek in July 1991.

Figure 2. Cross-section of barchan dunes on Slidre Fiord ice. Note the coarseness of the top clastic layer, which overlies relatively clean snow, which rests on a continuous layer of compacted dusty snow over sea ice.

Dust on snow

The snow survey identified regional differences in dust concentrations. East of Romulus Lake, the average eolian deposition was 1029 g/m^2, whereas it was approximately 100 g/m^2 farther east from Coal Lake to Gemini well site (Table 1). In other areas, the snow had only trace sediment

content. Snow pit excavations in May near the Gemini well head showed layers of snow with varying dust contents (Fig. 3).

Results of dusting experiment

The dusting experiment confirmed that dust on snow changes the energy balance at the snow surface and affects the rate of snowmelt (Woo and Dubreuil, 1985). Snow ablation began at the treated plot soon after dust was applied, even though maximum air temperature was below 0°C (Fig. 4). The control plot, however, showed little ablation until a week after the air temperature rose above freezing. This plot was bare one week after the snow was gone from the dusted plot. The advancement of the melt date resulting from the dusting which enabled ground thaw to start earlier. But by early July the frost table at the control plot was the same as the dusted plot. Towards the end of the summer there was little difference in the thaw depth at both plots.

Local eolian deposits and vegetation at Hot Weather Creek

Soon after snowmelt in early June, we found small eolian deposits 15-55 mm thick near Hot Weather Creek base camp which were composed entirely of unstratified silty clay (sand:silt:clay [SSC] ratio = 0:40:60). These deposits, which paralleled the lowermost segments of both north- and south-facing slopes, were 5-10 m wide and from 25-40 m long. They blanketed well vegetated hummocks developed on a large marine deposit. No eolian sediments were found in the adjacent valley bottoms; instead, there was an abrupt demarcation between blanketed slope foot and the fen vegetation of the valley bottom. Eolian sediments persisted on the tops of hummocks throughout the summer with only a slight loss of material on the edges of some hummocks.

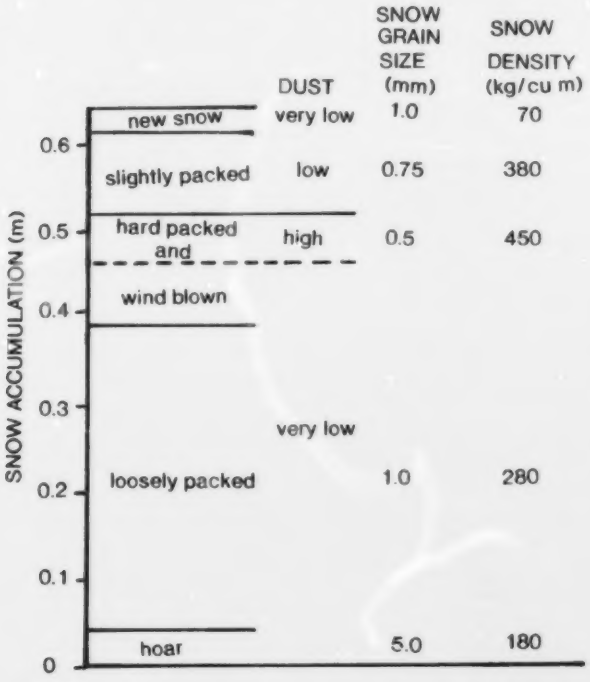

Figure 3. Stratigraphy of snow in a shallow polygonal depression near Gemini well head, 10 May 1991.

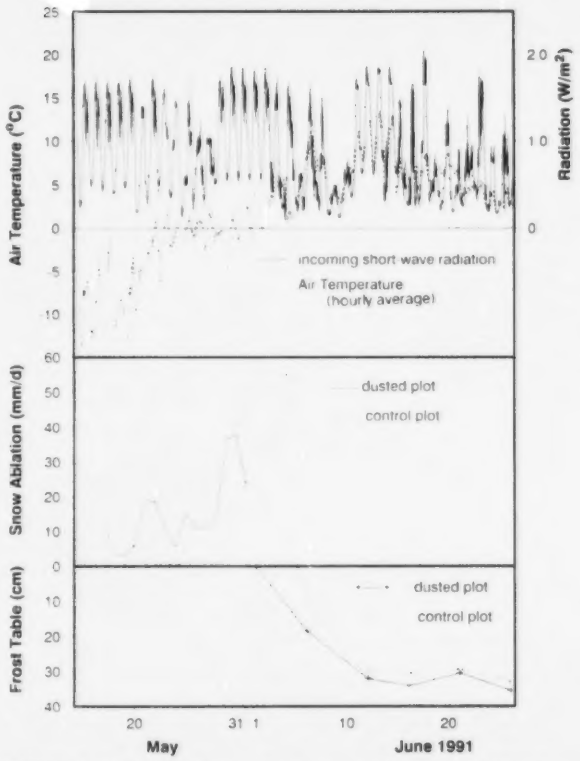

Figure 4. Air temperature, short-wave radiation (Hot Weather Creek automatic weather station), ablation and frost table development at the "dusted" and control plots.

The sediment smothered most vegetation (Table 2). While previous cover analyses showed that *Dryas* cover on the lower slopes was 40 to 75%, and Salix, from 5 to 15%, in June no plants were visible. In August a few *Dryas* leaves had emerged through thinner parts of the blanket, it consititued less than 1% and *Salix arctica*, constituted between 5 and 10%. There was no sign of *Cassiope tetragona*, which formerly had 5-10% cover.

Most species, except *Saxifraga oppositifolia*, were able to survive thinner blankets (<15 mm) of sediment in this first growing season. Of the woody species, only *Salix arctica* survived sedimentation of over 30 mm; no plants survived sediment accumulations greater than 50 mm. Grass-like herbs such as *Luzula nivalis*, *Kobresia myosuroides*, and *Arctagrostis latifolia*, and forbs with tall flowering stalks like *Eutrema edwardsii*, and *Pedicularis* species in places grew through silty clay. *Salix arctica*, which generally sprawls along the ground, in some places grew tangentially to protrude through up to 50 mm of sediment. Most plants that survived did not flower; none produced seed.

Upslope, the deposits feathered out over a distance of 2-5 m. The valley shoulders and broad crest showed evidence of fresh erosion, such as scour around the tussocks of grasses, and the baring of upper tap roots of some herbs. This marine deposit (SSC 12:38:50) has been the site of repeated deflation. Woody plants are absent and per cent cover is generally less than 5%. Only grasses such as *Agropyron latifolium, Alopecurus alpinus, Poa glauca, P. hartzii, Puccinnellia poacea* and forbs such as *Melandrium affine* and *M. triflorum, Oxyria digyna*, and *Papaver lapponicum* typical of early stage successsion occur there.

Figure 5. Well vegetated hummocks near the base of a slope blanketed with silt and clay to a depth of 30 mm.

Table 2. Survival of vascular plant species which experienced eolian deposition during winter 1991 near Hot Weather Creek

	DEPTH OF SEDIMENT BLANKET (mm)			
	<15	15-30	30-50	>50
SPECIES				
Luzula nivalis	+	+/-	-	-
Kobresia myosuroides	+	+/-	-	-
Arctagrostis latifolia	+	+/-	-	-
Salix arctica	+	+	+/-	-
Oxyria digyna	+/-	-	-	-
Polygonum viviparum	+/-	-	-	-
Papaver lapponicum	+/-	-	-	-
Stellaria longipes	+/-	-	-	-
Eutrema edwardsii	+	+/-	-	-
Saxifraga oppositifolia	-	-	-	-
Dryas integrifolia	+/-	-	-	-
Cassiope tetragona	+/-	-	-	-
Pedicularis arctica	+	-	-	-
Pedicularis capitata	+	+/-	-	-
Pedicularis lanata	+	+/-	-	-

+ = more than 10% survival
+/- = species occasionally survival (<10%)
- = no survivors

Many smaller (5-15 mm thick) eolian deposits were also observed in the region, generally on upper slopes where snow cornices develop. Such deposits most commonly occurred on both north- and south-facing slopes. While vegetation was initially masked by such deposits, little sediment was present on the surface at the end of the summer. Most had sifted through the foliage or had been washed 5-25 m downslope by heavy rains in August, as faint sediment trails downslope suggested.

Vegetative matter was also incorporated in winter eolian deposits. Leaves of *Dryas integrifolia* and/or *Salix arctica* were interspersed in snow and masked the surface of some snowbanks in the bottom of narrow valley near Slidre River. In some places the litter was so thick that snow was insulated so effectively that basal ice persisted until the third week of July. Woo et al. (1981) noted similar litter accumulations at Vendom Fiord, Ellesmere Island.

DISCUSSION

Eolian deposition on west-central Fosheim Peninsula commonly occurs as dustings of fine grained sediments interspersed through the snow, or locally as blankets of silt and clay. This is not unexpected, since the dominant surficial materials are fine grained marine deposits and sediment from the generally poorly consolidated Eureka Sound formation (Thorsteinsson, 1971a, b; Hodgson et al., 1991). In winter 1990-91, however, more substantial amounts of coarse grained materials were transported onto the Slidre Fiord ice and to a lesser extent, the adjacent land. High winds in early to mid winter probably redistributed the winter snow and created snow-free patches on ridges and knolls and cleared Black Top Ridge and uncovered slopes along the north shore of Slidre Fiord while the temperatures remained well below freezing. Because pickup and transport of such coarse clastic sediment requires extremely strong winds (50-100 km/h to pick of particles of 1-5 mm diameter; Pye and Tsoar, 1990), the major transport of sand and gravel onto the sea ice probably occurred in mid February when gusts exceeded 90 km/h or late March when there was a prolonged period of strong winds and gusts exceeded 80 km/h at Eureka.

Since the predominant surficial deposits in this area are silt and clay, the likely source of such coarse sediment is the unpaved runway 1 km inland from the coast to the north of the dune field. This airstrip receives regular applications of sand and gravel quarried from rock formations west of Eureka. Black Top Ridge crest and upper slopes are probably not a major source of eolian sediments, because the surface is mainly coarse boulders and cobbles, with few fines.

While eolian deposition of gravel is probably rare here, such a source should be taken into consideration when interpreting marine and lake sediment history. Gravel in subaqueous sediments may be derived from eolian deposits on seasonal ice, not just from ice rafting from shores or glaciers.

Elsewhere, in the vicinity of lower Hot Weather Creek and south of Slidre Fiord, the regional pattern of snow containing significant dust content corresponds to the zone of

early spring melt in 1990 and 1991. The source of dust east of Romulus Lake is most likely the extensive snow-free, poorly vegetated sand and silt in the lower Slidre River floodplain.

The absence of structure within the localized thick eolian deposits at Hot Weather Creek suggests that they were probably deposited during a single strong wind event when there was a period of significant southerly gusts, as well as northerly winds. The source of the silty clay is most likely the knoll of marine sediments upslope.

Evidence of deflation and deposition at this site has been noted each year since 1988. Until this year, however, thin deposition occurred only on poorly vegetated upper slopes near the crest and not on the nearly continuously vegetated lower slopes. This suggests that stronger winds occurred at this site this year, which moved the sediment downslope beyond the usual zone of accumulation. The sharp trimline on these deposits at the valley bottom suggests that the deposits accumulated on the winter snow cover and were subsequently removed by snowmelt runoff.

Accumulations of leaf litter within snow drifts in some valleys in the area suggest that snow removal was not confined to upper slopes and knolls but that snow was removed from nearby well vegetated slopes and plateaus. The terrain adjacent to the valleys has extensive *Dryas-Salix* hummocky tundra vegetation. Such communities ordinarily retain a protective snow cover throughout winter, but if exposed in winter would readily provide such litter.

Repeated eolian erosion, even on a local scale, retards the development of mature woody plant dominated communities so common on Fosheim Peninsula (Edlund et al., 1989). Upper slopes and crests, which are the source area for eolian sediments, are characteristically found in an early stage of succession, dominated by grasses and herbs.

If eolian deposition is light and infrequent, most mature plant communities would probably survive with little alteration except for lichens or mosses at the ground surface. Thick sedimentation, however, kills most if not all plants, and moderate amounts favour some species over others. *Salix arctica*, which can produce substantial increments of branch growth each year is able to survive major eposides of deposition by growing up through the deposits, whereas *Dryas integrifolia*, the most common plant where hummocks are present, is not.

The extent of terrain vegetated by nearly continuous *Dryas-Salix* tundra communities indicates that the exceptional accumulations of eolian deposits are rare and localized events. Should future climate changes accelerate winter eolian erosion and deposition, either by the reduction of winter precipitation or by increasing the intensity of winds, there may be expansion of wind scoured terrain and early melt zones, and an increase in eolian deposition on snow, leading to accretion on slopes. This could result in an expansion of successional communities, a loss of *Dryas* and heath dominated communities, and an alteration of species composition within communities.

ACKNOWLEDGMENTS

This work was funded by a research agreement with the Department of Energy Mines and Resouces and a grant from the Natural Sciences and Engineering Research Council. The logistical support of Polar Continental Shelf Project is gratefully acknowledged. We wish to thank Barry Goodison (AES) and the staff of Eureka Weather Station for lodging and for making the winter climate data available to us immediately. We also thank Andrej Saulesleja and Angus Headley (AES), and Bob Rowsell and Paul Wolfe for their assistance in the field. We also thank Douglas Hodgson for helpful comments on an earlier draft of this manuscript.

REFERENCES

Edlund, S.A., Alt, B.T., and Young, K.L.
1989: Interaction of climate, vegetation, and soil hydrology at Hot Weather Creek, Fosheim Peninsula, Ellesmere Island, Northwest Territories; in Current Research, Part D; Geological Survey of Canada, Paper 89-1D, p. 125-133.

Hodgson, D.A., St-Onge, D.A., and Edlund, S.A.
1991: Surficial materials of Hot Weather Creek basin, Ellesmere Island, Northwest Territories; in Current Research, Part E; Geological Survey of Canada, Paper 91-1E, p. 157-163.

Lewkowicz, A.G. and Young, K.L.
in press: Observations of aeolian transport and niveo-aeolian deposition at three lowland sites, Canadian Arctic Archipelago; Permafrost and Periglacial Processes.

Pye, K. and Tsoar, H.
1990: Aeolian Sand and Sand Dunes; Unwin Hyman, London, 396 p.

Thorsteinsson, R.
1971a: Geology, Eureka Sound North, District of Franklin; Geological Survey of Canada, Map 1302A.
1971b: Geology, Greely Fiord West, District of Franklin; Geological Survey of Canada, Map 1311A.

Woo, M-K. and Dubreuil, M-A.
1985: Emprical relationship between dust content and arctic snow albedo; Cold Regions Science and Technology, v. 10, p. 125-132.

Woo, M-K, Edlund, S.A., and Young, K.L.
1991: Occurrence of early snow-free zones on Fosheim Peninsula, Ellesmere Island, Northwest Territories; in Current Research, Part B; Geological Survey of Canada, Paper 91-1B, p. 9-13.

Woo, M-K., Heron, R., and Marsh, P.
1981: Basal ice layers of very cold arctic snowpack; in Proceedings, Eastern Snow Conference, 38th Annual Meeting, Syracuse, N.Y., June 4-5, 1981, p. 67-75.

Woo, M-K., Young, K.L., and Edlund, S.A.
1990: 1989 observations of soil, vegetation, and microclimate, and effects on slope hydrology, Hot Weather Creek basin, Ellesmere Island, Northwest Territories; in Current Research, Part D; Geological Survey of Canada, Paper 90-1D, p. 85-93.

Geological Survey of Canada Projects 880047 and 760058

Slope hummocks on Fosheim Peninsula, Ellesmere Island, Northwest Territories

Antoni G. Lewkowicz[1] and Kristinn A. Gudjonsson[1]
Terrain Sciences Division

Lewkowicz, A.G. and Gudjonsson, K.A., 1992: Slope hummocks on Fosheim Peninsula, Ellesmere Island, Northwest Territories; in Current Research, Part B; Geological Survey of Canada, Paper 92-1B, p. 97-102.

Abstract

Slope hummocks differ from earth hummocks in their size, distribution, and granulometry. At sites on the Fosheim Peninsula they are usually about 20 cm high, 60 cm long, and are composed of silty sand. Their distribution can be correlated with occurrences of deep winter snow accumulation. Their internal morphology exhibits a series of bands running sub-parallel to the surface and deformed in the downslope direction. These hummocks probably originate due to a combination of desiccation cracking, wash processes, and niveo-eolian deposition. Mass movement processes contribute to their preservation as hummocks move downslope by a combination of sliding and rolling.

Résumé

Les tertres de pentes diffèrent des tertres de toundra du point de vue de leurs dimensions, de leur distribution et de leur granulométrie. Dans les sites de la péninsule de Fosheim, ils ont habituellement 20 cm de haut, 60 cm de long et se composent de sable silteux. Il est possible de corréler leur distribution avec les accumulations épaisses de neiges hivernales. Leur morphologie interne se caractérise par une série de bandes disposées subparallèlement à la surface et déformées dans le sens de la pente. Ces tertres sont probablement le résultat combiné de fentes de dessication, de processus de ruissellement et de la sédimentation nivale et éolienne. Les processus de déplacement en masse contribuent à leur conservation, puisque les tertres se déplacent suivant la pente à la fois par glissement et par roulement.

[1] Department of Geography, Erindale College, University of Toronto, Mississauga, Ontario L5L 1C6

INTRODUCTION

Hummocks are dome-shaped forms that fit generally within the category of nonsorted nets in Washburn's (1956) classification of patterned ground. Earth hummocks, defined as "having a core of silty and clayey mineral soil and showing evidence of cryoturbation" (Permafrost Subcommittee NRCC, 1988) have received considerable attention in the literature. These features preferentially develop in the continuous permafrost zone, but similar forms are found in nonpermafrost areas where they are termed thufur (Schunke and Zoltai, 1988). The formation of earth hummocks has been discussed by a number of authors (e.g. Mackay, 1979; Schunke, 1977; Tarnocai and Zoltai, 1978; Van Vliet-Lanoë, 1991) and has variously been attributed to the processes of differential frost heave and thaw settlement, differential swelling, load-casting and cryostatic pressures, acting singly or in combination with one another.

A type of hummock that has received little study is commonly found on slopes in the Canadian High Arctic. It superficially resembles an earth hummock but can be differentiated by smaller size, composition, and lack of cryoturbation (Schunke and Zoltai, 1988, p. 243). This form, here termed slope hummock, was investigated during the summer of 1991 on the Fosheim Peninsula, Ellesmere Island (Fig. 1A).

METHODS

Two locations were selected, "Big Slide Creek" (unofficial name) (79° 42'N, 84° 23'W) and Hot Weather Creek (79° 58'N, 84° 23'W) (Fig. 1B). The distribution of slope hummock fields at each location was mapped and five plots chosen for more detailed study. Aspect and slope were determined at each detailed study site as well as overall hummock concentration (the number of hummocks per linear metre along a transect downslope). Hummock height, width, length, and orientation of long axis were measured and the

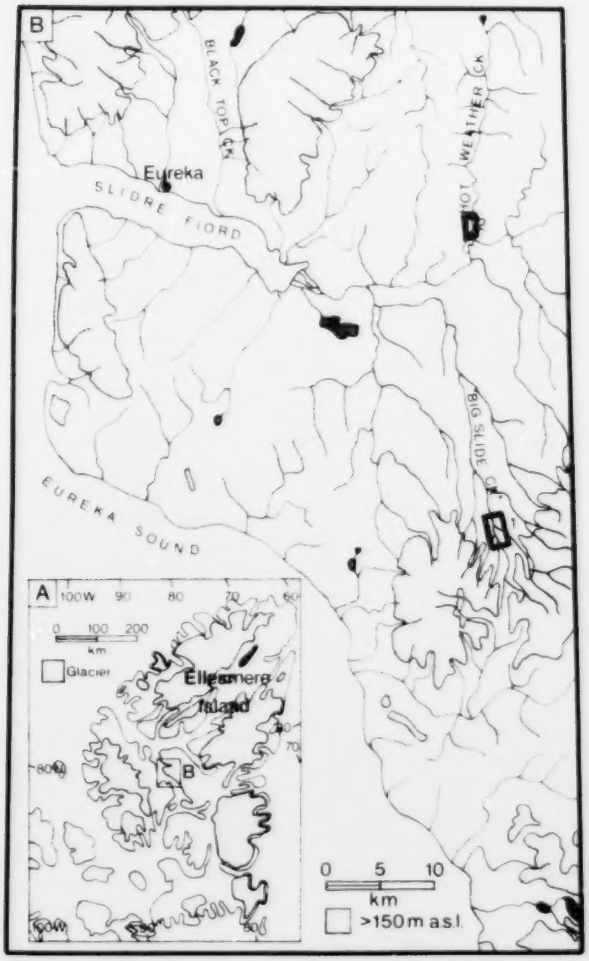

Figure 1. (**A**) Location map of Fosheim Peninsula study area on Ellesmere Island, Northwest Territories. (**B**) Study sites on the Fosheim Peninsula: 1- "Big Slide Creek", 2-Hot Weather Creek.

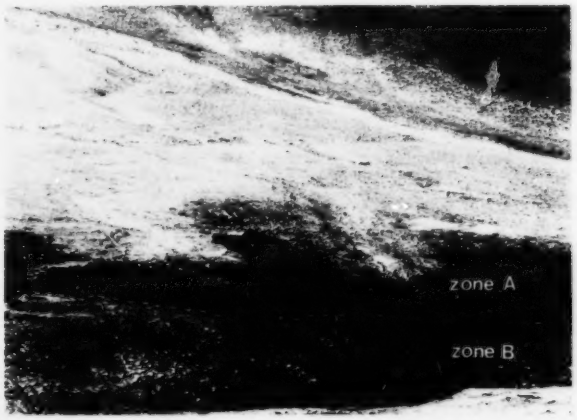

Figure 2. Hummock field at site 2, "Big Slide Creek". Dashed line separates upper zone A from lower zone B (see text). Hummocks illustrated in Figures 4-6 were exposed in trenches shown.

Figure 3. Niveo-eolian deposition of fine sand on the crowns of hummocks in zone B, site 2, "Big Slide Creek".

type and distribution of vegetation were noted. Trenches were dug through the plots both down and across the slope and the visible structures recorded. Undisturbed box cores were taken from the walls of the trenches for micromorphological study and grain size analyses. This report concentrates on preliminary results from one of the study sites at "Big Slide Creek".

RESULTS

Distribution and external morphology

The study area at "Big Slide Creek" lies above the Holocene marine limit of 140 m (Hodgson, 1985). The slopes are covered by a veneer of colluvium or residuum derived from the weathering of sands, siltstones, shales, and coal of the Eureka Sound Formation (Geological Survey of Canada, 1971). Eight hummock fields were identified in an area of 13.8 km^2. The total extent of these eight fields was 0.8 km^2 or 5.8% of the area mapped. The biggest hummock field was 0.2 km^2 while the smallest was 0.008 km^2. All of the fields were found on relatively steep (10-25°) north-facing slopes. Hummock fields at Hot Weather Creek developed on similar materials but exhibited greater variability in orientation, facing from northwest through to east. Snow accumulation is enhanced on these slopes and in some years may be twice as great as at plateau sites (Woo et al., 1991); vegetation cover is also greater.

The hummocks studied in detail displayed considerable similarity in external and internal morphology. The following is a description of site 2 at "Big Slide Creek" (Fig. 2).

The cross-slope length of site 2 was 260 m and the downslope width between 15-30 m. Superimposed on the hummock field is a network of ice-wedge polygons which on the average are 10 m wide. A break-of-slope divided the field into two parts: an upper section (zone A) with a mean gradient of 12° (range of 9.5°-15°) and a lower section (zone B) with a mean gradient of 21° (range 17°-26°). All the hummocks in the field were composed of silty sand, but at the boundary between the zones, vegetation changed from mainly Arctic

Table 1. Dimensions of hummocks at site 2, "Big Slide Creek"

	Length cm	Width cm	Height cm	W/L ratio	Hummocks per linear m downslope
Zone A	59.3	45.0	21.1	0.76	2.14
range	28-99	22-70	10-35	0.48-1.0	2.0-2.3
Zone B	59.6	40.6	25.4	0.71	1.57
range	25-94	20-56	15-48	0.45-1.0	1.5-1.6

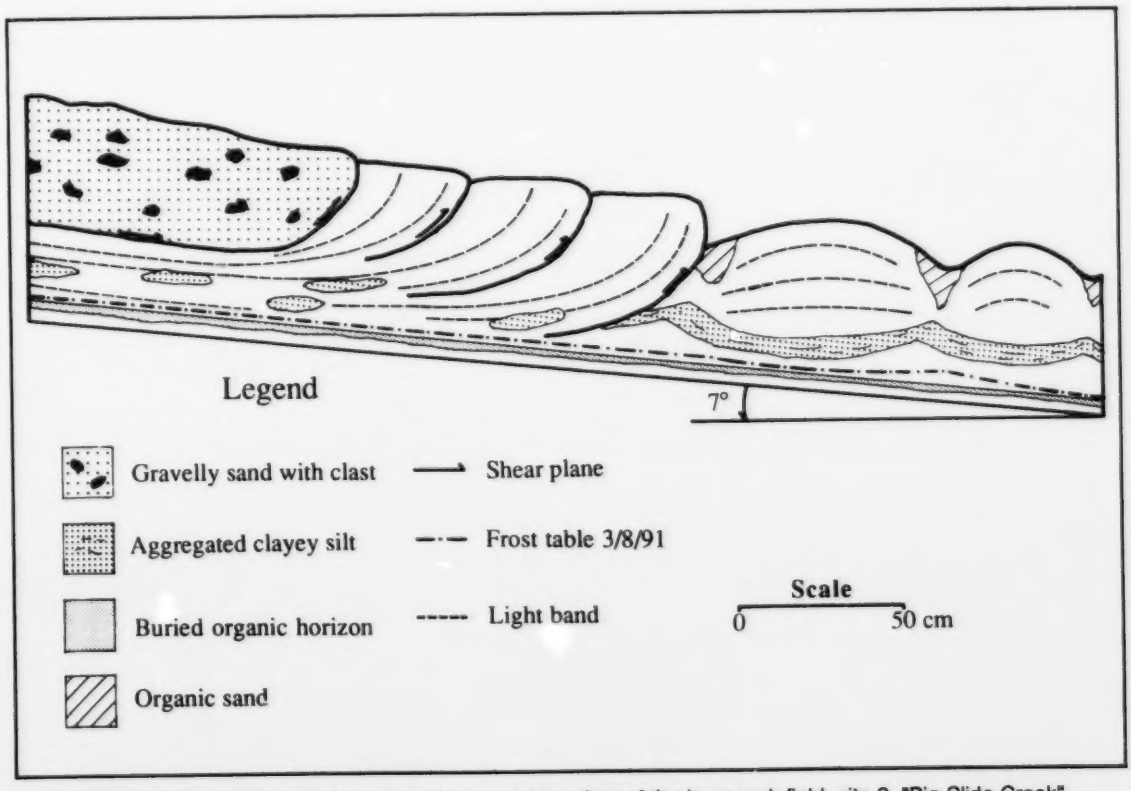

Figure 4. Downslope section across the upper boundary of the hummock field, site 2, "Big Slide Creek". Except where indicated, the hummocks are composed of silty sand.

Bell Heather (*Cassiope tetragona*) to dominated by willow (*Salix arctica*). Vegetation cover on the hummock crests was 85% in zone A, and 45% in zone B.

Average hummock height and length did not differ significantly between the two zones (Table 1). However, ignificant differences were present in the mean widths (at the p = 0.05 level) and in the width-to-length ratios, indicating that hummocks in zone B tend to be more elongate. Half of the hummocks in zone B were oriented with their long axes perpendicular to the slope, while this was true of only 26% of the hummocks in zone A.

Cracks were found in the inter-hummock troughs in both zones but they were much wider in the steeper B zone. These cracks were better developed cross-slope than downslope, and the former are attributed to tension associated with hummock movement. As a consequence, the average hummock density in zone A was 2.14 hummocks per linear metre, while it was 1.57 hummocks per metre in zone B. Many hummocks in zone B were partially detached from the surface at their upslope sides as if they were in the process of rolling over. Silt and fine sand deposits, 1-2 cm thick, were common on the crests of hummocks in zone B. Vegetation had barely penetrated through the uppermost layer indicating that it had been deposited within the last two years (Fig. 3).

Internal morphology

A distinct boundary occurred at the upslope end of zone A, site 2 (Fig. 4). Shear structures indicate that material has moved downslope from above the field, possibly as an active-layer detachment slide. A continuous organic layer of varying thickness was present at the base of the section (5 cm below the frost table). Dating of the organic material in this horizon may reveal whether burial took place catastrophically or if it resulted from slow mass movement.

No signs of convection type circulation were detected in the hummocks at site 2 but alternating light and dark arch-shaped bands were common. These bands ran subparallel to the hummock surface in both the downslope and cross-slope planes, but were deformed downslope in a manner analogous to structures that have been observed in solifluction lobes (e.g. Hirakawa, 1989) (Fig. 5). The degree of deformation increased downslope and was greatest in the lower part of zone B (Fig. 6). In this zone, some hummocks had caught up with, and rolled over hummocks previously located downslope. A continuous layer of rounded clayey-silt aggregates was present beneath the hummocks in zone B. This horizon probably resulted from development of ice lenses during freezing of the active layer upwards from the permafrost table. The layers beneath it were undeformed

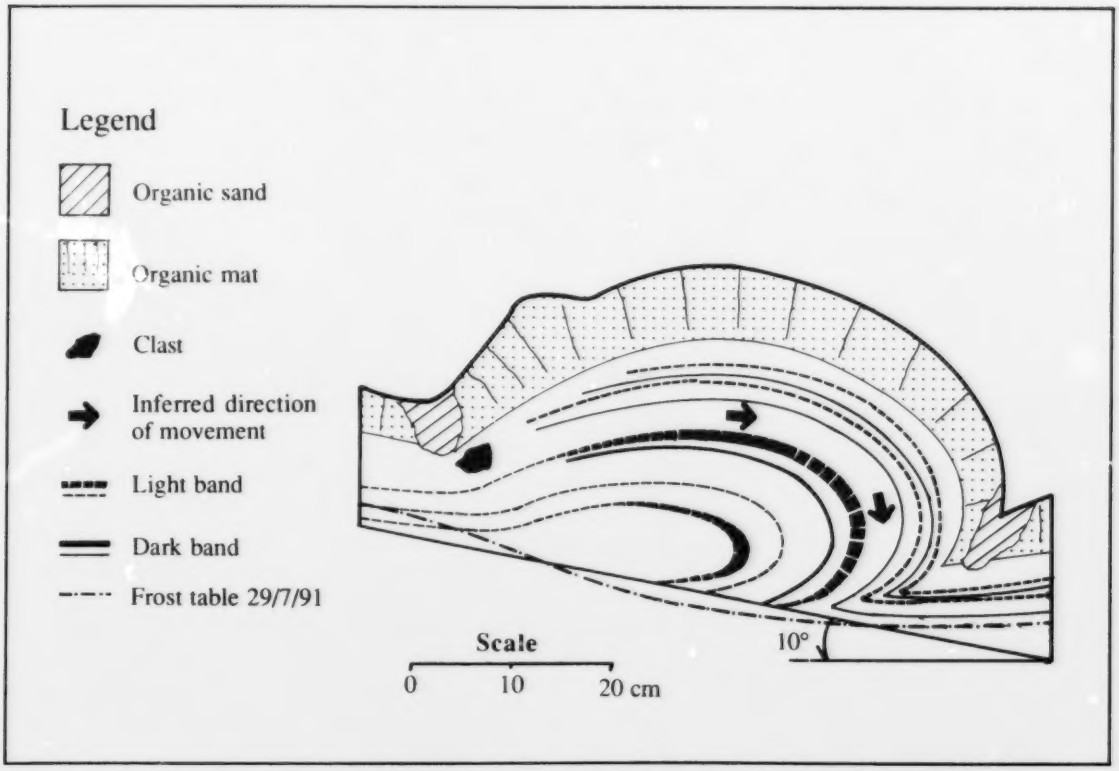

Figure 5. Downslope section of a hummock in the upper part of zone A, site 2, "Big Slide Creek". Except where indicated, the hummock is composed of silty sand. Note the relatively small amount of deformation within the banded structures.

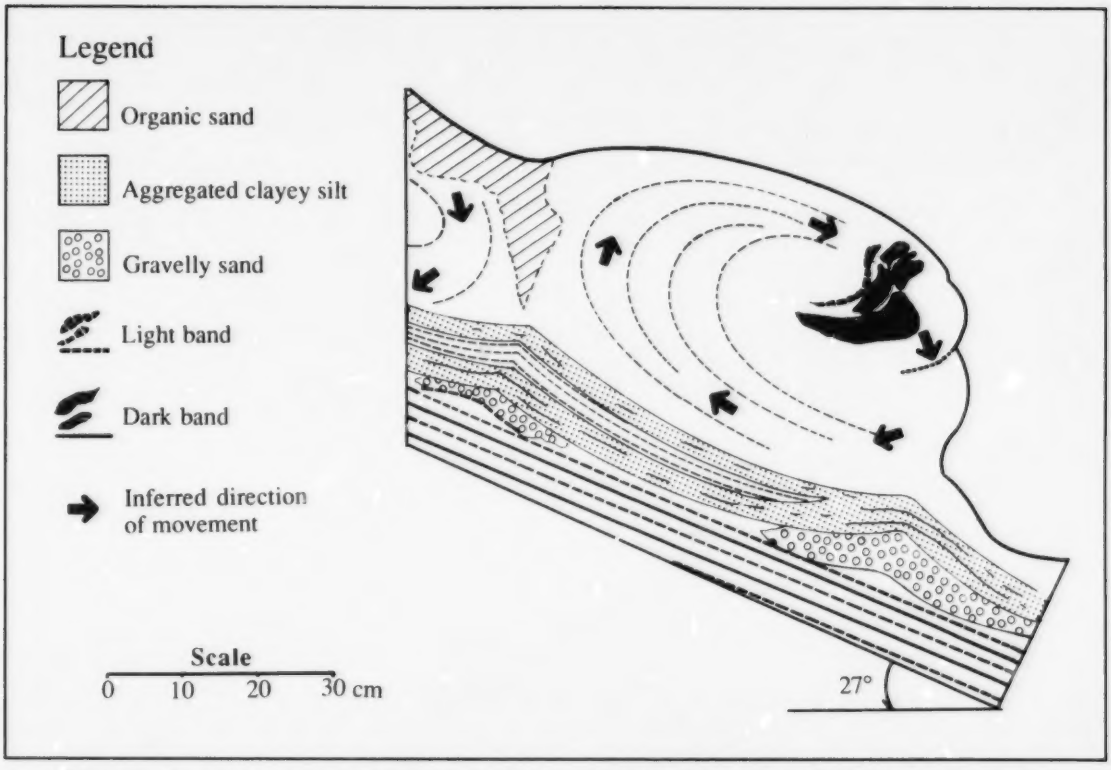

Figure 6. Downslope section of a hummock in the lower part of zone B, site 2, "Big Slide Creek". Except where indicated, the hummock is composed of silty sand. Note the high degree of internal deformation.

while the hummock's banded structure indicated that its core was rolling over as a unit within a cup-shaped indentation in the aggregated layer (see Fig. 6).

The frost table tended to be basin-shaped beneath the hummocks, with the lowest point under the hummock apex. This pattern was clear for hummocks on the more moderate slopes in zone A, but was not as evident on the steeper slopes in zone B.

DISCUSSION

Schunke and Zoltai (1988) have suggested that slope hummocks are formed by water eroding and overdeepening desiccation cracks that originate in a uniform fine sand. This could explain the correlation between snow and hummock distributions in the study areas. Desiccation cracks were observed upslope of most hummock sites and drying of the ground is particularly likely on the Fosheim Peninsula because of its warm summer climate (Edlund and Alt, 1989). Enhanced snowmelt in spring could maintain and deepen cracks by wash processes. However, observations at the study sites suggest that the development of slope hummocks is complex and that a suite of processes may be at work.

Deposition of wind-blown material on the tops of hummocks clearly contributes to their growth. Such accretion, described here for "Big Slide Creek" and previously for Hot Weather Creek (Lewkowicz and Young, in press), could account for their granulometry and the banded structures observed. The protection afforded by snow at hummock sites and the additional soil moisture during melt lead to the development of an extensive vegetation cover which increases hummock strength and helps maintain the form during movement downslope. The steepness of the slopes and the overall appearance of the hummock field (tension cracks and compression zones) indicate that mass movements play an important role. Internal structures demonstrate that hummocks at site 2 are generated at the upper part of zone A and then gradually move downward. It is possible to distinguish between two components in this downward motion: the movement of the active layer as a unit and the rolling motion of individual hummocks. Hummocks may have turned over several times before they reach the end of zone B and may, in some cases, have collided with other hummocks on their way down. Further work is required to evaluate which of these noncompeting factors is most important to the development of slope hummocks.

CONCLUSIONS

1. Slope hummocks are widespread on Fosheim Peninsula, in one area occupying 6% of the landscape. These forms are smaller than earth hummocks (typically 60 cm long and 20 cm high) and are found predominantly on steep slopes where substantial depths of snow accumulate in winter.

2. Slope hummocks are composed of silty sand which exhibits a banded structure both downslope and across the slope. These bands are deformed down-gradient and the degree of deformation increases downslope from the upper boundary of the hummock field.

3. Several factors probably contribute to hummock formation and preservation. These include desiccation cracking, wash processes, deposition of niveo-eolian sediment, the strengthening of the soil by vegetation, and mass movement. Micromorphological studies are in progress in an effort to identify which of these is the most important.

ACKNOWLEDGMENTS

Fieldwork was supported by a grant from the Natural Sciences and Engineering Research Council of Canada (to AGL) in addition to an EMR Research Agreement. Logistical support was kindly provided by the Polar Continental Shelf Project. H. Taylor ably assisted in the field. The authors wish to thank Dr. S.A. Edlund and Dr. M.-K. Woo for discussions in the field and elsewhere and all the personnel at the G.S.C. Hot Weather Creek camp for their kind hospitality.

REFERENCES

Edlund, S.A. and Alt, B.T.
1989: Regional congruence of vegetation and summer climate patterns in the Queen Elizabeth Islands; Arctic, v.42, p. 3-23.

Geological Survey of Canada
1971: Geology of Eureka Sound North, District of Franklin; Geological Survey of Canada, scale 1: 250 000, Map 1302A.

Hirakawa, K.
1989: Downslope movement of solifluction lobes in Iceland: a tephrostratigraphic approach; Geographical Reports, Tokyo Metropolitan University, v.24, p. 15-30.

Hodgson, D.A.
1985: The last glaciation of west-central Ellesmere Island, Arctic Archipelago; Canadian Journal of Earth Sciences, v.22, p. 347-368.

Lewkowicz, A.G. and Young, K.L.
in press: Observations of aeolian transport and niveo-aeolian deposition at three lowland sites, Canadian Arctic Archipelago; Permafrost and Periglacial Processes, v.2, in press.

Mackay, J.R.
1979: An equilibrium model for hummocks (nonsorted circles), Garry Island, Northwest Territories; in Current research, Part A, Geological Survey of Canada, Paper 79-1A, p. 165-167.

Permafrost Subcommittee, Associate Committee on Geotechnical Research, National Research Council of Canada
1988: Glossary of Permafrost and Related Ground-Ice Terms; National Research Council of Canada, Technical Memorandum no. 142, 156 p.

Schunke, E.
1977: Zur Ökologie der Thufur Islands; Berichte aus der Forschungsstelle Nedri As, Hveragerdi (Island), no. 26, 69 p.

Schunke, E. and Zoltai, S.C.
1988: Earth hummocks (thufur); in Advances in Periglacial Geomorphology, (ed.) M.J. Clark; John Wiley & Sons, Toronto, p.231-245.

Tarnocai, C. and Zoltai, S.C.
1978: Earth hummocks of the Canadian Arctic and Subarctic; Arctic and Alpine Research, v.10, p. 581-594.

Van Vliet Lanoë, B.
1991: Differential frost heave, load casting and convection: converging mechanisms; a discussion of the origin of cryoturbations; Permafrost and Periglacial Processes, v.2, p. 123-139.

Washburn, A.L.
1956: Classification of patterned ground and review of suggested origins; Geological Society of America, Bulletin no. 67, p. 823-866.

Woo, M.-K., Edlund, S.A., and Young, K.L.
1991: Occurrence of early snow-free zones on Fosheim Peninsula, Ellesmere Island, Northwest Territories; in Current Research, Part B, Geological Survey of Canada, Paper 91-1B, p. 9-14.

Geological Survey of Canada Project 880047

AUTHOR INDEX

Anderson, T.W. 7
Bégin, C. 13
Blake, W., Jr. 23
Boucher, S. 13
Bower, M.E. 31
de Freitas, T. 47, 53
Edlund, S.A. 91
Eisbacher, G.H. 37
Forsyth, D.A. 31
Gentzis, T. 79
Gibson, D. 79
Goodarzi, F. 79
Gudjonsson, K.A. 97
Hardwick, C.D. 31
Jackson, H.R. 23
Kjarsgaard, B.A. 1
Lewis, C.F.M. 7
Lewkowicz, A.G. 97
Loncarevic, B.D. 23
Macnab, R. 31
Marcotte, D.L. 31
Mayr, U. 47, 53, 65
Michaud, Y. 13
Nelson, J.B. 31
Okulitch, A.V. 31
Peterson, T.D. 1
Soule, G.S. 73
Spratt, D.A. 73
Teskey, D. 31
Thériault, P. 65
Woo, M-K. 91

NOTE TO CONTRIBUTORS

Submissions to the Discussion section of Current Research are welcome from both the staff of the Geological Survey of Canada and from the public. Discussions are limited to 6 double-spaced typewritten pages (about 1500 words) and are subject to review by the Chief Scientific Editor. Discussions are restricted to the scientific content of Geological Survey reports. General discussions concerning sector or government policy will not be accepted. All manuscripts must be computer word-processed on an IBM compatible system and must be submitted with a diskette using WordPerfect 5.0 or 5.1. Illustrations will be accepted only if, in the opinion of the editor, they are considered essential. In any case no redrafting will be undertaken and reproducible copy must accompany the original submissions. Discussion is limited to recent reports (not more than 2 years old) and may be in either English or French. Every effort is made to include both Discussion and Reply in the same issue. Current Research is published in January and July. Submissions should be sent to the Chief Scientific Editor, Geological Survey of Canada, 601 Booth Street, Ottawa, Canada, K1A 0E8.

AVIS AUX AUTEURS D'ARTICLES

Nous encourageons tant le personnel de la Commission géologique que le grand public à nous faire parvenir des articles destinés à la section discussion de la publication Recherches en cours. Le texte doit comprendre au plus six pages dactylographiées à double interligne (environ 1500 mots), texte qui peut faire l'objet d'un réexamen par le rédacteur scientifique en chef. Les discussions doivent se limiter au contenu scientifique des rapports de la Commission géologique. Les discussions générales sur le Secteur ou les politiques gouvernementales ne seront pas acceptées. Le texte doit être soumis à un traitement de texte informatisé par un système IBM compatible et enregistré sur disquette WordPerfect 5.0 ou 5.1. Les illustrations ne seront acceptées que dans la mesure où, selon l'opinion du rédacteur, elles seront considérées comme essentielles. Aucune retouche ne sera faite au texte et dans tous les cas, une copie qui puisse être reproduite doit accompagner le texte original. Les discussions en français ou en anglais doivent se limiter aux rapports récents (au plus de 2 ans). On s'efforcera de faire coïncider les articles destinés aux rubriques discussions et réponses dans le même numéro. La publication Recherches en cours paraît en janvier et en juillet. Les articles doivent être envoyés au rédacteur en chef scientifique, Commission géologique du Canada, 601, rue Booth, Ottawa, Canada, K1A 0E8.

Geological Survey of Canada Current Research, is now released twice a year, in January and in July. The four parts published in January 1992 (Paper 92-1, parts A to D) are listed below and can be purchased separately.

Recherches en cours, une publication de la Commission géologique du Canada, est publiée maintenant deux fois par année, en janvier et en juillet. Les quatre parties publiées en janvier 1992 (Étude 92-1, parties A à D) sont énumérées ci-dessous et vendues séparément.

Part A, Cordillera and Pacific Margin
Partie A, Cordillère et marge du Pacifique

Part B, Interior Plains and Arctic Canada
Partie B, Plaines intérieures et région arctique du Canada

Part C, Canadian Shield
Partie C, Bouclier canadien

Part D, Eastern Canada and national and general programs
Partie D, Est du Canada et programmes nationaux et généraux

Part E (this volume)
Partie E (ce volume)